Chemically- and photo-convertible dyes for fluorescence detection of biomolecules

Dissertation
for the award of the degree
"Doctor rerum naturalium" (Dr. rer. nat.)
of the Georg-August-Universität Göttingen

within the doctoral program in Chemistry
of the Georg-August University School of Science (GAUSS)

Submitted by
Elizaveta Savicheva
from Leningrad

Göttingen
2023

Thesis committee

Prof. Dr. Lutz Ackermann, Institute of Organic and Biomolecular Chemistry, Georg-August-Universität Göttingen

Prof. Dr. Dr. h.c. mult. Stefan W. Hell, Department of NanoBiophotonics, Max Planck Institute for Multidisciplinary Sciences

Dr. Vladimir N. Belov, Department of NanoBiophotonics, Max Planck Institute for Multidisciplinary Sciences

Members of the examination board

Reviewer: Prof. Dr. Lutz Ackermann, Institute of Organic and Biomolecular Chemistry, Georg-August-Universität Göttingen

Second reviewer: Prof. Dr. Dr. h.c. mult. Stefan W. Hell, Department of NanoBiophotonics, Max Planck Institute for Multidisciplinary Sciences

Further members of the Examination board

Dr. Grazvydas Lukinavicius, Research Group Chromatin Labeling and Imaging, Max Planck Institute for Multidisciplinary Sciences

Dr. Daniel Janßen-Müller, Institute of Organic and Biomolecular Chemistry, Georg-August-Universität Göttingen

Prof. Dr. Marina Bennati, Institute of Physical Chemistry, Georg-August-Universität Göttingen and Research Group Electron-Spin Resonance Spectroscopy, Max Planck Institute for Multidisciplinary Sciences

Date of oral examination: 20.12.2023

Abstract

Further progress in fluorescence microscopy and nanoscopy depends, among other factors, on the ease of detection, analysis, and selective imaging of bioconjugates prepared from fluorescent dyes with reactive groups and biomolecules. For that, new multifunctional fluorescent dyes which predictably change or acquire their emissive properties in the course of a chemical or photochemical transformation are highly demanded. These chemically- or photo-convertible dyes alter their spectral and emissive properties upon bioconjugation or photoactivation; they enable new imaging modalities and are highly favoured in fluorescence detection techniques.

In this work, chemically and photoconvertible dyes were designed, prepared and studied. The dissertation consists of three chapters and experimental part. The first chapter deals with the synthesis of yellow-emitting negatively charged aminopyrenes for reductive amination and fluorescence detection of sugars. The second chapter is devoted to photoconvertible cyanines containing 4-amino-1-diazobutanone fragment attached to the polymethine chain via amino group. The new cyanines undergo irreversible photolysis upon irradiation with UV light. In this chapter, synthetic challenges and features of cyanine dyes are discussed. Chapter three presents a novel approach to the late-stage functionalisation of rhodamines and photoactivatable phenoxazines. An oxidative olefination method via C–H activation was used to introduce a linker with a carboxyl group for bioconjugation. The photolysis experiments involving functionalised phenoxazines are described.

Table of contents

List of abbreviations

Chapter 1. **Negatively charged yellow-emitting aminopyrene dyes for reductive amination and fluorescence detection of glycans**

1.1 Introduction……..….10

1.2 Fluorescent dyes for glycan analysis ……..…..…….……12

1.3 Design of new dyes…….……..……14

1.3.1 Synthesis of pyrene sulfonamides..……..……..14

1.3.2 Synthesis of model sugar conjugates……...……..18

1.3.3 Photophysical properties of new dyes and their conjugates……...…….18

1.3.4 Determination of the Hammett σ-constants of the new substituents and evaluation of their electronic effects and influence on spectra…….……21

1.4 Reductive amination and detection of sugars…….……27

1.4.1 Reductive amination…….……..28

1.4.2 Polyacrylamide gel electrophoresis (PAGE)….…….……31

1.4.3 Desialylation studies…….... ……...…35

1.4.4 Capillary gel electrophoresis with laser-induced fluorescence detection (CGE-LIF)…….…….……...37

1.5 Conclusion…… ……38

1.6 References to Chapter 1…….…….……...40

Chapter 2. **Photoconvertible cyanine dyes**

2.1 Introduction……..…….……44

2.1.1 Wolff rearrangement…….……45

2.1.2 Cyanine dyes…….……47

2.1.3 Design and synthesis of photoconvertible cyanine dyes……..……..49

2.2 Trimethinecyanine dyes (Cy3)…….…….……51

2.2.1 Synthesis of the *meso* amino-substituted Cy3 ……...…….51

2.2.2 Photolysis of Cy3 incorporating 4-amino-1-diazobutanone fragment……...53

2.2.3 Photophysical properties of Cy3 dyes and their derivatives……..54

2.3 Pentamethinecyanine dyes (Cy5)……..55

2.3.1 Synthesis of the *meso* amino-substituted Cy5 through halogen substitution…….55
2.3.2 Synthesis of the *meso* amino-substituted Cy5 from malonic dialdehydes…….57
2.3.3 Intermezzo: *meso*-(2-carboxyphenyl)-Cy5 dye…….…….61
2.3.4 Photophysical properties of Cy5 dyes……62
2.4 Squaraines: synthesis, properties and photolysis……..65
2.5 Conclusion ……....68
2.6 References to Chapter 2…….…….……..……69
Chapter 3. **Late-stage transformation of fluorescent dyes via C–H activation**
3.1 Introduction…….…..73
3.2 C–H activation – general information……75
3.3 Rhodamines ……..78
3.3.1 *N*,*N'*-Bis(acetyl) rhodamine 110 as a substrate for oxidative olefination……....79
3.3.2 *N*,*N'*-Bis(trifluoroacetyl) rhodamine 110 as a substrate for oxidative olefination…..85
3.3.3 Photophysical properties of new rhodamine dyes……..87
3.4 Oxazines ……...90
3.4.1 *N*-Acetyl-protected phenoxazines……..93
3.4.2 *N*,*N'*-(*tert*-Butoxycarbonyl)-protected oxazines…….97
3.4.3 Synthesis of oxazine dyes from resorufin…….102
3.4.4 Photolysis of 10-*N*-Acetyl-protected phenoxazines……..……...105
3.4.5 Photophysical properties of new oxazine dyes……108
3.5 Conclusion and outlook……..…….110
3.6 References to Chapter 3……...…111
Chapter 4**. Experimental part**
4.1 General remarks……..114
4.2 Experimental procedures…….118
4.2.1 To Chapter 1…….118
4.2.1.1 Synthesis of new pyrene dyes……118
4.2.1.2 Synthesis of substituted fluorobenzenes……132
4.2.1.3 Synthesis of individual conjugates with glucose……135
4.2.1.4 Reductive amination of sugars …….140
4.2.1.5 Characterization of conjugates …….141

4.2.1.6 Desialylation studies…….153
4.2.2 To Chapter 2…….156
4.2.2.1 Preparation of DAK reagent……..156
4.2.2.2 Synthesis and properties of trimethine cyanines (Cy3)…….158
4.2.2.3 Synthesis and properties of pentamethine cyanines (Cy5)……172
4.2.2.4 Introduction of diazoketone moiety to the *Intermezzo* dye……..……..190
4.2.2.5 Synthesis and properties of squarylium dyes…….193
4.2.3 To Chapter 3…….197
4.2.3.1 Oxidative olefination of rhodamines…….197
4.2.3.2 Synthesis and properties of new rhodamine dyes……..204
4.2.3.3 Oxidative olefination of phenoxazines……..208
4.2.3.4 Synthesis and properties of new oxazine dyes……..214
4.2.3.5 Oxidative olefination of acetyl-protected resorufin **95** ……219
4.3 References to Chapter 4……..224
Acknowledgments……...225

List of abbreviations

Ac_2O - Acetic anhydride

AcOH - Acetic acid

APTS - 8-Aminopyrene-1,3,6-trisulfonic acid

BODIPY - Boron-dipyrromethene

CV - Column volume

C(G)E-LIF - Capillary (gel) electrophoresis with laser-induced fluorescence detection

DAK - Diazo ketone

DBN - 1,5-Diazabicyclo[4.3.0]non-5-ene

DCM - Dichloromethane

DFT - Density functional theory

DIEA - Diisopropylethylamine

DMAP - 4-*N*,*N*-Dimethylaminopyridine

DMF - *N*,*N*-Dimethylformamide

DMSO - Dimethyl sulfoxide

DP – degree of polymerisation

Dppf - 1,1'-bis(Diphenylphosphino)ferrocene

ESI - Electrospray Ionization

EI - Electron ionization

GU – glucose unit

HOMO - Highest occupied molecular orbital

HPLC - High performance liquid chromatography

HRMS - High Resolution Mass Spectrometry

IR - Infrared

LCMS - Liquid Chromatography – Mass Spectrometry

LSF - Late-stage functionalisation

LUMO – Lowest unoccupied molecular orbital

M - Molar concentration

MeCN - Acetonitrile

MINFLUX - Minimum fluxes nanoscopy technique

MINSTED - Minimum STED

ppm - Part per million

mCPBA - m-Chloroperbenzoic acid

NIR - Near-IR

NMR - Nuclear magnetic resonance

PAGE - Polyacrylamide gel electrophoresis

PALM - Photoactivation localisation microscopy

PET - Photoinduced electron transfer

RM - Reaction mixture

QY - quantum yield

R_f - Retention factor

r.t. - Room temperature

STED - Stimulated emission depletion

STORM - Stochastic optical reconstruction microscopy

TBDMS - *tert*-Butyldimethylsilyl

TBE - Tris/Borate/EDTA buffer

TFA -Trifluoroacetic acid

TFAA -Trifluoroacetic anhydride

TEA - Triethylamine

TEAB - Triethylammonium bicarbonate buffer

THF -Tetrahydrofuran

TLC - Thin layer chromatography

t_R -Retention time

% v/v -Volume/volume percent

UV -ultraviolet

Chapter 1.

Negatively charged yellow-emitting aminopyrene dyes for reductive amination and fluorescence detection of glycans

Two papers were published in *Angew. Chem. Int. Ed*.:

1. Negatively Charged Yellow-Emitting 1-Aminopyrene Dyes for Reductive Amination and Fluorescence Detection of Glycans, E. A. Savicheva, G. Y. Mitronova, L. Thomas, M. J. Böhm, J. Seikowski, V. N. Belov, S. W. Hell, *Angew. Chem. Int. Ed*. **2020**, *59*, 5505–5509; *Angew. Chem*. 2020, *132*, 5547–5551. **doi.org/10.1002/anie.201908063**

Contribution: I performed and optimised the synthesis of dye **6-H**, conjugates, and participated in writing of the manuscript.

2. Fluorescence Assisted Capillary Electrophoresis of Glycans Enabled by the Negatively Charged Auxochromes in 1-Aminopyrenes, E. A. Savicheva, J. Seikowski, J. I. Kast, C. R. Grünig, V. N. Belov, S. W. Hell, *Angew. Chem. Int. Ed*. **2021**, *60*, 3720–3726. **doi.org/10.1002/anie.202013187**

Contribution: I performed all synthetic work mentioned in the manuscript, measured photophysical properties and prepared the samples for electrophoresis. I also evaluated the Hammett constants and wrote the manuscript.

1.1 Introduction

Glycosylation is an enzymatic process that ensures the attachment of carbohydrates to proteins, lipids and other biomolecules. The resulting glycoconjugates represent a class of natural products that are unrivalled in structural and functional diversity and involved in fundamental biochemical processes in living organisms.[1] In the complex landscape of glycobiology, the role of these carbohydrate-rich molecules is only partially understood. Only few specific functions of these complex and carbohydrate-rich molecules have been well described so far. Further progress in glycomics and glycobiology depends on the advances in analytic techniques applicable to complex carbohydrates. This knowledge gap reveals the need for a deeper understanding of glycomics and glycobiology, aided by advances in analytical methods that correspond to the complex nature of carbohydrates. [2-7]

A major challenge in the analysis of carbohydrates relates to their innate properties. Carbohydrates do not absorb visible light, and require adequate derivatisation for efficient analysis. The derivatisation with a fluorescent tag by means of reductive amination has been the most widely used method applicable for glycan analysis.[3] Reductive amination of sugars is a two-step process involving the reversible formation of the Schiff base, which is then irreversibly reduced to a stable secondary amine (Scheme 1). This derivatisation enables analysis of glycans by sensitive detection of emission, probably combined with further detection modalities including mass spectrometry (MS),[4] chromatography,[5] capillary electrophoresis (CE),[6] and their combinations.[7]

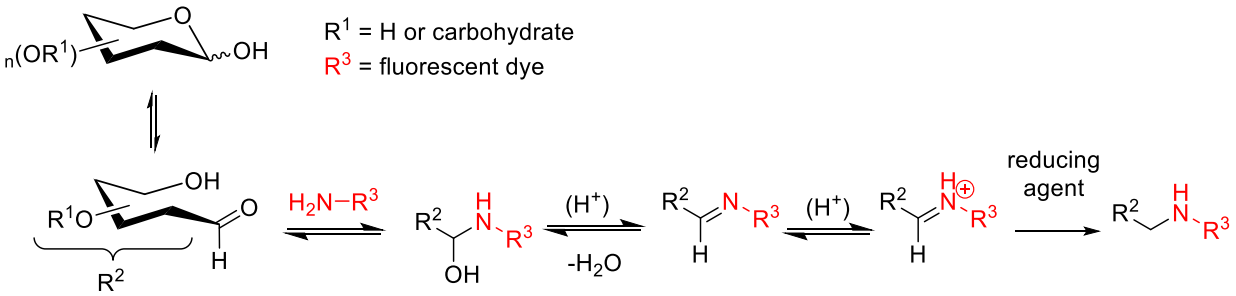

Scheme 1. Reductive amination of mono- and oligosaccharides. R^3-NH_2 is a fluorescent dye with an amino group capable of reaction with reducing sugars.

Capillary gel electrophoresis (CGE) combined with laser-induced fluorescence (LIF) has emerged as a powerful tool for the efficient separation and detection of enzymatically or chemically released glycans labelled with anionic fluorescent tags. This technique has found application in commercial DNA sequencers equipped with CGE-LIF modules operating with a 488 nm Ar lasers.[7] The efficiency of this approach depends on the properties of the fluorescent tag itself, which must fulfil certain criteria. The tag must have a strong absorbance at 488-505 nm and a high fluorescence quantum yield. In addition, the tag should include a reactive amino group for binding with glycans, be multicharged to provide high electrophoretic mobility, should be soluble in aqueous buffers, and stable against reduction with boranes or borohydrides in a wide pH range (3–8). The bright and negatively charged fluorescent dyes suitable for reductive amination of carbohydrates are rare. 8-Aminopyrene-1,3,6-trisulfonic acid (**APTS**, Figure 1) is up to now the standard and unique reagent which is widely used in CGE-LIF.[8-10] However, the overall performance of **APTS** as a single fluorescent tag is limited by one emission colour (green), improvable brightness and three negative charges. The prospective approach for the design of new dyes may rely on modifying sulfonate moieties within the pyrene core (Figure 1). The introduction of stronger acceptor groups to the "active" positions 3, 6 and 8 of pyrene core (in this case the amino group is at position 1) leads to the formation of a donor-acceptor dye with red-shifted bands. This red-shift is due to a "push-pull" effect between electron-donating amino group and electron-withdrawing groups. The introduction of electron-acceptors has to be combined with the presence of the negatively charged groups which enable moving in the electric field.

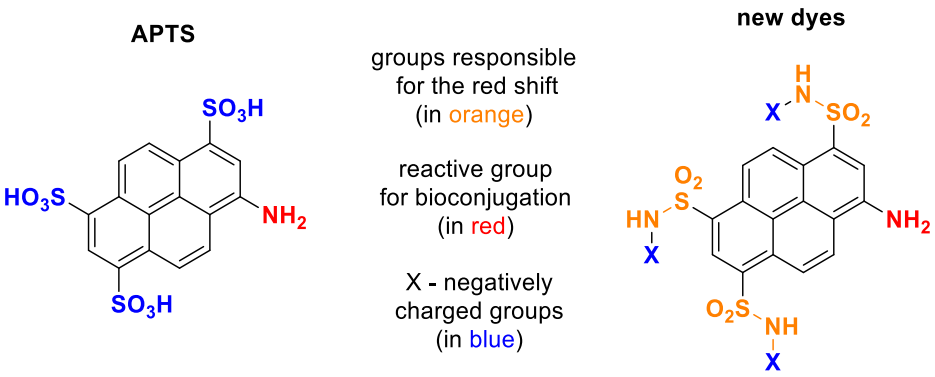

Figure 1. 8-Aminopyrene-1,3,6-trisulfonic acid (**APTS**) and general principle for the design of **APTS** analogues.

Here we stay within the family of aminopyrene dyes, because up to now it was represented only by **APTS** dye, and the potential of those dyes is far from being exhausted. Below, we will show that simple changes in aminopyrene structure will give dyes outperforming **APTS** in glycan derivatisation and analysis.

Hence, the main objective involved the development of a pyrene-based fluorescent tag superior to **APTS** in glycan detection. This goal was achieved through the transformation of the free sulfonic acid groups to substituted sulfonamides (Figure 1). The free **APTS** emits green-blue light, the **APTS** conjugates emit green. The new pyrene dyes were expected to exhibit yellow emission in conjugates, to have improved CGE-LIF performance, providing higher sensitivity, better separation and low cross-talk with other detection channels of a standard DNA-sequencer. Efficient labelling, easy separation and detection of carbohydrates featuring diverse structures and positional isomerism, such as mannose and sialic acid-rich structures were expected to be addressed by molecular design of aminopyrene.

1.2 Fluorescent dyes for glycan analysis

The introduction of **APTS** (Figure 1) as a label for the CGE-LIF technique marked significant progress in glycan analysis.[8a] **APTS** conjugates are excitable with an Ar laser and emit green light (512 nm). Up to now **APTS** has been employed in numerous studies involving not only CGE-LIF,[8-10] but also chromatography with fluorescent and/or mass detection techniques.[11]

The requirements for the dye suitable for reductive amination and sugar analysis are quite strict. Other dyes such as rhodamines[12] and cyanines[13] bleach upon reduction with borohydrides used for reductive amination and were not considered. For the past 25 years, **APTS** has dominated in the field of glycan analysis.

The fluorescence of **APTS** derivatives is detected in the "green" colour channel of the standard DNA sequencers. Emission of **APTS**-conjugates is somewhat red-shifted (compared with **APTS** itself), because *N*-alkylation takes place in the reaction with carbohydrates, and the donor properties of *N*-alkyl groups are stronger than that of the primary NH_2 group. These conjugates are excitable with an argon laser (emission line at 488 nm). However, the potential of **APTS** as a fluorescent tag providing only one emission colour, moderate brightness and three negative charges, is limited. After introduction of **APTS** for CGE-LIF in 1995, [8a] several attempts to modify

its structure have been reported. Other negatively charged dyes were developed for CE-LIF and CE-MS analysis of glycans, but their structures are either unknown, or they emit in the blue spectral region and cannot be excited with 488 nm light.[14] Shifting the absorption spectrum to the red can potentially help to get a better dye with reduced or even without cross-talk with **APTS** detection window. This kind of red shift can be achieved, first of all, by mono-alkylation of the amino group. This modification would convert the primary amino group to a more electron-donating secondary amine. However, it was shown that a secondary amino group did not participate in the reductive amination of glucose (even under harsh conditions).[15]

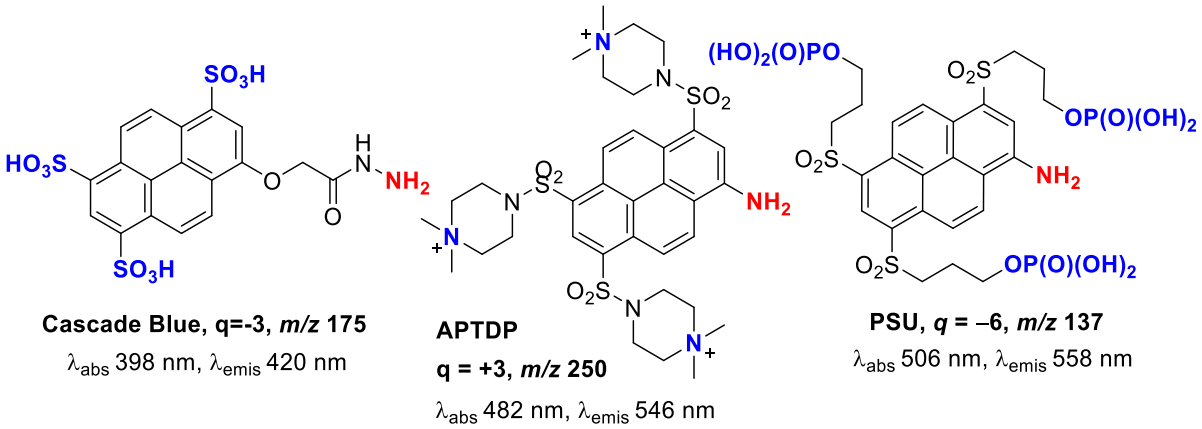

Figure 2. Pyrene based dyes for sugar analysis. Absorption and emission maxima are given for glycan-dye conjugate; q = net electric charge.

Interestingly, the use of hydrazide as a reactive group for the reductive amination of sugars has been reported. Cascade Blue dye[16] (Figure 2) appeared much more reactive in reductive amination than **APTS**, and it was successfully applied for labelling of glycans; the conjugates were separated by CE-LIF. However, the fluorescence cannot be excited with 488 nm light, because the absorption maximum of conjugates is at 398 nm and the emission at 420 nm.

The positively charged aminopyrene sulfonamide **APTDP** (Figure 2) has been reported very recently.[17] Remarkably, in this work the negatively charged **APTS** dye was converted to a positively charged derivative with q = +3. The positive charge was achieved by introduction of the piperazine fragment which provides a positive charge upon *N*-alkylation to *N,N*-dimethylammonio derivatives. The latter may be used in CE with the "reversed" polarity of the electric field. The dye **APTDP** and their conjugates showed red-shifted absorption and emission maxima compared to

APTS thanks to the presence of three electron-withdrawing sulfonamide groups (σ_m = 0.53, σ_p = 0.60 for SO_2NH_2).[18]

In our group a negatively charged aminopyrene sulfone **PSU** (Figure 2) was prepared.[15] Alkylsulfonates have higher values of the *Hammett* σ-constants (σ_m = 0.56-0.66, σ_p = 0.68-0.77 for SO_2Alkyl)[18] than ionised sulfonic acid residues in **APTS** (σ_m = 0.05, σ_p = 0.09).[19] The net charge -6 is provided by three primary phosphate groups (R-$OP(O)(OH)_2$) which ensure higher mobility in the electric field compared to **APTS**.

1.3 Design of new dyes

The high-performing fluorescent tags applicable in the reductive amination and CGE-LIF of glycans must have a primary amino group with pK_a of the conjugated acid in the range of 3–4 for the efficient reductive amination at pH ~ 3, stability against reduction with boranes or borohydrides (key reagents for reductive amination of glycans), net charge of –3...–6 at pH = 8 (pH of the buffer solution for electrophoresis) to provide high electrophoretic mobility. High absorption within the range of 488 – 505 nm provides the excitation efficiency with an argon laser and high brightness of the conjugates. Additionally, high brightness and minimal cross-talk with the "**APTS** channel" in the detector (*i.e.*, low emission of conjugates at 520 nm) are also required. These features are set by the reaction conditions in Scheme 1, and the spectral properties associated with standard DNA sequencing equipment used for the separation and detection of the fluorescent glycan derivatives.[21]

1.3.1 Synthesis of pyrene sulfonamides

The **APTS** core remains an attractive scaffold for further modifications. As demonstrated with **PSU** dye (Figure 2), the incorporation of acceptor groups at "active" positions 3, 6, and 8 of the 1-aminopyrene core results in a noticeable red shift in both absorption and emission maxima.[15] This red-shift is due to a “push-pull”-effect between the electron-donating amino group and electron-withdrawing groups at positions 3, 6 and 8. Another modification is the conversion of three sulfonic acid residues in **APTS** into another electron acceptors – sulfonamides (Scheme 2). The values of Hammett σ_p and σ_m constants were considered as a tool for evaluation of the acceptor

properties of the substituents "opposing" the donor amino group in 1-aminopyrene and providing the red-shifts in spectra. Sulfonamides have higher values of the Hammett σ-constants (σ_m = 0.53, σ_p = 0.60 for SO_2NH_2)[18] than ionised sulfonic acid residues in **APTS** (σ_m = 0.05, σ_p = 0.09).[19]

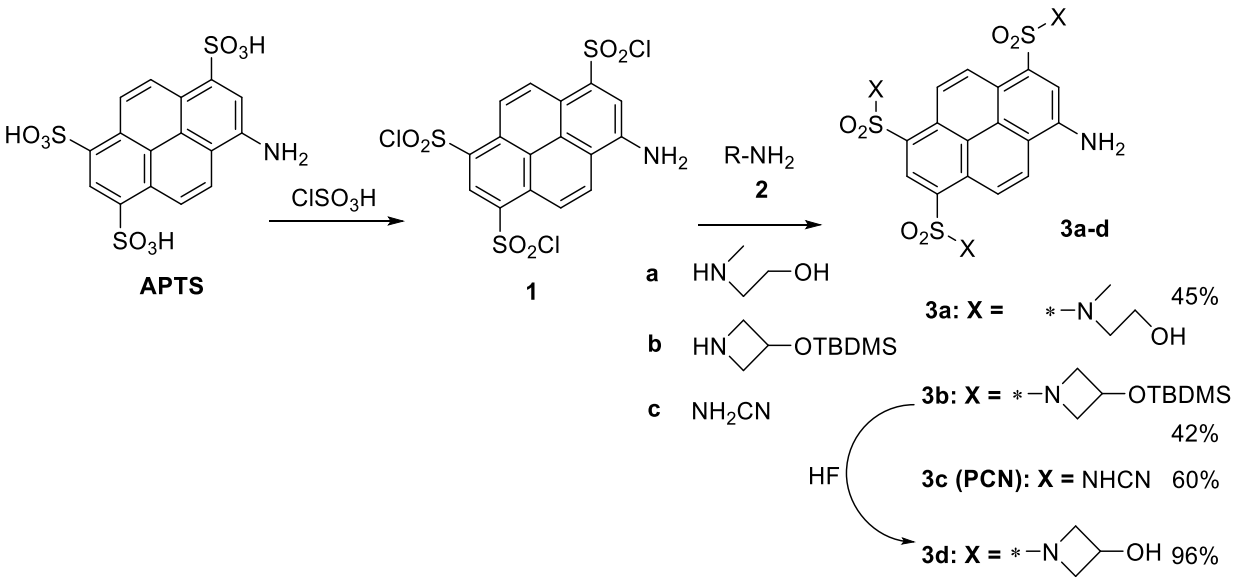

Scheme 2. Synthesis of pyrene-sulfonamides from **APTS**.

A simple two-step synthesis of sulfonamides involves **APTS** as a starting material which is converted to tris-chlorosulfonyl aminopyrene **1** as an intermediate (Scheme 2). The corresponding sulfonamides **3a-c** were prepared by reaction of **1** with amines **2a-b**, or cyanamide **2c**. The deprotection of *tert*-butyldimethylsilyl (TBDMS) ether **3b** to **3d** carried out using HF in MeCN.

The selection of amines was driven by intention to study and compare several features associated with the amine structure. A strained cyclic amine **2b**, containing an azetidine moiety, is less conformationally flexible than the linear counterpart **2a**. Dye **3d** was expected to have smaller hydrodynamic radius and provide higher mobility in conjugates than its acyclic analogue **3a**.

N-(Cyano)sulfonamide residue in dye **3c** (or **PCN** according its "published name")[24] is one of the most intriguing, promising and least studied groups. This substituent was mentioned in the context of medicinal chemistry,[22] but its impact on optical spectra and electric charge remained unknown. It was not clear, if this group will be negatively charged at pH = 8 (CE buffer) and have electron-acceptor properties when ionised. Nevertheless, it was expected that due to the presence of cyano group, *N*-(cyano)sulfonamide group would be a more powerful acceptor than SO_3^-. The

acidity of NH-proton is enhanced due to the neighbouring effects of two strong electron-acceptor residues – SO_2 and CN – and delocalisation of the negative charge between two nitrogen atoms (Scheme 3).

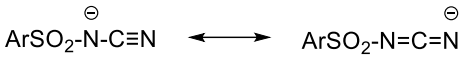

Scheme 3. Resonance structures of aryl *N*-(cyano)sulfonamide group.

In case of *N*-alkylsulfonamides, primary phosphates were chosen as ionisable groups to provide multiple negative charges and high electrophoretic mobility at pH 8. Their first and second pK_a values are in the range of 1.5-1.9 and 6.3-6.8, respectively.[23] In the electrophoresis buffer solution (pH = 8), one primary phosphate group introduces two negative charges. Direct phosphorylation of three hydroxyl groups in **3a,d** by $POCl_3$ followed by hydrolysis afforded dyes **PSN** (16% yield), and **PAZ** (13% yield), bearing six negative charges at pH 8 (Scheme 4).

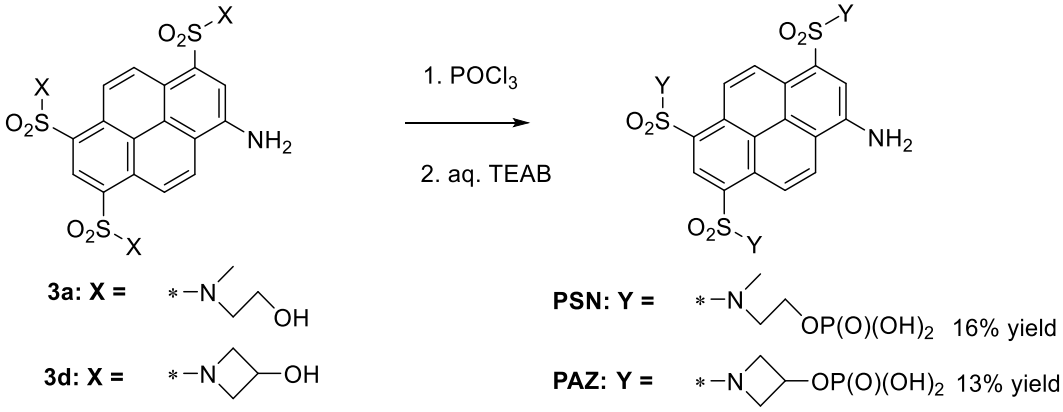

Scheme 4. Direct phosphorylation of hydroxyl groups in dyes **3a,d** with $POCl_3$ followed by hydrolysis with aq. triethylamine-CO_2 buffer (TEAB). Yields of isolated products are given.

Although the desired dyes were obtained, the yields were low. To improve the yields, the synthesis was modified (Scheme 5). The main change was based on the use of *O*-phosphorylated amines **6a** or **6b** (Scheme 5), which were applied as compounds with already phosphorylated hydroxyl groups. Thus, the step responsible for a low yield was omitted. Indeed, phosphorylation of benzyloxycarbonyl (Z) – protected amines **4** with phosphoramidite reagent followed by oxidation to appropriate *O*-protected phosphate occurs under mild conditions and provides good

yields (reaction 2, Scheme 5). After deprotection of the amino group, *O*-phosphorylated compounds **6a,b** react with 8-aminopyrene-1,3,6-trisulfonyl trichloride **1** to form intermediates **7a,b**. Their conversion into dyes **PSN** or **PAZ** is straightforward. Thus, the overall yield of the 5-step sequence (Scheme 5) turned to be superior to yields of the previous 3-step sequence (Schemes 2, 4). The final dyes **PSN** and **PAZ** were synthesised with 26% and 35% overall yields, respectively, instead of 7% and 3% respectively.

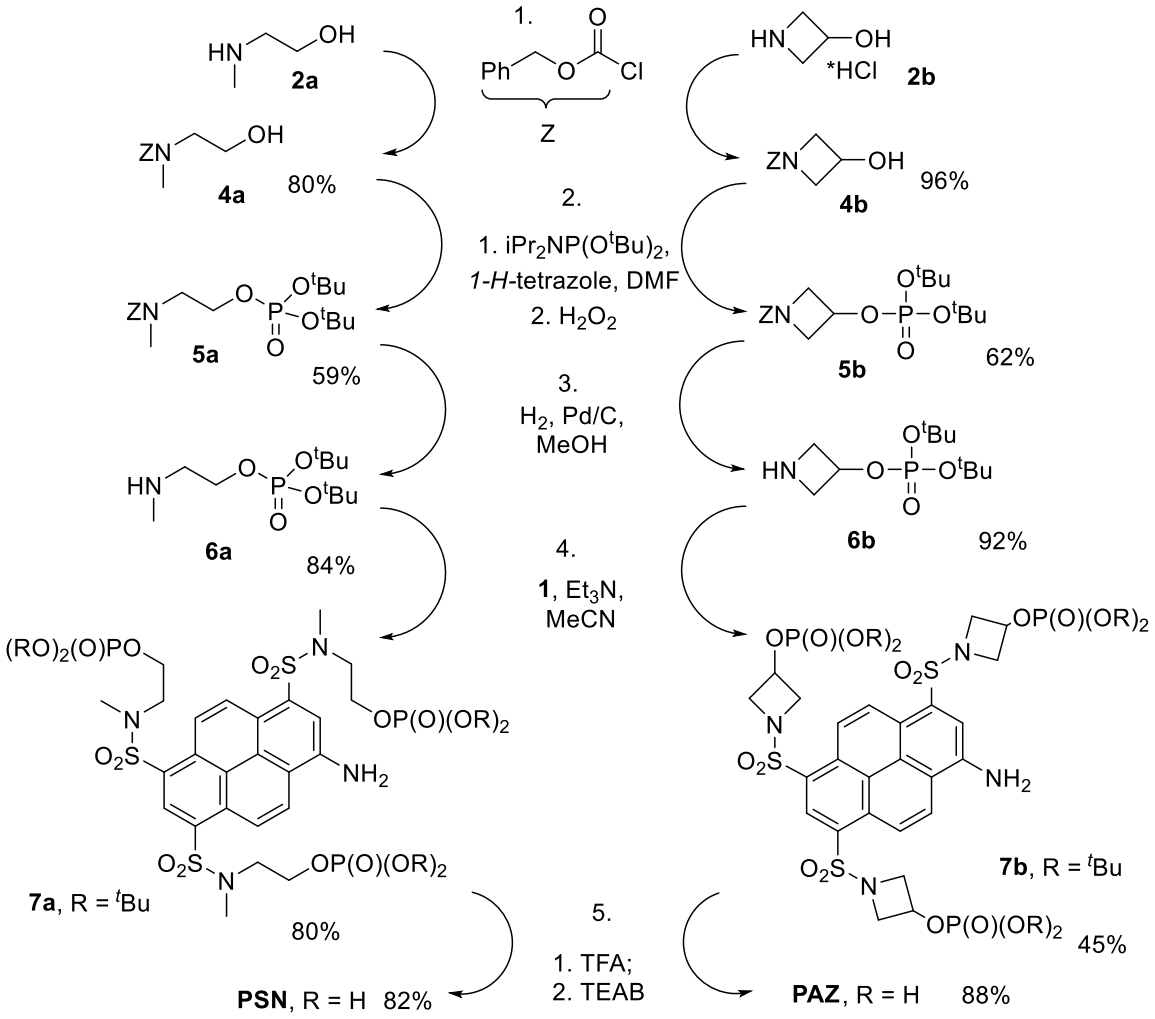

Scheme 5. Synthesis of phosphorylated trisulfonamide pyrene dyes **PSN** and **PAZ**. Yields of isolated products are given.

1.3.2 Synthesis of model sugar conjugates

The model conjugates of the new dyes with glucose (**G**) were prepared by reductive amination. The conjugates with glucose would allow us to measure the red shifts in the absorption and emission spectra, extinction coefficients and quantum yields. Commercially available **APTS** and previously prepared in our lab **PSU** dye were also included into this study. The **PSU** dye was prepared according the reported procedure.[15]

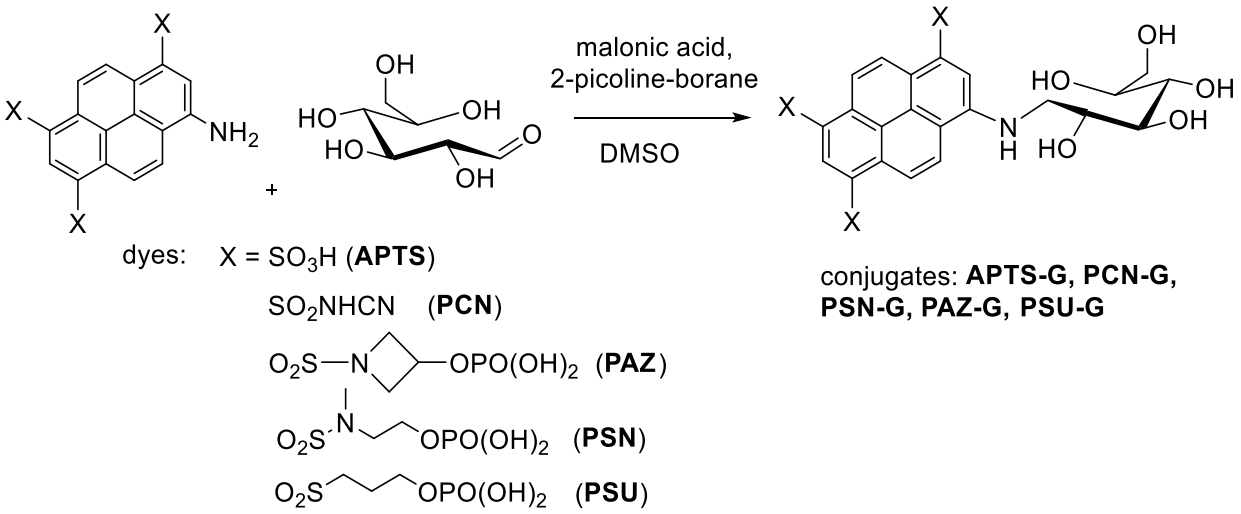

Scheme 6. Synthesis of dye-conjugates with glucose via reductive amination.

5-Fold excess of glucose was used in this reaction in order to facilitate the isolation of conjugates and not to waste the dye. The conjugates were isolated by reversed phase chromatography and their photophysical properties were measured.

1.3.3 Photophysical properties of new dyes and conjugates

The photophysical properties of **APTS**, new aminopyrene dyes, and their conjugates with glucose (dye-G) are given in Table 1. The compounds in Table 1 form two groups: free dyes with a primary amino group **(APTS**, **PCN**, **PSN**, **PAZ**, **PSU**), and conjugates possessing a secondary amino group (**APTS-G**, **PCN-G**, **PSN-G**, **PAZ-G**, **PSU-G**). Pyrenes of the first group absorb at 424 nm (**APTS**) to 477 nm (**PSU**). Compounds of the second group relate to the products formed

in the course of reductive amination (Scheme 6). As a result of *N*-alkylation, their absorption maxima are red-shifted compared to free dyes, and found in the range from 455 nm (**APTS-G**) to 506 nm (**PSU-G**) in aqueous solutions. Thus, *N*-alkylation shifts the absorption maximum to the red by 25-31 nm, while the emission underwent a smaller bathochromic shift of 11-21 nm. These red shifts are important, as the glycan conjugates of new dyes are intended to have minimal emission in the **APTS** detection window. The brightness of a glycan label is defined as a product of the extinction coefficient (at the excitation wavelength, *e.g.*, 488 nm) and the fluorescence quantum yield. For **APTS** conjugates, the extinction coefficient at the maximum (455 nm) is about 17000 $M^{-1}cm^{-1}$, and the absorption at 488 nm is *ca*. 35% of the maximal value. For all new conjugates (**PSN-G**, **PAZ-G**, **PSU-G**) we can assume the extinction coefficient at 488 nm to be about 18000 $M^{-1}cm^{-1}$ and 29000 $M^{-1}cm^{-1}$ for **PCN-G**. Therefore, the conjugates of new dyes are *ca*. 3 times brighter than **APTS** derivatives under excitation with the 488 nm laser. For all conjugates the Stokes shifts are quite large (52-62 nm), and the fluorescence quantum yields are high (>0.9). This combination is valuable and rare, because large Stokes shifts are often associated with reduced emission efficiencies. The large Stokes shifts allow more freedom in choosing the excitation wavelength and detection window, which is an important condition, as it reduces cross-talk between detection channels in the standard DNA sequencer (**APTS** on the one hand, and **PCN**/**PSN**/**PAZ**/**PSU** on the other hand).

The absorption (and emission) spectra of **PSN-G**, **PAZ-G**, and **PSU-G** conjugates were very similar: the positions of the maxima differ only by 6-10 nm. Probably, the amino group as a single donor is not capable to provide more electron density to the π-system decorated with three very powerful acceptor groups, whatever strong they are. Remarkably, the absorption and emission spectra of the **PCN** dye, which possesses a poorly studied *N*-(cyano)sulfonamide group, are also red-shifted compared to **APTS**. That confirms expectations that *N*-(cyano)sulfonamide group is more electron withdrawing than ionised sulfonic acid residue. However, it is weaker acceptor than sulfonamides in **PSN** and **PAZ**. We come to this conclusion if we compare the positions of the absorption and emission bands and assume the correlation between their positions and electronic effects of the substituents.

Table 1. Spectral properties of the dyes and their conjugates with glucose (dye-G) in aqueous solutions (pH 7.3)

Compound	Absorption λ_{max}, nm (ε)[a]	Emission λ_{max}, nm (Φ_{fl})[b]	Fluor. lifetime, ns	Stokes shift, nm
APTS[c]	424 (20600)	500 (0.95)	-	76
APTS-G[d]	455 (17160)	511 (0.92)	5.1	56
PCN	454 (23900)	531 (0.93)	5.6	77
PCN-G	484 (29000)	544 (0.92)	5.5	60
PSN	471 (18000)	544 (0.91)	5.6	73
PSN-G	496 (30000)	558 (0.91)	5.7	62
PAZ	476 (19000)	543 (0.92)	5.9	67
PAZ-G	505	564 (0.90)	5.8	59
PSU	477 (19600)	542 (0.92)	5.8	65
PSU-G	506	558 (0.95)	5.8	52

[a] molar extinction coefficient, $M^{-1}cm^{-1}$; [b] absolute values of fluorescence quantum yield; [c] data from ref. 7d; [d] data from ref. 7a.

The values of Hammett σ_p and σ_m constants for the acceptor substituents "opposing" the donor amino group in 1-aminopyrene were considered to be responsible for the red shift in spectra. These values, as well as the field and resonance parameters (σ_I and σ_R^0), for SO_2NHCN (*N*-(cyano)sulfonamide) and $SO_2NC_3H_5OH$ (*N*-[3-hydroxyazetidine]sulfonyl) groups were unknown. The new substituents are interesting as polar acceptor groups not only for 1-aminopyrene, but also for other "push-pull" chromophores. This is why we evaluated the values of Hammett σ-constants of these groups. The following chapter discusses the measurement of Hammett σ-constants and the influence of electronic effects on photophysical properties of the dyes.

1.3.5 Determination of the Hammett σ-constants of the new substituents, evaluation of their electronic effects and influence on spectra.

Traditionally, Hammett σ-constants have been obtained by measuring the constants of ionisation of benzoic acids in water, or ionisation of the protonated amines, but also through spectroscopic methods.[18] The use of nuclear magnetic resonance (NMR) spectroscopy, in particular, the measurement of ^{19}F chemical shifts, was shown to be a versatile and valuable technique for measuring and studying these values.[25] The chemical shifts in ^{19}F-NMR spectra relate to the electron density on fluorine nuclei and are very sensitive to the nature of *meta*- or *para*-substituents in the benzene ring. Therefore, the chemical shifts in ^{19}F-NMR spectra of *meta*- and *para*-substituted fluorobenzenes enable to calculate the inductive σ_I and resonance σ_R^0 values of the new substituents. For this purpose, *meta*- (compounds **8a** and **9a** on Scheme 7) and *para*- (compounds **8b** and **9b**, Scheme 7) substituted fluorobenzenes were prepared as model compounds from commercially available fluorobenzenesulfonyl chlorides (Scheme 7).

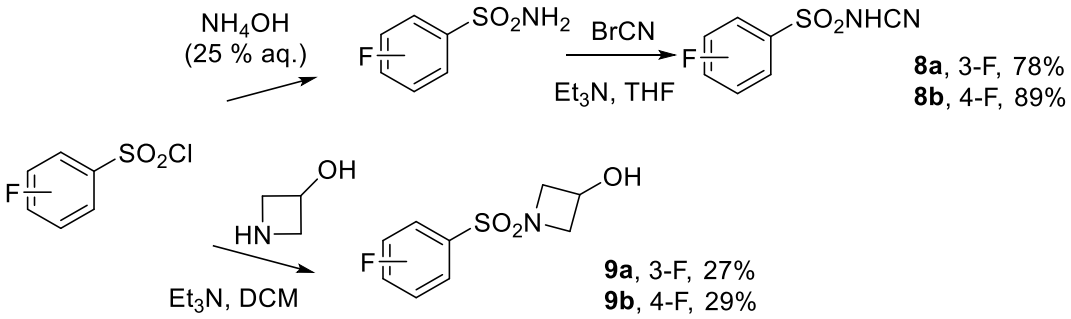

Scheme 7. Synthesis of *meta*- and *para*- substituted fluorobenzenes with sulfonamide substituents for evaluation of the Hammett σ-constants of sulfonamide groups.

The parameter σ_I reflects the polar effect of the substituent – combination of the inductive and field effects (transferred along σ-bonds and through space). The parameter σ_R^0 is associated with a pure resonance (mesomeric) effect of the group (transferred via π-systems, *d*-orbitals and their combination). Taft demonstrated that it is possible to separate the polar (σ_I) and resonance (σ_R^0) effects.[25a] He introduced the method to calculate σ_I (eq. 1) and σ_R^0 (eq. 2) using shielding parameters $\delta_H^{m(X)}$, $\delta_H^{p(X)}$, and their difference $\Delta\delta_H^{p(X)-m(X)}$. The shielding parameters $\delta_H^{m(X)}$, $\delta_H^{p(X)}$

represented the difference between chemical shifts of ^{19}F in the *meta*- and *para*-substituted fluorobenzenes and fluorobenzene; $\Delta\delta_H^{p(X)-m(X)} = \delta_H^{p(X)} - \delta_H^{m(X)}$.

Knowing the values of σ_{I} and σ_{R}^0, it is possible to calculate the Hammett substituent constants σ_p and σ_m according to eq. 3 and 4:[25]

$$\sigma_I = \frac{0.6+\delta_H^{m(X)})}{7.1} \quad (1); \qquad \sigma_R^0 = \frac{\Delta\delta_H^{p(X)-m(X)}}{29.5} \quad (2)$$

$$\sigma_p = \sigma_I + \sigma_R^0 \quad (3); \qquad \sigma_m = \sigma_{\mathrm{I}} + \alpha\,\sigma_{\mathrm{R}}^0; \quad 0 < \alpha < 1 \quad (4)$$

The physical sense of eq. 3 and 4 follows from the clear separation of the polar (σ_{I}) and resonance (σ_{R}^0) effects: σ_p is simply the sum of the parameters reflecting these two effects, while σ_m includes only a *constant* part of the resonance effect (due to less efficient conjugation with the *meta*-position). According to Taft[25c], $\alpha \approx 0.5$.

To confirm the reliability of this approach, several representative substituents were chosen, and the ^{19}F NMR spectra were measured for corresponding *meta*- and *para*-substituted fluorobenzenes (including compounds **8** and **9** containing studied substituents, Scheme 7). The substituent (X) shielding parameters $\delta_H^{m(X)}$, $\delta_H^{p(X)}$ were calculated (the difference between chemical shifts of ^{19}F in *meta*- and *para*-substituted fluorobenzenes and fluorobenzene itself). The values of σ_I, σ_{R}^0, σ_p and σ_m were calculated from equations (1-4), and are given in Table 2. For 11 substituents σ values are known and given in brackets (columns 4-7). The calculated values of Hammett σ_p and σ_m constants according to eq. 3 and 4 may be compared with previously reported σ values obtained from other methods. Indeed, the data in last two columns of Table 2 confirm that the σ_p and $\sigma_m$values derived from the ^{19}F NMR spectra are in satisfactory agreement with values reported in the literature.[18]

Table 2. Calculated δ[a] and σ[b] values; previously reported values[18] are given in brackets.

X	1	2	3	4	5	6	7
	$\delta_H^{p(X)}$	$\delta_H^{m(X)}$	$\Delta\delta_H^{p(X)-m(X)}$	σ_I	σ_R^0	σ_p	σ_m
H	0	0	0	0	0	0	0
NO_2	10.24	3.1	7.14	0.52 (0.65)	0.24 (0.13)	0.76 (0.78)	0.64 (0.71)
COMe	6.78	0.6	6.18	0.17 (0.33)	0.21 (0.17)	0.38 (0.50)	0.27 (0.38)
CN	9.87	2.58	7.29	0.45 (0.51)	0.25 (0.15)	0.70 (0.66)	0.57 (0.56)
SO_2NH_2	5	1.9	3.1	0.35 (0.49)	0.105 (0.11)	0.45 (0.60)	0.40 (0.53)
SO_2NHCN	5.16	2.06	3.1	0.375	0.105	0.48	0.42
SO_2NMe_2	6.94	2.78	4.16	0.48 (0.44)	0.14 (0.21)	0.62 (0.65)	0.55 (0.51)
$SO_2NC_3H_5OH$	7.61	2.93	4.68	0.5	0.16	0.66	0.58
CO_2Et	6.86	3.43	3.43	0.57 (0.34)	0.11 (0.11)	0.68 (0.45)	0.62 (0.37)
CCl_3	3	1.79	1.21	0.34 (0.38)	0.04 (0.09)	0.38 (0.46)	0.36 (0.40)
$CONH_2$	3.44	0.03	3.41	0.09 (0.26)	0.11 (0.10)	0.20 (0.36)	0.14 (0.28)
SO_3^-	-0.1	-0.5	0.4	0.014 (0.04)[c]	0.04 (0.05)[c]	0.06 (0.09)[c]	0.03 (0.05)[c]
Cl	-2.48	2.37	-4.85	0.42 (0.42)	-0.16 (-0.19)	0.26 (0.37)	0.34 (0.23)
OMe	-11.34	1.27	-12.61	0.26 (0.29)	-0.43 (-0.56)	-0.17 (-0.27)	0.05 (0.12)

[a] The substituent (X) shielding parameters $\delta_H^{m(X)}$, $\delta_H^{p(X)}$ represent the difference between chemical shifts of ^{19}F in *meta*- and *para*-substituted fluorobenzenes and fluorobenzene; [b] the values of σ_I, σ_R^0, σ_p and σ_m were calculated from equations (1-4); [c] data from ref. 19.

Another method for determining σ values involves the use of correlation curves. The linear correlation between the ^{19}F shielding parameters δ (derived from the values of ^{19}F chemical shifts) and values of σ_I and σ_R^0 is described.[25c] Thus, the inductive σ_I and resonance σ_R^0 values of the new substituents may be also estimated by fitting the measured ^{19}F NMR shielding parameters δ to the straight line plotted for other groups with already known values of σ_I and σ_R^0. This method allows us to obtain σ values for the new substituents not only from ^{19}F chemical shifts, but also considering other molecular properties, since the known values of σ_I and σ_R^0 were derived from a heterogeneous pool of data related to multiple reaction centres. This is why this approach was considered as more reliable and has been chosen for further measurements.

A good linear correlation between the measured ^{19}F shielding parameters δ and values of σ_I and σ_R^0 is observed with R^2 = 0.92 and 0.94 for parameters σ_I and σ_R^0, respectively. Figure 3 illustrates this approach, and provides the required values σ_I and σ_R^0 for the new substituents (SO_2NHCN and $SO_2NC_3H_5OH$) by interpolation of the experimental parameters $\delta_H^{m(X)}$ and $\Delta\delta_H^{p(X)-m(X)}$ to the straight line plotted on the basis of data obtained for other substituents with known σ_I and σ_R^0 values (taken from ref. 18). These values of inductive σ_I and resonance σ_R^0 constants for SO_2NHCN and $SO_2NC_3H_5OH$ groups determined by linear interpolation might be used in calculations of σ_p and σ_m according to equations 3 and 4. The correctness of these assumptions is confirmed by better prediction of the absorption and emission spectra (Figure 4) through the σ_p values derived from the interpolated σ_I and σ_R^0 constants (Figure 3) than through the σ_p values derived from the σ_I and σ_R^0 parameters calculated from eq. 1 and 2 (Table 2).

The values of σ_p and σ_m for the studied groups (SO_2NHCN and $SO_2NC_3H_5OH$) were compared with the known values for sulfonamides and sulfones (Table 3). Importantly, through both approaches *N*-(cyano)sulfonamide group turned out to be a stronger acceptor than sulfonic acid, but weaker than tertiary sulfonamide. *N*-(3-hydroxyazetidine)sulfonyl group is a stronger acceptor than *N*,*N*-dimethylaminosulfonyl residue; though both are tertiary sulfonyl amides.

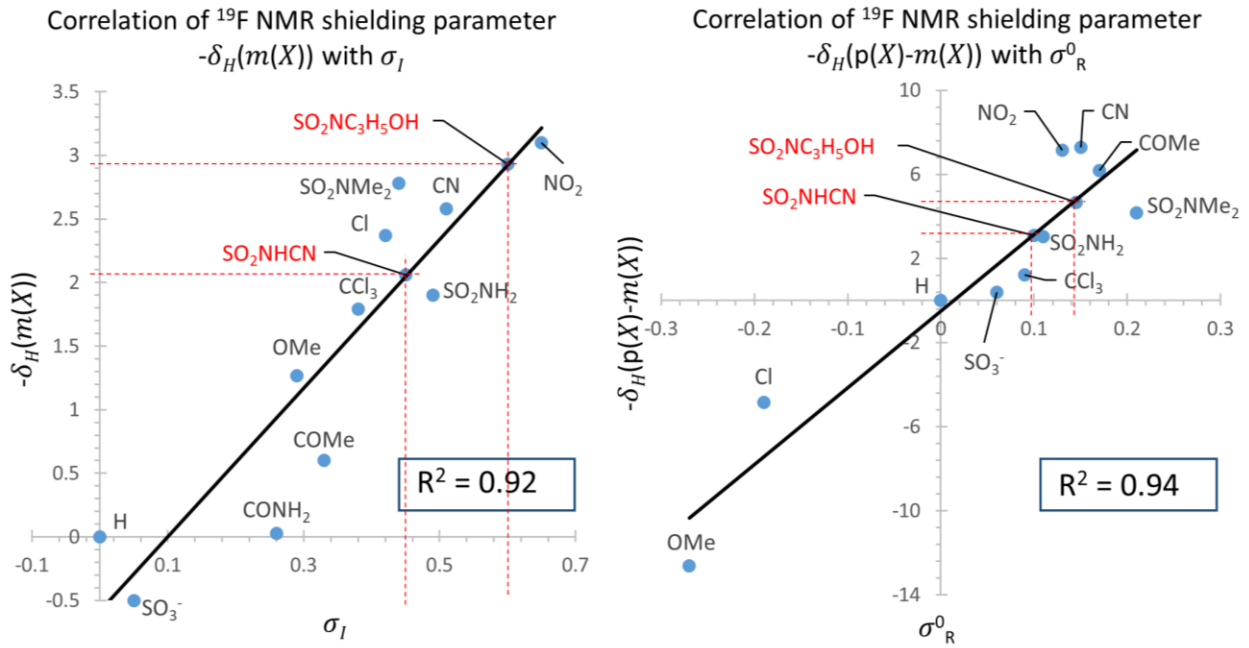

Figure 3. Linear correlations of ^{19}F NMR shielding parameters $\delta_H^{m(X)}$ and $\Delta\delta_H^{p(X)-m(X)}$ (ref. to fluorobenzene) with σ_I (left plot) and σ_R^0 (right plot) values from ref. 18. The interpolation is represented by red dashed lines, the studied substituents are displayed in red.

This data and σ_p, σ_m values in Table 3 indicate the trend and suggest substituents useful for the design of new "push-pull" dyes. If an electron-donor ("push") group is directly attached to the aromatic system, it can be opposed by one or several electron-acceptor ("pull") groups selected from sulfonic acid, *N*-(cyano)sulfonamide, sulfonamide and alkylsulfone residues. Alkyl sulfonates are the strongest acceptors in this series. The previous studies report the correlations between photophysical properties (*e.g.*, positions of absorption and/or fluorescence maxima) and Hammett σ_p constants.[26,27] The relationships between the positions of the absorption and emission maxima of new dyes (and their conjugates) and Hammett σ_p constants of the substituents present in their structures were evaluated (Figure 6). Remarkably, a better correlation was observed for absorption (R^2 = 0.97; 0.99) than for emission (R^2 = 0.89; 0.93). All these results support the power, accuracy and predictive force of the ^{19}F NMR method and Taft approach[25] that allowed us to determine the complete set of σ values.

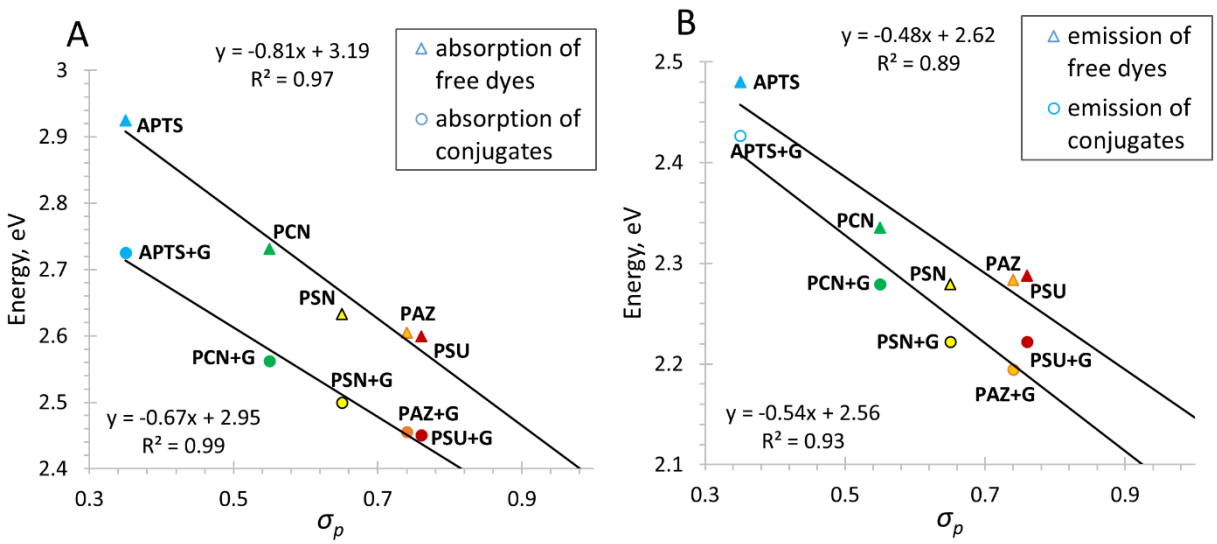

Figure 4. Correlations between σ_p values and positions of absorption (A) and emission (B) maxima of the free dyes and their conjugates with glucose.

Table 3. Hammett σ_p and σ_m values for sulfonamides, sulfones, and sulfonic acid.

Substituent	σ_p	σ_m
SO_3^-	0.35[a]	0.30[a]
SO_2NHCN	0.55[b]	0.49[b]
SO_2NH_2	0.60[a]	0.53[a]
SO_2NMe_2	0.65[a]	0.51[a]
SO_2Alk	0.72-0.77[a]	0.60-0.66[a]
$SO_2NC_3H_5OH$	0.74[b]	0.58[b]

[a] data from ref. 18; [b] calculated values of the present work.

To summarise, the acceptor properties of SO_2NHCN and $SO_2NC_3H_5OH$ groups were evaluated and these substituents were classified as members of a wide set of electron-acceptor groups (Table 3). The new substituents are interesting as polar acceptor groups not only for 1-aminopyrene, but also for other “push-pull” chromophores.[28]

1.4 Reductive amination and detection of sugars

To prove the applicability of new dyes for fluorescence-assisted detection of sugars, their conjugates with diverse carbohydrates and maltodextrin "ladder" were obtained. **APTS** conjugates were also obtained and analysed for comparison (Scheme 8).

In the context of analytical techniques, the maltodextrin ladder serves as a reference standard.[3] Maltodextrin is composed of glucose units linked together in chains, and the length of these chains can vary. The glucose units are linked with α(1→4) glycosidic bonds. Maltose, maltotriose, maltotetraose *etc.* belong to this family (Figure 5). The maltodextrin ladder typically includes molecules ranging from DP1 (glucose itself) up to DP20 or even higher. The use of fluorescently labelled maltodextrin ladder offers an opportunity to determine the values of retention time of "Glycan Units" (GU) pertaining to distinct structures. The sugar ladder allows to correlate the migration (electrophoresis) or retention time (chromatography) of new analytes with the known standard components of the ladder, aiding in the identification and quantification of the new or unidentified carbohydrates in various samples.

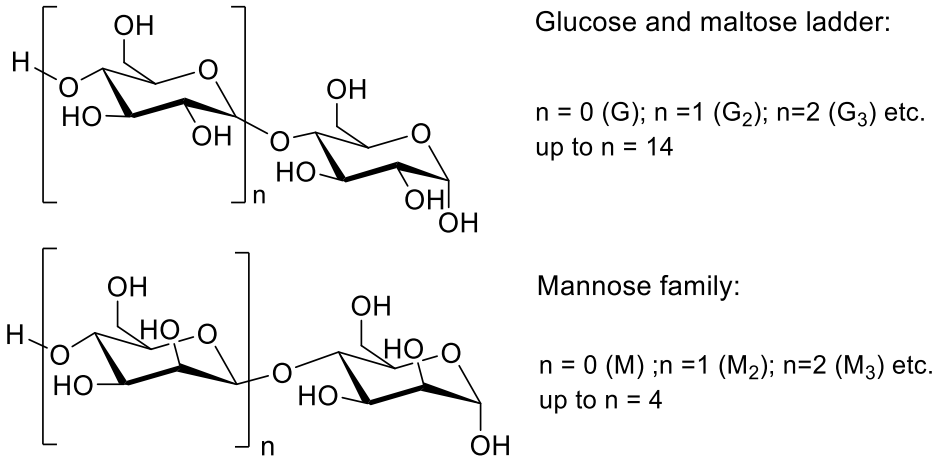

Figure 5. Glucose (G) and mannose (M) oligomers used in this study.

Linkage isomers of mannobioses (Figure 6) and sialyllactoses (Figure 7) were labelled with **PSU** dye to investigate the separation efficiency of the new label in comparison to **APTS**. A desialylation study (the loss of *N*-acetylneuraminic acid, Neu5Ac in the course of labelling) was performed using **PCN** dye.

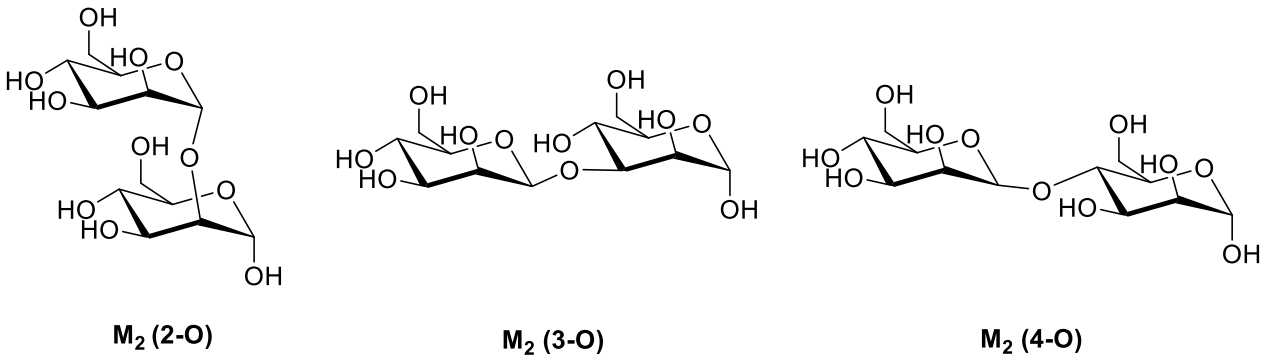

Figure 6. Mannobioses (M_2) and isomeric 2-*O*-, 3-*O*- and 4-*O*-(α-D-mannopyranosyl)-D-mannoses (M_2-2O, M_2-3O and M_2-4O).

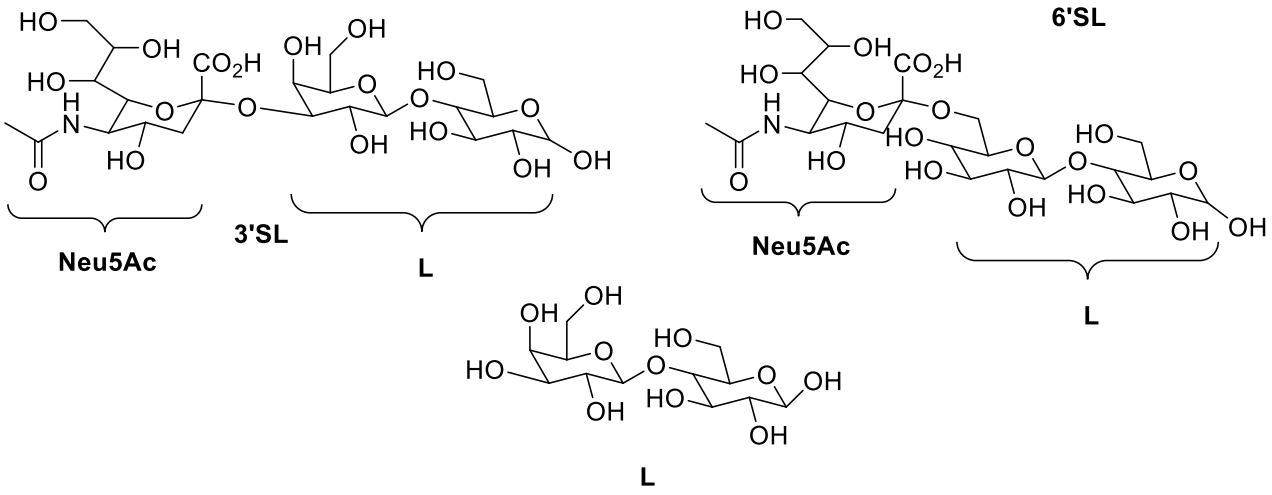

Figure 7. Neu5Ac - *N*-acetylneuraminic acid, 3'- (3'SL) and 6'-sialyllactoses (6'SL); lactose (L).

1.4.1 Reductive amination

Many various conditions were reported for efficient labelling of reductive sugars with **APTS**. The influence of concentration, temperature, time, the nature of acid and reducing agent were optimised for this dye.[8,9,29] Additional improvements, such as evaporative reductive amination, have been reported recently.[30] The combination of citric acid with $NaBH_3CN$ as a reducing agent in THF represents typical conditions for labelling with **APTS**.[31] Recently, 2-picoline-borane complex in DMSO was reported as an efficient and non-toxic reductant for this reaction.[32]

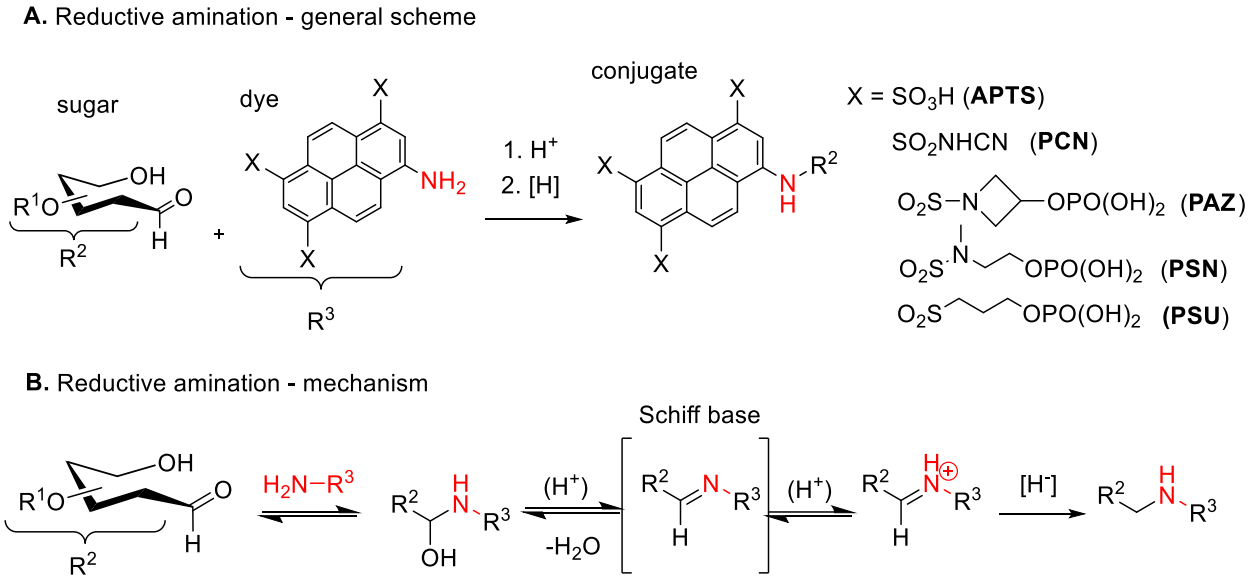

Scheme 8. Reductive amination of sugars: A) general scheme; B) mechanism.

HPLC analysis of the reaction mixtures revealed, that under standard conditions (classic – with $NaBH_3CN$/citric acid, and "modern" – with 2-picoline-borane complex/malonic acid) the labelling with new dyes (**PSN, PAZ, PSU**) is not complete. Due to the presence of strong acceptors groups, the new dyes undergo reductive alkylation more reluctantly than **APTS**. To enhance efficiency, the water-free protocol has been established for efficient labelling with new pyrene dyes. In this experiment, glucose was labelled with 2-fold excess of **PSN** dye in the presence of malonic acid to maintain pH level below 3, and 2-picoline borane complex in DMSO as a reducing agent. Malonic acid (pK_a^1 2.83)[29b] is stronger than citric acid (pK_a^1 3.13)[29b], and therefore protonates the weak amines **PSN**, **PAZ** and **PSU** (and Schiff base formed from them) easier. This was the reason why the malonic acid was used. Since reductive amination is a two-step process, our intention was to separate these steps in order to create best conditions for each step.

The first step results in the formation of the Schiff base in the presence of malonic acid; water is removed during this process (Scheme 8, B). The sample was shaken at 40 °C for 1 h in an Eppendorf ThermoMixer®. The equilibrium constant of this reaction is known to be low, and the amount of Schiff base does not accumulate with time. To assure complete formation of the Schiff base, we decided to eliminate water from the reaction mixture; the solvents were completely removed in a freeze-dryer. The complete formation of the Schiff base was observed through HPLC analysis once the reaction mixture had been thoroughly dried (Figure 8a). The absorption maximum

of the Schiff base is blue-shifted to 459 nm (compared to dye **PSN**, λ_{max} (absorption) 474 nm). The Schiff base was isolated and its constitution confirmed by HRMS. The second step related to the reduction of the Schiff base to the stable secondary amine. The reducing agent (2-picoline-borane complex in DMSO) was added, and the reduction step carried out (the sample stirred at 40°C for 16 h in an Eppendorf ThermoMixer®). The HPLC analysis of the reaction mixture upon reduction showed the formation of the desired conjugate **PSN-G** together with an excess of **PSN** dye (Figure 8b).

These observations explain the necessity of complete removal of water by drying the reaction mixture in vacuo, before addition of the reducing agent.

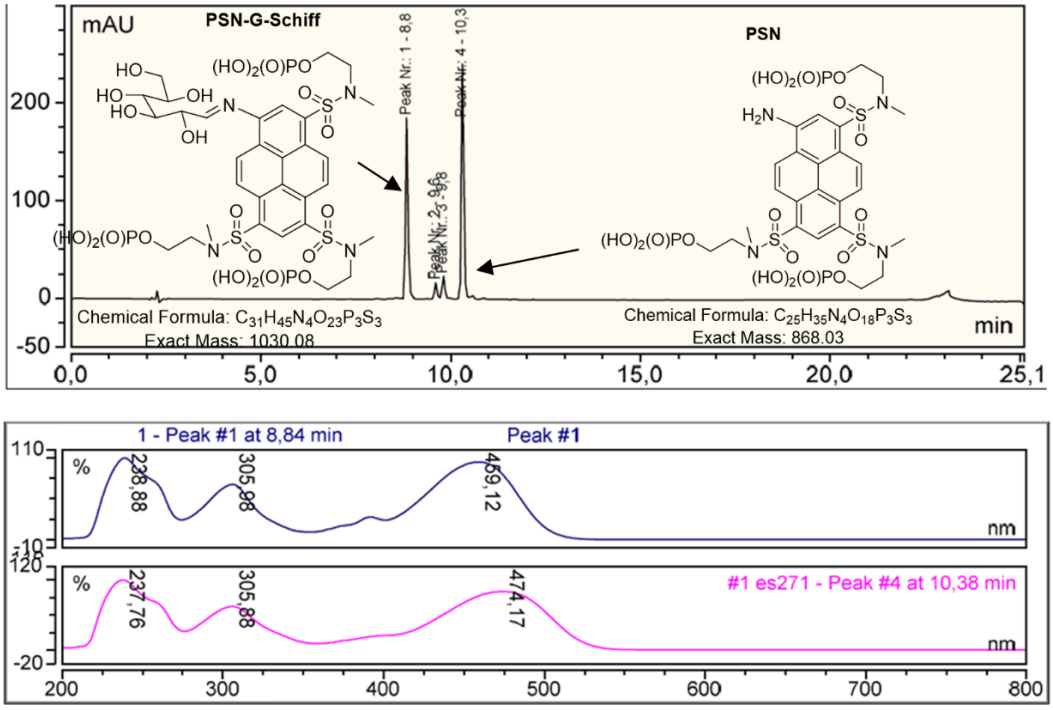

Figure 8a. HPLC traces of the reaction mixture after drying: dye **PSN** (t_R = 10.3, λ_{max} = 474 nm, magenta line), and the Schiff base formed from glucose (t_R = 8.8, λ_{max} = 459 nm, dark blue line) were observed.

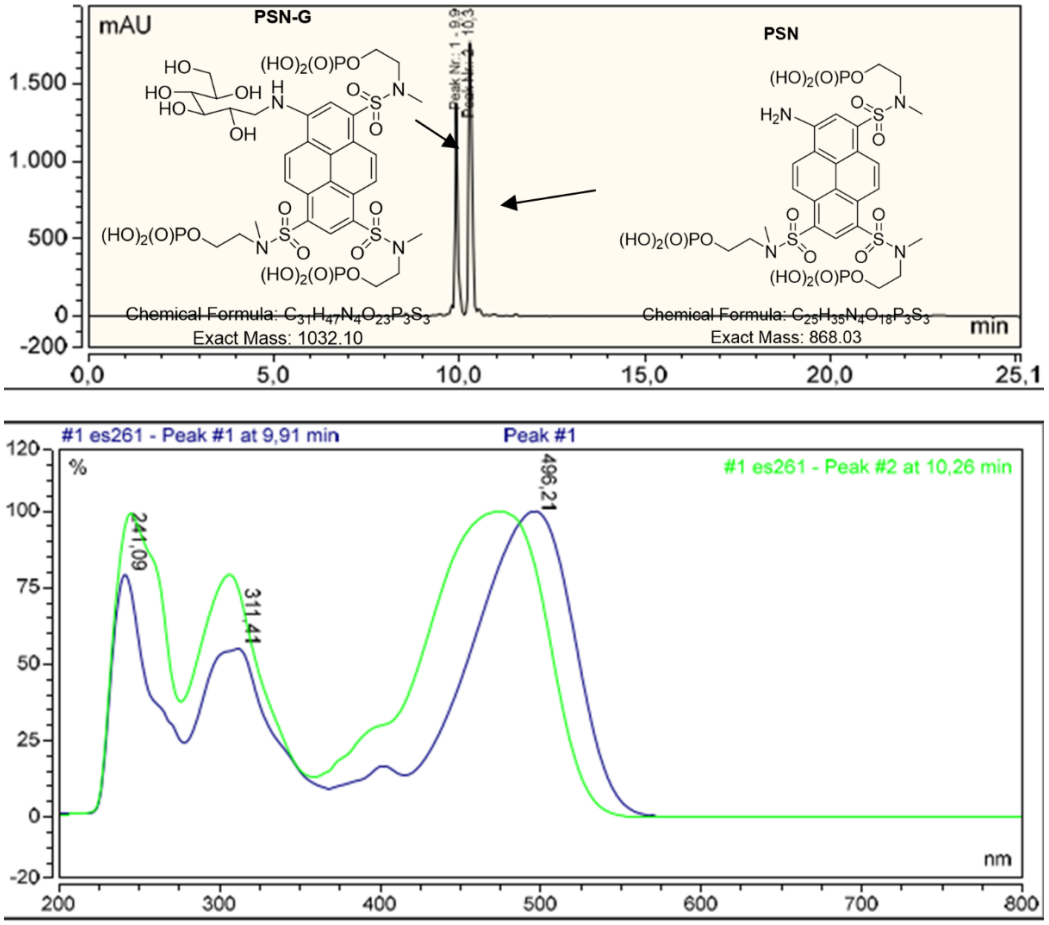

Figure 8b. HPLC traces of the reaction mixture after reduction with 2-picoline-borane complex in DMSO: dye **PSN** (t_R = 10.3, λ_{max} = 474 nm, green line), and the desired product **PSN-G** (t_R = 10.3, 9.9, λ_{max} = 496 nm, blue line).

1.4.2 Polyacrylamide gel electrophoresis (PAGE)

To evaluate the "separation power" and electrophoretic mobilities provided by the new pyrene dyes and **APTS** (as a standard marker), we prepared their conjugates with reducing sugars and analysed them by PAGE. Samples were applied on a freshly prepared polyacrylamide slab gel in TBE buffer (pH 8). The electrophoresis was performed at ambient temperature and constant power (35 W; 1750 - 2200 V) for 90 min. The bands were visualised by emission (excitation with 366 nm UV-lamp), and the pictures (Figures 9-12) were taken by using a digital camera. For structures of dyes see Scheme 8, for structures of sugars see Figures 5-7.

Figure 9 shows the gel electrophoresis results obtained with **APTS** and its conjugates (lanes 1, 3, 5), as well as **PSU** and its conjugates with the same reducing sugars (lanes 2, 4, 6). The conjugates of **PSU** move faster than the corresponding **APTS** conjugates. Due to higher net charge of **PSU** and its conjugates, the distances between yellow spots related to them are shorter than the distances between green bands of **APTS** conjugates.

In case of mannobiose isomers, the selectivity profile of **PSU** is different from that of **APTS** (Figure 9, lanes 3, 4). Conjugates of M_2-2O and M_2-3O with **APTS** move as one spot (lane 3, fourth spot from the top), and **APTS**-M_2-4O moves slower (lane 3, third spot). Conjugates of **PSU**-M_2-2O and **PSU**-M_2-4O move as one spot (lane 4, third spot from the top), and conjugate **PSU**-M_2-3O moves faster (lane 4, fourth spot). Each conjugate was also analysed separately (Figure 12).

Both dyes (**APTS** and **PSU**) easily resolve 3'- and 6'-isomers of sialyllactoses (lanes 5 and 6 of Figure 9).

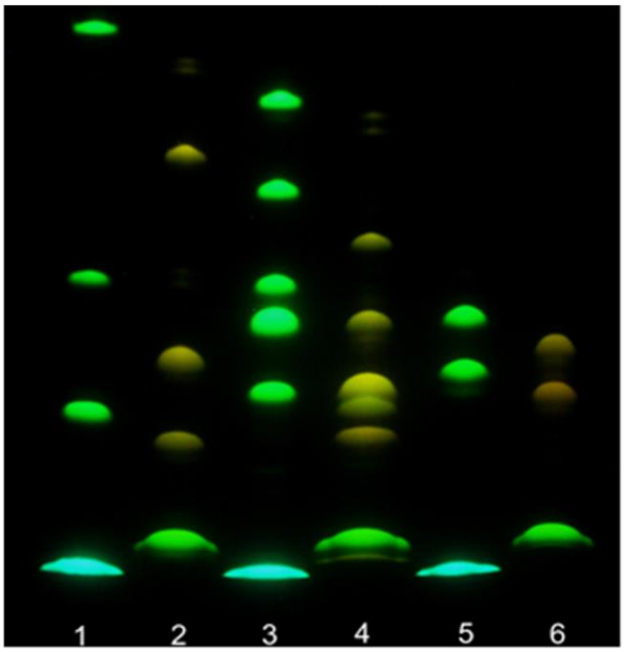

Figure 9. The PAGE plate (migration from “north” to “south”, pH 8.3). Lane 1: **APTS** (lowest bluish spot), **APTS**-G, **APTS**-G_3, **APTS**-G_7 (green spots). Lane 2: dye **PSU** (green spot), **PSU-G**, **PSU**-G_3, **PSU**-G_7 (yellow spots). Lane 3: **APTS**, **APTS**-M, **APTS**-M_2-2O/**APTS**-M_2-3O) (unresolved), **APTS**-M_2-4O, **APTS**-M_3 and **APTS**-M_4. Lane 4: **PSU**, **PSU**-M, **PSU**-M_2-3O, **PSU**-**M_2**-2O/**PSU**-M_2-4O (unresolved), **PSU**-M_3 and **PSU**-M_4. Lane 5: **APTS**, **APTS**-3'SL, **APTS**-6'SL. Lane 6: **PSU**, **PSU**-3'SL, **PSU**-6'SL.

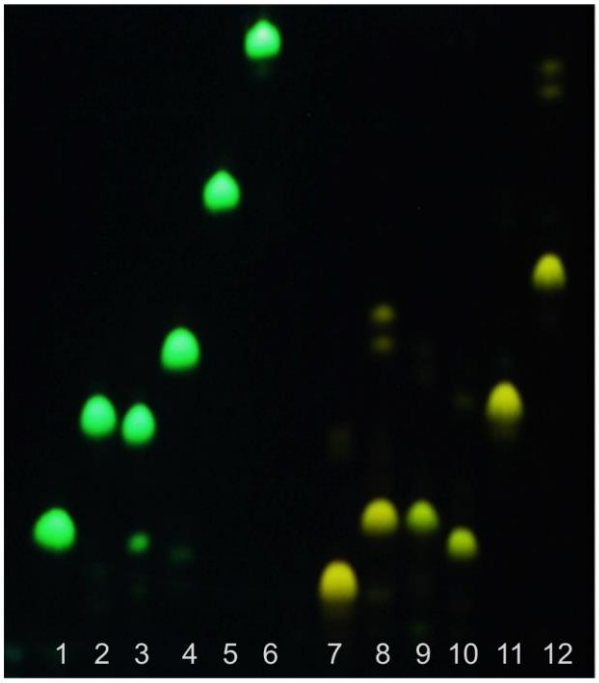

Figure 10. The PAGE plate (migration from "north" to "south", pH 8.3) of **APTS** conjugates with mannose and its oligomers (lanes 1-6, green spots) and conjugates of dye **PSU** with mannose and its oligomers (lanes 7-12, yellow spots). Lanes 1-6, green spots, from left to center: **APTS**-M, **APTS**-M_2-2O, **APTS**-M_2-3O, **APTS**-M_2-4O, **APTS**-M_3 and **APTS**-M_4. Lanes 7-12, yellow spots, from center to right: **PSU**-M, **PSU**-M_2-4O, **PSU**-M_2-2O, **PSU**-M_2-3O, **PSU**-M_3 and **PSU**-M_4.

The labelled ladders for all new pyrene dyes were analysed by PAGE and separated into individual fluorescent zones (Figure 11). The runs with **APTS** (q=-3, SO_3H) and **PCN** (q=-3, SO_2NHCN) are shown in lanes 1 and 2, and the runs with phosphorylated six-charged **PSN**, **PSU** and **PAZ** dyes (q=-6, $OPO(OH)_2$) – in lanes 3-5. The conjugates migrate according to their charge-to-mass ratio, or, more strictly, the charge-to-hydrodynamic ratio.[3] The bands of individual saccharides were well resolved and detectable up to G_{12}. **APTS** and **PCN** in lanes 1 and 2 have the same net electrical charge (q=-3), but due to slightly higher molecular mass, **PCN** conjugates move slower. **PCN** dye is fully ionised at pH 8.3. Due to much higher brightness, **PCN** dye is perspective as an alternative or complementary reagent (in the sense of separation performance and selectivity towards isomeric carbohydrates) to **APTS**.

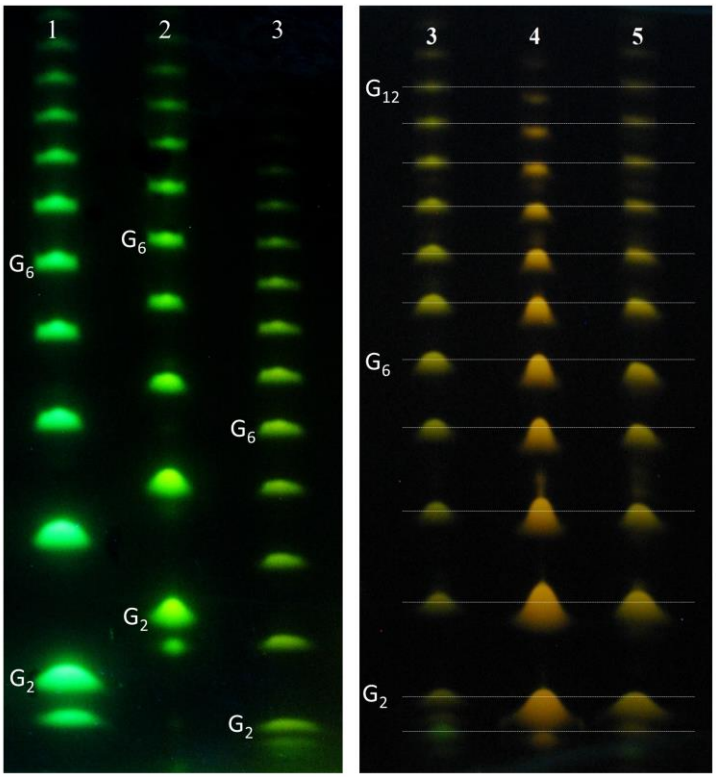

Figure 11. PAGE plates (migration from “north” to “south”, pH 8.3) show maltodextrin ladder labelled with negatively charged aminopyrenes from Scheme 8. Left plate: triple-charged **APTS** and **PCN** (lanes 1 and 2, respectively) and **PSN** (lane 3) having 6 charges. Right plate: triple-phosphorylated pyrenes **PSN**, **PAZ** and **PSU** (lanes 3, 4, and 5 respectively). Weak horizontal lines enable to compare the positions of spots.

Conjugates of all phosphorylated dyes (Figure 11, lanes 3-5) with 6 negative charges move faster than **APTS** and **PCN** derivatives having three negative charges (lanes 1, 2). The *m/z* ratio of **PAZ** (144) is not lower than *m/z* values of **PSN** (145) and **PSU** (137), but **PAZ** (lane 4) shows higher mobility in conjugates. It is visible for heavier oligomers (G_8–G_{12}) on the right panel of Figure 13. Due to the gel’s sieving effect, electrophoretic mobility of a labelled sugar depends on the size (shape) of the molecule.

The electrophoretic mobility is inversely proportional to hydrodynamic radius.[3] Sulfonamides **PSN** and **PAZ** differ only by 6 hydrogen atoms, but the azetidine-containing molecule of **PAZ** has 3 cycles and, therefore, enjoys much less “conformational freedom” than the linear sulfonamide **PSN**. Due to the presence of sulfonyl groups in the **PAZ** (into which the lone

pair on nitrogen may delocalise), the inversion barrier of nitrogen in *N*-sulfonyl azetidines is possibly lower than 30 kJ/mol observed for azetidine itself or *N*-alkylated derivatives. This became visible in the sum of the bond angles centred at the nitrogen atom (334° for *N*-methylsulfonylazetidine), which is higher than the value for azetidine (320°).[33] To evaluate that, ^{1}H-NMR spectra of 3-hydroxy-*N*-(3-/4-fluorophenyl)sulfonyl azetidines **9** (Scheme 7) were measured at +25°… -100 °C in diethylether-d_{10}, and observed no broadening or signal splitting, which indicates the free inversion of the nitrogen "pyramide" in 3-hydroxy-*N*-arylazetidines and the absence of *syn-anti* isomerism in **PAZ**.

1.4.3 Desialylation studies

Sialic acids are acidic sugars that are often found at the end of glycan chains in glycoproteins, glycolipids, and gangliosides. Sialic acids play important roles in various biological processes, such as cell-cell interactions, neural transmission in synaptogenesis, and immune responses. Due to its exposed location, sialic acids often participate as recognition sites in biological processes including cancerogenesis.[34] As linkage isomers can be responsible for different types of cancer, it is important to analyse the sialic acid linkage type and possible desialylation degree (the loss of sialic acid residue;[29,34] Scheme 9) in the course of labelling.

Desialylation level in the reaction with **APTS** is reported to be 2-15% depending on the reaction conditions.[29a,b] Desialylation study was performed for **PCN** dye. Two commercially available 3'- and 6'-sialyllactoses as well as lactose were labelled with **PCN**. The conjugate with lactose (**PCN-L**) was required to calculate desialylation level.

It was found that **PCN**-labelled 3'- and 6'-sialyllactoses as well as lactose are separable by HPLC. The conjugates were prepared, and isolated. The mixture containing equal amounts of **PCN-L**, **PCN-3'SL** and **PCN-6'SL** was prepared as a reference standard. Then the reductive amination of 3'SL and 6'SL with 1.5 eq. of the dye was conducted at "classic" conditions ($NaBH_3CN$/citric acid in THF) and "modern" (2-picoline-borane complex/malonic acid in DMSO), and the reaction mixtures analysed by HPLC. The conversion degrees and desialylation level were determined by measuring peak areas of the residual dye and product(s) at isosbestic point (469 nm). The results are given in Table 4.

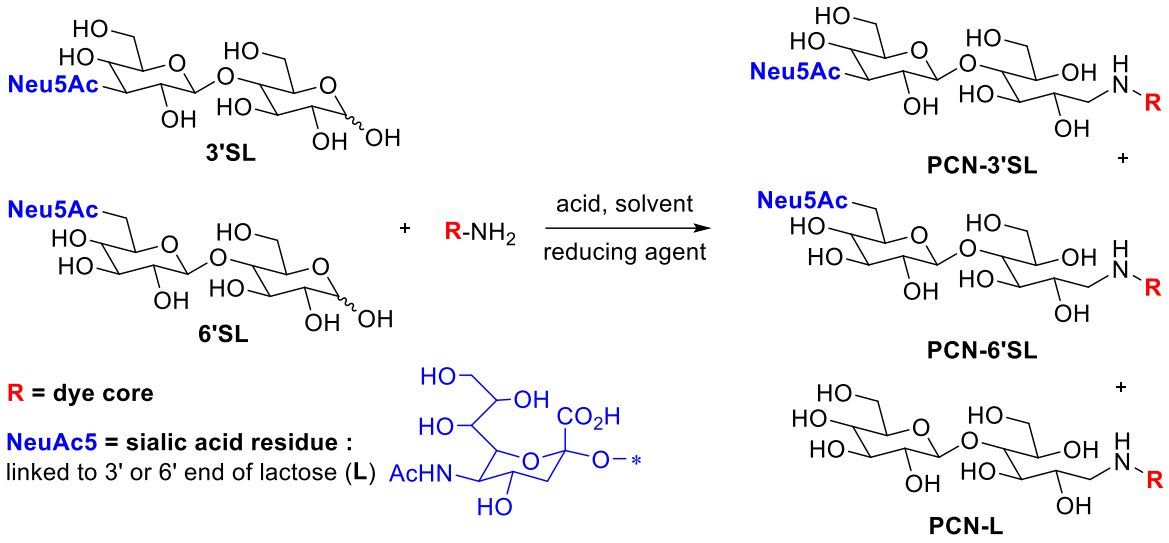

Scheme 9. Reductive amination of 3' (**3'SL**) and 6' -sialyllactoses (**6'SL**) with **PCN**-dye.

To determine the separation profile of **PCN** dye, the labelled isomeric sialic acids were analysed by PAGE and their mobilities were compared with those of the corresponding **APTS** derivatives (Figure 12).

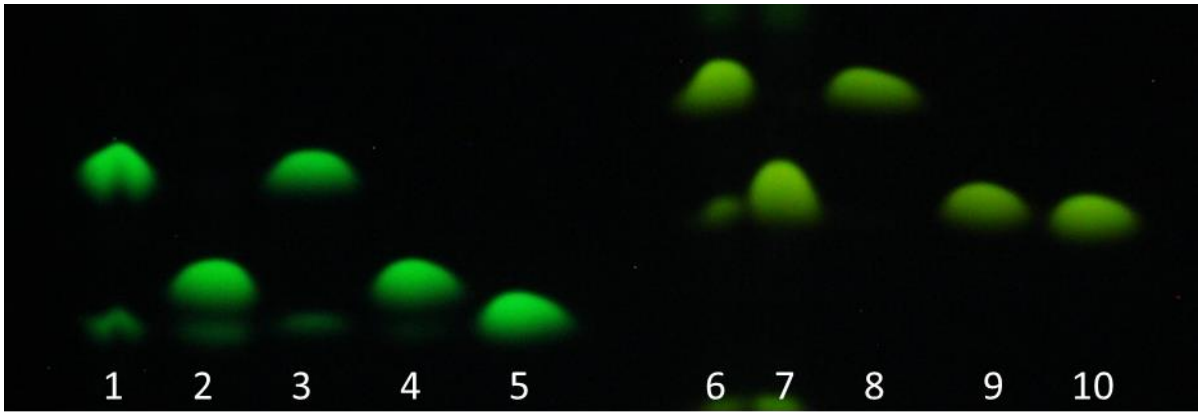

Figure 12. The PAGE plate (migration from “north” to “south”, pH 8.3) of **APTS** and **PCN** labelled isomeric sialyllactoses. Lane 1: **APTS**-3'SL, the reaction mixture; Lane 2: **APTS**-6'SL, the reaction mixture; Lane 3: **APTS**-3'SL, isolated conjugate; Lane 4: **APTS**-6'SL, isolated conjugate; Lane 5: **APTS**-L, isolated conjugate (side product); Lane 6: **PCN**-3'SL, the reaction mixture; Lane 7: **PCN**-6'SL, the reaction mixture; Lane 8: **PCN**-3'SL, isolated conjugate; Lane 9: **PCN**-6'SL, isolated conjugate; Lane 10: **PCN**-L, isolated conjugate (side product).

Table 4. Desialylation degree (%) in the reductive amination of isomeric sialyllactoses.

Isomer\conditions	"classic", desialylation %	"modern", desialylation %
3'SL	5	6
6'SL	6	3

It is clear that both dyes (**APTS** and **PCN**) easily resolve 3'- and 6'-isomers of sialyllactoses (**APTS**: lanes 3, 4; **PCN**: lanes 8, 9 of Figure 12). Nevertheless, there is a slight difference in the separation profile: the **PCN**-conjugates move slower compared to those of **APTS**. While the level of desialylation in reductive amination with the new **PCN** dye is slightly lower than that with **APTS**, desialylation still takes place. To entirely prevent this side reaction, further investigations of the labelling conditions are required.

1.4.4 Capillary-Gel Electrophoresis with Laser Induced Fluorescence detection

Commercial DNA sequencers represent standard devises for glycan analysis. The DNA analysers are equipped with LIF detectors and excitation sources. These devises offer the possibility of multicolour detection. There are 5 colour channels – called (conditionally) "blue", "green", "yellow", "orange", and "red" – reserved for four nucleotides and a reference (DNA ladder labelled with a red-emitting dye). We used the ABI 3730 XL DNA Analyser platform having a CE-LIF unit and a laser diode emitting 505 nm light. Figure 13 illustrates the CE-LIF results obtained with glucose oligomers labelled with **APTS** (~1 pmol), **PCN** (~1 pmol) and **PSU** (~0.1 pmol) dyes. The **PCN** dye provides *ca*. four-fold better signal level than **APTS**, but somewhat higher cross-talk with the second "green" detection window. If the dye is used alone in the application (this is now the case with **APTS**), the cross-talk with any detection windows, except the red one, may be tolerated. The **PSU** dye in the green detection channel provides the similar signal level as **PCN** in the green channel. However, nearly half of the emission of **PSU** "leaks" into the yellow slot.

With the colour settings standard for the DNA analyser, the **PSU** dye has a non-zero cross-talk with the "blue" detection window (positive or negative signal; it depends on concentration of **PSU** conjugates). The recalibration of the colour settings of the DNA analyser is possible by using a new set of fluorescent dye conjugates and creating a new matrix file. For the **PSU** dye, that would enable to collect more light, which is now distributed between green and yellow detectors, and

probably fully avoid the cross-talk with the **APTS** detection window. If so, **PSU** could be used not only as brighter or "rapid" (swifter moving) alternatives to **APTS** (which is now possible), but also for creating new internal standards for glycan analysis based on natural carbohydrates and compatible with **APTS** in one run.

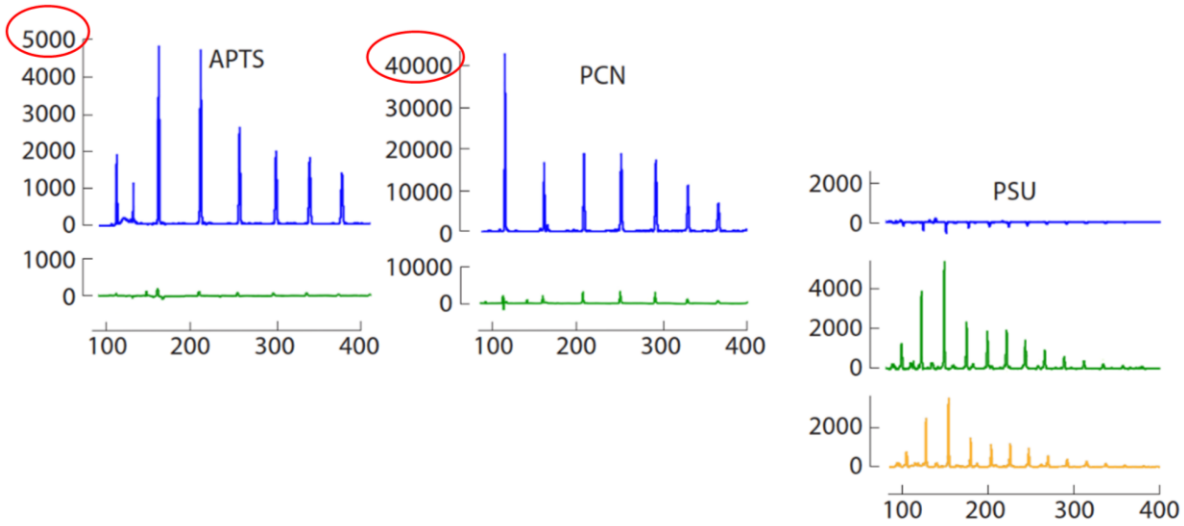

Figure 13. CE-LIF traces of maltodextrin ladder labelled with **APTS** (1 pmol), **PCN** (1 pmol) and **PSU** (0.1 pmol) dyes; for PAGE electrophoresis, see Figure 13. X-axis: retention time (a.u.), y-axis – emission intensity (a.u.). Blue, green and yellow detection channels are shown with corresponding colours. The averaged relative peak widths at half maxima are 1.42, 1.35 and 1.00 for **APTS**, **PCN** and **PSU** conjugates, respectively.

1.5 Conclusion

Sulfonic acid residues in **APTS** were successfully transformed into various sulfonamides. The presence of the electron-donating amino group at position 1 and three electron-acceptor groups at "active" positions (3, 6, and 8) of the pyrene system led to the emission of green (**PCN**) or yellow (**PSN**, **PAZ**) light for the "push-pull" dyes. The electronic effects (Hammett σ values) of *N*-(cyano)sulfonamide or 3-hydroxyazetidine-*N*-sulfonyl residues were evaluated, and these groups were identified as strong electron-acceptors and auxochromes.

The new sulfonamide dyes **PCN**, **PSN**, and **PAZ**, as well as sulfone **PSU**, were conjugated with various reducing sugars and compared with corresponding **APTS** analogues as references.

The “water-free” protocol for the reductive amination of sugars has been developed. The new dyes offer a different selectivity profile for isomeric carbohydrates. The separation profile revealed for **PSU** demonstrated the successful separation of positional (linkage) isomers of mannobioses and sialyllactoses. Desialylation studies performed for **PCN** dye showed a relatively low level of desialylation (3-6%).

The conjugates of **PSN**, **PAZ**, and **PSU** dyes exhibit absorption and emission maxima at approximately 500 nm and 560 nm, respectively, and carry six negative charges (pH ≥ 8) with low *m/z* ratios. Due to their higher absorption between 488–506 nm, the conjugates of **PSN**, **PAZ**, and **PSU** dyes are about 3 times brighter than **APTS** derivatives, with excitation performed using 488 nm or 505 nm light. The phosphate groups in dyes **PSN**, **PAZ**, and **PSU** are hydrolytically stable within a broad pH range: from 3 (under reductive amination conditions) to 8.3 (during electrophoresis) and beyond. These groups contribute to low *m/z* ratios and high mobilities in the electric field. The *N*-(cyano)sulfonamide group is fully ionised at pH 8.3, providing 3 negative charges in **PCN** dye. The absorption maxima of **PCN** conjugates nicely match the emission lines (488 nm) of the Ar laser used in DNA analysers. Higher absorption at 488 nm improves the brightness of the new fluorescent tags by a factor of 3-4 (compared with **APTS**).

Conjugates of **APTS**, **PCN**, and **PSU** dyes were analysed using CE-LIF in the DNA sequencer. The average peak width at half maximum is approximately 30% smaller for **PSU**-conjugates compared to **APTS**- or **PCN**-labelled sugars, which is advantageous for analytical purposes. **PCN** derivatives were detected in the blue channel (similar to **APTS**) with a signal intensity around 4 times higher than that of **APTS** derivatives at equal quantities. There was low cross-talk with the green detection window. The signal of **PSU** derivatives was evenly distributed between the green and yellow detectors. The envisaged implementation of a new colour calibration of DNA sequencer is expected to further enhance signal intensity, potentially doubling the detection efficiency for **PSU**.

To end up, the new dyes are expected to complement **APTS** in sugar analysis thereby accelerating progress in glycomics.

1.6 References to Chapter 1

1. a) M. Dalziel, M. Crispin, C. N. Scanlan, N. Zitzmann, R. A. Dwek, *Science* **2014**, *343*, 1235681-1–1235681-8; b) S. S. Pinho, C. A. Reis, *Nat. Rev. Cancer* **2015**, *15 (9)*, 540–555; c) A. Varki, *Glycobiology*, **2017**, *27*, 3–49.

2. K. Villadsen, M. C. Martos-Maldonado, K. J. Jensen, M. B. Thygesen, *ChemBioChem* **2017**, *18*, 574-612.

3. A. Guttman, L. Hajba, *Capillary Gel Electrophoresis and Related Microseparation Techniques*, Elsevier B.V., **2022**, pp. 298-324.

4. L. R. Ruhaak, G. Xu, Q. Li, E. Goonatilleke, C. B. Lebrilla, *Chem. Rev*. **2018**, *118*, 7886-7930

5. T. Ikegami, *J. Sep. Sci*. **2019**, *42*, 130–213.

6. a) N. Volpi, *Capillary electrophoresis of carbohydrates*. *From monosaccharides to complex polysaccharides*, Humana Press, N. Y. **2011**, pp. 1-51; b) V. Mantovani, F. Galeotti, F. Maccari, N. Volpi, *Electrophoresis* **2018**, *39*, 179-189.

7. G. Lu, C. L. Crihfield, S. Gattu, L. M. Veltri, L. A. Holland, *Chem. Rev*. **2018**, *118*, 7867-7885

8. **APTS** in CGE LIF: a) R. A. Evangelista, M.-S. Liu, F.-T. A. Chen, *Anal. Chem.* **1995**, *67*, 13, 2239-2245; b) F.-T. A. Chen, R. A. Evangelista, *Electrophoresis* **1998**, *19*, 2639-2644; c) F.-T. A. Chen, T. S. Dobashi, R. A. Evangelista, *Glycobiology* **1998**, *8*, 11, 1045-1052; d) R. W. Sabnis in *Handbook of Fluorescent Dyes and Probes*, John Wiley & Sons Inc. **2015**, chapter 22, p. 63.

9. L. R. Ruhaak, R. Hennig, C. Huhn, M. Borowiak, R. J. E. M. Dolhain, A. M. Deelder, E. Rapp, M. Wuhrer, *J. Proteome Res.* **2010**, *9*, 6655-6664.

10. T. Kawai, N. Ota, A. Imasato, Y. Shirasaki, K. Otsuka, Y. Tanaka, *J. Chromatogr. A* **2018**, *1565*, 138-144.

11. H. Suzuki, O. Müller, A. Guttman, B. Karger, *Anal. Chem.* **1997**, *69*, 4554-4559.

12. K. Kundu, S. F. Knight, N. Willett, S. Lee, W. R. Taylor, N. Murthy, *Angew. Chem. Int. Ed*. **2009**, *48*, 299-303.

13. Carlini, A. Benke, L. Reymond, G. Lukinavičius, S. Manley, *ChemPhysChem* **2014**, *15*, 750-755.

14. H.-T. Feng, P. Li, G. Rui, J. Stray, S. Khan, S.-M. Chen, S. F. Y. Li, *Electrophoresis* **2017**, *38*, 1788-1799.

15. E. A. Savicheva, G. Y. Mitronova, L. Thomas, M. J. Böhm, J. Seikowski, V. N. Belov, S. W. Hell, *Angew. Chem. Int. Ed*. **2020**, *59*, 5505-5509.
16. J. Krenkova, F. Dusa, R. Cmelik, *Electrophoresis* **2020**, *41*, 684-690.
17. J. Krenkova, M. Liskova, R. Cmelik, G. Vigh, F. Foret, *Anal. Chim. Acta* **2020**, *1095*, 226-232.
18. C. Hansch, A. Leo, R. W. Taft, *Chem. Rev.* **1991**, *91*, 165-195.
19. H. Zollinger, W. Büchler, C. Wittwer, C. *Helv. Chim. Acta.* **1953**, *36*, 1711-1722; larger values for SO_3^- (σ_m = 0.30 and σ_p = 0.35) are mentioned in ref. 18, but these are solely based on a private communication of Viktor Palm.
20. a) E. K. Hill, A. J. de Mello, H. Birrell, J. Charlwood, P. Camilleri, *J. Chem. Soc., Perkin Trans. 2*. **1998**, 2337-2341; b) M. A. Fomin, J. Seikowski, V. N. Belov, S. W. Hell, *Anal. Chem*. **2020**, *92*, 5329-5336.
21. ABI PRISM®, 310 Genetic Analyser**.** User's Manual, **2010** Applied Biosystems, pp. 2.20-
22. C. T. Supuran, A. Scozzafava, F. Briganti, *J. Enzyme Inhib.* **1999**, *14*, 289-306.
23. F. Wold, C. E. Ballou, *J. Biol. Chem.* **1957**, *227*, 301–312.
24. E. A. Savicheva, J. Seikowski, J. I. Kast, C. R. Grünig, V. N. Belov, S. W. Hell, *Angew. Chem. Int. Ed*. **2021**, *60*, 3720–3726.
25. a) R. W. Taft, E. Price, I. R. Fox, I. C. Lewis, K. K. Andersen, G. T. Davis, *J. Am. Chem. Soc.* **1963**, *85*, 3146-3156; b) R. W. Taft, *J. Phys. Chem*. **1960**, *64*, 12, 1805-1815; c) R. W. Taft, E. Price, I. R. Fox, I. C. Lewis, K. K. Andersen, G. T. Davis, *J. Am. Chem. Soc.* **1963**, *85*, 709-724.
26. a) L. Cisse, A. Djande, M. Capo-Chichi, A. Khonté, J.-P. Bakhoum, F. Delattre, J. Yoda, A. Saba, A. Tine, J.-J. Aaron, *J. Phys. Org, Chem*. **2020**, *33*, e4014; b) A. Marchesi, S. Brenna, G. A. Ardizzoia, *Dyes Pigm*. **2019**, *161*, 457-463; c) E. Yamaguchi, F. Shibahara, T. Murai, *J. Org. Chem*. **2011**, *76*, 6146-6158.
27. C. Rouxel, C. Le Droumaguet, Y. Mac, S. Clift, O. Mongin, E. Magnier, M. Blanchard-Desce, *Chem. Eur. J*. **2012**, *18*, 12487-12497.
28. a) F. Bureš, *RSC Adv.* **2014**, *4*, 58826-58851; b) C. Pigot, G. Noirbent, D. Brunel, F. Dumur, *Eur. Polym. J*. **2020**, *133*, 109797.
29. a) A. Guttman, F.-T. A. Chen, R. A. Evangelista, N. Cooke, *Anal. Biochem.* **1996**, *233*, 234-242; b) R. A. Evangelista, F.-T. A. Chen, A. Guttman, *J. Chromatogr. A* **1996**, *745*, 273-280; c) R. A. Evangelista, A. Guttman, F.-T. A. Chen, *Electrophoresis* **1996**, *17*, 347-351.

30. B. Reider, M. Szigeti, A. Guttman, *Talanta* **2018**, *185*, 365-369.

31. Z. Szabo, A. Guttman, T. Rejtar, B. L. Karger, *Electrophoresis* **2010**, *31*, 1389-1395.

32. L. R. Ruhaak, E. Steenvoorden, C. A. M. Koeleman, A. M. Deelder, M. Wuhrer, *Proteomics* **2010**,*10*, 2330–2336.

33. O. P. Blahun, A. B. Rozhenko, E. Rusanov, S. Zhersh, A. A. Tolmachev, D. M. Volochnyuk, and O. O. Grygorenko, *J. Org. Chem.* **2020**, *85*, 5288-5299.

34. N. de Haan, S. Yang, J. Cipollo, M. Wuhrer, *Nat. Rev. Chem*. **2020**, *4*, 229-242.

Chapter 2.

Photoconvertible cyanine dyes

A paper was published in *ChemPhotoChem*:

Introduction of the functional amino group at the *meso* position of Cy3 and Cy5 dyes: synthesis, stability, spectra and photolysis of 4-amino-1-diazo-2-butanone derivatives, E. A. Savicheva, M. L. Bossi, V. N. Belov, S. W. Hell, *ChemPhotoChem* **2022**, e202200222. **doi.org/10.1002/cptc.202200222**

Contribution: Together with Dr. Vladimir N. Belov, I designed the study and was responsible for writing the manuscript. I performed all synthetic work and measurement of photophysical properties. The photolysis was performed by Dr. Mariano L. Bossi.

2.1 Introduction

The ability to induce transitions between non-fluorescent (dark) and fluorescent (bright) molecular states forms the basis of superresolution microscopy.[1] In superresolution microscopy, the diffraction unlimited optical resolution enables to see fine details within biological specimen which remain unresolved in confocal microscopy. For image acquisition, fluorescent markers are brought to a bright state for registration, while adjacent fluorophores remain in a dark state. This selective activation of individual fluorophores enables the precise localisation and imaging of subcellular structures. The transitions into the bright state may occur spontaneously (blinking), or can be induced photochemically.[1-6] Modern superresolution microscopy techniques, such as MINSTED[2] (MINimum Stimulated Emission Depletion), MINFLUX[3] (MINimum FLUXes), PALM[4] (PhotoActivated Localisation Microscopy), and STORM[5] (Stochastic Optical Reconstruction Microscopy), rely on the use of photoactivatable and photoconvertible dyes and their ability to transition between dark and bright states.[6] Breaking the diffraction limit revolutionised imaging of cellular and subcellular structures by providing unprecedented clarity and detail.

Further progress in the development of fluorescent dyes for superresolution microscopy is based on the introduction of various photoactivatable groups to the dyes of different types.[6] Cyanine dyes are known for their strong emission, which make them excellent for the fluorescent labelling and imaging applications.[7] However, photoactivatable cyanines remain unknown. As candidates, we considered cyanines with a 4-amino-1-diazo-2-butanone[8] fragment ($H_2N(CH_2)_2COCH=N_2$) attached to the polymethine chain via the amino group (Scheme 10). Upon irradiation with UV light, diazoketones (DAK) eliminate nitrogen, and the intermediate acylcarbenes undergo a Wolff rearrangement.[9] The photoconversion process induced by diazoketone fragments can modulate the fluorescence properties of the dye, such as its emission wavelength, intensity, or fluorescence lifetime.

If the diazoketone group is separated from the amino group by two methylene residues, the intermediate ketene is expected to spontaneously cyclise to 5-membered pyrrolidone (Scheme 10). This kind of intramolecular amidation (unrelated to the Wolff rearrangement) was reported for a Cy7 dye.[10] It was accompanied by a red shift (+174 nm) and a significant increase in emission at 807 nm. The symmetrical amino-modified Cy7 dyes were obtained from the corresponding

halogenated derivatives (Cl, Br) by nucleophilic substitution with amines.[11] However, the emission of Cy7 dyes in the IR region does not fit the common detection window of current nanoscopy techniques (650 – 750 nm).[1]

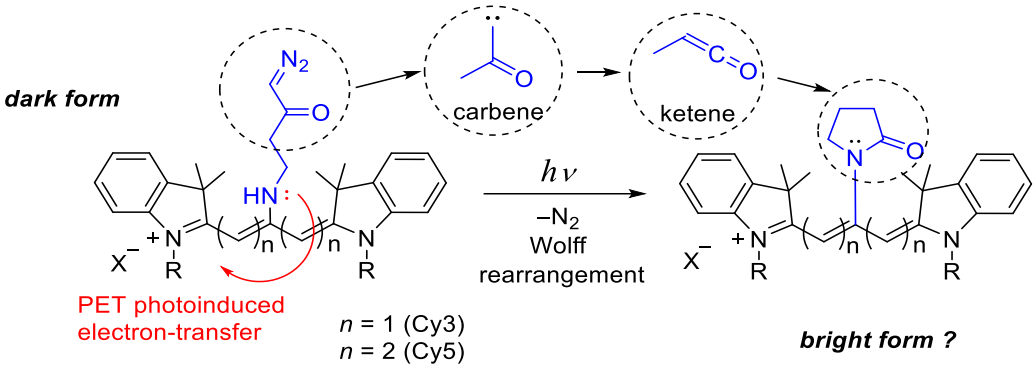

Scheme 10. The concept of photoconversion applied to Cy3 and Cy5 dyes.

Therefore, as primary synthetic goals, we have chosen amino-modified Cy3 and Cy5 dyes (Scheme 10) with estimated emission maxima at 550 nm and 660 nm, respectively. The substituent at the *meso* position of the chromophore may reduce photobleaching and increase the fluorescence quantum yield.[12] Thus, the introduction of the (ω-aminoalkyl)diazoketone moiety and amino group alone to the *meso* position of the chromophore was interesting and challenging. The same as for amino-substituted Cy7 dyes[10], we expected initial compounds in Scheme 10 to be non-fluorescent due to photoinduced electron transfer (PET).[7,13]

2.1.1 Wolff rearrangement

The transformation of α-diazo ketones into ketenes and the products of their reactions with nucleophiles was first reported by Ludwig Wolff in 1902.[14] The Wolf rearrangement produces ketene as an intermediate, which can undergo nucleophilic attack (by water, alcohols, and amines), and give carboxylic acid derivatives (Scheme 11), or undergo other reactions such as cycloaddition. The Wolff rearrangement typically occurs under photolysis conditions, although other triggers, such as catalysis by transition metals or thermolysis, have also been reported.[9]

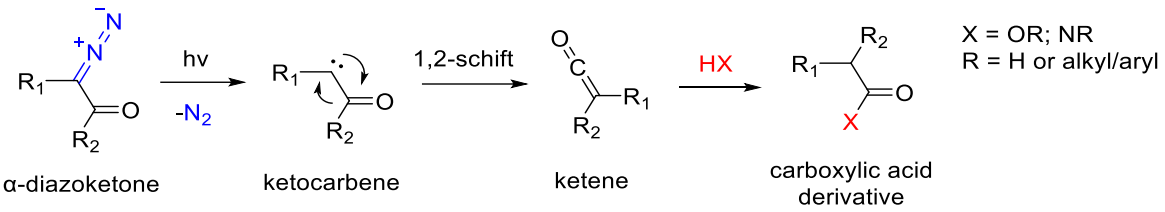

Scheme 11. General mechanism of the Wolff rearrangement.

The most common application involves trapping the ketene intermediate by nucleophiles to form carboxylic acid derivatives. This transformation is known as Arndt-Eistert homologation, where a carboxylic acid can be extended by a methylene unit.[15] Another common use is based on ring-contraction: if the α-diazo ketone is cyclic, the Wolff rearrangement leads to a product with a smaller ring.[9]

In addition to numerous applications in organic synthesis, the Wolff rearrangement has also been used in the photoactivation of caged dyes.[6c,d, 16a-c] Caged dyes exist in a non-fluorescent and stable form and can be converted into a fluorescent form through irradiation with near-UV light followed by a chemical reaction. The use of diazoketone as a photocaging group for fluorescent dyes was first reported in 2010.[16a] One of the most significant features is that the photochemical cleavage of diazoketone generates only molecular nitrogen as a byproduct. This simple and compact photocaging group was incorporated into a rhodamine dye (compound **BNN**, Scheme 12). The so-called rhodamines NN[16a] rapidly undergo uncaging under irradiation with light (λ<420 nm), resulting in the formation of highly fluorescent rhodamine derivatives.

When UV light was used to irradiate rhodamine **BNN**, two products – “bright” and “dark” were observed (Scheme 12). The major product resulting from the Wolff rearrangement was the fluorescent rhodamine derivative ("bright"). The Wolff rearrangement of carbene **C** to ketene **K** (with the migration of the bond **b**, or 1,2 shift) leads to the ring-contraction. Reaction of the unstable ketene **K** with MeOH leads to elongation of the carbon chain, introducing an additional methylene group between the *ortho*-substituted phenyl residue and CO_2Me group. A minor "dark" product was also isolated. Its formation may be explained by migration of the bond “**a**” in the intermediate carbene **C**.[16a]

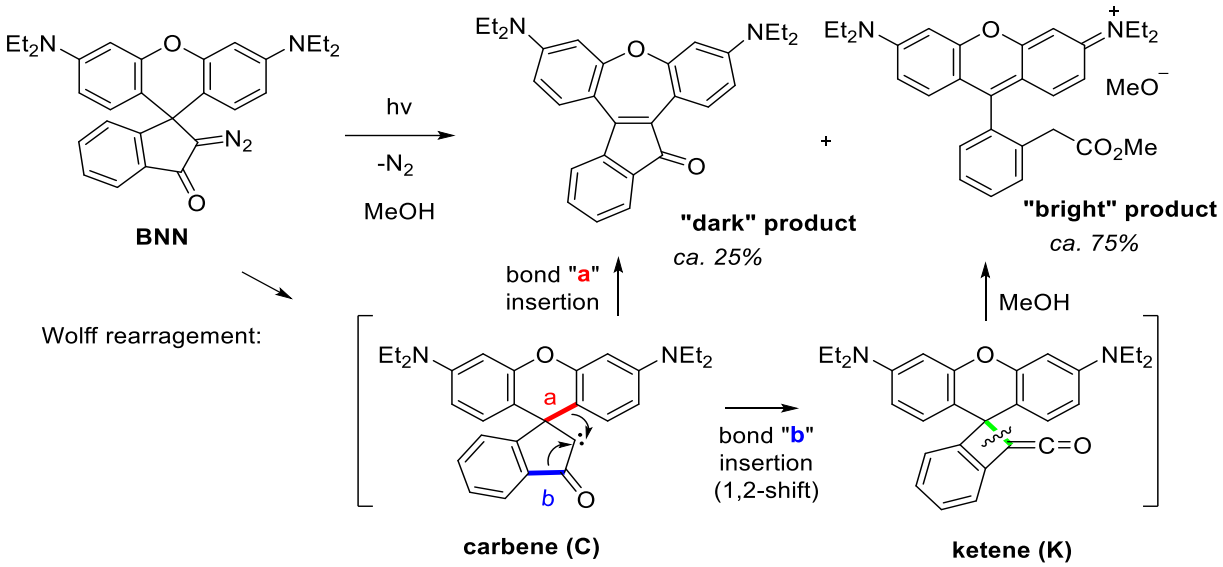

Scheme 12. Photolysis of the caged rhodamine **BNN** in methanol using UV light (λ 320 nm). This example is taken from ref. [16a].

The successful application of these newly developed caged fluorophores in superresolution optical microscopy[16d] confirmed the suitability and potential of diazoketone as a caging group for the further design of photoconvertible fluorescent dyes.

2.1.2 Cyanine dyes

Cyanines are fluorophores based on a polymethine chain, representing a series of conjugated carbon-carbon double bonds (alternating single and double bonds) incorporated between two nitrogens. The terminal nitrogen-containing groups and the polymethine chain bear one positive charge, so that one nitrogen atom (uncharged) acts as a donor, while another nitrogen represents an acceptor. The simplest type of polymethine dyes is termed streptocyanines; they lack unsaturated heterocycles (Figure 14). A (formal) ring closure within the polymethine chain, creating aza-heterocycles at each end, leads to the classic cyanine dyes (**Cy**). If one end terminates with a nitrogen atom that does not form an unsaturated heterocycle, it is referred to as hemicyanine. Cyanine dyes are also classified by the number of presented methine groups: monomethine cyanine (one methine unit), trimethine cyanine or carbocyanines (three methine groups, Cy3), pentamethine cyanine (five methine groups, Cy5) and heptamethinecyanine dyes (seven methine groups, Cy7) (Figure 14). Extension of the polymethine chain exhibits a red shift of absorption.[7]

As important analogues of cyanines, it is worth mentioning squarylium dyes (**Sq**).[17] They contain a negatively charged squaraine moiety in the center of the conjugated double bond system (Figure 14). The **Sq** dyes exhibit a zwitterionic structure and are generally considered more polar molecules compared to cationic cyanines.

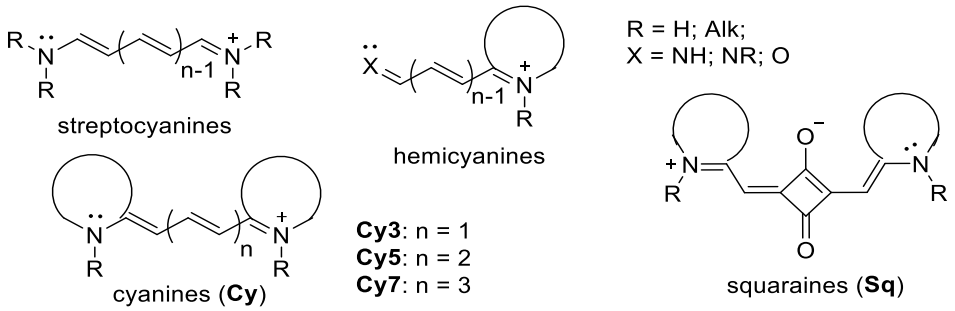

Figure 14. Classification of cyanine dyes.

The name "cyanine" indicates their characteristic blue-green colour. Absorption in the visible region of the spectrum is determined by the presence of the delocalised π-electron system and depends on the length of the polymethine chain.[7] The polymethine chain forms a fully conjugated structure, with a positive charge mostly located on nitrogen atoms. The charge delocalisation between two nitrogen atoms can be represented by two resonance structures (Scheme 13). This conjugation imparts unique optical properties to cyanines. Cyanine dyes feature very high molar extinction coefficients, and satisfactory fluorescence efficiencies which makes them bright dyes suitable for a variety of applications, including fluorescence microscopy and imaging.[7] Furthermore, the optical properties of cyanine dyes can be tuned, as their chemistry enables to perform various structural modifications influencing the photophysical properties.

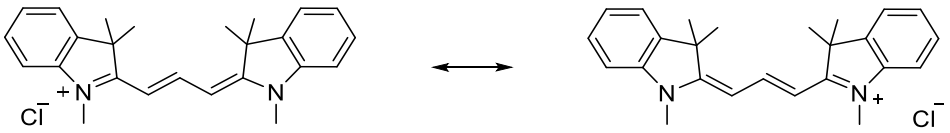

Scheme 13. Main resonance structures of Cy3 dye involve charge delocalisation between two nitrogens.

2.1.3 Design and synthesis of photoconvertible cyanine dyes

Synthesis of unsubstituted cyanines usually involves the condensation of cationic heterocyclic compounds containing an activated methylene group with *ortho* esters or formamidinium salts[18] (to obtain Cy3 dyes), or derivatives of malondialdehydes[19] (to obtain Cy5). The synthesis of cyanines having an amino group at the *meso* position of the polymethine chain might be achieved in the course of nucleophilic substitution of the halogen atom by functionalised amines. This reaction was reported for Cy7 dyes.[11] The proposed synthesis strategy for Cy3 and Cy5 is shown in Schemes 14, 15; the synthesis of **DAK** reagent is shown in Scheme 16.

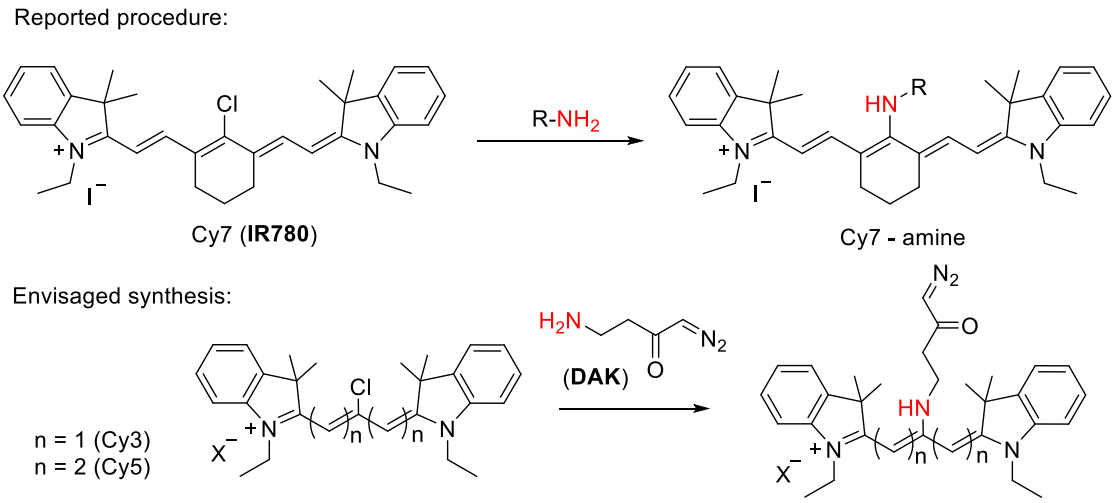

Scheme 14. Nucleophilic substitution in *meso* chloro-substituted cyanine dyes.

The alternative synthesis of *meso* amino-substituted Cy3 dyes is based on the condensation of isocyanates or phosgene (or its solid substitute triphosgene[20]) with methylene bases (Fischer base, Scheme 15).[21-23] One equivalent of phosgene reacts with two equivalents of Fischer base to give an unsaturated ketone.[22-23] It was mentioned that Cy3-ketone and $POCl_3$ gave Cy3-enyne – an acetylenic dye, which undergoes a nucleophilic addition of amines to the conjugated triple bond to yield Cy3-NHR (R = $(CH_2)_3Si(OEt)_3$, Scheme 15). We expected, that the addition of amines to the electron-poor conjugated system of Cy3-enyne proceeds under mild conditions and gives symmetric *meso* amino-substituted Cy3-NHR (R = $(CH_2)_2COCHN_2$, Scheme 15).

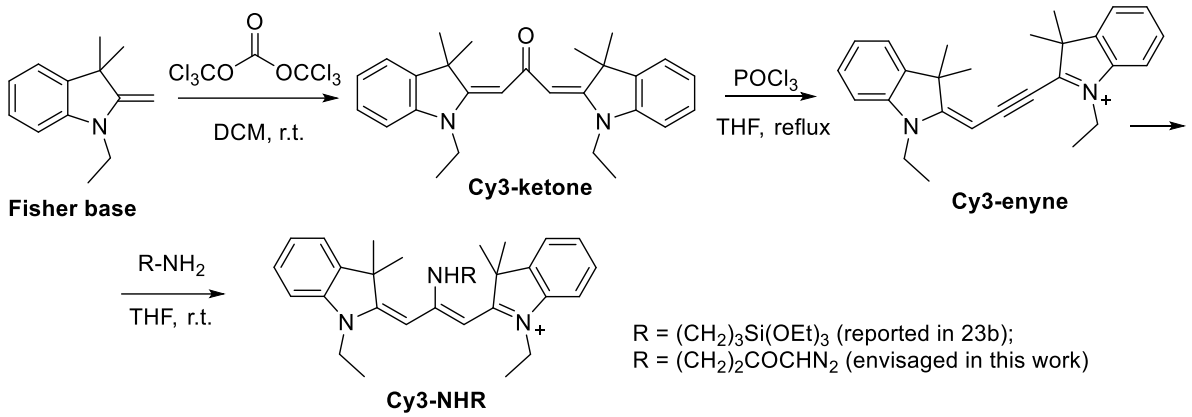

Scheme 15. Reported[23b] (R = $(CH_2)_3Si(OEt)_3$) and envisaged (R = $(CH_2)_2COCHN_2$) synthesis of *meso* amino-substituted Cy3 dyes.

As a final substance, it was necessary to prepare the compound that incorporates both diazoketone and amino groups separated by CH_2CH_2 linker. Diazoketones can be synthesised from diazomethane and acyl chlorides or mixed anhydrides.[8] The envisaged synthesis of the reagent **DAK** from commercially available β-alanine is shown in Scheme 16.

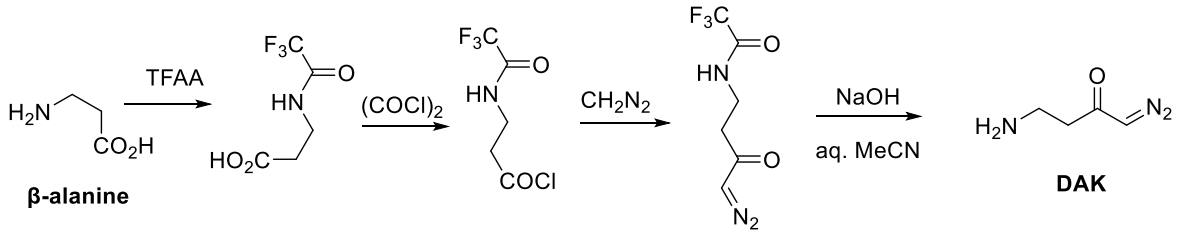

Scheme 16. Preparation of 4-amino-1-diazobutan-2-one[8] (**DAK**).

2.2 Trimethinecyanines (Cy3)

2.2.1 Synthesis of the *meso* amino-substituted Cy3

Indeed, the most straightforward route to the cyanine dyes with an amino group at the *meso* position is based on the nucleophilic substitution of the halogen atom. This reaction is widely used for Cy7 dyes (Scheme 14).[11] We attempted to apply this method to the Cy3 dyes. The first challenge included the preparation of the *meso* halogenated Cy3, which are unknown. The synthesis of unsubstituted Cy3 dye **12a** includes the condensation of a formamidinium salt (the source of a *meso* carbon) with 1,2,3,3-tetraalkyl-3*H*-indolium salts **10** (Scheme 17).[18] In order to obtain *meso* halogenated dye **12b**, the halogenated precursor *N,N'*-diphenylchloroformamidinium hydrochloride **11b**[24] was prepared and introduced in the reaction with indolium iodide **10**. Surprisingly, this reaction did not produce linear cyanine **12b** (Scheme 17), but gave several side products including hemicyanine **13**, unsubstituted cyanine **12a**, *meso N*-phenyl-substituted cyanine **12e**, and trinuclear cyanines **14** and **15**. We constated that this method is not applicable for the synthesis of *meso* substituted Cy3 dyes.

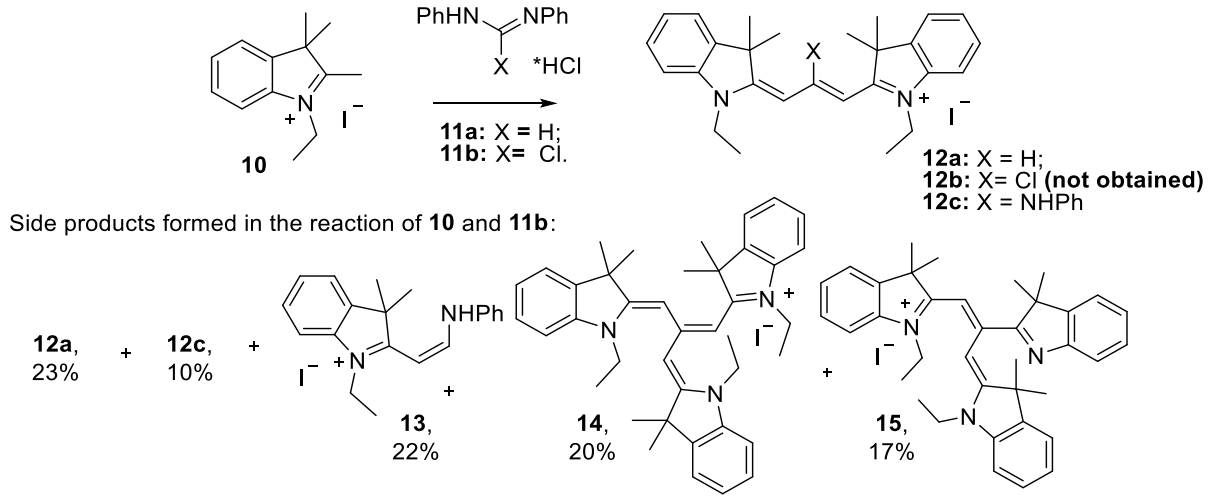

Scheme 17. Reaction of indolium iodide **10** with *N,N'*-diphenylformamidinium hydrochloride **11a**, or *N,N'*-diphenylchloroformamidinium hydrochloride **11b**. *Meso* chloro-substituted cyanine **12b** was not detected, side products (**12a, 12c, 13-15**) were isolated and characterised. Yields of isolated products are given.

Next, we tried to reproduce the synthesis reported in [23b] to obtain compound Cy3-enyne (Scheme 15) as it was expected to react with amines of interest. In the reaction between Fischer base **16** and triphosgene (Scheme 18), ketone **17** was detected in the reaction mixture as an intermediate (confirmed by NMR, LCMS), but its isolation failed. Surprisingly, the final product of this reaction was squaraine **18** even if an excess of the Fischer base was used. Among side products, unsubstituted cyanine **19** together with trinuclear cyanine **20** and the derivative of 1,3,5-cyclohexanetrione **21** were found.

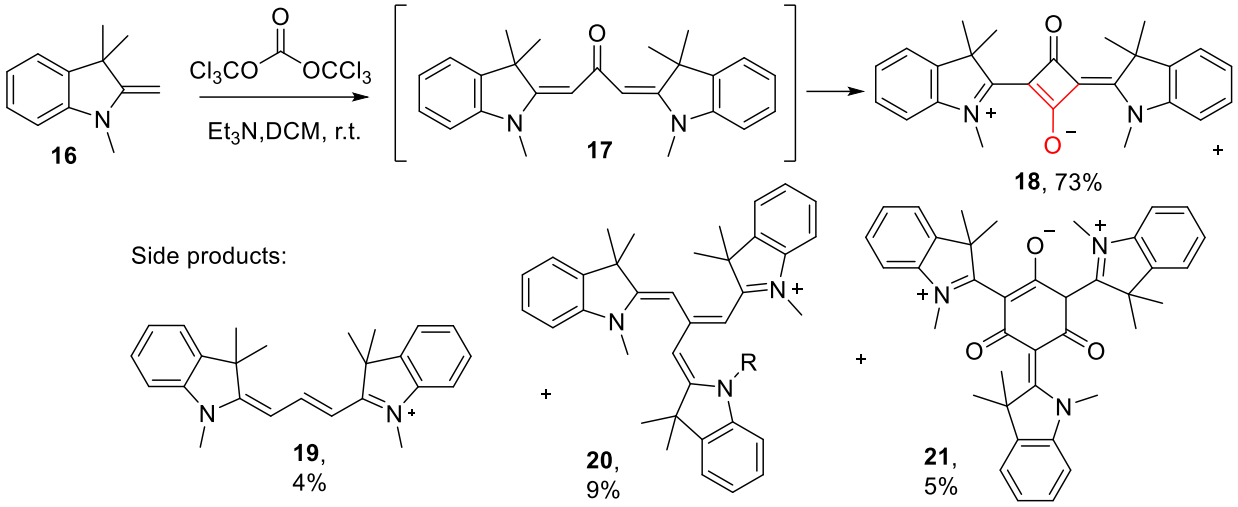

Scheme 18. Reaction of the Fischer base with triphosgene. Yields of isolated products are given.

The structure of compound **18** was confirmed by ^{1}H, ^{13}C NMR, and HRMS. This compound has never been reported in the literature, and its properties and reactivity were unknown. To check the reactivity, the squaraine dye **18** was introduced in the reaction with $POCl_3$ (Scheme 19). Surprisingly, it reacts with $POCl_3$ and gives the required acetylenic carbocyanine **23**. The plausible mechanism includes phosphorylation of the hydroxyl group followed by elimination of a good leaving group ($OPOCl_2^-$), and the loss of CO (intermediate **22** in Scheme 19). To check the reactivity of compound **23** with amines, we introduced compound **23** in the reaction with β-alanine *t*-butyl ester and obtained amino ester **24**. The target compound **25** was obtained by direct addition of freshly prepared 4-amino-1-diazobutan-2-one (**DAK**) to compound **23** (Scheme 19). The synthesis of **DAK** is given in Scheme 16.

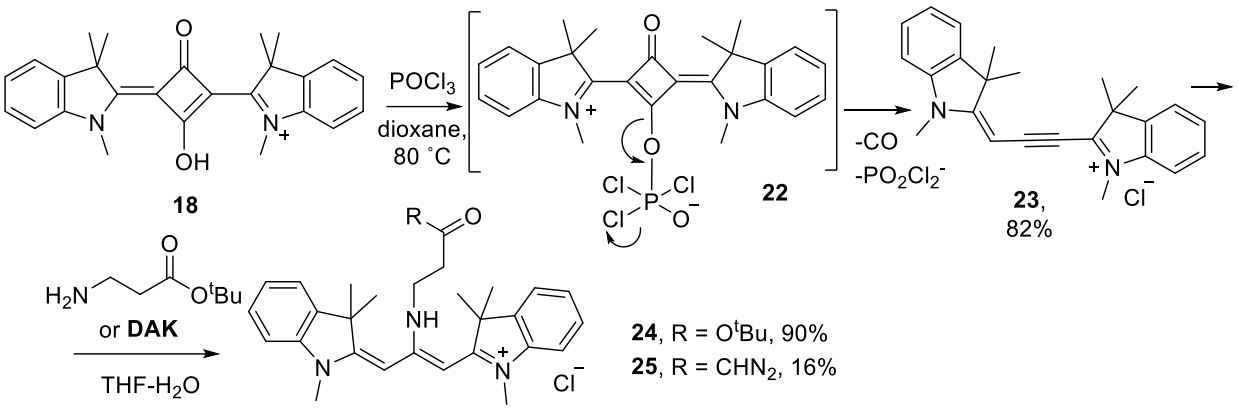

Scheme 19. Synthesis of the *meso* amino-substituted Cy3 derivatives including the target diazoketone **25**. Intermediate **22** was not isolated. Yields of isolated products are given.

2.2.2 Photolysis of Cy3 incorporating 4-amino-1-diazobutanone fragment

Photolysis of compound **25** was performed in methanol and in acetonitrile – aq. buffer 4:1 (Scheme 20, Figure 15). The reaction rates in both solvents were nearly the same. In methanol, a clean reaction to a more polar compound with λ_{abs} = 535 nm and *m/z* = 440 was observed. As expected, diazoketone dye **25** underwent a Wolff rearrangement under irradiation with UV light and formed pyrrolidone **26**. In acetonitrile – aq. buffer (4:1), along with minor amounts of pyrrolidone **26**, an even more polar compound with *m/z* = 458 and an absorption spectrum similar to the starting diazoketone dye **25** (λ_{abs} = 458 nm), was observed as the main photolysis product. We assign its structure to the amino acid **27**, formed from the intermediate ketene, which added water. The bathochromic shift in the transformation **25** – **26** was large (77 nm); however, both products (**26** and **27**) were non-fluorescent.

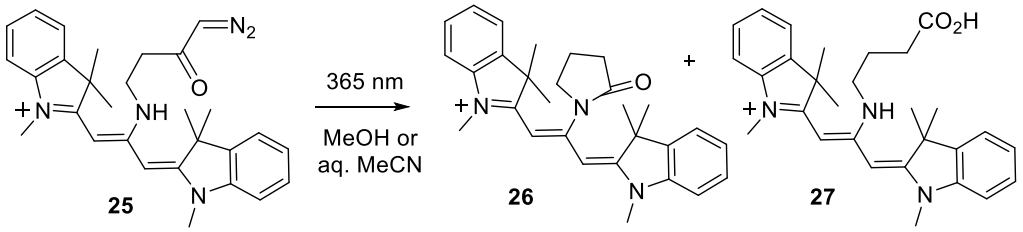

Scheme 20. Photolysis of trimethine cyanine **25**.

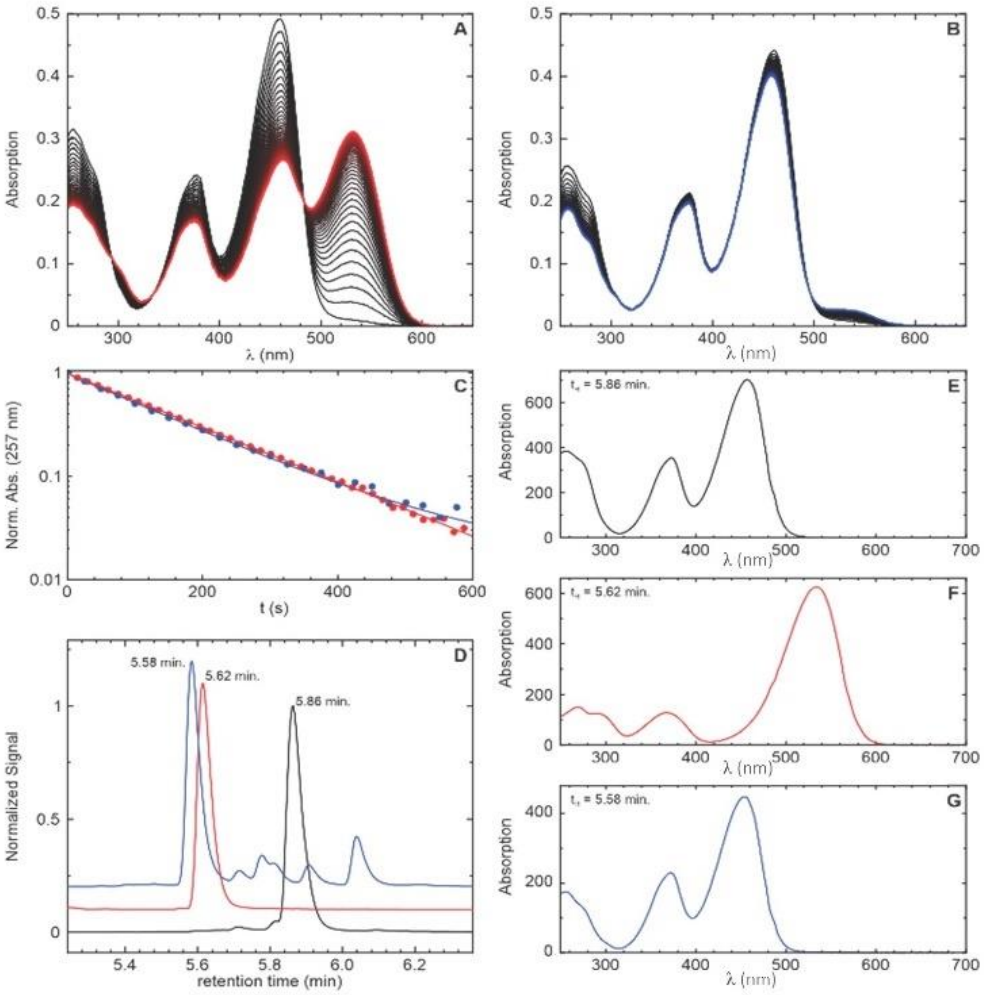

Figure 15. Photolysis of compound **25** in MeOH (A) and in an MeCN – aq. buffer (4:1) mixture (B). The initial spectra are plotted in black; the data for products **26** and **27** are in red and blue, respectively. (C) Normalised transients (absorption at 257 nm) upon consumption of **25**. (D) HPLC traces of **25** (black line), **26** (photolysis in MeOH; red line), and **27** (MeCN – aq. buffer (4:1); blue line). (E-F): absorption spectra of the main peaks with indicated retention times corresponding to each HPLC trace in (D).

2.2.3 Photophysical properties of Cy3 and their derivatives

The photophysical properties for all new compounds were measured and given in Table 5. The presence of (alkyl)amino group at the *meso* position of Cy3 (compounds **24**, **25**, **27**) showed a significant hypsochromic shift (-87 nm) compared to unsubstituted Cy3, and a very weak fluorescence, which confirmed the initial assumption. The presence of *N*-phenyl substituent

(compound **12c**) showed a hypsochromic shift of -47 nm. However, amidation of the basic amino group results in a bathochromic shift of absorption maxima (+77 nm). Other derivatives of Cy3 such as trinuclear cyanines **14** and **15**, Cy3-squaraine **18**, Cy3-enyne **23**, are not fluorescent.

Table 5. Photophysical properties of Cy3 derivatives in MeCN.

Dye	λ_{abs}, nm	λ_{em}, nm	ε,[a] $M^{-1}cm^{-1}$	Φ_{fl}[b], %
12a; 19	545	560	90 000	10
12c	498	595	72 000	1
14	553	613	65 000	1
15	577	-	92 000	0
18	473	483	66 000	1[c]; 4[d]
23	513	-	84 000	0
24	458	-	65 000	0
25	458	-	65 000	0
26	535[c]	-	-	0[c]
27	458[e]	-	-	0[e]

[a] molar extinction coefficient; [b] absolute values of fluorescence quantum yield; [c] in MeOH; [d] in dioxane; [e] in MeCN-buffer mixture (4:1).

2.3 Pentamethinecyanines (Cy5)

2.3.1 Synthesis of the *meso* amino-substituted Cy5 through halogen substitution

Unlike amino-substituted Cy3[23b] and Cy7[10,11] dyes, Cy5 dyes with a basic amino group at the *meso* position of the pentamethine chain were unknown. However, symmetric Cy5 dyes with a halogen atom at the *meso* position are well known,[19,26] and, like Cy7 analogues,[11] they may serve as direct precursors for amino modified Cy5 dyes. We prepared compounds **29a-c** (Scheme 21, I) according to reported procedures[19], and attempted to substitute the halogen atom in compounds **29b,c** with an amino or hydroxyl group by using compounds **30a-e** as nucleophiles (Scheme 21, II). Unfortunately, this reaction leads to the decomposition of the Cy5 fluorophore yielding hemicyanines **31a-e**. Further studies revealed that no halogen substitution occurred, and

the chlorine atom remained attached, while the polymethine chain became shorter, and one indolenine fragment was replaced with a nucleophile RYH (compounds **31a-e** in Scheme 21). This kind of reactivity of Cy5 core has been unknown so far. The resulted hemicyanines **31a-e** are not fluorescent.

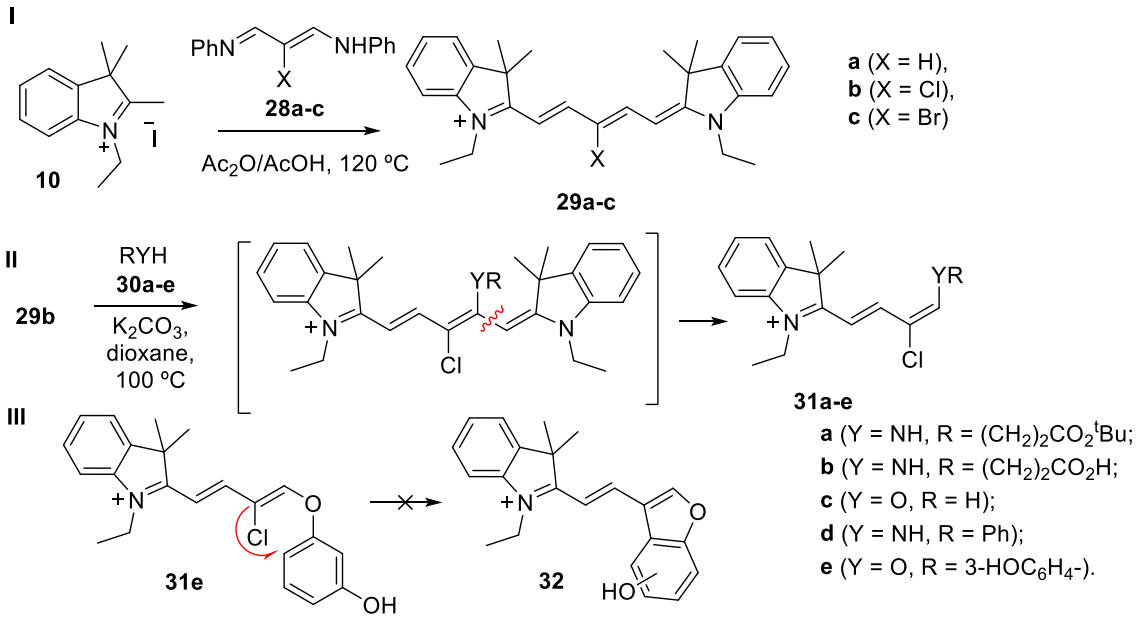

Scheme 21. I: Synthesis of unsubstituted and *meso* halogen-substituted Cy5; II: attempted halogen substitution (compounds **31a-e**); III: Expected intermolecular cyclization in **31e**.

In related transformations, the aromatic nucleophiles such as resorcinol **30e** was found to attack and cut the long methine chain of Cy7.[27] The donor substituent (in resorcinol) favoured the intramolecular electrophilic cyclization leading to cyclic hemicyanines. However, such kind of reaction did not occur for Cy5: in the reaction of **29b** with resorcinol **30e**, we observed only the product of Cy5 destruction **31e** which did not undergo the intramolecular cyclisation to form **32** (Scheme 21, III).

Cy5 dyes with bromine atom at the *meso* position are reported to be suitable substrates for Suzuki coupling with boronic derivatives.[28] We attempted another cross-coupling reaction widely used for C-N bond creation – Buchwald-Hartwig amination.[29] Unfortunately, the *meso* brominated cyanine **29c** proved to be inert in the Pd-catalysed Buchwald-Hartwig reaction and the desired aminocyanine **33** was not obtained (Scheme 22).

We also tried to obtain the acetylenic type of Cy5 (as was done for Cy3; see compound **23** in Scheme 19). The dehydrohalogenation methods reported for vinyl halides[30] incorporated into a conjugated system were applied to compounds **29b** and **29c** in Scheme 22. The use of strong and non-nucleophilic bases such as DBN (widely employed for dehydrohalogenation reactions[30]) did not result in the required acetylenic compound **34**. Numerous products with short absorption wavelengths ("destroyed" chromophores) were detected by LCMS analysis of the reaction mixture.

We have to conclude, that both strong bases and nucleophiles (Schemes 21, 22) destroyed the pentamethine fluorophore.

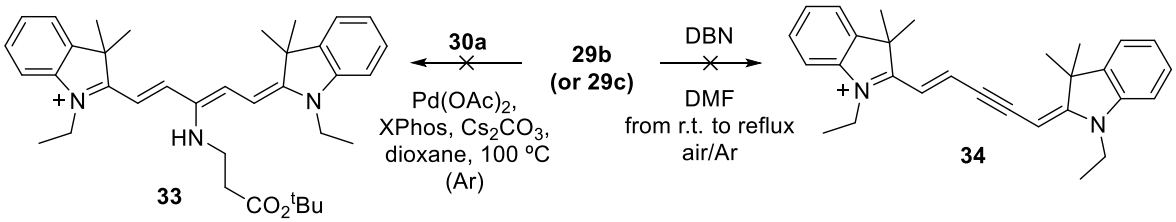

Scheme 22. Attempted Pd-catalysed Buchwald-Hartwig amination (expected compound **33**) and dehydrohalogenation (expected compound **34**). Both reactions did not work.

2.3.2 Synthesis of the *meso* amino-substituted Cy5 from malonic dialdehydes

Other methods of introducing a functional group to the *meso* position of the polymethine chain in Cy5 include the use of 2-substituted malondialdehydes OHCCHRCHO (R = NO_2, CN, aryl, etc.) or their synthetic equivalents.[31]

Free aminomalondialdehydes OHCCHRCHO (R = NHR′) are unstable, but the corresponding bis-dimethylacetals, and *N*-(acylamino) malondialdehydes were obtained through Vilsmeier-Haack formylation of glycine.[32] In our case, trifluoroacetylation looked promising, because it would allow further functionalisation of the amino group via *N*-alkylation,[33] and the trifluoroacetyl residue as a protecting group which is known to be easily removable by alkaline hydrolysis.[34]

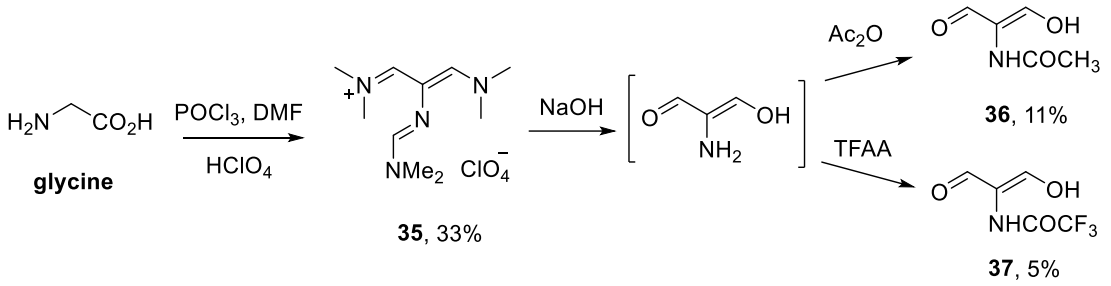

Scheme 23. Synthesis of the *meso* substituted malonic dialdehydes.

We prepared both *N*-acetyl- and *N*-trifluoroacetyl aminomalondialdehydes **36** and **37** according to the method reported by Arnold[32] and condensed them with indolium salt **10** to afford dyes **40** and **41** (Scheme 24). The possibility of further modification via *N*-alkylation was proved by methylation with methyl iodide to afford model compounds **43** and **44** (Scheme 24).

Amide **43** was of particular interest, because it structurally relates to *N*-pyrrolidone (Scheme 10), and it was important to study its photophysical properties. Amide **41** (Scheme 24) was prepared as a precursor for *N*-alkylation. Amide **44** was prepared as a model compound for investigating the cleavage of the trifluoroacetyl protecting group and assessing the stability of *meso* aminocyanine **45**-Me. Surprisingly, compounds **41** and **44** could not be transformed to *meso* pentamethineamines **45**-R. Under basic conditions, the hydrolysis resulted in hemicyanines (Scheme 25, Figure 16) and was accompanied by the disruption of the polymethine chain and the disappearance of the typical blue colour. Several compounds were detected by LCMS, but none of them was of particular interest as a fluorescent dye.

We also checked whether an amino group may be introduced via reduction of the nitro group. For this purpose, the nitro compound **42** (Scheme 24) was prepared[31g] and subjected to the catalytic reduction with hydrazine or hydrogen.[35] The desired pentamethineamine **45**-H was not detected in the reaction mixture. Among the decomposition products, compounds with Cy3 fluorophore were found. Interestingly, the related "downgrade" of fluorophores was observed in the row Cy7-Cy5-Cy3 by photolysis, but in our case this transformation occurred without application of light.[36]

Our attempts to introduce a donor amino group to the *meso* position of Cy5 failed due to the instability of the target compounds **45**-R. We introduced another donor group (OH) to Cy5 fluorophore (compound **46**, Scheme 24). To the best of our knowledge, it has been the first strong donor group (σ_p = -0.37)[37] attached to the *meso* position of Cy5. Compound **46** was obtained

through the condensation of commercially available hydroxymalondialdehyde **39** and indolium salt **10** in butanol – toluene solution. If this reaction was carried in acetic anhydride – acetic acid (typical solvent mixture for cyanine synthesis), the hydroxyl group was *in situ* acylated, and ester **47** formed (Scheme 24).

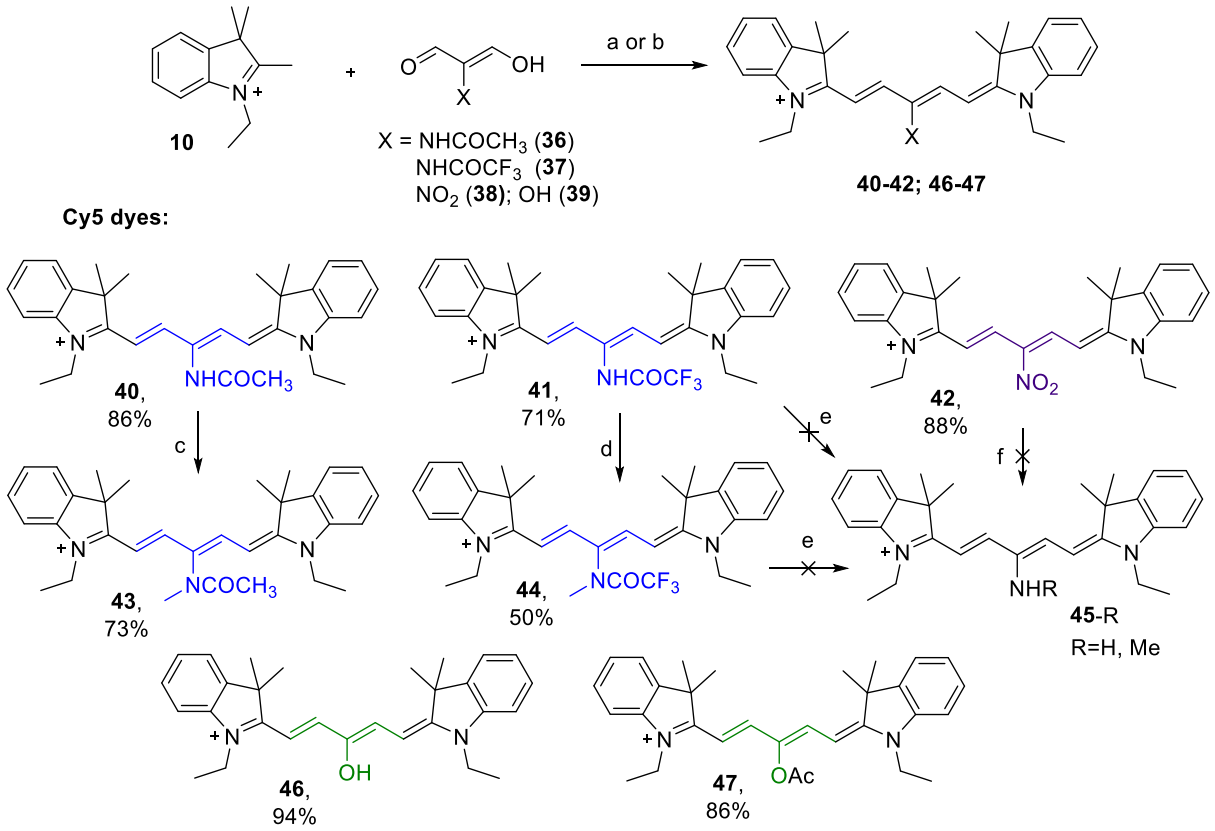

Scheme 24. Synthesis of Cy5 derivatives *via* substituted malondialdehydes **36-39** and structures of the *meso* substituted Cy5 dyes. Compounds **45**-R were not detected. Reagents and conditions: a) Ac_2O, NaOAc, 120 ˚C; b) BuOH/ toluene 1:1, pyridine, 100 ˚C; c) MeI, NaH, DMF, 0 ˚C - r.t. d) MeI, Cs_2CO_3, DMF, 100 ˚C; e) 1 M aq. NaOH, MeCN, r.t.; f) $N_2H_4*H_2O$, $FeCl_3*6H_2O$, active carbon, MeOH, 60 ˚C or H_2, Pd/C, MeOH, 60 ˚C. Counterions are omitted (undefined). Yields of isolated compounds are given.

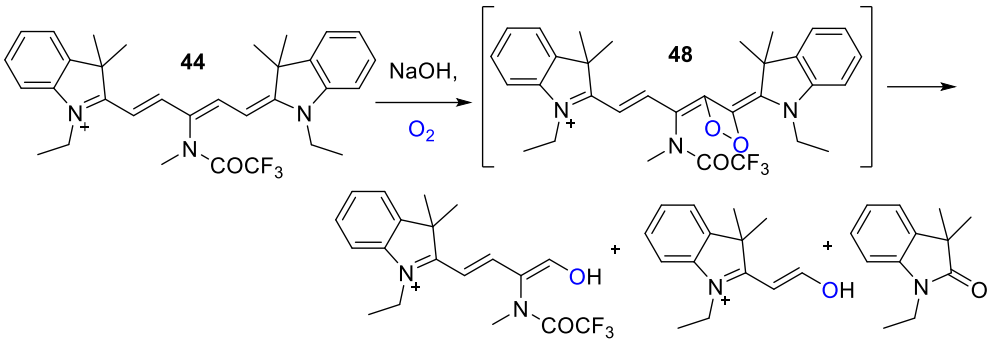

Scheme 25. Oxidative alkaline hydrolysis involving Cy5 derivative **44**. Compound **48** proposed as an intermediate. The reaction products are detected by LCMS (not isolated).

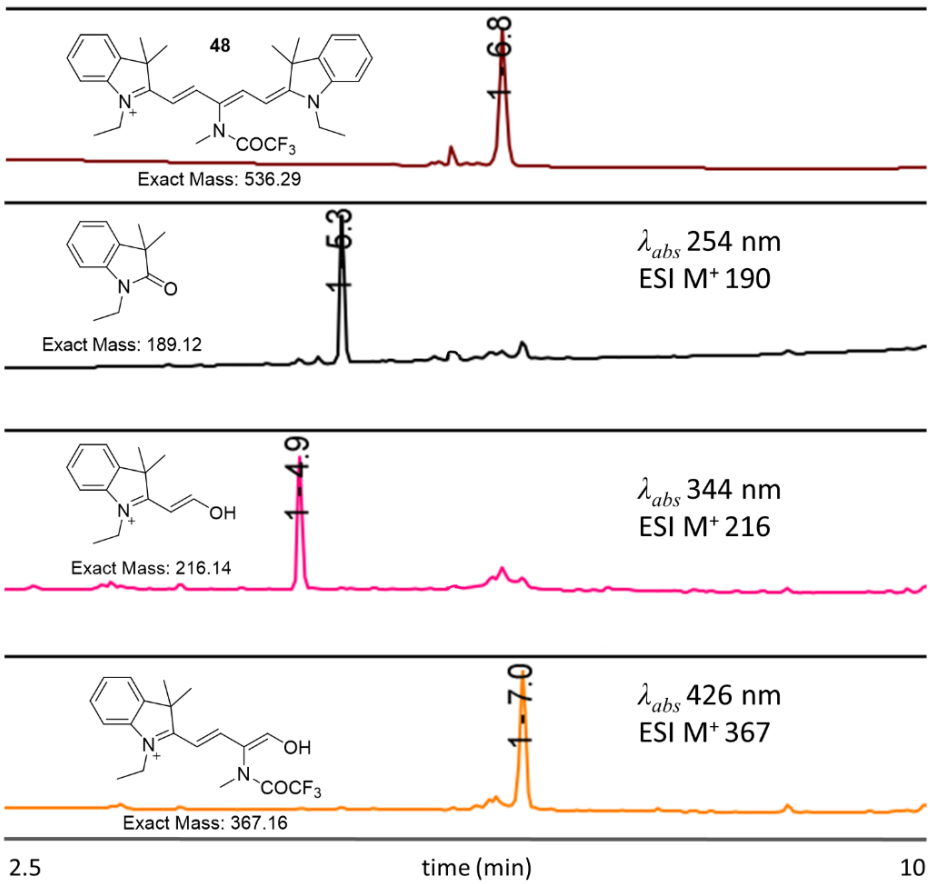

Figure 16. LCMS traces of the oxidative alkaline hydrolysis involving Cy5 derivative **44**.

When irradiated with light, polymethine dyes are capable of reacting with singlet oxygen, and the intermediate 1,2-dioxetane (*i.e.* compound **48** in Scheme 25) may decompose with breaking of the polymethine chain. This transformation reminds ozonolysis.[38] Cy7 dyes with a basic

(electron-donating) amino group at the *meso* position are reported to show lower photostability than the acylated analogues.[39] The hypothesis was that an iminium intermediate facilitates the incorporation of the singlet oxygen species into the polymethine chain.[39] Acylation of the heteroatom (N, O) reduces the electron density on the free amino or hydroxyl group and minimizes the photoinduced addition reactions to the chromophore. Thus, *N*-, or *O*-acylation increases photo- and chemical stability, as we observed for dyes **40**, **41**, **43**, **44**, **47** (Scheme 24). They are stable as solids and solutions in MeCN for weeks and can be kept at r.t. without exclusion of air oxygen. Compound **46** is unstable; it decomposed faster than other Cy5 derivatives mentioned here.

2.3.3 Intermezzo: *meso*-(2-carboxyphenyl)-Cy5 dye

We briefly checked another option which may lead to the photoactivatable Cy5 dyes having 2-diazo-3-spiro-1-indanone unit (compound **50** in Scheme 26). This group incorporated into rhodamine dyes made them colourless (pale yellow) and non-fluorescent, due to spontaneous cyclization to the spiro-form with broken conjugation.[6c, 16] The existence of spirolactam capped Cy7 dyes[40] with similar molecular architecture confirmed the possibility to mask the cyanine chromophore by intramolecular addition of a nucleophilic group (-**CH**=N_2, -CO**NH**R) to polymethine chain. Photolysis of 2-diazo-3-spiro-1-indanones (in protic solvents) obtained from rhodamines was accompanied by Wolff rearrangement and led to fluorescent analogues of the initial dyes with an additional CH_2 group between the phenyl ring and the carboxylic acid function (COOH, COOR or COONHR).[16]

The starting *meso*-(2-carboxyphenyl)-Cy5 dye **49** was obtained from the corresponding brominated derivative **29c** and 2-carboxyphenyl boronic acid via Suzuki coupling.[28] Diazoketone **50** was generated from the acyl chloride of acid **49** and diazomethane. It turned out to be unstable and decomposed in the reaction mixture giving a non-fluorescent product, to which we can assign either structure **53**, or **54**. The former (**53**) corresponds to carbene insertion into the carbon-carbon bond, and the latter (**54**) – to carbene insertion into carbon-hydrogen bond. The similar process – formation of a dark by-product via carbene insertion into a carbon-carbon bond – was observed in the photolysis of 2-diazo-3-spiro-1-indanones obtained from rhodamines, but these diazoketones were quite stable.[16a-c]

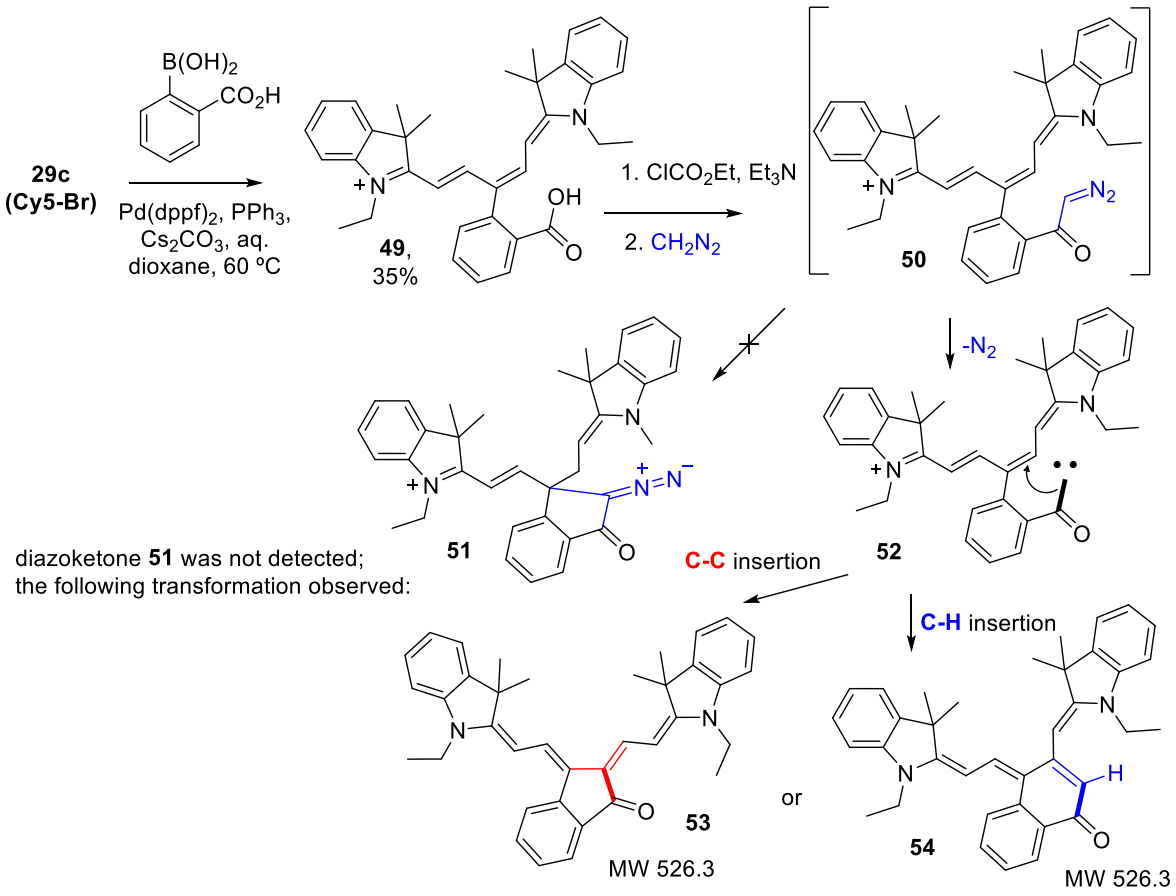

Scheme 26. Generation of instable diazoketone **50** leads to the formation of non-fluorescent products **53** ("Cy6 analogue") and **54** (Cy5 derivative). Counterions are omitted (undefined).

2.3.4 Photophysical properties of Cy5 dyes

The photophysical properties of Cy5 derivatives are given in Table 6. The introduction of acylamino group (σ_p = 0.0 – 0.39)[37] to the *meso* position of the pentamethine chain (compounds **40**, **41**, **43**, **44**, Scheme 24) produces a small blue shift of the absorption (up to -14 nm) and emission (up to -19 nm) maxima compared to unsubstituted dye **29a** (Scheme 21). For the nitro group (σ_p = 0.78[37] compound **42**, Scheme 24), this effect is much stronger (-45 nm). The only group with donor properties (OH, σ_p = -0.37)[37] induces a red shift in both absorption (+28 nm) and emission (+28 nm) maxima (compound **46**, Scheme 24).

In our previous publication, we reported the linearized correlations between the Hammett σ_p constants and positions of absorption and fluorescence maxima.[33] In the present case, we plotted the values of the Hammett σ_p constants and the positions of absorption and emission maxima (in

eV) for Cy5 derivatives (data from this study) and Cy7 analogues (data from ref. 41) in Figure 17. If we consider the influence of the substituents at the *meso* position on the spectra of cyanine dyes, we can conclude that Cy7 and Cy3 dyes demonstrate similar trends, while the Cy5 fluorophore demonstrates the opposite trend. The explanation of this phenomena can be found in the localisation of HOMO and LUMO.[42] According to DFT-calculations, the highest occupied molecular orbital (HOMO) is localised on the entire pentamethine chromophore including the *meso* carbon atom (and an adjacent substituent). The lowest unoccupied molecular orbital (LUMO) is localised on the pentamethine chain, excluding the *meso* carbon atom. Thus, the electron donor groups at the *meso* position of the Cy5 chromophore increase the energy of the HOMO, reduce the energy gap between HOMO and LUMO, and produce bathochromic shift of the absorption and emission maxima. The localisations of HOMO and LUMO at the *meso* amino-substituted Cy7 and Cy3 dyes are opposite to Cy5. In these dyes, the electron donors increase the energy of the LUMO and produce hypsochromic shift of the absorption and emission bands. Indeed, the blue shifts in absorption and emission maxima are observed for compounds **24** and **25** (Scheme 19, Table 5) compared to unsubstituted dye **19** (Scheme 18, Table 5). Thus, our experimental data confirm the trends based on DFT calculations.[42]

The correlation coefficients are positive for Cy5 dyes (*ca*. 0.9) and negative for Cy7 derivatives (*ca*. -0.9; Figure 17). Compared to the non-fluorescent *meso* pyrrolidone-substituted Cy3 (**26**, QY 0, Scheme 20, Table 5), and Cy7 (QY 0.075 in MeCN),[10] the fluorescence quantum yield of **43** (which is structurally related to pyrrolidone; Scheme 24) was found to be high enough for Cy5 dyes: 0.22 in MeCN (Table 6).

Table 6. Photophysical properties of **Cy5** derivatives in MeCN.

Dye	Substituent at the *meso* position	σ_p[a]	λ_{abs}, nm	λ_{em}, nm	ε,[b] $M^{-1}cm^{-1}$	Φ_{fl}[c]
29a	H	0	639	664	191 000	0.17
29b	Cl	0.23	640	659	193 700	0.07
29c	Br	0.23	636	658	179 000	0.06
40	NHCOMe	0	637	660	180 000	0.15
41	$NHCOCF_3$	0.12	631	651	175 000	0.15
42	NO_2	0.78	594	641	160 000	0.02
43	NMeCOMe	0.26	631	651	175 000	0.22
44	$NMeCOCF_3$	0.39	625	645	175 000	0.22
46	OH	-0.37	667	692	190 000	0.14
47	OCOMe	0.31	642	663	176 000	0.11
49	*o*-$CO_2HC_6H_4$	-	640	664	168 000	0.11

[a] data from ref. 37; [b] molar extinction coefficient; [c] absolute values of fluorescence quantum yield.

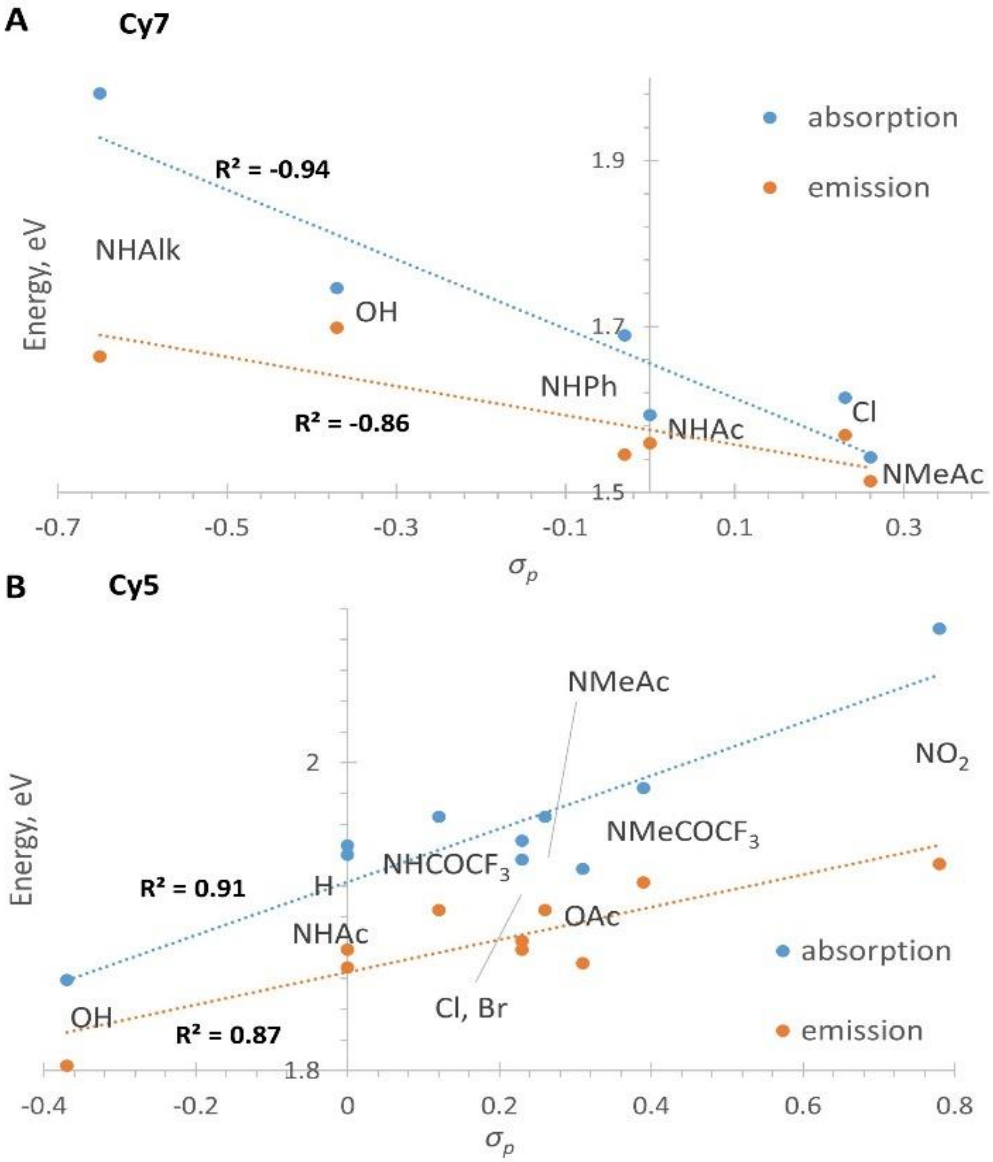

Figure 17. Correlations of the σ_p values with positions of absorption and emission maxima (in eV) of Cy7 (A, data from ref. 41) and Cy5 (B, this work).

2.4 Squaraines: synthesis, properties and photolysis

Squarylium dyes combine good photostability with high quantum yields, and some stabilized squaraines are used as fluorescent probes and labels for biomedical applications.[43] The stabilization (often in the supramolecular guest-host complex) is required, as the "naked" squarylium dyes are hydrolytically unstable and readily react with nucleophiles. However, the

facile synthesis makes them attractive platform for the design of the far-red emitting fluorescent probes.[44] The incorporation of the squaraine residue into Cy3 fluorophore (compound **18**, Scheme 18) allowed us to obtain the acetylenic compound (**23**, Scheme 19), which was an important substrate for the preparation of the amino-substituted Cy3 dyes **24** and **25** (Scheme 19). We decided to incorporate the squarylium moiety into Cy5 core (Scheme 27), because this approach helped us to achieve the synthetic goal for the Cy3 chromophore (Schemes 18, 19), and we thought that it will also work for Cy5 chromophore.

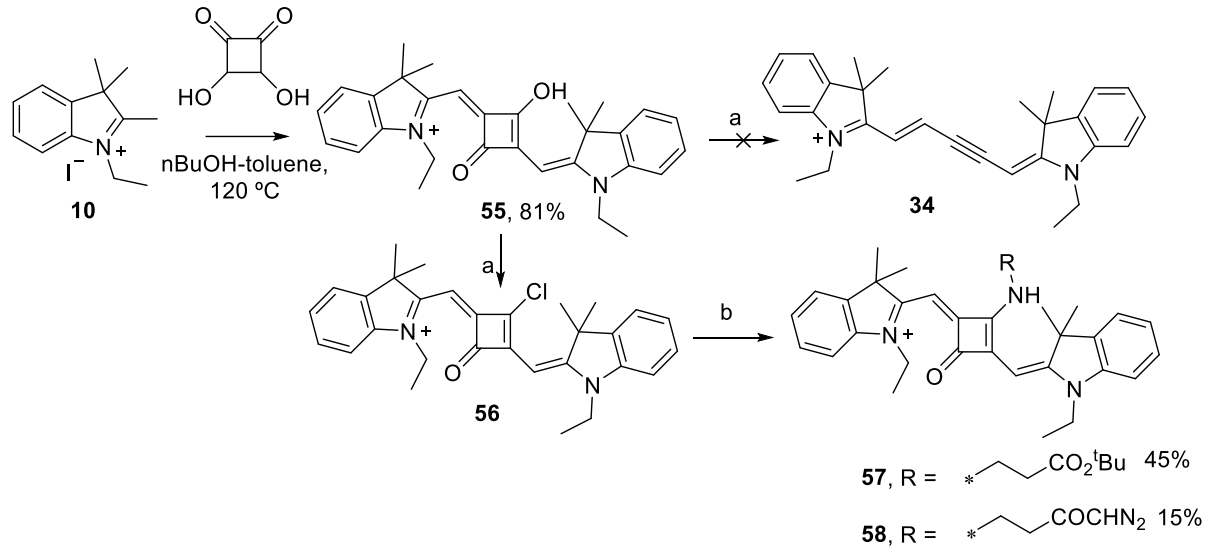

Scheme 27. Synthesis of amino-squaraine based Cy5 dyes. Reagents and conditions: a) $POCl_3$, Et_3N, 1,4-dioxane, 80 ˚C; b) K_2CO_3, THF, r.t., β-alanine *t*-butyl ester to obtain dye **57**; reagent **DAK** (Scheme 16) to obtain dye **58**. Counterions are omitted (undefined). Yields of isolated products are given.

Squaraine **55** (Scheme 27) was obtained according to the reported methods.[43-44] In the reaction with $POCl_3$ compound **55** did not lose CO and gave no acetylenic derivative **34**, but rather formed chloride **56**, which readily reacted with β-alanine *t*-butyl ester and afforded amino-squaraine **57**. In comparison with the parent squarylium cyanine **55**, amino-squaraine **57** displays a small bathochromic shift of the absorption band (+12 nm) and shows very weak fluorescence (Table 7), as required for the initial "dark state" of the photoactivatable dyes. Further transformation was based on the introduction of the diazoketone moiety (reaction with **DAK**

reagent) and resulted in dye **58**. This modification did not increase the fluorescence quantum yield, and dye **58** was subjected to photolysis (Scheme 28 and Figure 18).

Table 7. Photophysical properties of squarylium derivatives in MeCN.

Dye	λ_{abs},nm	λ_{em}, nm	ε,[a] $M^{-1}cm^{-1}$	Φ_{fl}[b]
55	631	644	210 000	0.08
57	643	659	150 000	0.01
58	643	659	150 000	0.01
59	620	654[c]	≈100 000[d]	0.007[c]
60	643	651[e]	≈139 000[d]	0.008[e]

[a] molar extinction coefficient; [b] absolute values of fluorescence quantum yield; [c] in MeOH; [d] assuming full conversion; [e] in MeCN-buffer mixture (4:1).

Diazoketone **58** was subjected to photolysis at 365 nm in methanol and in aqueous acetonitrile (Scheme 28, Figure 18). The products are similar to the products obtained from trimethine cyanine **25** (Scheme 20, Figure 15). In methanol, the main product with t_R = 6.27 min, λ_{abs} = 620 nm and *m/z* = 520 is pyrrolidone **59**. In acetonitrile – aqueous buffer (4:1) solution, the main product with t_R = 6.06 min, λ_{abs} = 643 nm and *m/z* = 538 is amino acid **60**. Unfortunately, both photolytic products **59** and **60** were found to be poorly fluorescent (Table 7), with emission quantum yields as low as that of compound **58**.

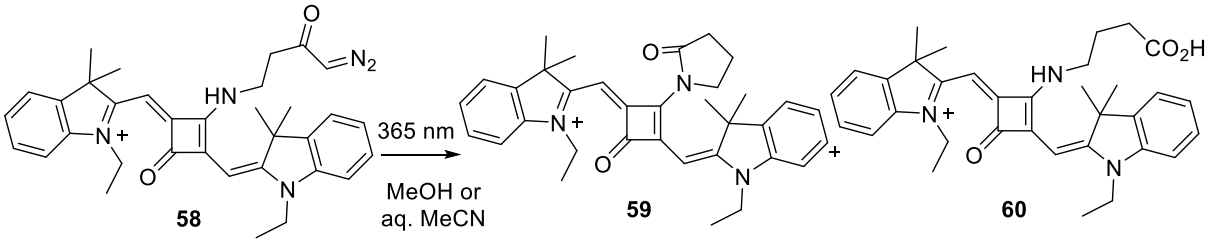

Scheme 28. Photolysis of compound **58**.

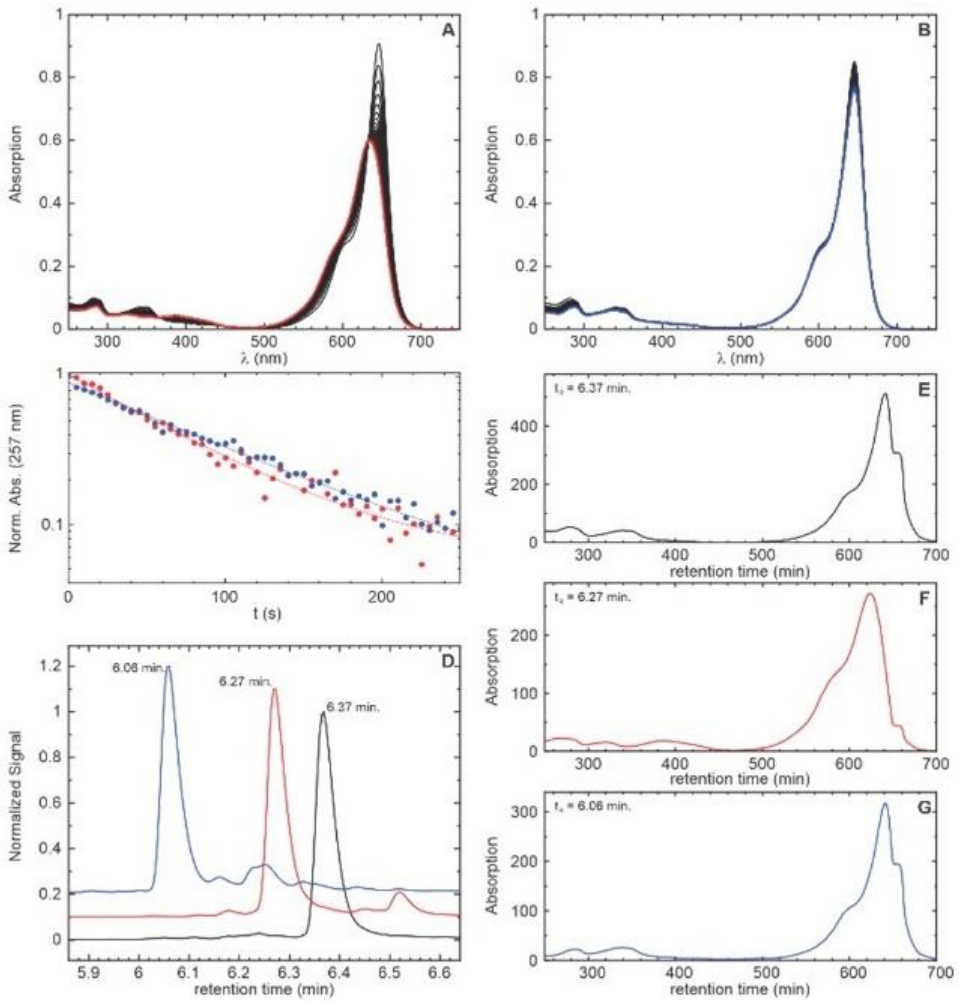

Figure 18. Photolysis of compound **58** in MeOH (A) and in an MeCN - aq. buffer (4:1) mixture (B). The initial spectra are plotted in black. The data for products **59** and **60** are in red and blue, respectively. (C) Normalised transients (absorption at 257 nm) by consumption of **58**. (D) HPLC traces of compound **58** (black line) and the reaction mixtures after photolysis in MeOH (red line, compound **59**) and in the MeCN - aq. buffer (4:1) mixture (blue line, compound **60**). (E-F) Absorption spectra of **58** (black line) and the main peaks (products) in red and blue HPLC traces in (D) (with indicated retention times).

2.5 Conclusion

Not like Cy3 dyes, Cy5 derivatives with a basic amino group at the *meso* position of the fluorophore were found to be unstable and decomposed with the disruption of the polymethine chain. The presence of an amino group at this position quenches the fluorescence of Cy3 and, as

an additional functionality, provides a certain degree of synthetic freedom. To demonstrate this, we prepared 4-amino-1-diazo-2-butanone ($H_2N(CH_2)_2COCH=N_2$) and attached it via an amino group to Cy3 and squaraine dyes. Photolysis of these compounds was accompanied by Wolff rearrangement and led to pyrrolidones (in methanol and aprotic solvents) formed via intramolecular cyclization of the intermediate ketenes with an amino group. In aqueous acetonitrile, ketenes reacted with water and gave carboxylic acids. Though the products of these reactions were found to be non-fluorescent, synthesis and incorporation of the fragment $H_2N(CH_2)_2COCH=N_2$ into other chromophores is interesting, and may be a promising tool for obtaining photoconvertible (or photoactivatable) dyes. In our case, the initial dyes were non-fluorescent; probably, due to photoinduced electron transfer (PET) from the basic amino group.[7,13] For other dyes, like BODIPYs or oxazines, these aspects remain unexplored. Importantly, we established that the intramolecular acylation of the amino group takes place if the photolysis is carried out in methanol or aprotic solvents. Thus, the use of photoconvertible dyes (dye-$HN(CH_2)_2COCH=N_2$) in aqueous solutions may be limited, but applications in material science (in organic solvents, polymer matrices, etc.) are more promising.

2.6 References to Chapter 2

1. (a) K. Uno, V. N. Belov, M. L. Bossi, Photoswitscable fluorophores for super-resolution optical microscopy in *Molecular Photoswitches*: *Chemistry, Properties, and Applications*, Wiley VCH GmbH, **2022**, pp. 606-626; (b) T. Fukaminato, *J. Photochem. Photobiol. C: Photochem. Rev*. **2011**, 12, 177-208.

2. M. Weber, M. Leutenegger, S. Stoldt, S. Jakobs, T. S. Mihaila, A. N. Butkevich, S. W. Hell *Nat. Photonics* **2021**, *15*, 361-366.

3. F. Balzarotti, Y. Eilers, K. C. Gwosch, A. Gynnå, V. Westphal, F. D. Stefani, J. Elf, S. W. Hell, *Science* **2017**, *355*, 606-612.

4. E. Betzig, G. H. Patterson, R. Sougrat, O. W. Lindwasser, S. Olenych, J. S. Bonifacino, M. W. Davidson, J. Lippincott-Schwartz, H. F. Hess, S*cience*, **2006**, *313*, 1642-1645.

5. M. J. Rust, M. Bates, X. Zhuang, *Nat. Methods*. **2006**, *10*, 793-795.

6. a) A. N. Butkevich, M. Weber, A. R. Cereceda Delgado, L. M. Ostersehlt, E. D'Este, S. W. Hell. *J. Am. Chem. Soc*. **2021**, *143*, 18388-18393; b) A. Aktalay, T. A. Khan, M. L. Bossi, V. N. Belov,

S. W. Hell, *Angew. Chem. Int. Ed*. **2023**, e202302781; c) B. Roubinet, M. Bischoff, S. Nizamov, S. Yan, C. Geisler, S. Stoldt, G. Y. V. N. Belov, M. L. Bossi, S. W. Hell, *J. Org. Chem.* **2018**, *83*, 6466-6476; d) J. B. Grimm, B. P. English, H. Choi, A. K. Muthusamy, B. P. Mehl, P. Dong, T. A. Brown, J. Lippincott-Schwartz, Z. Liu, T. Lionnet, L. D. Lavis, *Nat. Methods* **2016**, *13*, 985-988.

7. a) A. P. Gorka, R. R. Nani, M. J. Schnermann, *Org. Biomol. Chem*. **2015**, *13*, 7584-7598; b) M. Levitus, S. Ranjit, *Q. Rev. Biophys*. **2011**, *44*, 123-151.

8. A. M. Sipyagin, V. G. Kartsev, *Russ. Zh. Org. Khim.* **1986**, *22*, 401-409.

9. W. Kirmse, *Eur. J. Org. Chem*. **2002**, 2193-2256.

10. X. Hu, Y. Su, Y. Ma, X. Zhan, H. Zheng, Y. Jiang, *Chem. Commun*. **2015**, *51*, 15118-15121.

11. (a) X. Peng, F. Song, E. Lu, Y. Wang, W. Zhou, J. Fan, Y. Gao, *J. Am. Chem. Soc.* **2005**, *127*, 4170-4171; (b) K. Kiyose, S. Aizawa, E. Sasaki, H. Kojima, K. Hanaoka, T. Terai, Y. Urano, T. Nagano, *Chem. Eur. J.* **2009**, *15*, 9191-9200; (c) W. Pham, L. Cassell, A. Gillman, D. Koktysh, J. C. Gore, *Chem. Commun*. **2008**, 1895–1897.

12. A. Descalzo, K. Rurack, *Chem. Eur. J*. **2009**, *15*, 3173-3185.

13. Y. Gidi, L. Payne, V. Glembockyte, M. S. Michie, M. J. Schnermann, G. Cosa, *J. Am. Chem. Soc*. **2020**, *142*, 12681-12689.

14. L. Wolff, *Justus Liebigs Ann. Chem.* **1902**, *325*, 129-195.

15. F. Arndt, B. Eistert, *Ber. Dtsch. Chem. Ges. B* **1935**, *68*, 200-208.

16. a) V. N. Belov, C. A, Wurm, V. P. Boyarskiy, S. Jacobs, S. W. Hell, *Angew. Chem. Int. Ed*. **2010**, *49*, 3520-3523; b) V. N. Belov, G. Y. Mitronova, M. L. Bossi, V. P. Boyarskiy, E. Hebisch, C. Geisler, K. Kolmakov, C. A. Wurm, K. I. Willig, S. W. Hell, *Chem. Eur. J*. **2014**, *20*, 13162-13173; c) K. Kolmakov, C. Wurm, M. V. Sednev, M. L. Bossi, V. N. Belov, S. W. Hell, *Photochem. Photobiol. Sci.* **2012,** *11*, 522-532; d) S. J. Sahl, J. Matthias, K. Inamdar, T. A. Khan, M. Weber, S. Becker, C. Griesinger, J. Broichhagen, S. W. Hell, bioRxiv 2023.07.07.548133; doi: https://doi.org/10.1101/2023.07.07.548133.

17. S. Yagi, H. Nakazumi, Squarylium dyes and related compounds in *Heterocyclic polymethine dyes*, Springer, **2010**, pp. 133-181.

18. Z.-H. Peng, L. Qun, X.-F. Zhou, S. Carroll, H. J. Geise, B. Peng, R. Dommisse, R. Carleer, *J. Mater. Chem.*, **1996**, *6*, 559-565.

19. E. A. Owens, H. Hyun, J. G. Tawney, H. S. Choi, M. Henary, *J. Med. Chem*. **2015**, *58*, 4348-4356.

20. L. Cotarca, P. Delogu, A. Nardelli, V. Sunjic, *Synthesis* **1996**, *5*, 553-576.

21. a) M. Coenen, *Chem. Ber*. **1947**, *80*, 546-533; b) M. Coenen, *Chem. Ber*. **1949**, 66-72; c) M. Coenen, *Angew. Chem*. **1949**, *61*, 11-17.

22. M. Coenen, Chem. Ber. **1960**, 633, 102-110.

23. a) D. Zhang, J. Su, X. Ma, H. Tian, *Tetrahedron* **2008**, *64*, 8515-8521; b) G. Chen, F. Song, X. Wang, S. Sun, J. Fan, X. Peng, *Dyes & Pigm*. **2012**, *93*, 1532-1537.

24. H. Eilingsfeld, G. Neubauer, M. Seefelder, H. Weidinger, *Chem. Ber*. **1964**, *97*, 1232-1245.

25. a) D. Dukanya , T. R. Swaroop, S. Rangappa, K. S. Rangappa, B. Basappa, *SynOpen* **2019**, *3*, 71-76; b) M. R. Kelley, J.-U. Rohde, *Inorg. Chem*. **2013**, *52*, 5, 2564–2580.

26. Q. Zhang, S. Xu, F. Lai, Y. Wang, N. Zhang, M. Nazare, H.-Y. Hu, *Org. Lett*. **2019**, *21*, 2121-2125.

27. a) L. Li, Z. Li, W. Shi, X. Li, H. Ma, *Anal. Chem*. **2014**, *86*, 6115-6120; b) S.-Y. Liu, H. Xiong, R.-R. Li, W.-C. Yang, G.-F. Yang, *Anal. Chem*. **2019**, *91*, 3877-3884; c) M. Santra, M. Owens, G. Birch, M. Bradley, *ACS Appl. Bio Mater*. **2021**, *4*, 8503-8508.

28. a) Y. Ji, Y. Wang, N. Zhang, S. Xu, L. Zhang, Q. Wang, Q. Zhang, H.-Y. Hu, *J. Org. Chem*. **2019**, *84*, 1299-1309; b) X. Zhao, Q. Yao, S. Long, W. Chi, Y. Yang, D. Tan, X. Liu, H. Huang, W. Sun, J. Du, J. Fan, X. Peng, *J. Am. Chem. Soc.* **2021**, *143*, 12345-12354.

29. R. Dorel, C. P. Grugel, A. M. Haydl, *Angew. Chem. Int. Ed.* **2019**, *58*, 17118-17129; *Angew. Chem.* **2019**, *131*, 17276-17287.

30. a) G. M. Mkryan, A. A. Pogosyan, A. A. Kaitsuni, *Russ. Zh. Org. Khim.* **1978**, *14*, 1810-1814; b) C. K. Skepper, J. B. MacMillan, G.-X. Zhou, M. N. Masuno, T. F. Molinski, *J. Am. Chem. Soc*. **2007**, *129*, 4150–4151.

31. a) C. Reichardt, W. Mormann, *Chem. Ber*. **1972**, *105*, 1815-1839; b) Yu. L. Slominskii, N. I. Efimenko, N. V. Kuznetsov, I. I. Krasavtsev, *Ukr. Khim. Zh.* **1977**, 713-716; c) N. S. Spasokukotskii, A. F. Vompe, I. I. Levkoev, N. N. Sveshnikov, *Russ. Zh. Org. Khim*. **1980**, 2427-2434 (Engl. Transl. **1981**, pp. 2080-2087); d) V. M. Zubarovskii, Yu. L. Briks, G. P. Hodot, *Ukr. Khim. Zh.* **1981**, *47*, 525-528; e) C. Reichardt, U. Rust, *Z. Naturforsch. B* **1982**, 236-245; f) A. Mehranpour, S. Hashemnia, R. Maghamifar *Synth. Commun*. **2010**, *40*, 3594-3602; g) S. Miltsov, V. S. Karavan, M. Goikhman, I. Podeshvo, S. Gomez-de Pedro, M. Puyol, J. Alonso-Chamarro, *Dyes & Pigm.* **2014**, *109*, 34-41; h) T. Briza, S. Rimpelova, J. Kralova, K. Zaruba, Z. Kejik, T. Ruml, P. Martásek V. Kral *Dyes & Pigm.* **2014**, *107*, 51-59.

32. Z. Arnold, J. Sauliova, V. Krchnak *Coll. Czech. Chem. Commun*. **1973**, *38*, 2633-2640.

33. E. A. Savicheva, G. Y. Mitronova, L. Thomas, M. J. Boehm, J. Seikowski, V. N. Belov, S. W. Hell, *Angew. Chem. Int. Ed.* **2020**, *59*, 5505-5509; *Angew. Chem.* **2020**, *132*, 5547-5551.

34. T. Greene, G. M. Peter, Protection for the amino group in *Protective groups in Organic Synthesis*, John Wiley & Sons, 2nd ed., **1991**, 343-344.

35. a) S. A. Shevelev, A. Kh. Shakhnes, B. I. Ugrak, S. S. Vorob'ev, *Synth. Commun.* **2001**, *31*, 2557-2561; b) M. M. Zanardi, A. G. Suarez, *Tetrahedron Lett*. **2015**, *56*, 3762-3765.

36. a) Y. Cho, H. J. An, T. Kim, C. Lee, N. K. Lee, *J. Am. Chem. Soc*. **2021**, *143*, 14125−14135; b) S. S. Matikonda, D. A. Helmerich, M. Meub, G. Beliu, P. Kollmannsberger, A. Greer, M. Sauer, M. J. Schnermann, *ACS Centr. Sci.* **2021**, *7*, 1144−1155.

37. C. Hansch, A. Leo, R. W. Taft, *Chem. Rev*. **1991**, *91*, 165-195.

38. T. J. Fisher, P. H. Dussault, *Tetrahedron* **2017**, *73*, 4233-4258.

39. A. Samanta, M. Vendrell, R. Das, Y.-T. Chang, *Chem. Comm*. **2010**, *46*, 7406-7408.

40. a) L. He, W. Lin, Q. Xu, M. Ren, H. Wie, J.-Y. Wang, *Chem. Sci*. **2015**, *6*, 4530-4536; b) C. Kar, Y. Shindo, K. Oka, S. Nishiyama, K. Suzuki, D. Citterio, *RSC Adv*. **2017**, *7*, 24970-24980.

41. a) L. Feng, W. Chen, X. Ma, S. H. Liu, J. Yin, *Org. Biomol. Chem*. **2020**, *18*, 9385-9397; b) R. M. Exner, F. Cortezon-Tamarit, S. I. Pascu, *Angew. Chem. Int. Ed.* **2021**, *60*, 6230-6241; *Angew. Chem.* **2021**, *133*, 6295-6306.

42. J. Cao, J. Fan, W. Sun, Y. Guo, H. Wu, X. Peng, *RSC Adv*. **2017**, *7*, 30740-30746.

43. a) M. Collot, R. Kreder, A. L. Tatarets, L. D. Patsenker, Y. Mely, A. S. Klymchenko, *Chem. Comm*. **2015**, *51*, 17136-17139.

44. a) K. D. Volkova, V. B. Kovalska, A. L. Tatarets, L. D. Patsenker, D. V. Kryvorotenko, S. M. Yarmoluk, *Dyes and Pigments* **2007**, *72*, 285-292; b) F. Mandim, V. C. Graça, R. C. Calhelha, I. L. F. Machado, L. F. V. Ferreira, I. C. F. R. Ferreira, P. F. Santos, *Molecules*, **2019**, *24*, 863-877.

Chapter 3.

Late-stage transformation of fluorescent dyes via C–H activation

3.1 Introduction

Multifunctional organic dyes modulating their emissive properties in the course of a chemical or photochemical reaction are highly favoured as "smart" fluorescent probes and indispensable for the progress in life sciences and optical microscopy.[1,2] Rhodamines constitute very important fluorophores for applications in live-cell fluorescence microscopy.[2] Despite recent advances in "tuning" rhodamines by structure changes, novel synthetic tools to get tailor-made dyes for the specific imaging and labelling techniques are in high demand. In comparison with rhodamines, oxazine fluorescent dyes[3,4] feature red-shifted absorption and emission bands and are important dyes used in superresolution STED (stimulated emission depletion) microscopy and single-molecule switching techniques.[4] The synthesis of newly designed oxazines is a highly challenging task, as this class of dyes has been relatively understudied. However, despite the tedious synthesis, asymmetric rhodamines and oxazines hold significant potential and attractiveness for further studies. Substituents at the dye core influence the photophysical and photochemical properties of the dyes. The introduction of a simple acrylate function to the dye core brings two valuable functionalities (Figure 19). Firstly, it expands the conjugation chain, which can enhance the dye's absorption and emission and potentially improve its performance in various applications. Additionally, the acrylate group provides an excellent site for bioconjugation, allowing the dye to be linked to biomolecules for various bioimaging or targeted delivery applications.

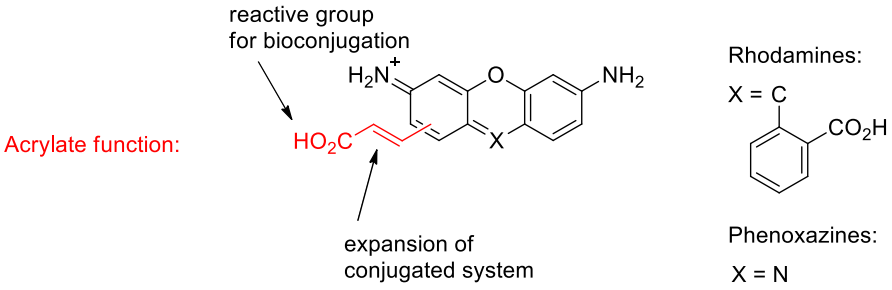

Figure 19. Rhodamines and oxazines with an acrylate function.

The presence of a double bond in the acrylate function offers the possibility of its reduction, which can change the dye's structures, and consequently, its photophysical properties. Investigating the impact of these changes on the dye's properties will contribute to a deeper understanding of how the structure influences the positions of absorption and emission, quantum yield, and fluorescence lifetime.

As previously mentioned, the synthesis of asymmetric dyes is quite challenging, often involving far more than 10 complex steps, which demands much work in the laboratory and financial resources. To overcome these drawbacks, a promising approach is the late-stage functionalisation (LSF), which offers the opportunity to diversify key compounds in a stepwise and atom-economic manner.[5] The C–H activation strategy that takes advantage of designed directing groups has pioneered the field of LSF in drug development.[5-7] However, these methods remain scarce in the context of dye design. The full control of regioselectivity constitutes a major challenge in C–H transformations, as there are omnipresent C–H bonds in complex molecules. One way to address this challenge lies in the use of directing groups (DG),[6,7] ideally exploiting innate, naturally occurring functional groups or applying transient directing groups. Therefore, the primary objective of this work was to focus on the LSF of rhodamines and oxazines using a C–H activation approach and functional groups pertinent to these fluorophores. To introduce the acrylate functional group to rhodamines and oxazines, we chose the method of oxidative olefination (Scheme 29). The study of the resulting dyes and the analysis of their photophysical behaviour was thought to contribute to a deeper understanding of their structure-spectra relationships and perspective applications in various fluorescence techniques. The ultimate goal was to develop new synthetic methodologies that facilitate the creation of novel dyes with required properties.

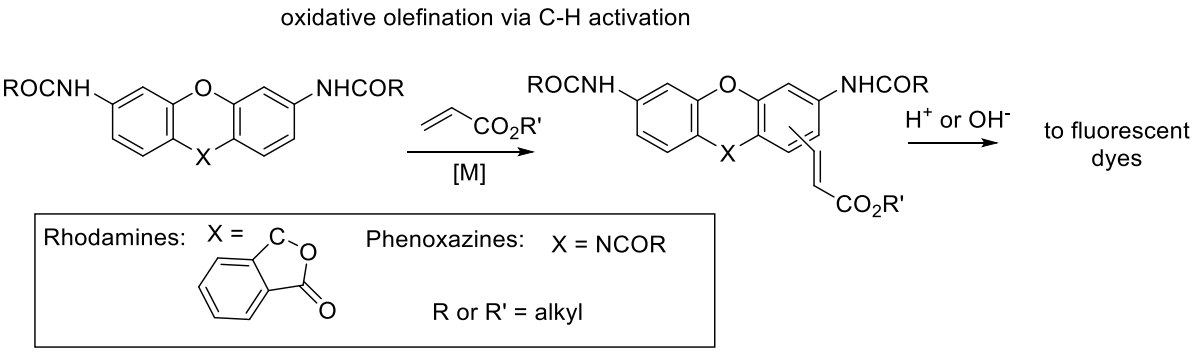

Scheme 29. General synthetic route towards rhodamine and oxazine dyes.

3.1 C–H activation – general information

When discussing carbon-carbon bond formation, the most prominent methods that come to mind are transition metal (TM) catalysed cross-coupling reactions (2010 Nobel Prize in Chemistry for palladium-catalysed cross-couplings in organic synthesis).[8] Despite undeniable advances, cross-couplings require two pre-functionalised substrates, and therefore lead to lengthy syntheses and the formation of undesirable side products in stoichiometric amounts. As a better alternative, TM catalysed C–H activation allows C–C bond formation through the cleavage of an available C–H bond without any pre-functionalisation, minimizing the generation of often hazardous waste. There is a broad scope of C–C bond formation reactions enabled by C–H activation. They include arylation, alkenylation, allylation, alkylation, cyanation, and other chemical transformations.[5-7] The original Fujiwara-Moritani reaction refers to the introduction of olefin moiety to arene (Scheme 30A), was reported in 1967.[9] However, it was not widely used by organic chemists due to its typically harsh reaction conditions, such as acidic, or oxidative reagents, and heating at high temperatures: the conditions which most functional groups cannot tolerate. Moreover, this reaction involves non-directed C–H activation with poor selectivity, and the use of an excess of arenes (solvent amounts). Despite these inconveniences and challenges, the mentioned reaction has gained a significant importance in modern organic synthesis and established itself as a valuable methodology in the field of C–H transformations. One of the most important advancements in this reaction is the use of directing groups[10] that influence the regioselectivity and/or stereoselectivity[11] of the transformation (Scheme 30B).

Thus, the directed C–H oxidative olefination represents a significant advantage compared to non-directed reaction. The term "directed" refers to the selectivity of the reaction: it means that the catalyst is designed in such a way that it targets the specific C–H bonds within the organic substrate. This kind of selectivity is essential, because most organic compounds contain multiple C–H bonds, and if the reaction is directed to a specific site, the unwanted side reactions are “blocked” and the regioselectivity is improved.

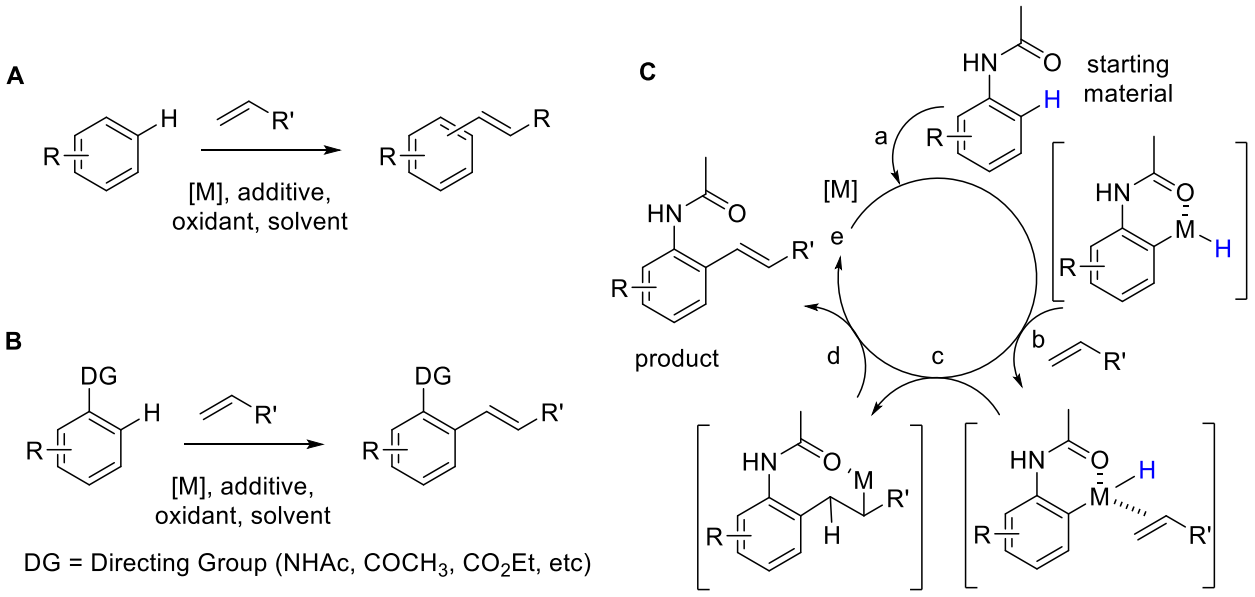

Scheme 30. A: Non-directed Fujiwara-Moritani oxidative olefination; B: Directed C–H oxidative olefination; C: Mechanism of the *ortho*-directed M-catalysed oxidative olefination of arenes, M = metal catalyst; a) coordination of the arene *via* C–H activation; b) olefin insertion; c) migratory olefin insertion; d) reductive elimination upon β-hydride elimination; e) catalyst regeneration.

The directing groups are Lewis-basic functional groups with lone electron pairs that influence the regioselectivity and/or stereoselectivity of a chemical reaction. In the process of C–H activation, the directing groups form and hold the catalytic metal complex in the close proximity to the certain ("desired") C–H site to be functionalised, and thereby, these DGs increase reactivity and improve selectivity. This approach is known as chelation-assisted C–H activation, as the catalyst forms a chelate complex with the substrate (Scheme 30C).[5-7] This is why the majority of directing groups are *ortho*-directing groups.[10,12] For example, amides[12a-c] and structurally related 2-pyrrolidones[12d] and 2-pyridones[12e] are widely used as *ortho*-directing groups for oxidative olefination. Various metal complexes based mostly on ruthenium,[12a,d,e] rhodium,[12b,c] and palladium[12f] (Figure 20) have shown high catalytic activity in various oxidative olefinations that proceed via C–H activation. The exact mechanism can vary depending on the specific catalytic system and reagents used. Scheme 30C briefly illustrates the general mechanism of the *ortho*-directed metal-catalysed oxidative olefination of arenes which includes 3 important steps:[12]

1. Coordination of the arene *via* C–H activation: The aromatic compound coordinates to the activated metal catalyst. This interaction is guided by DG (route a), and the chelate metal-aryl intermediate is formed. This step is often considered as one of the key steps in the reaction.

2. Olefin insertion: The metal-aryl intermediate coordinates the olefin (route b). Thereafter, migratory olefin insertion delivers a new C–C bond between aryl and olefin species (route c).

3. Reductive elimination: The final step of the cycle involves the reductive elimination (route d) of the metal species from the olefinated product upon β-hydride elimination, regenerating the active metal catalyst by oxidation (route e) for the next catalytic cycle. This is why there is "oxidative" in the name of reaction (oxidative olefination), as it indicates that the reaction involves the use of an oxidizing agent, typically molecular oxygen (O_2) from air, or a metal-based oxidant. The oxidant serves as the terminal acceptor of the hydrogen atom removed from the C–H bond, leading to the formation of the carbon-carbon double bond.

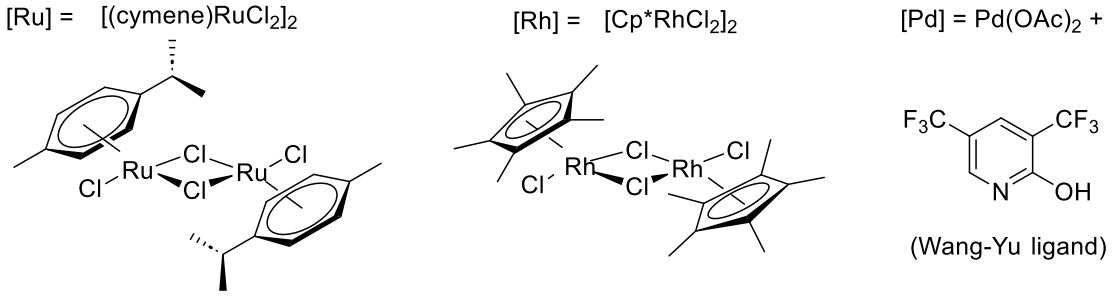

Figure 20. The most used catalysts for oxidative C–H olefination.

Although the majority of chelation-assisted C–C bond-forming reactions involve an *ortho*-selective transformation, various directing patterns have been developed based on distance and geometry correlations for use in C–H *meta*- and *para*- selective activation reactions.[13]

Diverse directing groups incorporating heteroatoms, such as nitrogen, oxygen, phosphorus and sulfur as coordinating sites have been designed and are currently in use.[5-7] Nevertheless, certain groups are neither easily installed, nor easily removed or converted into more useful functionalities. One of the most important features of organic dyes is that they naturally possess amino groups, that can be easily transformed into directing groups like amides.[14] Unfortunately, despite many examples available for oxidative olefination of arenes[6-13], no data was reported for the domain of fluorescent dyes.

3.3 Rhodamines

Discovered in the late 19th century, the chemistry of rhodamines continuously evolved and expanded over the years.[2] These remarkable compounds belong to the family of xanthene, sharing structural similarities with rhodol and fluorescein (Figure 21). The presence of a carboxyl group at the *ortho* position of the phenyl ring attached to the *meso* position (C-9) of the xanthene core is very important, as this group is responsible for the equilibrium between open (zwitterion, fluorescent) and closed (spirolactone, non-fluorescent) forms (Scheme 31). The spirolactone form is more hydrophobic than the zwitterion, which makes rhodamine-based fluorescent probes cell-permeable.[15] Commercially available rhodamine 110 was chosen as a model compound for studying C–H activation and performing optimisation of the reaction conditions. The sequence of derivatisation involves only three steps: protection of the amino group, C–H functionalisation via oxidative olefination, and final deprotection (Scheme 32).

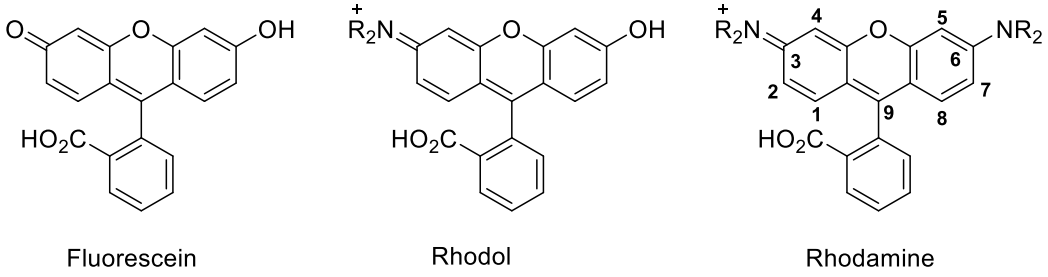

Figure 21. Xanthene dyes.

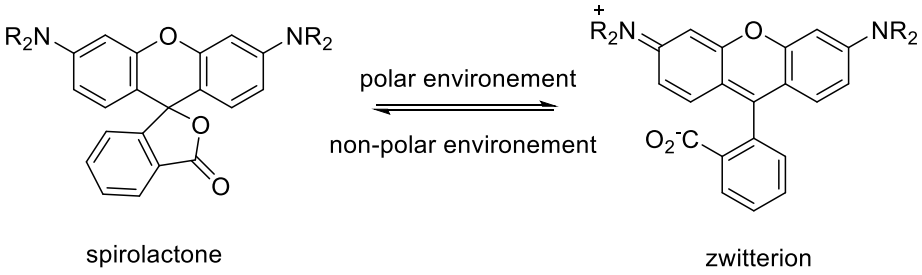

Scheme 31. Equilibrium of rhodamine between two forms: an "open"/fluorescent (zwitterion) form and a "closed"/nonfluorescent (spirolactone) form.

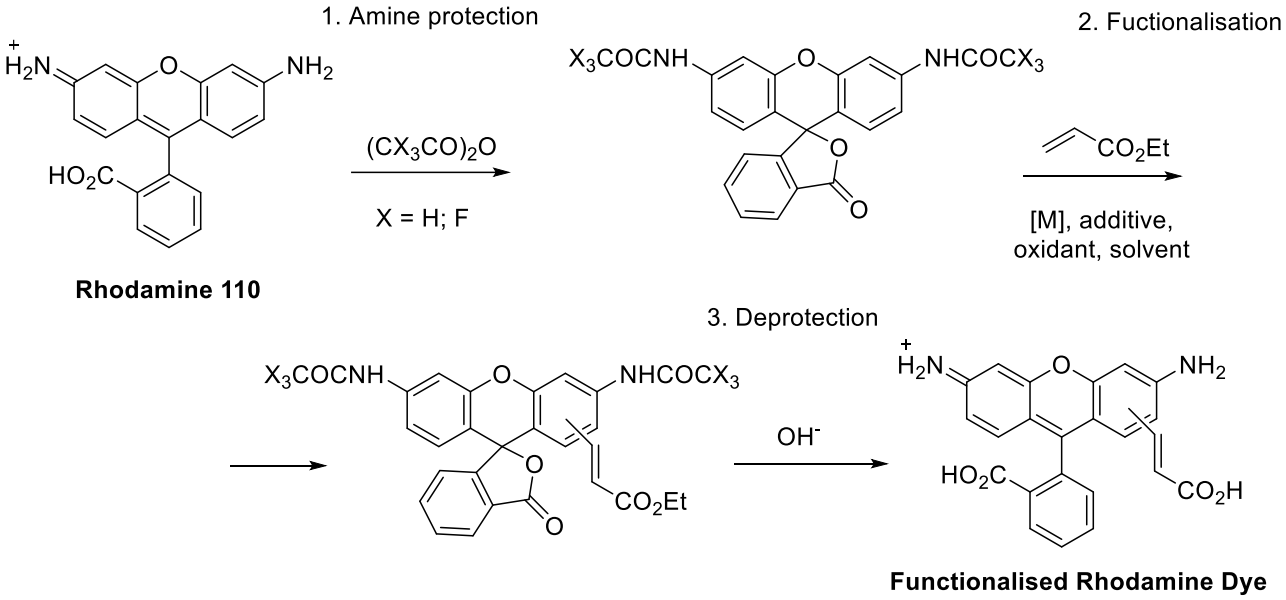

Scheme 32. Synthesis of functionalised rhodamines by C–H activation.

3.3.1 *N,N′*-bis(acetyl) rhodamine 110 as a substrate for oxidative olefination

Rhodamine 110 (compound **61**) is a commercially available dye, in which two amino groups can be easily acetylated to form NHAc directing group (Scheme 33).[16] The *N,N′*-bis(acetyl) rhodamine 110 (compound **62**) exists as spirolactone, and is colourless due to its closed-ring structure and the absence of a conjugated system. The formation of **62** goes smoothly and with a good yield (80%).

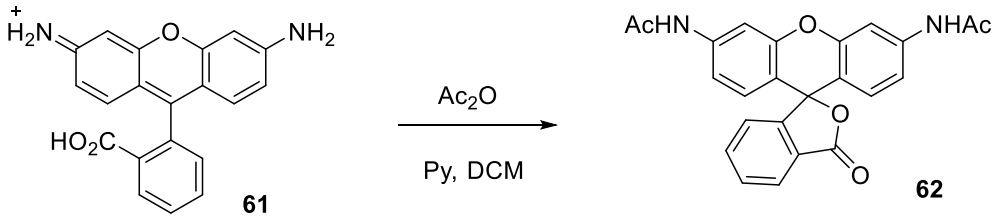

Scheme 33. Synthesis of *N,N′*-bis(acetyl) rhodamine 110 (compound **62**).

The selection of ethyl acrylate as a coupling partner in C–H olefination of **62** was driven by the need to achieve simultaneous deprotection of amino and carboxyl groups under the same (basic) conditions.[14] Various reaction conditions for oxidative olefination have been tested in order to find the most suitable ones for involving rhodamine 110 *N,N′*-diacetate **62** (Scheme 34).

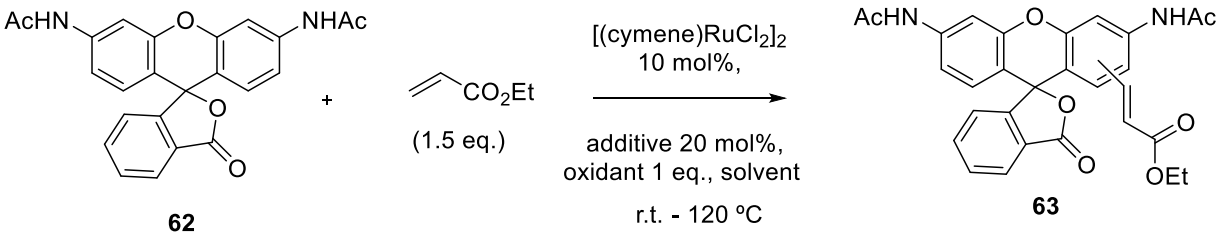

62 **63**

Scheme 34. Ru-catalysed oxidative olefination of *N*,*N'*-bis(acetyl) rhodamine 110 (**62**) for the optimisation of reaction conditions and studying product distribution.

The initial conditions were as follows: 1.5 eq. of ethyl acrylate, dimeric complex of Ruthenium(II) $[(cymene)RuCl_2]_2$ (for the structure, see Figure 20) as a catalyst (10 mol%), KPF_6 as a chloride scavenger (20 mol%), and $Cu(OAc)_2*H_2O$ as an oxidant (1 eq.) in DMA as a solvent. The reaction was carried at 120 °C, under Ar, for 16 h. Pleasingly, the first test gave the desired oxidative olefination products, but resulted in a mixture. The change of the scavenger to $AgSbF_6$ led to a better conversion (64% instead of 45%, HPLC calculated, entry 3, Table 8). However, the mixture of olefinated products was still present. This mixture was separated by reversed-phase chromatography, and the structure of each compound was established by means of 1D and 2D NMR. The structures of the isolated products are given in Figure 22. Among two mono-olefinated isomers (referred to as isomers "A" **63a** and "B" **63b**, Figure 22), several poly-olefinated compounds (**64**-**65**, Figure 22) were found. The 1,2-disubstituted CH=CH double bond in compounds **63**-**65** displayed *E*-configuration according to the high values of $^3J_{H,H}$ coupling constant (*ca*. 16 Hz).[17] The trace amount of *Z*-olefin was also detected (for compound **63b**) with $^3J_{H,H}$ coupling constant of 12 Hz. The formation of a mixture of positional isomers was not surprising, as each NHAc directing group has two *ortho* C–H bonds. Achieving full control over regioselectivity is challenging in C–H transformations, as in complex molecules like rhodamines, the "guidance" of the DG alone is not sufficient for good regioselectivity. This is why further changes of the reaction conditions were made.

We sought the optimal conditions that favour the formation of only one isomer. The use of benzoquinone as oxidant (entries 5, 6, Table 8) did not result in any conversion. Changing the solvent drastically affected the outcome. The reaction in a less polar dioxane offered better conversion in the presence of air (82%, entry 10, Table 8), but still produced 2 mono-isomers A

and B that were difficult to separate. The use of acetone as solvent in the presence of air resulted in 90% conversion of compound **62** and selective formation of one mono-olefinated positional isomer A (entry 12, Table 8). However, bis- and tris- olefinated products were still present. Changing the oxidant and decreasing the temperature did not lead to any improvement (entries 11, 13, 14, Table 8). The isolated yield of each isomer is given in Table 9, column [Ru].

Table 8. Optimisation of the reaction conditions for Ru-catalysed oxidative olefination of *N*,*N'*-bis(acetyl) rhodamine 110 (**62**, Scheme 34).

Entry	Additive	Solvent	Oxidant	T, ºC	Air/Ar	Conversion
1	KPF_6	DMA	$Cu(OAc)_2*H_2O$	120	Ar	45%
2	KPF_6	DMA	$Cu(OAc)_2*H_2O$	120	air	0
3	$AgSbF_6$	DMA	$Cu(OAc)_2*H_2O$	120	Ar	64%
4	$AgSbF_6$	DMA	$Cu(OAc)_2*H_2O$	60	Ar	<5%
5	KPF_6	DMA	benzoquinone	120	Ar	0
6	KPF_6	DMA	benzoquinone	120	air	0
7	KPF_6	H_2O	$Cu(OAc)_2*H_2O$	120	Ar	0
8	KPF_6	1,4-dioxane	$Cu(OAc)_2*H_2O$	120	Ar	13%
9	$AgSbF_6$	1,4-dioxane	$Cu(OAc)_2*H_2O$	110	Ar	20%
10	$AgSbF_6$	1,4-dioxane	$Cu(OAc)_2*H_2O$	110	air	82%
11	$AgSbF_6$	1,4-dioxane	benzoquinone	110	air	<5%
12	**$AgSbF_6$**	**acetone**	**$Cu(OAc)_2*H_2O$**	**70**	**air**	**90%**
13	$AgSbF_6$	acetone	benzoquinone	70	air	<5%
14	$AgSbF_6$	acetone	$Cu(OAc)_2*H_2O$	25	air	<5%

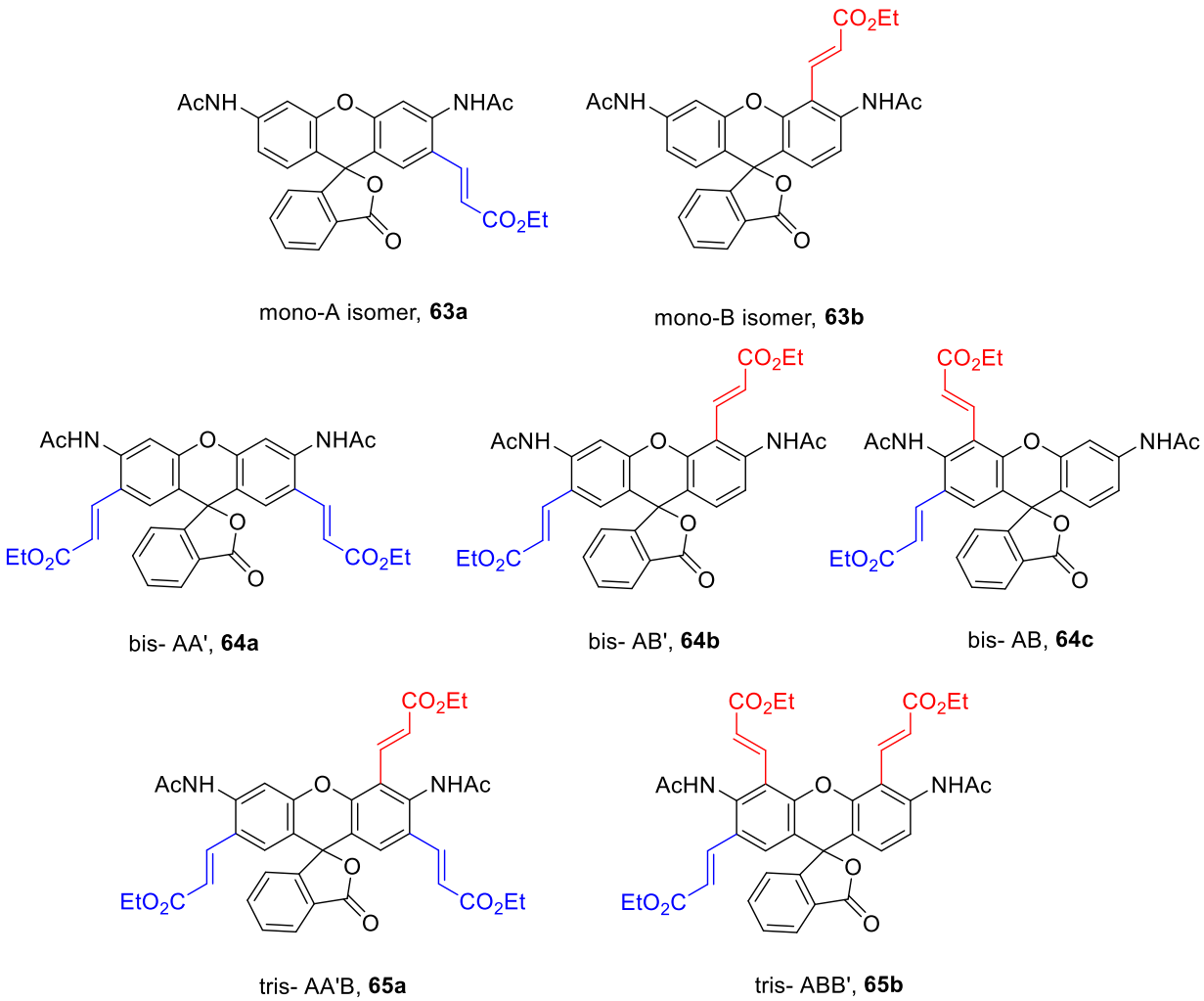

Figure 22. Structures of isolated products of Ru/Rh-catalysed oxidative olefination of compound **62** reacting with ethyl acrylate.

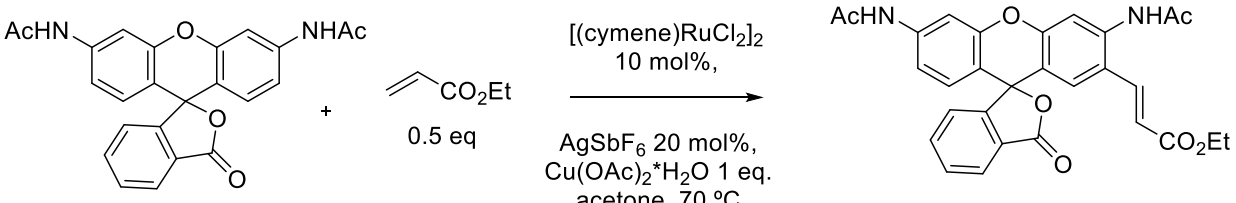

Scheme 35. Ru-catalysed oxidative olefination of *N*,*N'*-bis(acetyl) rhodamine 110 (**62**) under optimised conditions.

To avoid formation of poly-olefinated products, the reaction was carried out with a smaller amount of acrylate (0.5 eq. instead of 1.5). The preparative yield of the desired isomer A (**63a**, Scheme 35) slightly diminished (35% instead of 40%), but the separation became easier, and the unreacted starting material can be easily recovered from the reaction mixture.

Inspired by these promising results, we wondered whether we could selectively obtain isomer B (**63b**, Figure 22). The term "directed" refers to the selectivity of the reaction, meaning that the catalyst is also designed to target specific C–H bonds within the organic substrate. This is why in the next experiments we opted to investigate the catalyst's impact on the C–H activation process. Among the developed catalytic systems, a notable candidate is a dimeric rhodium complex with a pentamethylcyclopentadienyl (Cp*) ligand known as $[Cp^*RhCl_2]_2$, which proved to be an efficient catalyst for directed C–H oxidative olefination of arenes (Figure 20).[12b] Additionally, a complex with modified cyclopentadienyl ligand, bis[(1,2,3,4,5-η)-1,3-bis(ethoxycarbonyl)-2,4,5-trimethyl-2,4-cyclopentadien-1-yl]di-μ-chlorodichlorodirhodium has been reported to catalyse the reaction at room temperature[12c], which may be crucial for unstable compounds.

In following experiments, the performance of the $[Cp^*RhCl_2]_2$ catalyst was evaluated (Scheme 36). The conditions established for [Ru] catalysis were used. The reaction resulted in the preferential formation of the isomer B (compound **63b**) together with poly-olefinated products. The isolated yield of each product is given in Table 9, column [Rh]. Unfortunately, compound **62** doesn't undergo C–H activation process at room temperature. Same as for ruthenium, the double bond showed *E*-configuration according to the values of $^3J_{H,H}$ coupling constant (*ca.* 16 Hz)[17] observed for the olefinic protons by means of ^{1}H NMR spectroscopy. To prevent the formation of poly-olefinated products, the reaction was carried with 0.5 eq. of ethyl acrylate. The resulting **63b** was isolated in 30% yield, the separation was facile, and the unreacted starting material was successfully recovered (Scheme 36).

Table 9. Isolated yields of products forming under Ru or Rh catalysis at optimised conditions (ethyl acrylate 1.5 eq., [M] 10 mol%, $AgSbF_6$ 20 mol%, $Cu(OAc)_2*H_2O$ 1 eq., air, acetone, 70 ºC).

Entry	Compound	[Ru], isolated yield, %	[Rh], isolated yield, %
1	**63a**	40	10
2	**63b**	2	38
3	**64a**	24	Not found
4	**64b**	6	7
5	**64c**	Traces, not isolated	10
6	**65a**	6	Traces, not isolated
7	**65b**	Traces, not isolated	29

In following experiments, the performance of the $[Cp*RhCl_2]_2$ catalyst was evaluated (Scheme 36). The conditions established for [Ru] catalysis were used. The reaction resulted in the preferential formation of the isomer B (compound **63b**) together with poly-olefinated products. The isolated yield of each product is given in Table 9, column [Rh]. Unfortunately, compound **62** doesn't undergo C–H activation process at room temperature. Same as for ruthenium, the double bond showed *E*-configuration according to the values of $^3J_{H,H}$ coupling constant (*ca.* 16 Hz)[17] observed for the olefinic protons by means of ^{1}H NMR spectroscopy. To prevent the formation of poly-olefinated products, the reaction was carried with 0.5 eq. of ethyl acrylate. The resulting **63b** was isolated in 30% yield, the separation was facile, and the unreacted starting material was successfully recovered (Scheme 36).

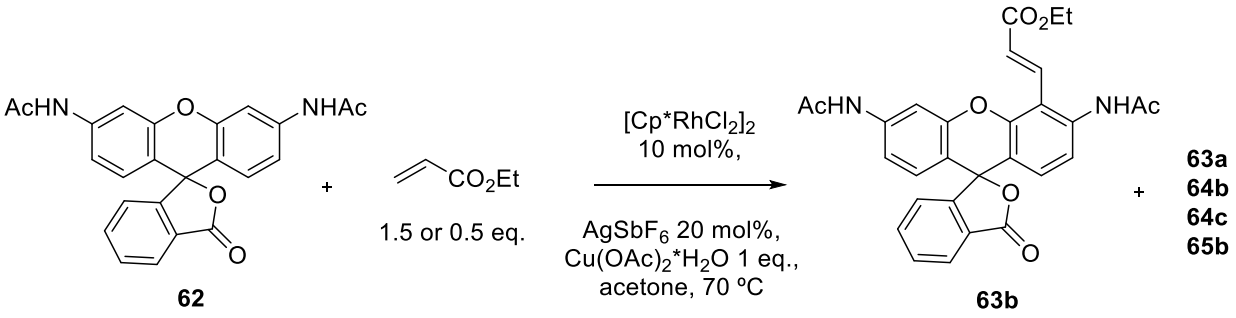

Scheme 36. Rh-catalysed oxidative olefination of *N*,*N'*-bis(acetyl) rhodamine 110 (**62**) under optimised conditions.

3.3.2 *N,N'*-Bis(trifluoroacetyl) rhodamine as a substrate for oxidative olefination

After conducting the oxidative olefination reactions of *N,N'*-bis(acetyl) rhodamine 110 (**62**) and finding conditions providing catalyst-dependent regioselectivity and satisfactory conversion, we became curious about the influence of the directing group on the reaction outcome. The rationale behind choosing trifluoroacetyl amide as a new directing group stems from its advantages over acetyl. Previous studies on pyrenes[18] and cyanines[19] have demonstrated that the trifluoroacetyl group permits *N*-alkylation under milder conditions, thereby facilitating further functionalisation of rhodamine. This feature allows the introduction of different substituents at nitrogen, resulting in a red shift of the absorption and emission maxima.[20] Additionally, the cleavage of the trifluoroacetyl group is known to occur more easily than that of the acetyl, as the latter often requires boiling with HCl or NaOH.[14] Finally, we did not find any results in the literature, where the trifluoroacetamide group was mentioned as a DG for oxidative olefination, which makes it more intriguing to investigate its directing ability in this case.

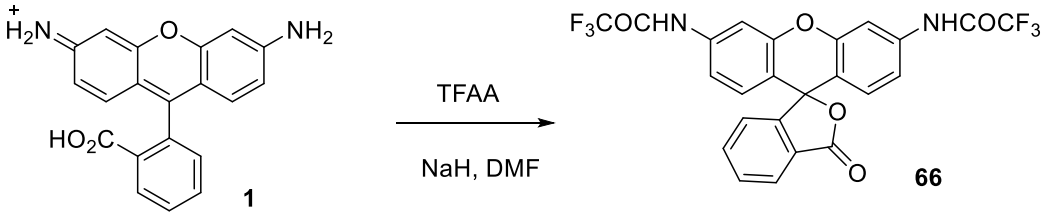

Scheme 37. Synthesis of *N,N'*-bis(trifluoroacetyl) rhodamine 110 (compound **66**).

N,N'-Bis(trifluoroacetyl) rhodamine 110 (**66**, Scheme 37) was successfully obtained (with 75% yield) following a reported procedure.[21] Then, we investigated the applicability of the established oxidative olefination protocol on compound **66** (Scheme 38). Unfortunately, the optimised conditions using the ruthenium catalyst did not result in any conversion of the starting material. Alternatively, employing the rhodium catalyst resulted only in a modest conversion after 18 h (20%, Table 10). Even with an extended reaction time of 72 h, the improvement in conversion was minimal, reaching only 23%. The reason for such a poor reactivity probably lies in the electronic properties of the molecule. By comparing the electron-withdrawing abilities of the directing groups, we found evident that the CF_3CONH group exhibits a slightly stronger electron-

accepting effect (σ_m 0.30, σ_p 0.12) compared to the CH_3CONH group (σ_m 0.21, σ_p 0.00).[22] This may explain the inertness of **66** (Scheme 38) compared to **62** (Schemes 35, 36).

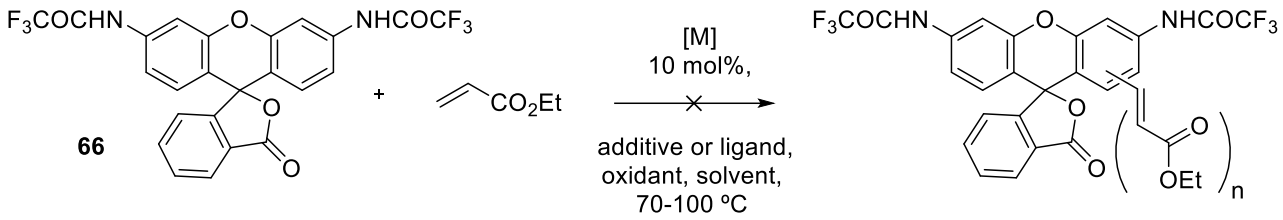

Scheme 38. M-catalysed oxidative olefination of *N*,*N'*-bis(trifluoroacetyl) rhodamine 110 (**66**). For details, see Table 10.

To sum up, it appears that *N*-trifluoroacetyl amide is not a suitable directing group for the Ru/Rh catalysed oxidative olefination. The *N*-trifluoroacylated compound requires additional "guidance" to undergo the desired transformation. Luckily, there has been recent progress in the development of a catalytic system that allows ligand-controlled C–H activation,[23] even for substrates lacking an appropriate directing group (*e.g.*, NHAc). This innovative system involves a complex of a substituted 2-pyridone ligand (commercially available as the Wang-Yu ligand, see Figure 20) bound to palladium. The presence of this ligand significantly accelerates the non-directed C–H oxidative olefination of arenes, enabling the successful olefination of less-reactive electron-deficient arenes as well.[23]

Hence, the introduction of *N*,*N'*-bis(trifluoroacetyl) rhodamine 110 (**66**, Scheme 38) into oxidative olefination under Pd catalysis was attempted, using conditions previously reported in [23]. Unfortunately, even with an excess of acrylate (2 eq.), no conversion has been achieved within 24 h (Table 10, entry 4). The change of the solvent to acetone brought only a slight improvement and led to conversion of 12% (Table 10, entry 5).

Due to the challenges presented by Pd-catalysed oxidative olefination, including the less favourable reaction conditions compared to Ru or Rh catalysis (the need for a large amount of oxidant AgOAc – 3 eq., and the expense of the ligand itself - 266 EUR for 250 mg, available at Sigma Aldrich), the Pd-catalysed ligand-controlled C–H activation of *N*,*N'*-bis(trifluoroacetyl) rhodamines does not seem to be a superior alternative for preparing new rhodamine fluorophores. However, it has been demonstrated that the rhodamine 110 protected by trifluoroacetyl group did not undergo deprotection under reaction conditions, and showed partial activity under Rh or Pd

catalysis. These findings may be significant for the further development of C–H activation studies involving trifluoroacetyl protected arylamines. This may be crucial for the compounds having the trifluoroacetyl group as the only possible protection of the amino group.

Table 10. M-catalysed oxidative olefination of **66** (Scheme 38).

Entry	[M] catalyst, 10 mol %	Additive /ligand, 20 mol %	Oxidant, 1 eq.	Time, h	Temperature, ºC	Conversion (HPLC)
1	[Ru]	$AgSbF_6$	$Cu(OAc)_2*H_2O$	18	70	0
2	[Rh]	$AgSbF_6$	$Cu(OAc)_2*H_2O$	18	70	20
3	[Rh]	$AgSbF_6$	$Cu(OAc)_2*H_2O$	72	70	23
4	[Pd][a]	Wang-Yu ligand	AgOAc, 3 eq.	24	100	0
5	[Pd][b]	Wang-Yu ligand	AgOAc, 3 eq.	24	75	12

[a] in HFIP; [b] in acetone.

3.3.3 Photophysical properties of new rhodamine dyes

The deprotection of amino groups in derivatives of rhodamine 110 (compounds **63**-**65**, Figure 22) leads to the formation of fluorescent dyes. Acetamides are rather difficult to hydrolyse.[14] The test hydrolysis experiments were performed for compound **63a** under both basic and acidic conditions (Scheme 39). Boiling with 25% HCl in EtOH results in a mixture of products where the "destroyed" rhodamine core was present (Scheme 39, A). The acidic hydrolysis (HCl, or TFA) at r.t. requires longer reaction time (approx. 1 week), but shows more pure reaction. Boiling with 20% aq. NaOH in EtOH (1:1) leads to a mixture of compounds too, but the fluorophore is not touched by destruction, and the product of intramolecular cyclization **69** was found (Scheme 39, B). A similar result was obtained after the basic hydrolysis of **63b** (Scheme 40) and **64a** (Scheme 41): partial lactamization of functionalised rhodamines **68**, **70**, **72** takes place in the presence of base (NaOH). To confirm the structure of lactam, compound **73** (Scheme 41) was isolated and its structure was confirmed by ^{1}H NMR. This type of cyclization leading to lactams might be useful in the synthesis of the fused-ring rhodamines such as Q-Rhodamine.[24]

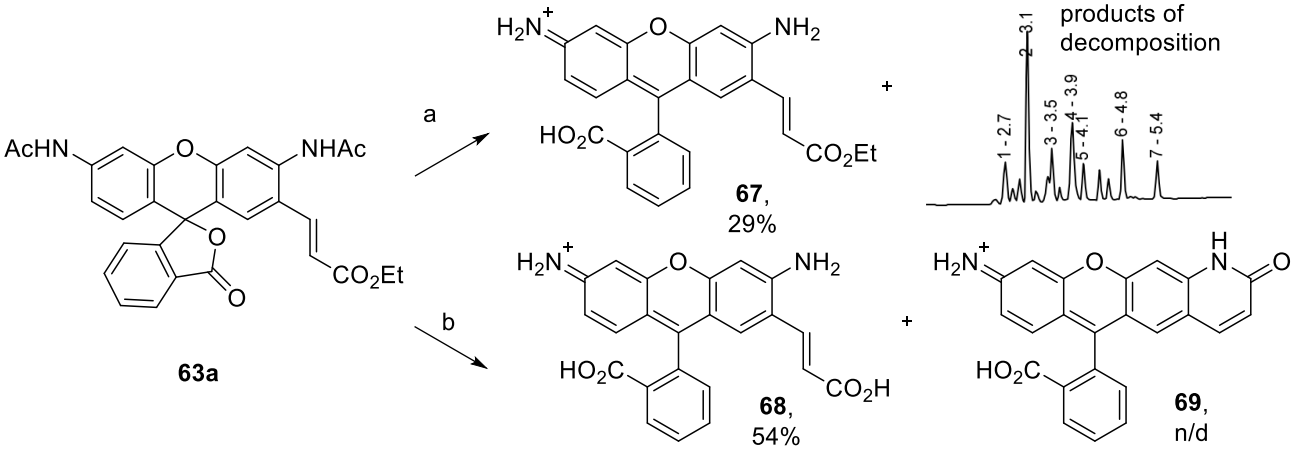

Scheme 39. Hydrolysis of **63a** under acidic (pathway a: 25% aq. HCl, EtOH, 90 ºC) and basic (pathway b: 20% aq. NaOH, EtOH, 90 ºC) conditions. Yields of isolated products are given.

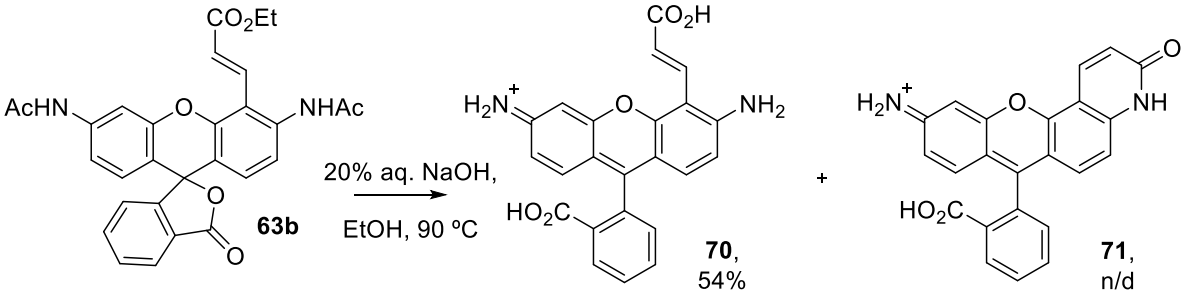

Scheme 40. Basic hydrolysis of compound **63b**.

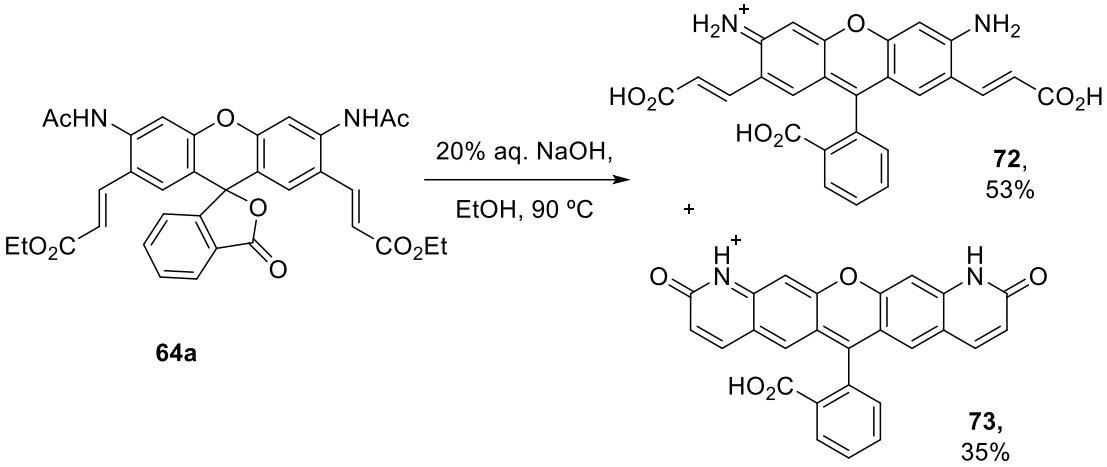

Scheme 41. Basic hydrolysis of compound **64a**.

Rhodamines owe their name to the beautiful pink to red hues observed when they are exposed to light (Greek *rhodon* (ῥόδον) meaning "rose"). The orange-pink-coloured rhodamines **68**, 7**0**, 7**2**, 7**4** (Figure 23) were isolated and their photophysical properties were measured in EtOH (Table 11). For comparison, the properties of the parental rhodamine 110 (**61**, Figure 23) are also given in the same table.

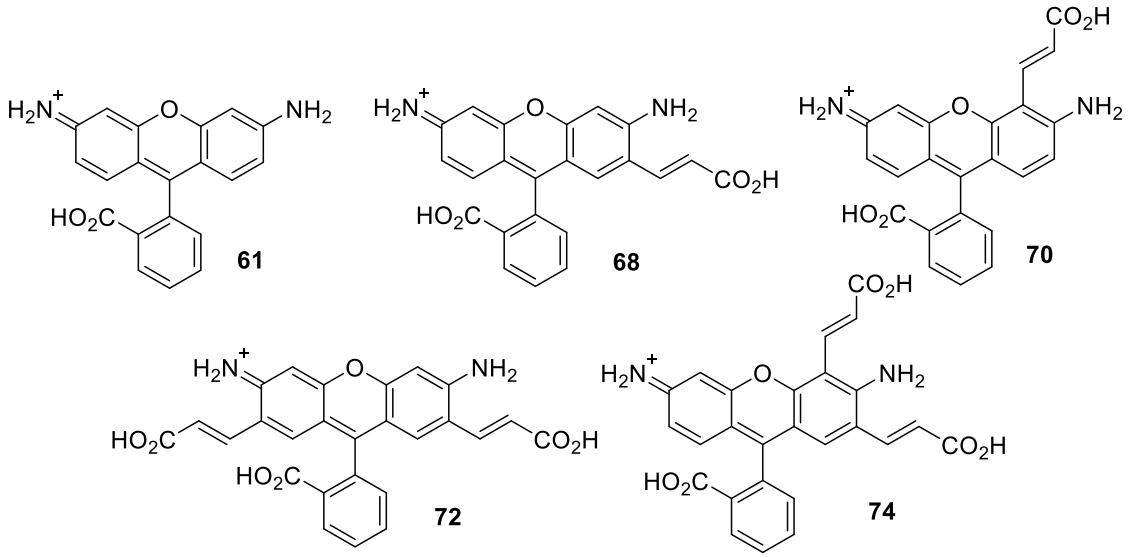

Figure 23. Parental rhodamine 110 (**61**) and its derivatives – acrylated rhodamines **68**, **70**, **72**, **74**.

The presence of an acrylate moiety (σ_m 0.30, σ_p 0.12)[22] at position 4 (compound **70**) or 2 (compound **68**) of the xanthene chromophore provided a bathochromic effect for both the absorption and emission maxima, and this effect is stronger for the compound having a substituent at position 2 (compound **68**). However, the fluorescence efficiency (fluorescence quantum yield) remains similar for all compounds. The new dyes **68**, **70**, **72**, **74** have larger Stokes shift, which is due to the asymmetry[20] of the fluorophore (Table 11). Asymmetrical molecules may be more sensitive to variations in solvent polarity, molecular conformation, or interactions with neighbouring molecules, all of which can influence the energy levels and relaxation pathways involved in absorption and emission processes.

Table 11. Photophysical properties of rhodamine 110 derivatives in EtOH.

Dye	λ_{abs}, nm	λ_{em}, nm	Stokes shift	ε,[a] $M^{-1}cm^{-1}$	Φ_{fl}[b], %	Fluor. lifetime, ns
61	501	524	23	75 000	88	3.9
68	518	548	30	77 000	88	3.6
70	505	533	28	74 000	77	3.2
72	545	580	35	77 000	88	3.5
74	524	556	32	75 000	85	3.3

[a] molar extinction coefficient; [b] absolute values of fluorescence quantum yield.

3.4 Oxazines

Oxazines, also known as phenoxazinium dyes, represent a class of organic compounds applicable as dyes and staining agents across various scientific and industrial domains.[3] Structurally, they comprise two phenyl rings fused with a 1,4-oxazine ring, as depicted in Figure 24. 3,7-Dihydroxy-substituted derivatives relate to the resorufin type fluorescent dyes which are widely used for detecting various analytes, as redox-sensitive indicators and other.[25] The presence of amino groups at positions 3 and 7 imparts distinct photophysical and chemical attributes to these dyes. They exist in oxidised form as phenoxazinium salt (fluorescent) and reduced form (non-fluorescent) 3,7-diaminophenoxazine (Scheme 42). Prominent examples, such as Oxazine 1, Atto 655, along with benzophenoxazines Nile Blue and Nile Red, find extensive use as staining reagents for biological samples, chemical reaction indicators, and drugs for photodynamic therapy.[26-29]

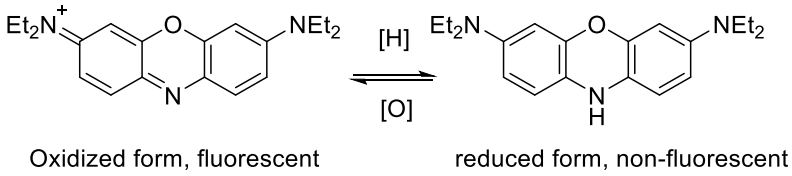

Scheme 42. Oxidised and reduced forms of oxazine 1.

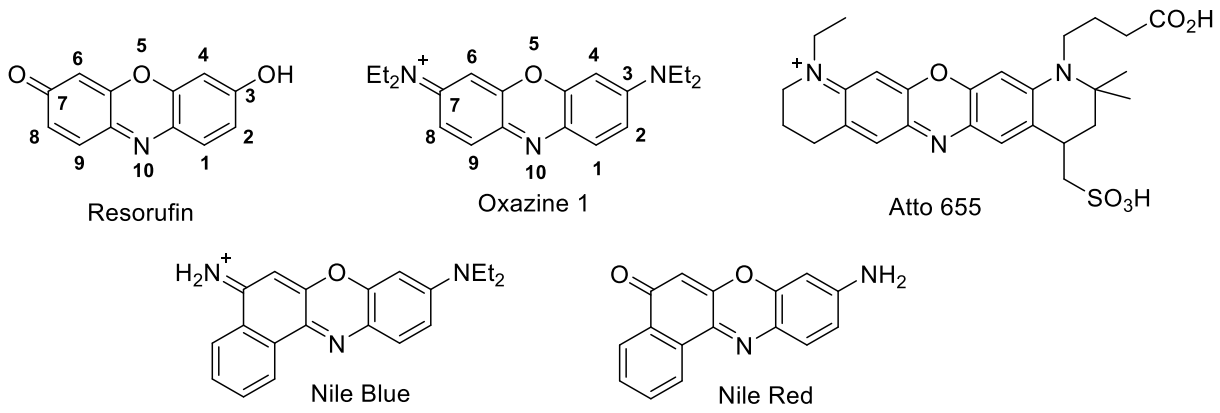

Figure 24. Oxazine dyes (resorufin, oxazine 1, and Atto 655) and benzophenoxazine (Nile Blue and Nile red) dyes.

Although some 3,7-diaminophenoxazines have found application in fluorescent microscopy,[4] the set of useful oxazines remains limited, especially if we consider the absence of naturally occurring carboxylic groups for biomolecule conjugation in most of them. Consequently, a reliable method for diversification of the oxazine core could unlock a treasure trove of valuable structural possibilities for various applications, making oxazines an attractive and ever-evolving field of study.

Unlike rhodamines, 3,7-diaminophenoxazines and 3,7-diaminophenoxazinium salts are not commercially available and have to be prepared. The conventional approach for preparation of 3,7-diaminooxazine derivatives relies on acid-catalysed condensation of nitroso intermediates of 3-aminophenols.[3,29] This methodology often results in moderate to poor yields, and the complexity of the entire procedure limits its applicability for the synthesis of oxazine dyes. The synthesis of 3,7-diaminophenoxazines from unsubstituted phenoxazine was reported in 2003.[30] This method is attractive, because triacetylated precursor **78** is promising for C–H activation studies, and could be prepare in three steps from commercially available phenoxazine 7**5** (Scheme 43).

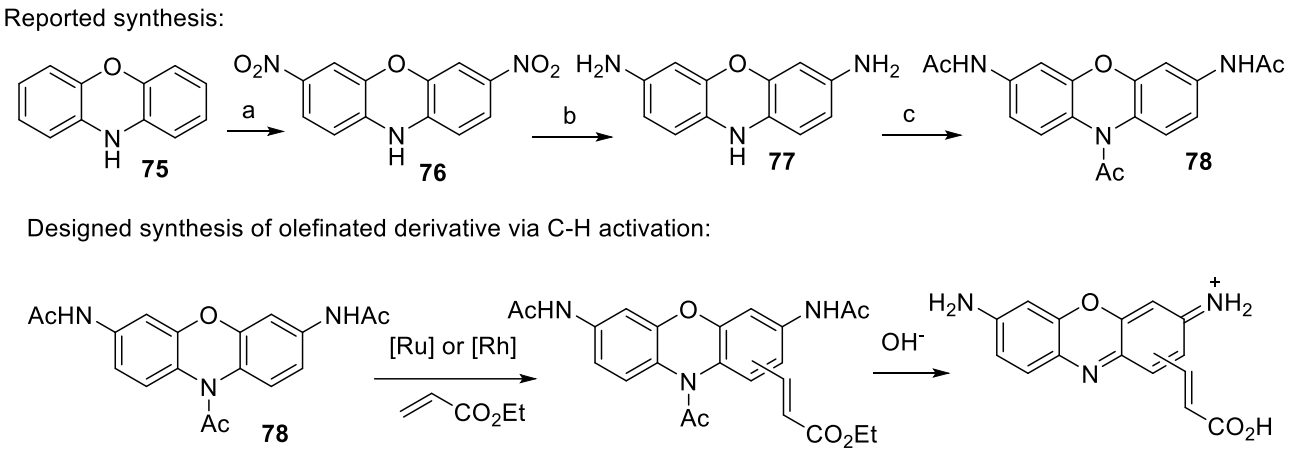

Scheme 43. Proposed synthetic route towards new oxazine dyes. Reagents and conditions: a) $NaNO_2$, AcOH, 3 days, r.t.; b) Fe, HCl, EtOH, 2 h, r.t.; c) AcCl, Et_3N, 1 h, r.t.

The choice of acetamide as a protecting is not solely determined by its directing ability in C–H activation. The bridged *N*-acetate provides an additional advantage, as it has been proved to be photocleavable, leading to an oxazine dye (as illustrated in Scheme 44). Notably, neither acid nor base was necessary for this transformation. The photolysis study was accomplished for 9-acetyl (or benzoyl) protected 3,7-bis(diethylamino)oxazines.[26, 31]

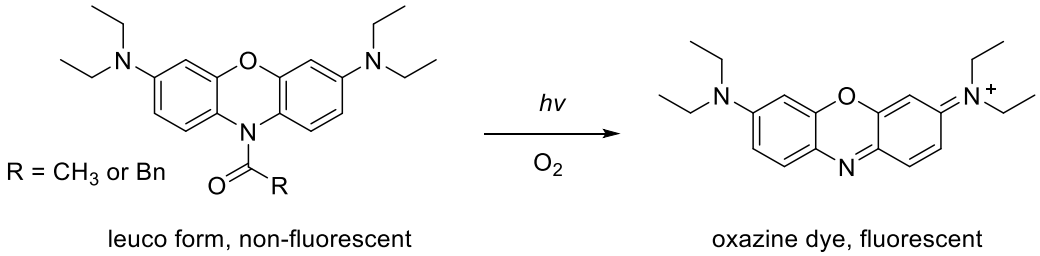

Scheme 44. Photolysis of 10-*N*-acyl phenoxazines (data from ref. 31).

Therefore, we focused on the development of a methodology allowing us to obtain functionalised oxazines using the C–H activation approach. As it was shown for rhodamines, this method allowed us to extend the conjugation and introduce a group for bioconjugation (acrylate) in 3 steps. Triacetylated 3,7-diaminophenoxazine **78** was required as a starting compound for oxidative olefination. The functionalised oxazines are expected to find applications in various fluorescent techniques.

3.4.1 *N*-Acetyl protected phenoxazines

To prepare compound **78**, commercially available phenoxazine **75** was subjected to nitration with sodium nitrite in the presence of acetic acid. It was then reduced using molecular hydrogen, and the resulting 3,7-diamino phenoxazine 7**7** was acetylated by acetic anhydride (as shown in Scheme 43, 1st line). Despite the reported procedure indicated good yields and a smooth process,[30] we encountered obstacles and very poor reproducibility at every step.

Firstly, the nitration with sodium nitrite resulted in a mixture of mono-, bis-, and tris-nitro phenoxazines that were difficult to separate (Scheme 45). Variation of the reaction time, temperature, and solvent, did not provide any improvement. Mono-, bis-, and tris- nitro phenoxazines exhibited poor solubility in common solvents. They tend to crystallize together and have nearly identical R_f values. The yield of the desired 3,7-dinitro phenoxazine **76** was only around 25%, and the reaction was difficult to scale up.

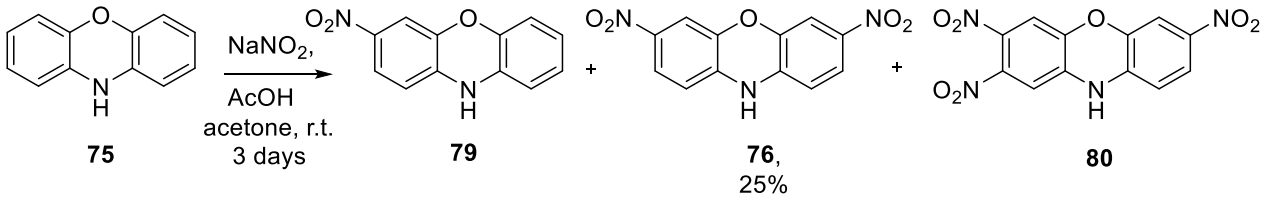

Scheme 45. Nitration of unsubstituted phenoxazine **75** provides a mixture of nitro-substituted compounds (**76**, **79**, **80**).

The reduction proceeds as described, but the stability of the resulting 3,7-diamino phenoxazine **77** is doubtful. To put it more exactly, compound **77** undergoes rapid oxidation upon exposure to air, forming dye **81** (Scheme 46). It was confirmed by ^{1}H NMR and HRMS measurements of the reaction product. A search of the literature revealed a study confirming that the colourless leuco dye **77** is oxidized immediately upon exposure to air, and gives the brilliant red fluorescent compound **81** as a free base.[32] However, in the original work from 2003,[30] no specific conditions for the isolation of compound **17** were mentioned (such as an inert atmosphere to avoid spontaneous oxidation on air).

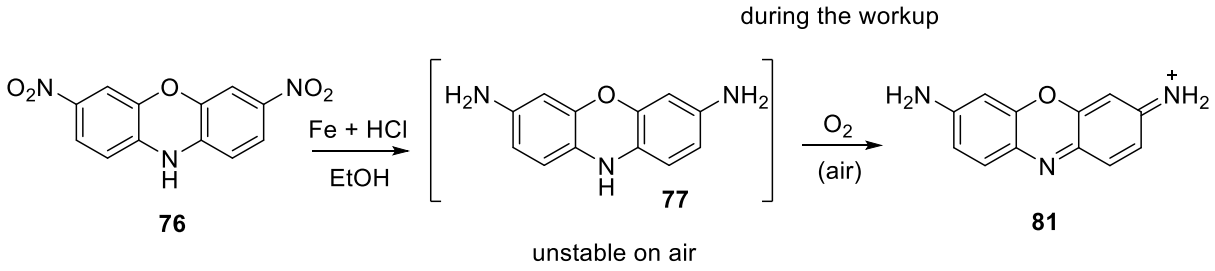

Scheme 46. Reduction of **76** followed by oxidation on air to give dye **81**.

To overcome these obstacles and make the method applicable and preparatively useful, the nitration procedure was combined with acetylation (these modifications are shown in Scheme 47). Upon nitration of phenoxazine **75**, the reaction mixture containing mono-, bis-, tris-, and (probably) tetrakis- nitrophenoxazines **76**, **79**, and **80** (Scheme 45) was subjected to acetylation in boiling acetic anhydride. It was observed that the isolation and purification of acetylated compound **82** by column chromatography was easier and more efficient than the isolation of amine **76** (Scheme 45). The desired compound **82** was isolated with a yield of 73%. This compound is more synthetically useful than amine **16**, as the bridged nitrogen is protected by the acetyl group, preventing oxidation when exposed to air.

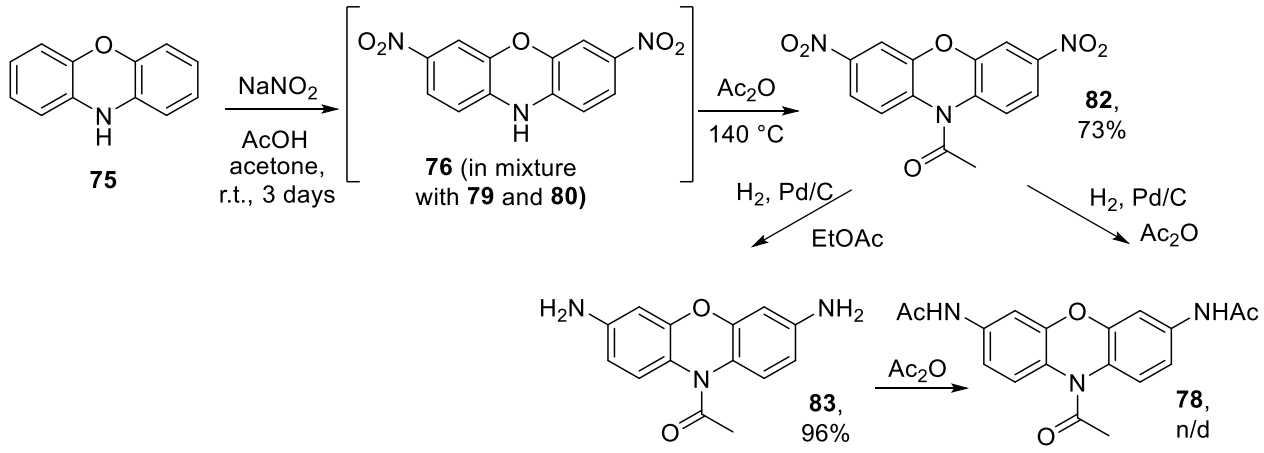

Scheme 47. An efficient route to triacetylated 3,7-diaminophenoxazine 7**8**.

Compound **82** was reduced to *N*-Acetyl-3,7-diaminophenoxazine **83**, which can be subsequently acetylated to yield the triacetylated compound **78** (Scheme 47). Additionally, it was demonstrated that the mono-acetylated compound **82** can be directly converted to **78** when

hydrogenation is carried out in acetic anhydride. However, both methods encountered unforeseen difficulties. The conversion **82** → **78** (or **83** → **78**) showed promising analytical results (TLC and LCMS indicated full conversion of the starting material, with the major component corresponding to the triacetylated product **78**), but the isolation of the target compound **78** proved unsuccessful. Various column chromatography techniques were tested, including both silica and alumina as stationary phases, and also reversed phase (C18), with various eluent systems (DCM-MeOH as reported in the original work,[30] DCM-acetone, or hexane-ethyl acetate). Unfortunately, none of these methods led to the successful isolation of the desired product. Curiously, the referenced paper[30] reports the easy purification of the target product on alumina with DCM-MeOH (0-10% gradient) as eluent affording a 91% yield of **78**.

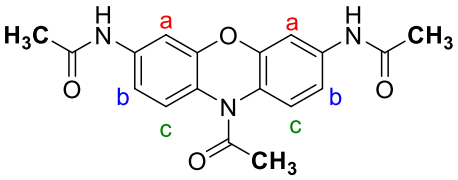

78

Chemical Formula: $C_{18}H_{17}N_3O_4$
Exact Mass: 339.12

Reported in ref. [30], δ in Me_2CO-d_6:

Acetyl protons:	3.75 (br s, 6H) 3.94 (br s, 3H)
Aromatic protons:	8.49 (m, 2H), 8.22 (m, 2H), 8.10 (m, 2H)
Amide protons:	10.38 (br s, 2H)

This study: δ in Me_2CO-d_6:

Acetyl protons:	2.08 (s, 6H) 2.27 (s, 3H)
Aromatic protons:	7.70 (d, J_{ab} = 2.3 Hz, 2H), 7.48 (d, J_{bc} = 8.7 Hz, 2H), 7.27 (dd, J_{cb} = 8.7, J_{ba} 2.4 Hz, 2H)
Amide protons:	9.34 (br s, 2H)

Figure 25. The structure of triacetylated 3,7-diaminophenoxazine **78** and the proton chemical shifts in acetone-d_6 from ref. [30] (on the left) and measured in this study (on the right).

The best achieved outcome was the isolation of only 3 mg of the compound **78** after loading approximately 70 mg of the crude product onto the column. Such a poor result is probably due to the instability of compound **78** on the column material (SiO_2 or Al_2O_3). It was a discouraging result, and we tried to find out the reason for the non-reproducibility by comparing the properties of the isolated compound with the reported data. Comparison of ^{1}H NMR spectra seemed to be as the most straightforward and reliable method. The signals were divided into three groups: acetyl ($C\underline{H}_3CONH$), aromatic (phenoxazine core), and amide ($CH_3CON\underline{H}$) protons (Figure 25). The ^{1}H NMR spectrum of isolated compound **78** was measured in acetone-d_6 as reported in [30]. The

proton spectrum of isolated compound **78** shows one singlet at 2.08 ppm (6H), and another one at 2.27 ppm (3H); they perfectly confirm the presence of two equivalent acetamide groups (s 2.08, 6H) and the bridged one (s 2.27, 3H) (Figure 25). The signals at 7.70-7.27 ppm correspond to the AMX spin system (confirmed by measuring *J* constants, Figure 25). The amide protons appeared at 9.34 ppm as a broad singlet which is typical for anilides.[33] Thus, the measured ^{1}H NMR spectrum of the isolated compound **78** perfectly fits the expected structure. The similar spectrum was obtained after measuring in MeOD; ^{1}H NMR (400 MHz, MeOD) δ 7.58 (d, *J* = 2.3 Hz, 2H), 7.47 (d, *J* = 8.7 Hz, 2H), 7.25 (dd, *J* = 8.7, 2.3 Hz, 2H), 2.31 (s, 3H), 2.13 (s, 6H). HRMS analysis confirmed the constitution of compound **78**: found 340.1292 $[M+H]^+$, calculated 340.1297 for $C_{18}H_{18}N_3O_4^+$. However, the reported ^{1}H NMR spectrum for the "same" compound is very different from the spectrum obtained by us, and in our opinion, these two spectra cannot be attributed to the same structure of compound **78**. The signal of acetyl protons of acetamide $\underline{CH_3}CONHR$ is normally located at around 2 ppm and rarely exceeds 2.5 ppm,[33] while the reported signals are around 3.7-3.9 ppm.[30] Due to this observation, we believe that the triacetylated phenoxazine **78** was not obtained by the reported procedure.

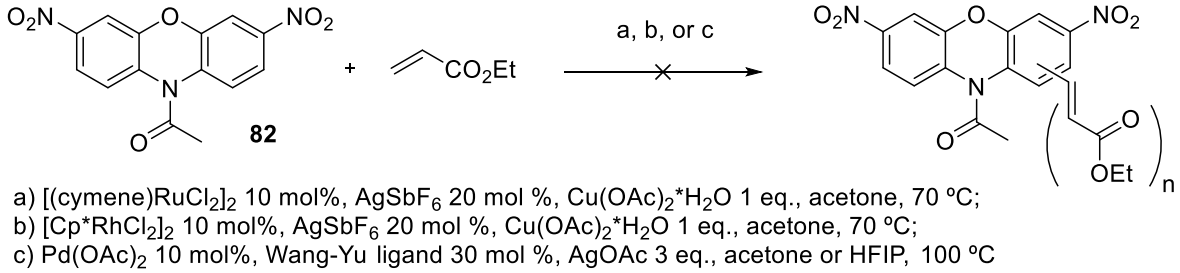

a) $[(cymene)RuCl_2]_2$ 10 mol%, $AgSbF_6$ 20 mol %, $Cu(OAc)_2{*}H_2O$ 1 eq., acetone, 70 ºC;
b) $[Cp^*RhCl_2]_2$ 10 mol%, $AgSbF_6$ 20 mol %, $Cu(OAc)_2{*}H_2O$ 1 eq., acetone, 70 ºC;
c) $Pd(OAc)_2$ 10 mol%, Wang-Yu ligand 30 mol %, AgOAc 3 eq., acetone or HFIP, 100 ºC

Scheme 48. Metal-catalysed oxidative olefination of 3,7-dinitro-10-acetylphenoxazine **82**.

Though the isolation of the target compound **78** failed, an error in the reported procedure[30] was identified. Unfortunately, due to the difficulties associated with the isolation of compound **78**, its application for further transformations was not possible. Nonetheless, testing the performance of compound **82** (which features a single directing NHAc group) in C–H activation proved to be intriguing. This compound was introduced into the reaction with ethyl acrylate under conditions established for acetylated rhodamines (Scheme 48). However, this attempt did not yield positive results; neither under Ru nor under Rh catalysis. It appears that the presence of single NHAc as a directing group is not enough to activate the C–H bond in the presence of two highly electron-

withdrawing NO_2 groups (σ_m 0.71, σ_p 0.78).[22] The reported Pd-catalysed ligand-accelerated approach[23] was also inefficient for such an inert compound.

3.4.2 *N,N'*-(*tert*-Butoxycarbonyl) protected oxazines

Considering the instability of triacetylated compound **78**, we reasoned whether alternative protective groups could be employed and whether this change could improve the compound's stability and ease of isolation. Compound **83** (Scheme 47) has two important features: the bridged nitrogen is protected by acetyl group which was reported to be photocleavable[31], and there is a possibility of introducing different protecting (and directing) groups to the nitrogen atomss at positions 3 and 7. Among the numerous substituents that could serve as directing groups, carbamates deserve special attention. While both carbamates and acetamides share some electronic similarities due to the presence of an amide bond, the additional oxygen atom in the carbamate imparts distinct electronic characteristics. The *tert*-butoxycarbonyl (Boc) is one of the widely used protecting groups for the amino group[14], and it has been reported as *ortho*-directing group in the oxidative olefination of arenes.[34] Another aspect to consider when applying the directing ability of carbamates is the fact that several photolabile protecting groups (PPGs), such as those based on 2-nitrobenzyl or 2-nitroveratryl, possess carbamate nature (Figure 26).[35] Protecting a substrate with PPG is commonly referred to as "photocaging" which find a wide application in modern nanoscopy techniques. Consequently, Boc was selected as a protecting and directing moiety owing to its affordability, as well as facile protection and deprotection protocols.

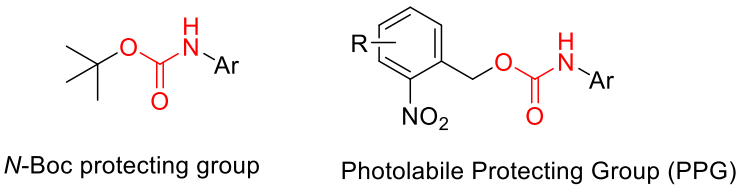

N-Boc protecting group Photolabile Protecting Group (PPG)

Figure 26. Carbamate protecting groups.

The desired bis-*N*-Boc-protected 3,7-diaminophenaxozine **84** was successfully prepared (Scheme 49). Surprisingly, its purification by the column chromatography on silica went smooth and without any problems compared to isolation of the structurally related triacetylated

phenoxazine **78** (Scheme 47). Compound **84** can also be obtained directly from *N*-Acetyl-3,7-dinitrophenoxazine **82** in the course of its reduction, if the reaction is carried in presence of Boc_2O. However, the yield of one-step transformation was significantly lower than the overall yield of the two-step procedure (30% vs. 84%).

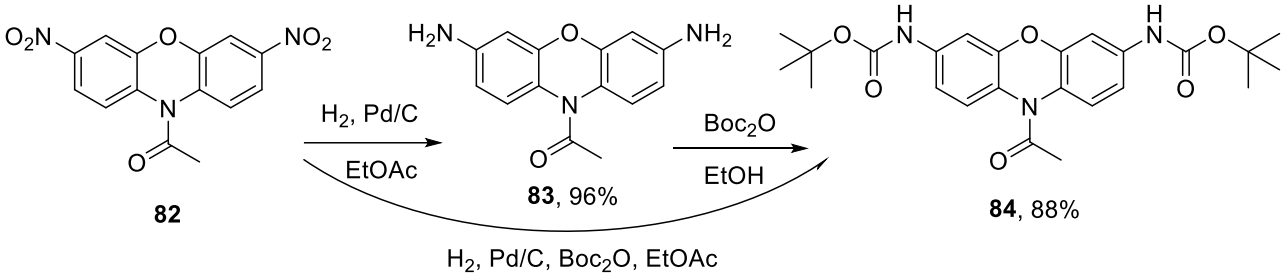

Scheme 49. Synthesis of bis-*N*-Boc-protected compound **84**.

Eventually, the applicability of the Ru- or Rh- catalysed oxidative olefination under conditions established above was demonstrated for Boc-protected compound **84** (Scheme 50). *tert*-Butyl acrylate was chosen as the coupling partner, in order to facilitate the cleavage of the *tert*-butyl ester, together with the Boc group, as both require acidic hydrolysis.[14]

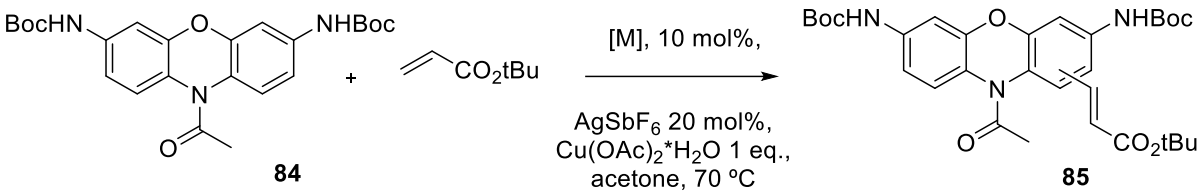

Scheme 50. M-catalysed oxidative olefination of bis-*N*-Boc-protected phenoxazine **84** to study of product distribution. [M] = $[(cymene)RuCl_2]_2$ or $[Cp^*RhCl_2]_2$. For details, see Table 12 and Figure 27.

Under Ru catalysis, the full conversion has not been achieved, even with an excess of acrylate (3 eq.). Surprisingly, the reaction yielded only one of the two possible mono-olefinated products (compound **85b**, Figure 27), and the degree of polyolefination was quite low. The products of bis-olefination were found in trace amounts (<5%), presented in a mixture of isomers, and were not isolated. Tris- and tetrakis- olefinated products were not detected. Despite the low degree of polyolefination, the yield of the desired compound **85b** (Figure 27, Table 12) was quite low. This

may be due to partial decomposition of the starting material (or product) in the course of reaction. A violet substance was isolated by column chromatography (representing 30% of the mass of the loaded sample), and further analysis revealed that it is not a pure compound, but rather a highly complex mixture. Carrying out the reaction at lower temperature (50 ºC and r.t.) resulted in a very low conversion (25 and <5%, respectively).

Under Rh catalysis, the reaction proceeded slightly different. Firstly, both mono-olefinated isomers **85a** and **85b** (Figure 27) were found in a 1:1 ratio. Secondly, poly-olefinated products were present in considerable amounts when an excess of acrylate (3 eq.) was used. Products resulting from the cleavage of protecting groups and decomposition of the fluorophore were also present (as violet mixture). No reaction was observed at r.t. (conversion <5%). In summary, under the given conditions the rhodium complex didn't prove to be a regioselective catalyst for oxidative olefination of Boc-protected phenoxazines.

Table 12. Isolated yields after reaction of **84** with 1.5 eq. of *tert*-butyl acrylate.

Catalyst	Recovered starting material, %	Isomer **85a**, %	Isomer **85b**, %
[Ru]	25	3	28
[Rh]	11	14	14

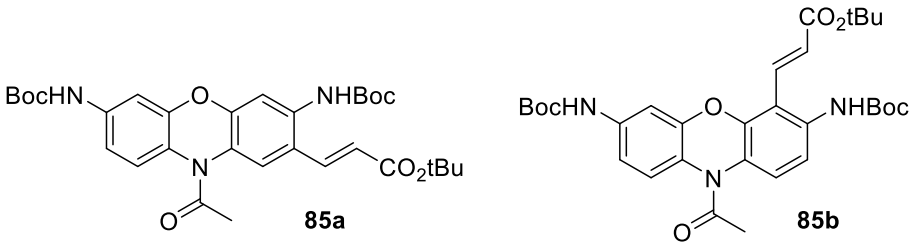

Figure 27. Structures of the mono-olefinated phenoxazines prepared by reaction on Scheme 50.

The double bond attached to the planar fluorophore results in a new planar structure with restricted rotational freedom and increased rigidity of the whole molecule.[7] The double bond can be reduced to a single bond, allowing free rotation around sp^3-carbon bonds. It was interesting to explore the alterations in properties associated with the presence of both saturated (sp^3) and unsaturated (sp^2) linkers. The reduction of the double bond was carried out for isomer **85b**, which

was obtained in a larger quantity. The compound with saturated linker was isolated with a 97% yield (compound **86**, Scheme 51).

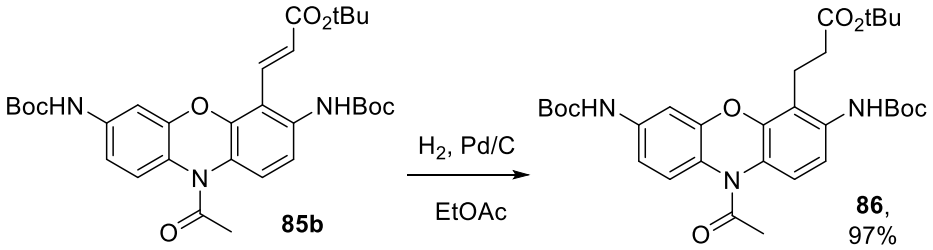

Scheme 51. Reduction of the double bond in compound **85b**.

The cleavage of *tert*-butyl ester and *tert*-butyl carbamates was performed for compounds **85a**, **85b**, and **86** using 10% v/v solution of TFA in DCM. The acidic hydrolysis of **85a** did not result in a clean reaction and gave by-products (Scheme 52). The desired compound **87** was isolated with only 22% yield. As for side reactions, the photocleavable bridged *N*-acetyl has been partially cleaved off resulting in the brilliant red fluorescent dye **88**. The second side reaction gave 6-membered lactam **89**, due to the intramolecular cyclization involving the amino and carboxyl groups. The same cyclization was observed for free dye **88** (compound **90** was isolated in trace amount which was not enough to confirm its structure by NMR).

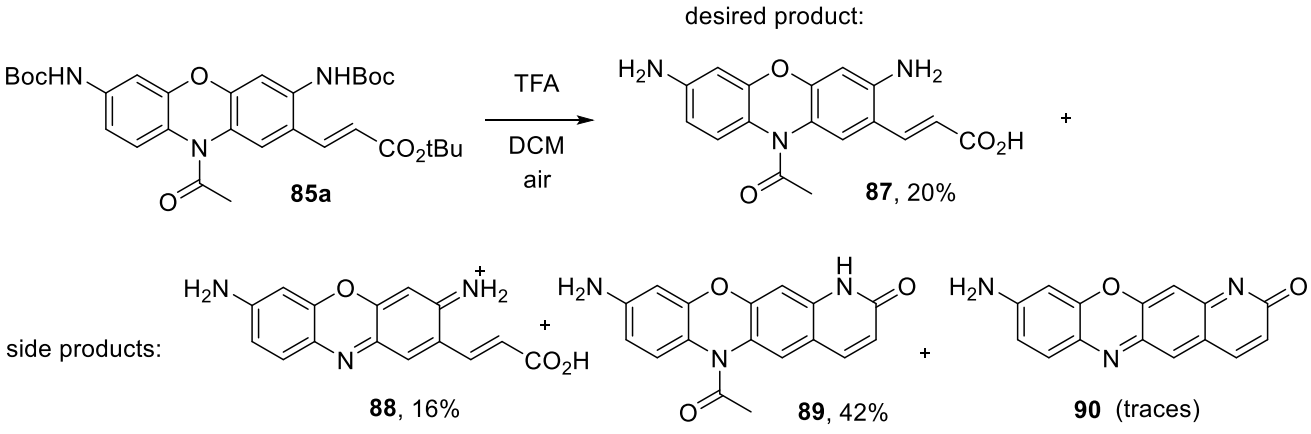

Scheme 52. Acidic hydrolysis of acrylated phenoxazine **85a**.

The acidic hydrolysis of isomer **85b** exhibited a cleaner reaction. Although the product of lactamization was not observed, the bridged acetate underwent partial cleavage, enabling the

oxidation of the molecule, and resulting in the formation of dye **92** (Scheme 53). This sequential process involving the cleavage of the bridged acetate, followed by oxidation (upon exposure to air) of resulting phenoxazine **91** made us consider the deprotection under inert conditions.

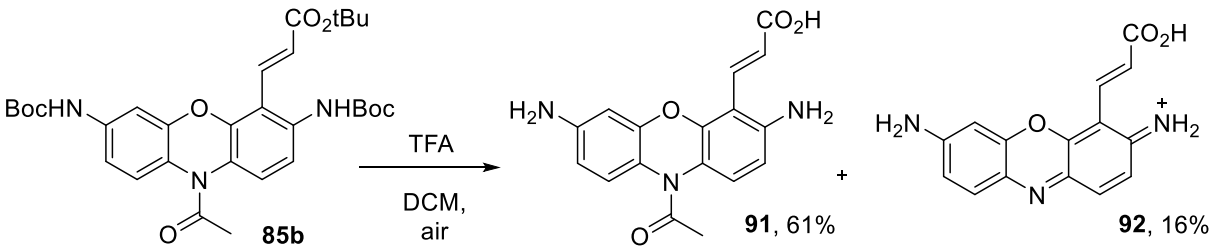

Scheme 53. Acidic hydrolysis of acrylated phenoxazine **85b**.

It has been reported in the literature[31] that the presence of oxygen amplifies the photolytic generation of the dye by a factor of 2.5 compared to the rate observed in its absence. Although the reaction under Ar and in the absence of light looked cleaner, the dye still persisted in the reaction mixture.

The acidic hydrolysis of compound with reduced linker resulted in full conversion of protected phenoxazine **86** to phenoxazinium dye **94** (Scheme 54). Compound **93** featuring bridged photocleavable *N*-acetyl was not detected.

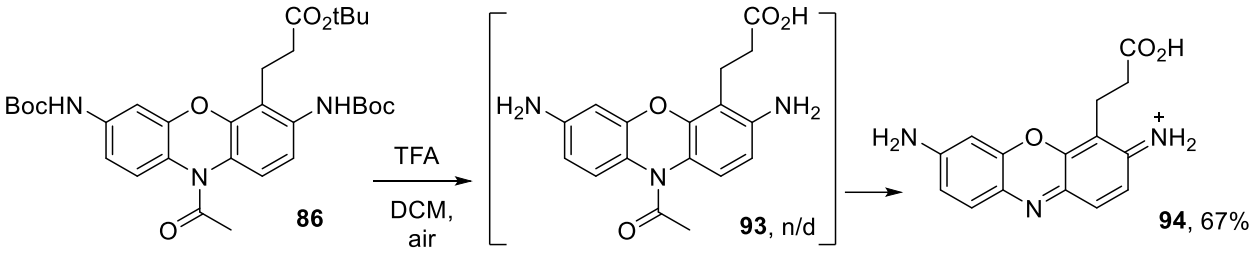

Scheme 54. Acidic hydrolysis of compound **86**. *N*-Acetylphenoxazine **93** was not detected.

The photophysical properties of the new dyes are discussed in section 3.4.5.

3.4.3 Synthesis of oxazine dyes through resorufin

While it has been demonstrated that acrylated phenoxazines can be obtained through *N*-Boc-directed C–H olefination, this transformation is hampered by several limitations. The reaction exhibits a low yield, faces challenges in the separation of isomers, and is prone to side reactions that result in decomposition of the dye core. In addition, this approach exclusively produces dyes with primary amino groups in the dye, which are suspectable to spontaneous lactamisation. Although the transformation to the secondary amino groups might be performed through *N*-alkylation of *N*-Boc-protected phenoxazines, the introduction of tertiary amino groups presents a novel synthetic challenge. Dyes featuring substituted amino groups are particularly interesting due to the capability of alkyl substituents attached to the nitrogen atoms to induce a red shift in both absorption and emission spectra.[20] Considering these regularities, we sought an alternative strategy to obtain functionalised oxazine dyes. Inspired by the late-stage fluorescein-to-rhodamine conversion strategy developed by Lavis[36], which permits to obtain bis-(*N*,*N*-dialkyl)-substituted rhodamines and oxazines from the corresponding fluoresceins and resorufins (which represent oxygen analogues of rhodamines and oxazines; see Figures 21, 24), we incorporated the C–H functionalisation step in this strategy. We considered the potential of phenylacetate as a directing group which exhibits electronic similarities to anilide. Importantly, acetate is reported as a suitable *ortho*-directing group for Ru-catalysed oxidative olefination of arenes.[37]

Thus, the new strategy for obtaining functionalised oxazines from commercially available resazurin *N*-oxide was designed (Scheme 55). It involved the use of tris-acetylated compound **95** as a substrate for oxidative olefination with *tert*-butyl acrylate. The double bond of acrylated compound **96** was then reduced yielding compound **97** with saturated linker. Compound **97** was then converted to corresponding triflate **98**. This compound underwent Pd-catalysed C–N cross-coupling with azetidine, leading to 3,7-diazetidinyl phenoxazine **99**. The choice of azetidine as a coupling partner was motivated by the fact that this substituent increases the quantum yield when incorporated into dyes.[36]

The designed strategy also enables to get functionalised resorufin derivatives **96** and **97** by alkaline hydrolysis of acetate protecting groups.

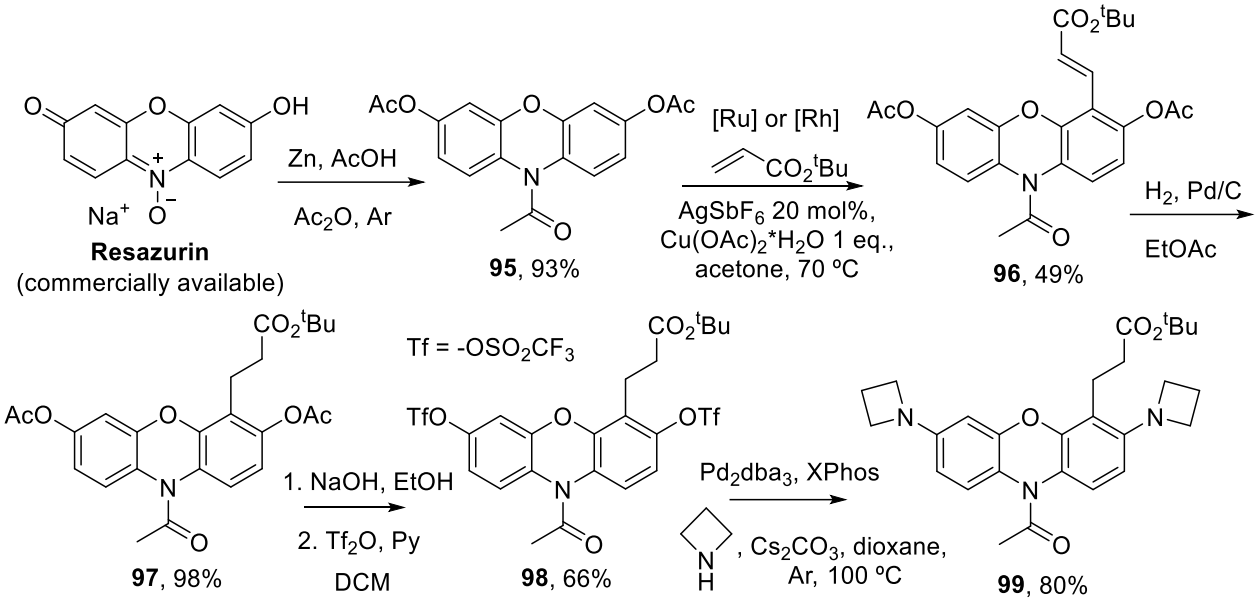

Scheme 55. Synthetic route to functionalised phenoxazine **99** from commercially available resazurin *N*-oxide. [Ru] = $[(cymene)RuCl_2]_2$, [Rh] = $[Cp^*RhCl_2]_2$; for the structures see Figure 20.

The initial step – the reduction of resazurin sodium salt led to compound **95** (Scheme 55). The reduction of resazurin sodium salt with zinc powder in glacial acetic acid to obtain dihydroresorufin is reported.[38] However, this compound is known to be air-sensitive and requires inert atmosphere for isolation. To skip this requirement, we combined the reduction with acetylation conducting the reaction in acetic anhydride (Scheme 55). This modification resulted in an efficient reaction with an excellent yield of 93%, and compound **95** demonstrated easy isolation and high stability.

Then, compound **95** was introduced to Ru-catalysed oxidative olefination with *tert*-butyl acrylate to get compound **96** under conditions established before (Scheme 55). The full conversion has not been achieved even when an excess of acrylate (3 eq.) was used. Fortunately, the reaction found to be clean, as it resulted in formation of only one mono-olefinated isomer **96**. Products of double and triple olefination were detected in trace amounts. The isolated yield of compound **96** in the Ru-catalysed oxidative olefination was 49%.

Surprisingly, the same isomer **96** was obtained under the Rh catalysis. However, the conversion was lower than for Ru (50% for Rh, up to 90% for Ru), and the isolated yield of compound **96** under the Rh catalysis was only 20%. Nevertheless, this is an unexpected observation

that under the direction of OAc both catalysts demonstrated the ability to activate the same position C-4 of the phenoxazine core (compound **96**, Scheme 55).

Further steps in the development of functionalised oxazines included reduction of the double bond and was performed on compound **96** (to yield compound **97**, Scheme 55). This step was implemented in order to have a suitable substrate for Buchwald-Hartwig amination with the secondary amine (which represents a Michael donor) to avoid Michael addition to activated double bond (which is a Michael acceptor). Secondary cyclic amines are generally stronger nucleophiles than primary amines and therefore, are more reactive as Michael donors.[39]

The subsequent transformation involved deacylation-triflation to replace acetate with triflate -OSO_2CF_3 (compound **98**, Schemes 55, 56). The triflate group is an excellent leaving group used in organic reactions, notably in cross-coupling reactions.[8; 40] Both *O*-acetates in compound **97** underwent alkaline hydrolysis. It is worth mentioning that bridged *N*-acetate tolerated these conditions and was not cleaved off. The intermediate *N*-acetyl-protected dihydroresorufin **100** was not isolated; it was directly sulfonated with triflic anhydride. Following this two-step procedure, the desired triflate **98** was obtained with a yield of 66% (Scheme 56).

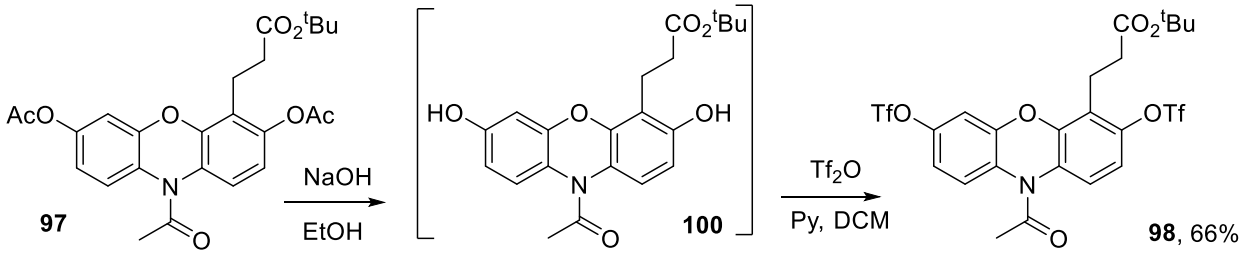

Scheme 56. Deacylation-triflation of functionalised *N*-acetyl resorufin **97**.

Triflate **98** may be coupled with secondary amines to obtain fluorogenic 3,7-diaminophenoxazines. An efficient Pd-catalysed cross-coupling reaction (so-called Buchwald-Hartwig amination[40]) was used to attach the azetidine substituent to the phenoxazine core. The choice of azetidine as a coupling partner was influenced by previous results indicating improved absorption and emission maxima (by the red shift)[20, 36], along with higher quantum yields demonstrated for azetidinyl-substituted rhodamines, acridines, oxazines, rhodols, and coumarines.[36] The Pd-catalysed C–N cross-coupling between triflate **98** and azetidine showed a clean reaction with the yield of desired 3,7-diazetidinyl phenoxazine **99** of 80% (Scheme 55).

To obtain compound **101** with the free carboxylic group, the deprotection of *tert*-butyl ester was performed for compound **99** (Scheme 57). The use of 0.3 M HCl solution in eq. EtOH led to the destruction of the azetidine cycle and formation of compound **101** (confirmed by LCMS and HRMS; not isolated). Deprotection with 10% v/v TFA in DCM under Ar resulted in the desired acid **102**.

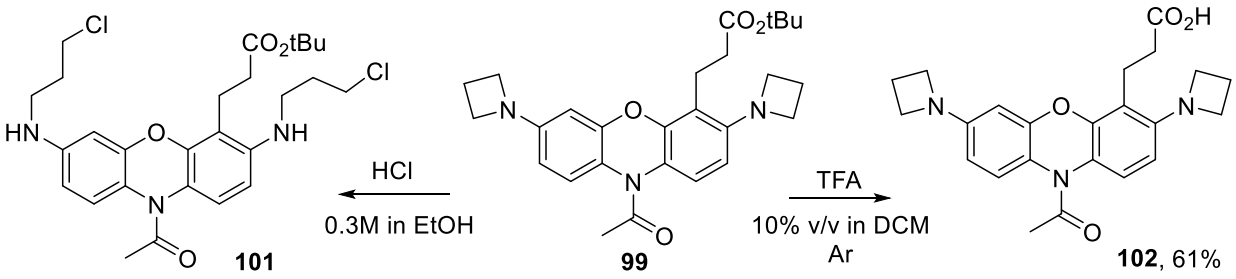

Scheme 57. Deprotection of *tert*-butyl ester in compound **99**. Compound **101** was not isolated. Compound **102** isolated with a yield of 65%.

3.4.4 Photolysis of 10-*N*-acetyl phenoxazines 91 and 99.

Photolysis of compound **91** was performed in acetonitrile (Scheme 58, Figure 28) and in aq.100 mM phosphate buffer (pH = 7) (Scheme 58, Figure 29). The reaction is 10-times slower in aqueous solution than in acetonitrile. As anticipated, 10-*N*-acetyl-protected phenoxazine **91** was converted to fluorescent products, and there is clear red shifting of the absorption maximum in the course of photolysis. In acetonitrile, irradiation at 365 nm led to a mixture of compounds with max λ_{abs} varying from 580 to 593 nm. The expected product **92** was not detected by LCMS analysis of the reaction mixture after photolysis. In aq. phosphate buffer the reaction was much cleaner, and compound **103** (with λ_{abs} 593 nm, λ_{emis} 617 nm) was identified as a main product with *m/z* 280 for M^+ (we assign its structure to the product of intramolecular C–H amination of the double bond).

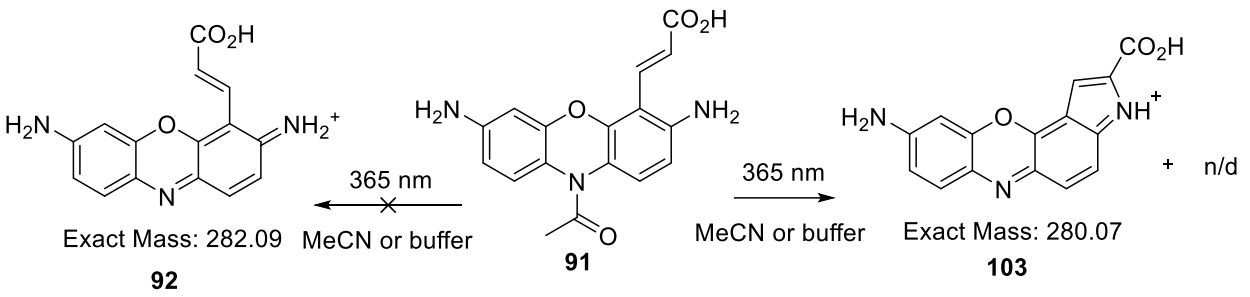

Scheme 58. Photolysis of compound **91** in acetonitrile and 100 mM phosphate buffer.

Photolysis of compound **99** was performed in acetonitrile (Scheme 59, Figure 28). The reaction was much slower than the photolysis of compound **91** with unsubstituted amino groups (>30 h). 10-*N*-Acetyl-protected phenoxazine **99** was converted to fluorescent products and there was clear red shifting of the absorption maximum in the course of irradiation. The photolysis at 365 nm led to a compound with λ_{abs} 620 nm and λ_{emis} 650 nm. Although the reaction was not clean, the expected fluorescent product **104** (with *m/z* 364 for M^+) was identified as a main component of the reaction mixture.

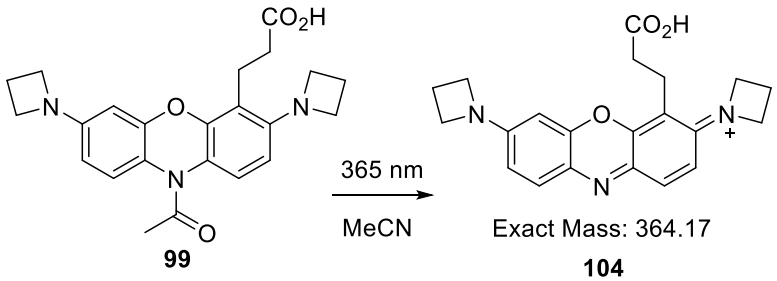

Scheme 59. Photolysis of compound **99** in acetonitrile.

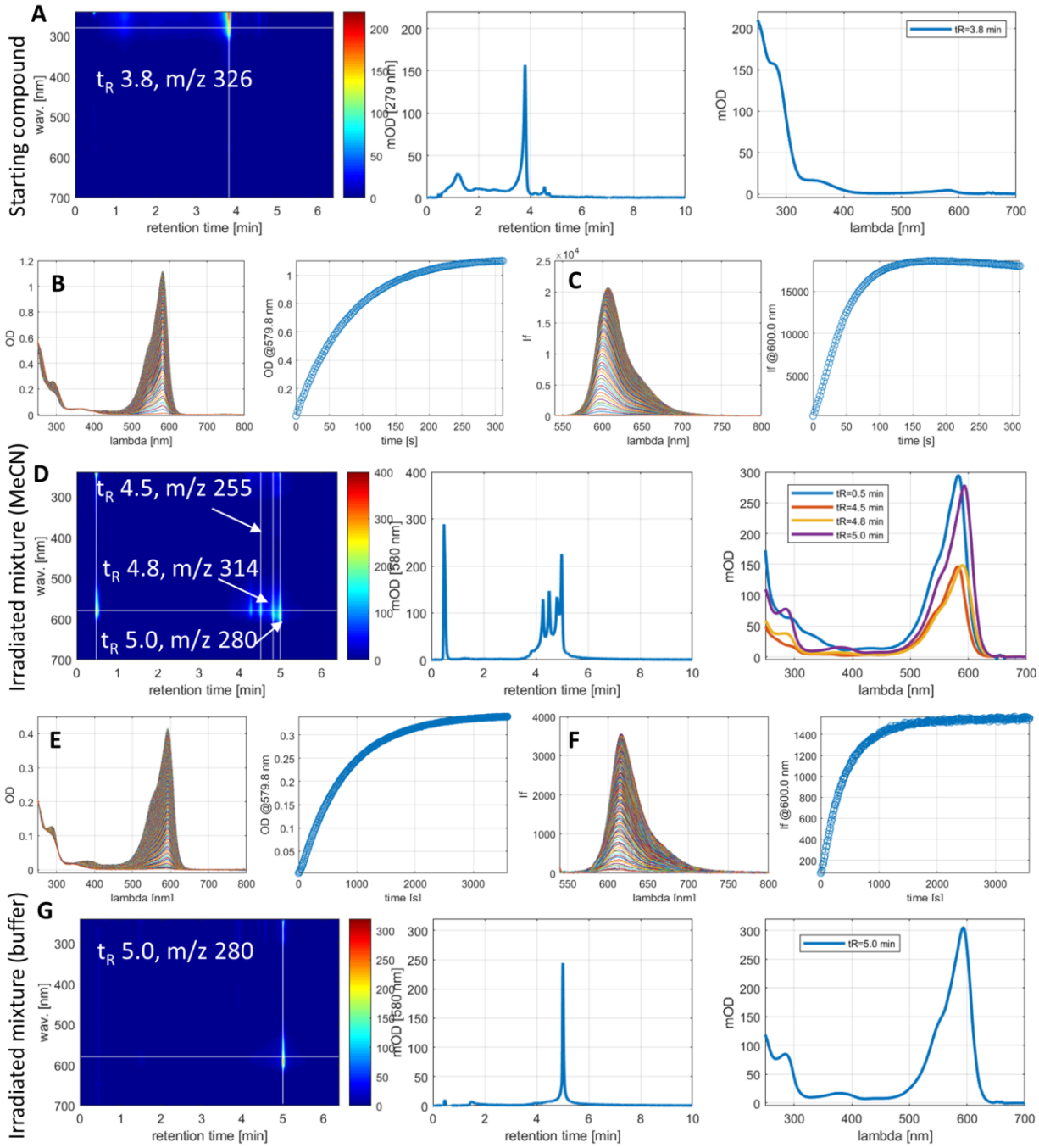

Figure 28. Photolysis of compound **91**: (A) HPLC traces and absorption spectrum of the starting compound **91**; (B) absorption spectra changes of **91** in MeCN as a function of time upon irradiation with 365 nm light; (C) emission spectra changes of **91** in MeCN as a function of time upon irradiation with 365 nm light; (D) HPLC traces of reaction mixture after photolysis with *m/z* values of the main peaks and absorption spectra of the main peaks; (E) absorption spectra changes of **91** in buffer as a function of time upon irradiation with 365 nm light; (F) emission spectra

changes of **91** in buffer as a function of time upon irradiation with 365 nm light; (G) HPLC traces of reaction mixture after photolysis with *m/z* values of the main peak and absorption spectra of the main peak.

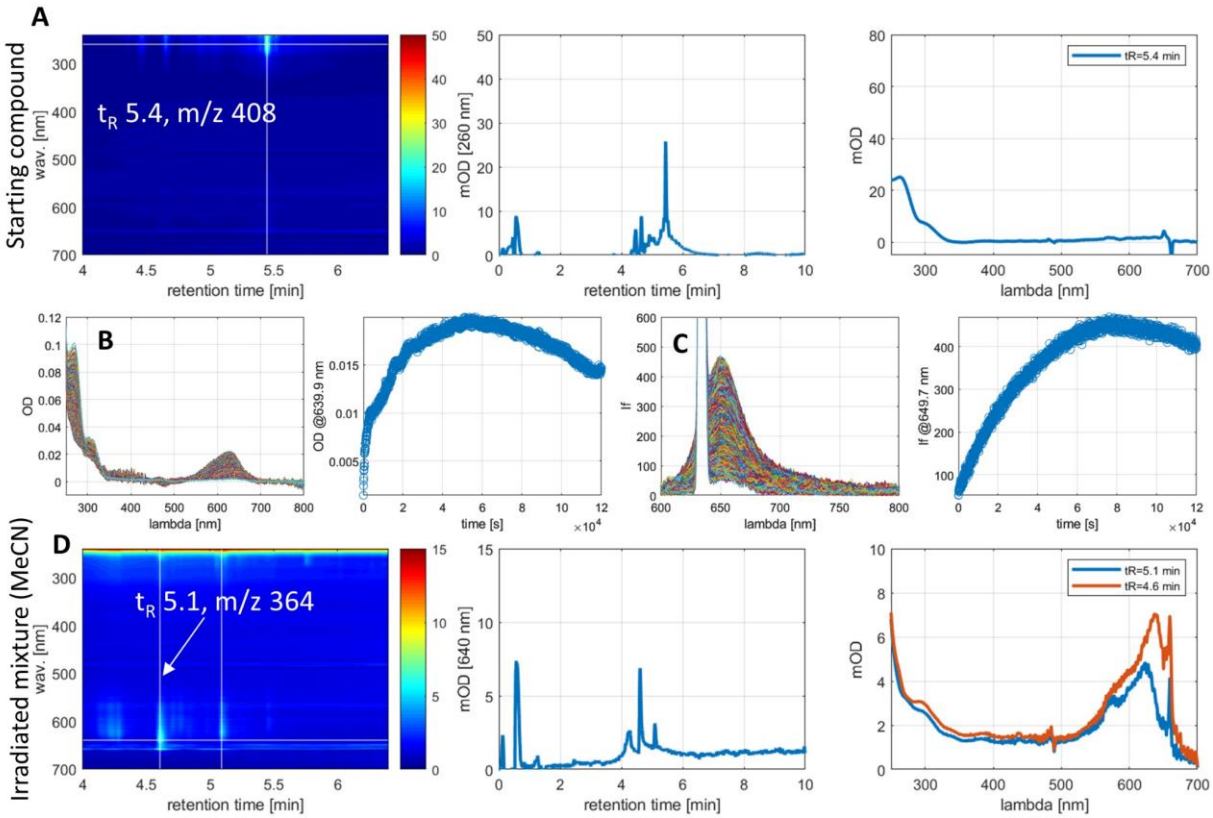

Figure 29. Photolysis of compound **99**: (A) HPLC traces and absorption spectrum of starting compound **91**. The ionisation was found to be poor. (B) absorption spectra changes of **99** in MeCN as a function of time upon irradiation with 365 nm light; (C) emission spectra changes of **99** in MeCN as a function of time upon irradiation with 365 nm light; (D) HPLC traces of the reaction mixture after photolysis with *m/z* values of the main peak and absorption spectra of the main peak (red line).

3.4.5 Photophysical properties of new dyes

The photophysical properties of parental (unsubstituted) oxazines and new oxazines (Figure 30) are given in Table 13. The introduction of the acrylate function produces a red shift in both absorption and emission spectra (dyes **88** and **92**). This effect is stronger when the substituent is at

position C-2 (dye **88**). The presence of a saturated linker at position C-4 produces a small shift of absorption and emission maxima to the red (dye **94**).

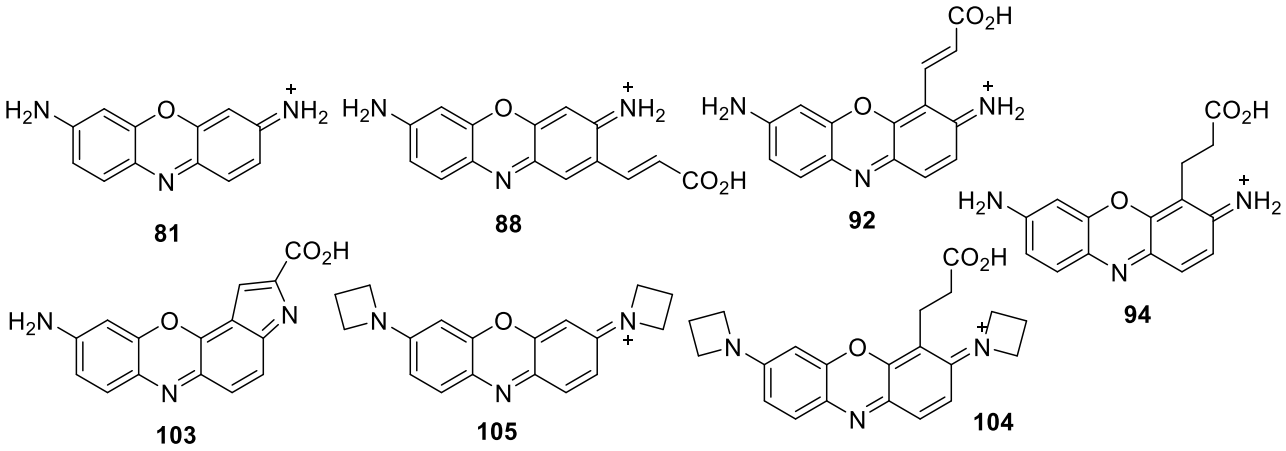

Figure 30. Parental unsubstituted oxazine dyes (**81**, **105**) and new functionalised oxazines (**88**, **92**, **103**, **104**). The structures **103** and **104** have not been yet confirmed, they are proposed as the products of the photolysis on the basis of the absorption spectra and LCMS analysis data.

Table 13. Photophysical properties of oxazine dyes in EtOH.

Dye	λ_{abs}, nm	λ_{em}, nm	Stokes shift	ε,[a] $M^{-1}cm^{-1}$	Φ_{fl},[b] %	Fluor. lifetime, ns
81	583	594	11	110 000	48	3.5
88	604	630	26	100 000	41	2.4
92	597	607	10	105 000	46	3.4
94	590	600	10	100 000	54	3.6
103[c]	592	615	23	47 000	n/d	n/d
104[c]	630	650	20	n/d	n/d	n/d
105[d]	647	661	14	99 000	24	n/d

[a] molar extinction coefficient; [b] absolute values of fluorescence quantum yield; [c] in MeCN; [d] data from ref. 36.

3.5 Conclusion and outlook

The catalyst-dependent regioselectivity in the reactions of oxidative olefination of *N,N'*-bis(acetyl) rhodamine and *N,N'*-bis(*tert*-butoxycarbonyl) phenoxazine with acrylates has been established. The (*p-cymene*) ruthenium dichloride dimer complex leads to a regioselective reaction activating C-2 position of the rhodamine core, and C-4 of phenoxazine. *N*-Trifluoroacetate proved to be an inappropriate directing group for Ru- Rh- or Pd-catalysed oxidative olefination. *O*-Acetyl as a directing group showed the same selectivity for both Rh and Ru catalysis. The products of oxidative olefination have acrylate fragments attached to the fluorophore.

The introduction of an acrylate function results in a red shift in both absorption and emission maxima (from +4 to 26 nm). The acrylate moiety can be reduced. For oxazines, the reduction of the double bond of the acrylate linker is expected to prevent the intramolecular (photoinduced) cyclization involving an amino group of the fluorophore and the adjacent C=C fragment of the acrylate. Lactamisation which found to occur in acrylated rhodamines and oxazines represents a pathway promising for the synthesis of the new dyes.

The results of this work not only shed light on the complex regioselectivity of C–H functionalisation reactions in rhodamines and phenoxazines, but also open new ways for improving and facilitating the synthesis of new photoconvertible dyes.

3.6 References to Chapter 3

1. a) M. Lelek, M.T. Gyparaki, G. Beliu, F. Schueder, J. Griffié, S. Manley, R. Jungmann, M. Sauer, M. Lakadamyali, C. Zimmer, *Nat Rev Methods Primers*, **2021**, 1:39; b) M. Olesińska-Mönch, C. Deo, *Chem. Commun*., **2023**, *59*, 660-669; c) R. Lincoln, M. L. Bossi, M. Remmel, E. D'Este, A. N. Butkevich, S. W. Hell, *Nature Chem.* **2022**, *14*, 1013-1020.

2. a) F. Chen, W. Liu, H. Li, T. Deng, B. Xing, F. Liu, *Analysis& Sensing* **2022**, *2*, e20210006; b) N. Lardon, L. Wang, A. Tschanz, P. Hoess, M. Tran, E. D'Este, J. Ries, K. Johnsson, *J. Am. Chem. Soc.* 2021, *143*, 36, 14592-14600; c) J. Bucevičius, R. Gerasimaitė, K. A. Kiszka, S. Pradhan, G. Kostiuk, T. Koenen, G. Lukinavičius, *Nat. Comm*. **2023**, *14*(1), 1306.

3. C. Sabhu, A. K. Mitra, *Mol Divers.* **2023**, https://doi.org/10.1007/s11030-023-10619-5.

4. K. Kolmakov, E. Hebisch, T. Wolfram, L. A. Nordwig, C. A. Wurm, H. Ta, V. Westphal, V. N. Belov, S. W. Hell, *Chem. Eur. J.* **2015**, *21*, 13344-13356.

5. L. Guillemard, N. Kaplaneris, L. Ackermann, M. J. Johansson, *Nat. Rev. Chem*. **2021**, *5*, 522-545.

6. T. Rogge, N. Kaplaneris, N. Chatani, J. Kim, S. Chang, B. Punji, L. L. Schafer, D. G. Musaev, J. Wencel-Delord, C. A. Roberts, R. Sarpong, Z. E. Wilson, M. A. Brimble, M. J. Johansson, L. Ackermann, *Nat Rev Methods Primers* **2021**, 1:43.

7. J. H. Docherty, T. M. Lister, G. Mcarthur, M. T. Findlay, P. Domingo-Legarda, J. Kenyon, S. Choudrhary, I. Larossa, *Chem. Rev*. **2023**, *123*, 7692-7760.

8. A. Biffis, P. Centomo, A. Del Zotto, M. Zecca, *Chem. Rev*. **2018**, *118*, 2249−2295.

9. a) I. Moritani, Y. Fujiwara, *Tetrahedron Lett*. **1967**, *8*, 1119-1122; b) Y. Fujiwara, I. Moritani, S. Danno, R. Asano, S. Teranishi, *J. Am. Chem. Soc*. **1969**, *91*, 7166-7169.

10. B. L. Tóth, A. Monory, O. Egyed, A. Domján, A. Bényei, B. Szathury, Z. Novák, A. Stirling, *Chem. Sci*. **2021**, *12*, 5152-5163.

11. H. Liang, J. Wang, *Chem. Eur. J.* **2023**, *29*, e202202461.

12. a) L. Ackermann, L. Wang, R. Wolfram, A. V. Lygin, *Org. Lett*. **2012**, *14*(3), 728-731; b) F. W. Patureau, F. Glorius, *J. Am. Chem. Soc*. **2010**, *132*, 9982-9983; c) Y. Takahama, Y. Shibata, K. Tanaka, *Chem. Eur. J*. **2015**, *21*, 9053-9056; d) Y.-C. Yuan, C. Bruneau, T. Roisnel, R. Gramage-Doria, *Cata. Sci. Technol.* **2019**, *9*, 4711-4717; e) S. R. Mohanty, N. Prusty, T. Nanda, S. K.

Banjare, P. C. Ravikumar, *J. Org. Chem*. **2022**, *87*(9), 6189-6201; f) D.-H. Wang, K. M. Engle, B.-F. Shi, J.-Q. Yu, *Science* **2010**, *327*, 315-319.

13. a) D. Leow, G. Li, T.-S. Mei, J.-Q. Yu, *Nature* **2012**, *486*, 518-522; b) A. Dey, S. K. Sinha, T. K. Achar, D. Maiti, *Angew. Chem. Int. Ed*. **2019**, *58*, 10820-10843.

14. T. Greene, G. M. Peter, in *Protective groups in Organic Synthesis*, John Wiley & Sons, 2nd ed., **1991**, pp. 343-344.

15. a) G. Lukinavičius, G. Y. Mitronova, S. Schnorrenberg, A. N. Butkevich, H. Barthel, V. N. Belov, S. W. Hell, *Chem. Sci.* **2018**, *9*, 3324-3334; b) G. Lukinavičius, L. Reymond, K. Umezawa, O. Sallin, E. D'Este, F. Gottfert, H. Ta, S. W. Hell, Y. Urano, K. Johnsson, *J. Am. Chem. Soc*., **2016**, *138*, 9365-9368.

16. L. D. Lavis, T.-Y. Chao, R. T. Raines, *ACS Chem. Biol*. **2006**, *1(*4), 252-260.

17. E. Pretsch, P. Bühlmann, C. Affolter, in *Structure Determination of Organic Compounds*, Springer-Verlag Berlin Heidelberg, **2000**, pp. 168.

18. E. A. Savicheva, G. Y. Mitronova, L. Thomas, M. J. Boehm, J. Seikowski, V. N. Belov, S. W. Hell, *Angew. Chem. Int. Ed*. 2020, *59*, 5505-5509; *Angew. Chem*. **2020**, *132*, 5547-5551.

19. E. A. Savicheva, M. L. Bossi, V. N. Belov, S. W. Hell, *ChemPhotoChem* **2022**, e202200222.

20. K. H. Dexhage, J. Res. *Natl. Inst. Stand. Technol*. **1976**, *80*(3), 421-428.

21. K. K. Abney, S. J. Ramos-Hunter, I. M. Romaine, J. S. Goodwin, G. A. Sulikowski, C. D. Weaver, *Chem. Eur. J*. **2018**, *24*, 8985-8988.

22. C. Hansch, A. Leo, R. W. Taft, *Chem. Rev*. **1991**, *91*, 165-195.

23. P. Wang, P. Verma, G. Xia, J. Shi, J. X. Qiao, S. Tao, P. T. W. Cheng, M. A. Poss, M. E. Farmer, K.-S. Yeung, J.-Q. Yu, *Nature* **2017**, *551*, 489-494.

24. a) E. A. Halabi, R. Weissleder, *J. Am. Chem. Soc*. **2023**, *145*(15), 8455-8463; b) K. R. Gee, E. S. Weinberg, D. J. Kozlowski, *Bioorg. Med. Chem. Lett*. **2001**, *11*, 2181-2183.

25. L. Tian, H. Feng, Z. Dai, R. Zhang, *J. Mater. Chem. B*, **2021**, *9*, 53-79.

26. A. V. Anzalone, Z. Chen, V. W. Cornish, *Chem. Commun*. **2016**, *52*, 9442-9445.

27. D. Danylchuk, P.-H. Jouard, A. S. Klymchenko, *J. Am. Chem. Soc*. **2021**, *143*, 912-924.

28. S. Jenni, K. Renault, G. Dejouy, S. Debieu, M. Laly, A. Romieu, *ChemPhotoChem* **2022**, *6*, e202100268.

29. M. I. P. S. Leitão, B. R. Raju, S. Naik, P. J. G. Coutinho, M. J. Sousa, M. S. T. Gonçalves, *Tetrahedron Lett*. **2016**, *57*, 3936-3941.

30. H. Maas, A. Khatyr, G. Calzaferri, *Microporous Mesoporous Mater*. **2003**, *65*, 233-242.
31. M. Akiba, A. S. Dvornikov, P. M. Rentzepis, *J. Photochem. Photobiol. A* **2007**, *190*, 69-76.
32. D. Creed, N. C. Fawcett, R. L. Thompson, *J. C. S. Chem. Commun*. **1981**, 497-499.
33. E. Pretsch, P. Bühlmann, C. Affolter, in *Structure Determination of Organic Compounds*, Springer-Verlag Berlin Heidelberg, **2000**, pp. 224-226.
34. T. Morita, T. Satoh, M. Miura, *Org. Lett.* **2017**, *19*, 1800-1803.
35. a) P. Klán, T. Šolomek, C. G. Bochet, A. Blanc, R. Givens, M. Rubina, V. Popik, A. Kostikov, J. Wirz., *Chem. Rev.* 2013, *113*, 119-191; b) L. M. Wysocki, J. B. Grimm, A. N. Tkachuk, T. A. Brown, E. Betzig, L. D. Lavis, *Angew. Chem. Int. Ed*. **2011**, *50*, 11206-11209; c) M. Weber, T. A. Khan, L. J. Patalag, M. Bossi, M. Leutenegger, V. N. Belov, S. W. Hell, *Chem. Eur. J*. **2021**, *27*, 451-458.
36. J. B. Grimm, B. P. English, J. Chen, J. P. Slaughter, Z. Zhang, A. Revyakin, R. Patel, J. J. Macklin, D. Normanno, R. H. Singer, T. Lionnet, L. D. Lavis, *Nat. Methods* **2015**, *12*(3), 244-250.
37. M. C. Reddy, M. Jeganmohan, *Eur. J. Org. Chem*. **2013**, 1150-1157.
38. Z. Han, X. Liang, X. Ren, L. Shang, Z. Yin, *Chem. Asian J*. **2016**, *11*, 818-822.
39. G. J. Noordzij, C. H. R. M. Wilsens, *Front. Chem.* **2019**, *7*, 729.
40. R. Dorel, C. P. Grugel, A. M. Haydl, *Angew. Chem. Int. Ed*. **2019**, *58*, 17118-17129.

Chapter 4.

Experimental part

4.1 General remarks

The reagents were purchased from commercial suppliers – Sigma Aldrich (Merck), ABCR, Carbosynth, TCI, Alfa Aesar – and stored according recommendations of the producers. Solvents were obtained from Merck. Anhydrous solvents were stored over molecular sieves. Deuterated solvents were purchased from Deutero GmbH ($CDCl_3$, CD_3OD, D_2O, $(CD_3)_2CO$ DMSO-d_6, Et_2O-d_{10}. All commercially available substances were used without further purification. Triethylammonium bicarbonate buffer (TEAB, pH = 8) was prepared from 1 M aq. Et_3N and CO_2 gas obtained by evaporation of solid CO_2.

Preparative chromatographic methods

Flash chromatography (normal phase; regular silica gel) was performed on an automated *Isolera™ One* system with commercially available cartridges (*Biotage GmbH*). For isolation of dyes and sugar conjugates, flash chromatography on reversed phase Interchim puriFlash™ was used (For pyrene dyes and conjugates: RP C18, 15C18AQ-F0025 cartridge, solvents MeCN and aqueous 20 mM TEAB; gradient of MeCN is given below for each individual run; for isolation of cyanine dyes: cartridges Interchim puriFlash™ 15C18AQ, acetonitrile gradient 30–100% over 12 CV in H_2O (0.1% v/v TFA/MeCN mixture); for isolation of rhodamine and oxazine dyes preparative column: Interchim Uptisphere Strategy C18-HQ, 10 μm, 250×21.2 mm (Article No. US10C18HQ-250/212, Interchim), typical flow rate: 20mL/min (if not stated otherwise).

Thin Layer Chromatography (TLC)

Normal phase TLC was performed on regular *silica gel 60 F_{254}* (*Merck Millipore*). Reversed phase TLC was performed on *silica gel RP-60 F_{254}* (*Merck Millipore*). Spots of compounds were detected by exposing TLC plates to UV-light (254 or 366 nm).

Analytical HPLC was performed on a Knauer Azura liquid chromatography system with a binary P 6.1L pump, dynamic mixing chamber V7119-1, UV diode array detector DAD 6.1L working in the range of 200–800 nm, an injection valve with a 20 µL loop and two electrical switching valves V 2.1S with 6-port multiposition valve heads. Three different columns were used; the solvent's gradient is given for each individual run:

A: *Knauer Eurospher II 100-5 C18,* 5 µm, 150x4 mm, 1.2 mL/min, solvents: water + 0.1% v/v trifluoroacetic acid (TFA); MeCN + 0.1% v/v TFA; gradient is given for MeCN;

B: *Interchim Uptisphere C18-HQ,* 10 µm, 250x4.6 mm, 1.2 mL/min, solvents: aqueous TEAB buffer 0.05 M; MeCN; gradient is given for MeCN;

C: *Kinetex C18 100,* 5 µm, 250x4 mm, 1.2 mL/min, solvents: aqueous TEAB buffer 0.05 M; MeCN; gradient is given for MeCN.

Analytical LCMS was performed on Ultimate 3000 system with *Phenomenex C18* column (2.6 µm, 75x3 mm, flow 0.5 ml/min; solvents: 0.1% v/v HCO_2H/MeCN + 0.1% v/v HCO_2H/water; gradient of MeCN 20/80 – 100/0 if not stated otherwise) coupled to Thermo Fisher Scientific ISQ EM mass spectrometer.

Absorption Spectroscopy

Absorption spectra were recorded with a double-beam UV–vis spectrophotometer (*Varian 4000*) in quartz cuvettes with 1 cm path length. Emission spectra were recorded on a Cary Eclipse fluorescence spectrometer (*Varian*). Fluorescence quantum yields (absolute values) were obtained on a *Quantaurus-QY Absolute PL* quantum yield spectrometer C11347 (*Quantaurus QY*). Excited states lifetimes were measured with *Quantaurus-Tau* device with TDC Unit M12977-01 (Hamamatsu).

Nuclear Magnetic Resonance (NMR)

NMR spectra were recorded at 25 °C with an Agilent 400-MR spectrometer at 400.1 MHz (^{1}H), 376.4 MHz (^{19}F), 161.9 MHz (^{31}P) and 100.6 MHz (^{13}C) and are reported in ppm. All ^{1}H spectra are referenced to tetramethylsilane (δ = 0 ppm) using the signals of the residual protons of HDO (4.79 ppm) in D_2O, CHD_2OD (3.31 ppm) in CD_3OD, CHD_2COCD_3 (2.05 ppm) in $(CD_3)_2CO$, CHD_2CN (1.94 ppm) in CD_3CN, DMSO-d_5 (2.50 ppm) in DMSO-d_6, $CHCl_3$ (7.26 ppm) in $CDCl_3$,

C_4H_7DO (1.73 ppm) in C_4D_8O. Multiplicities of the signals are described as follows: s = singlet, br. s = broad singlet, d = doublet, dd = doublet of doublets, t = triplet, q = quartet, m = multiplet. ^{13}C spectra are referenced to tetramethylsilane (δ = 0 ppm) using the signals of the solvent: CD_3CN (1.32 ppm), CD_3OD (49.00 ppm), $(CD_3)_2CO$ (29.84 ppm), DMSO-d_6 (39.52 ppm), $CDCl_3$ (77.36 ppm).

Mass-Spectrometry (MS)

Low resolution mass spectra (50 - 3500 m/z) with electro-spray ionization (ESI) were obtained on a *Varian 500-MS* spectrometer (Agilent). High resolution mass spectra (HRMS) were obtained on a *Bruker maXis* (ESI-QTOF-HRMS) or *Bruker Autoflex Speed* (MALDI-TOF HRMS) spectrometer (Institut für Organische und Biomolekulare Chemie, Georg-August-Universität Göttingen).

NMR measurement

Measurements of ^{19}F chemical shifts were performed at 20 ± 2 °C in DMSO-d_6 according to the reported procedures.[1] Approximately 2% solutions of substituted fluorobenzenes were used. Chemical shifts of ^{19}F stay constant, even in mixtures, if the concentration of the solute is low (0.01 M), and it chemically stable. The average deviation (reproducibility) of chemical shifts was better than ±0.03 ppm. Spectra were recorded on an Agilent 400-MR spectrometer (376 MHz ^{19}F) using standard fluorine parameters. Substituent (X) shielding parameters $\delta_H^{m(X)}$, $\delta_H^{p(X)}$, $\Delta\delta_H^{p(X)-m(X)}$ are referenced to fluorobenzene (in DMSO-d_6 δ -113.05 – -113.13), which was added as an internal standard. The spectra were recorded without suppression of ^1H-^{19}F spin-spin couplings. Under these conditions, the signals were multiplets, and the shielding parameters were measured by taking the distance between the center of a multiplet and the reference peak of fluorobenzene (-113.09). Each spectrum was recorded twice.

Low-temperature ^1H-NMR spectra of **9a** and **9b** were recorded in Et_2O-d_{10} at six temperatures: +25, 0, -25, -50, -75, -100 °C. Except some drift of the chemical shifts, no changes in the number of signals and their multiplicities were observed.

Electrophoresis

PAGE – was performed together with Jan Seikowski (Facility for Synthetic Chemistry, MPINAT).

Ca. 2 nmol of each conjugate (15 nmol for ladders) was dissolved in 15 µL of ultrapure water, mixed with an equal volume of loading solution (80% formamide, 52 mM EDTA. 89 mM Tris, 89 mM boric acid) and separated on a denaturated 20% polyacrylamide gel (7 M urea). The sugar-dye-conjugates were detected under UV-light of 366 nm. All individual conjugates and "ladders" were analysed by PAGE. Samples were applied to a 20% (w/v) polyacrylamide slab gel (0.7 mm x 230 mm x 300 mm) in TBE buffer (pH 8). The electrophoresis was performed at ambient temperature and constant power (35 W; 1750 - 2200 V) for 90 min. The bands were visualised by emission (excitation with 366 nm UV-lamp), and the pictures were taken by using a digital camera.

CE-LIF – was performed by Jeannette I. Kast, Microsynth AG, Schützenstrasse 15, CH-9436, Balgach, Switzerland.

0.001 to 1 pmol of each conjugate was diluted in 20 µL ddH_2O. The capillary electrophoresis was performed on an Applied Biosystems 3730XL DNA Analyser with the following conditions: injection time, 20 s; injection voltage, 2.0 kV; run time, 300 s; run voltage, 15 kV; capillary length, 50 cm; polymer, POP7; filter, Dye Set G5. The raw data .fsa files were analysed with GeneMarker V2.6.4.

Photolysis

Was performed by Dr. Mariano Bossi (Department of Optical Nanoscopy, Max-Planck-Institute for Medical Research, Jahnstrasse 29, 69120 Heidelberg, Germany).

Irradiation experiments were performed in a home-build setup, using a 365 nm LED as irradiation source (M365-L2, Thorlabs), and to monitor the advance of the reaction, a single beam absorption spectrometer with a deuterium/xenon lamp (DH-2000-BAL, Ocean Optics) as an illumination source (for recording absorption spectra), and a diode array spectrometer (FLAME-S-UV−VIS−ES, Ocean Optics). The intensity of the irradiation light was calibrated with a chemical actinometer (Azobenzene in MeOH). The samples were kept at 20 °C and continuously stirred with a Peltier-based temperature controller (Luma 40, Quantum Northwest, Inc.). The absorption of the samples was recorded at a right angle with respect to the irradiation source, at fixed irradiation

intervals until complete conversion to the final product. LCMS experiments (Shimadzu LCMS-2020) were performed on the starting solution (before irradiation), and after the photolysis.

4.2 Experimental procedures

4.2.1 To Chapter 1

4.2.1.1 Synthesis of new pyrene dyes

8-Amino-1,3,6-pyrenetrisulfonyl trichloride (1) [2]

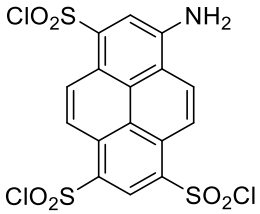

1

Chemical Formula: $C_{16}H_8Cl_3NO_6S_3$
Exact Mass: 510.86

Trisodium salt of 8-aminopyrene-1,3,6-trisulfonic acid (**APTS**) (446 mg, 0.98 mmol) was introduced into a 10 mL flask, cooled to 0 ˚C in an ice bath, and then chlorosulfonic acid (8.5 mL, 0.12 mol) was added dropwise with stirring. The reaction mixture was stirred at r.t. for 4 h, cooled to 0 ˚C, and carefully transferred onto crushed ice (100 g). The red precipitate of trisulfonyl chloride was washed with ice water (3 × 50 mL) and centrifuged. The crude compound was freeze-dried to afford 437 mg of **1** (87% yield) as a dark-red powder. The flask was purged with Ar and kept in the freezer (-20 °C).

^{1}H NMR (400 MHz, CD_3CN) δ 9.26 (d, *J* = 9.8 Hz, 1H), 9.20 (s, 1H), 8.85 (d, *J* = 9.7, 2.7 Hz, 2H), 8.60 (d, *J* = 9.7 Hz, 1H), 8.30 (s, 1H).

^{13}C NMR (101 MHz, CD_3CN) δ 148.9, 142.0, 134.5, 132.8, 132.2, 131.7, 130.0, 129.0, 128.9, 125.6, 121.7, 119.4, 117.5, 116.7.

$C_{16}H_8Cl_3NO_6S_3$, M = 510.9 for $^{35}Cl^{x}3$. EI-MS: *m/z* = 510.9 [$M^{+\cdot}$]

8-Amino-[*N*,*N*′,*N*′′-tris(2-hydroxyethyl)-*N*,*N*′,*N*′′-trimethyl]pyrene-1,3,6-trisulfonamide (3a) [2a]

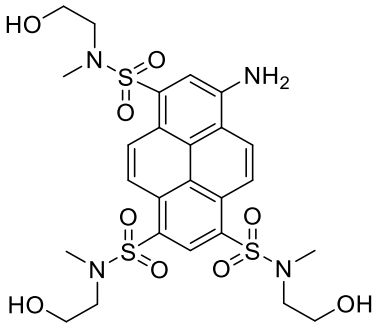

3a

Chemical Formula: $C_{25}H_{32}N_4O_9S_3$
Exact Mass: 628.13

8-aminopyrene-1,3,6-trisulfonyl trichloride **1** (462 mg, 0.90 mmol) was added to a stirred solution of *N*-(methylamino)ethanol (1.0 g, 13 mmol) in aqueous acetonitrile (1:1, 25 mL) at 0 ˚C. The reaction mixture was vigorously stirred at room temperature, until it became homogeneous, and then lyophilized. The title compound **3a** was isolated by chromatography on SiO_2 (100 g) with $CHCl_3$/MeOH/H_2O (80:18:2) mixture as an eluent. Yield – 252 mg (45%) of a brown-orange solid obtained after two purification steps by chromatography.

^{1}H NMR (400 MHz, DMSO-*d*$_6$) δ 9.01 (d, *J* = 9.7 Hz, 1H), 8.86 (s, 1H), 8.79 (d, *J* = 9.7 Hz, 1H), 8.75 (d, *J* = 9.7 Hz, 1H), 8.64 (d, *J* = 9.7 Hz, 1H), 8.06 (s, 1H), 7.58 (br. s, 2H, NH_2), 4.76 (s, 3H, OH), 3.55 – 3.45 (m, 6H), 3.29 – 3.21 (m, 6H), 2.90 (s, 3H), 2.86 (s, 3H), 2.85 (s, 3H).

^{13}C NMR (101 MHz, DMSO-*d*$_6$) δ 147.9, 136.5, 132.9, 131.8, 129.4, 128.6, 127.6, 126.9, 126.8, 126.7, 126.2, 121.5, 118.9, 115.9, 115.6, 115.4, 59.2, 59.0, 58.9, 51.7, 51.5, 51.4, 35.5, 35.2, 35.1.

ESI-HRMS: found 651.1227 $[M+Na]^+$, calculated 651.1229 for $C_{25}H_{32}N_4O_9S_3Na$.

λ_{max} (absorption) = 477 nm (ε = 22 400 M^{-1} cm^{-1}, MeOH), λ_{max} (emission) = 535 nm (MeOH, excitation at 470 nm); fluorescence lifetime 5.6 ns (MeOH); fluorescence quantum yield (0.96; absolute value in MeOH).

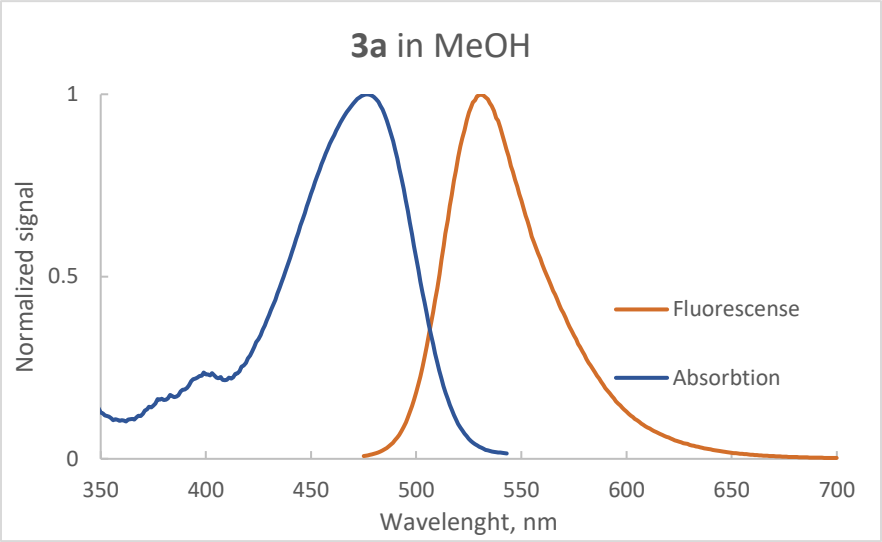

3,6,8-tris((3-((tert-butyldimethylsilyl)oxy)azetidin-1-yl)sulfonyl)pyren-1-amine (3b)

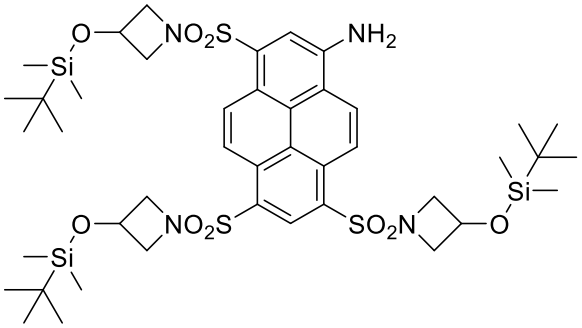

3b

Chemical Formula: $C_{43}H_{68}N_4O_9S_3Si_3$
Exact Mass: 964.35

A solution of sulfonyl chloride **1** (0.2 mmol, 110 mg) in 3 mL of MeCN was added dropwise to a stirred and cooled (0 °C) solution of azetidine-3-OTBDMS (1.35 mmol, 253 mg) and TEA (176 µL, 1.35 mmol) in MeCN (1 mL). 1 h after, the RM was analysed by TLC (DCM/MeOH, 10:1), a spot with R_f = 0.8 was detected. The reaction mixture was lyophilized, the residue was submitted to flash chromatography (SNAP Ultra cartridge with 25 g SiO_2, DCM/MeOH with 1-10% MeOH gradient over 15 CV) to provide the title compound **3b** (48 mg, 42 % yield) as an orange solid.

ESI-HRMS: found 965.3522 $[M+H]^+$, calculated 965.3529; found 987.3341 $[M+Na]^+$, calculated 987.3348.

^{1}H NMR (400 MHz, CD_3CN) δ 9.24 (d, *J* = 9.8 Hz, 1H), 9.08 (s, 1H), 9.06 (d, *J* = 9.6 Hz, 1H), 8.90 (d, *J* = 9.7 Hz, 1H), 8.57 (d, *J* = 9.7 Hz, 1H), 8.22 (s, 1H), 6.11 (s, 2H), 4.55 – 4.43 (m, 3H), 4.11 – 4.01 (m, 6H), 3.75 – 3.62 (m, 6H), 0.67 (d, *J* = 0.7 Hz, 18H), 0.61 (s, 10H), -0.09 (d, *J* = 0.5 Hz, 12H), -0.13 (s, 6H).

^{13}C NMR (126 MHz, CD_3CN) δ 147.7, 135.4, 134.4, 131.9, 130.3, 128.0, 127.3, 127.2, 127.1, 126.6, 124.2, 121.4, 119.5, 61.5, 61.4, 61.3, 61.2, 25.8, 25.7, 18.3, -5.0, -5.05, -5.1.

1,1',1''-(8-aminopyrene-1,3,6-trisulfonyl)tris(azetidin-3-ol) (**3d**)

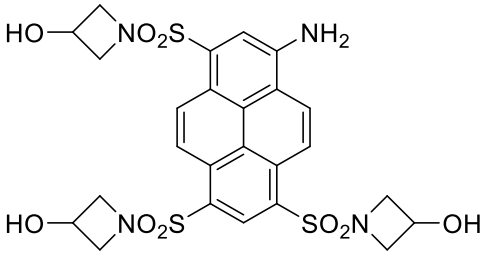

3d

Chemical Formula: $C_{25}H_{26}N_4O_9S_3$
Exact Mass: 622.09

To a stirred solution of tris-silyl ether **3b** (44 mg, 0.45 mmol) in MeCN at 0 °C, HF (74 µL, 2.33 mmol) was added. After stirring for 4h an extra amount of HF was added (74 µL, 2.33 mmol) and the RM was stirred overnight at r.t. The RM was analysed by TLC (DCM/MeOH, 10:1), a spot with R_f = 0.25 was detected. The RM was quenched by the addition of an aqueous sodium bicarbonate solution (5%, 10 mL), then brine. The product was extracted with DCM/iPrOH (1:1; 3×100 mL). The combined organic extracts were dried over $MgSO_4$ and concentrated in vacuo. The residue was submitted to flash chromatography (SNAP Ultra cartridge with 25 g SiO_2, DCM/MeOH with 2-20% MeOH gradient over 15 CV) to provide the title compound **3d** (27 mg, 96 % yield) as an orange solid.

ESI-HRMS: found 623.0913 $[M+H]^+$, calculated 623.0935; found 621.0773 $[M-H]^-$, calculated 624.0789.

^{1}H NMR (400 MHz, DMSO-*d6*) δ 9.06 (d, *J* = 9.7 Hz, 1H), 8.91 (s, 1H), 8.87 (d, *J* = 9.7 Hz, 1H), 8.83 (d, *J* = 9.7 Hz, 1H), 8.70 (d, *J* = 9.8 Hz, 1H), 8.16 (s, 1H), 7.70 (s, 2H), 5.72 – 5.59 (m, 3H), 4.38 – 4.24 (m, 3H), 4.07 – 3.91 (m, 6H), 3.65 – 3.45 (m, 6H).

^{13}C NMR (101 MHz, DMSO-*d6*) δ 148.2, 134.3, 133.3, 133.1, 130.6, 129.1, 127.1, 126.6, 125.9, 125.0, 124.0, 121.9, 119.1, 117.1, 116.7, 115.8, 60.2, 60.0, 58.6, 58.5, 40.4.

λ_{max} (absorption) = 483 nm (ε = 19000 M^{-1} cm^{-1}, MeOH), λ_{max} (emission) = 534 nm (MeOH; excitation at 450 nm); fluorescence lifetime 5.6 ns (MeOH), fluorescence quantum yield: 0.77 (absolute value in MeOH).

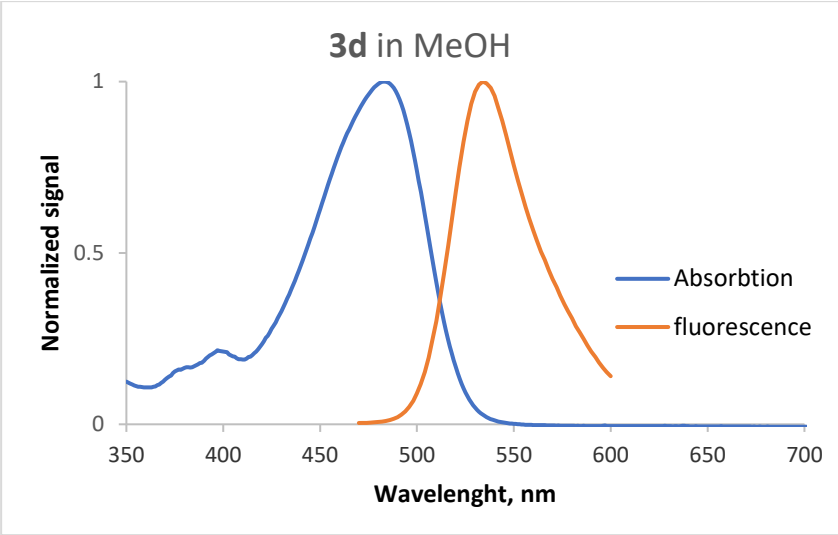

8-Amino-1,3,6-*tris*-[(cyanamido)sulfonyl]pyrene, triethylammonium salt (3c, PCN) [2b]

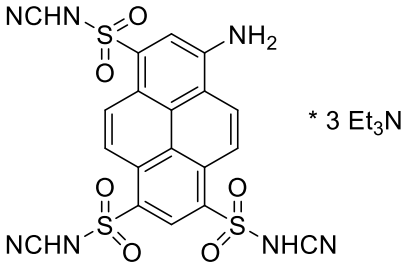

3c (PCN)

Chemical Formula: $C_{19}H_{11}N_7O_6S_3$
Exact Mass: 528.99

To a stirred solution of cyanamide (50 mg, 1.2 mmol) and triethylamine (100 µL, 0.72 mmol) in aqueous MeCN (1 mL) the solid sulfonyl chloride **1** (21 mg, 0.04 mmol) was added at 0 °C in portions. The colour of the reaction mixture became orange. Approx. 10 min after addition of the last portion, the reaction mixture was diluted with aqueous TEAB (2 mL, pH = 8), frozen and lyophilized. The title compound was isolated as a *tris* triethylammonium salt by flash chromatography on reversed phase (15C18AQ-F0025 cartridge) Interchim puriFlash™ (MeCN gradient 0-12% v/v over 12 CV in 25 mM TEAB/MeCN mix). Yield 60 % (orange solid, 20 mg).

^{1}H NMR (400 MHz, D_2O) δ 9.14 (s, 1H), 8.84 (d, *J* = 9.7 Hz, 1H), 8.57 (d, *J* = 9.6 Hz, 1H), 8.52 (d, *J* = 9.7 Hz, 1H), 8.03 (d, *J* = 9.6 Hz, 1H), 7.99 (s, 1H), 2.82 (q, *J* = 7.3 Hz, 18H, CH_2 in Et_3N in salt), 0.99 (t, *J* = 7.3 Hz, 27H, CH_3 in Et_3N in salt).

^{13}C NMR (101 MHz, D_2O) δ 144.8, 138.2, 131.3, 131.1, 130.8, 130.4, 128.2, 126.4, 125.5, 124.8, 124.7, 122.5, 120.1, 116.6, 116.0, 115.4, 46.4, 8.0; three carbons (namely SO2-NH-CN) are missing in ^{13}C NMR because the signals are too weak.

ESI-HRMS: found 527.9850 $[M-H]^-$; calculated 527.9860.

λ_{max} (absorption) = 454 nm (H_2O), ε = 23 900 M^{-1} cm^{-1}, λ_{max} (emission) = 531 nm (excitation at 440 nm); Stokes shift 77 nm, fluorescence lifetime 5.6 ns (H_2O; excitation at 440 nm); fluorescence quantum yield: 0.93 (H_2O).

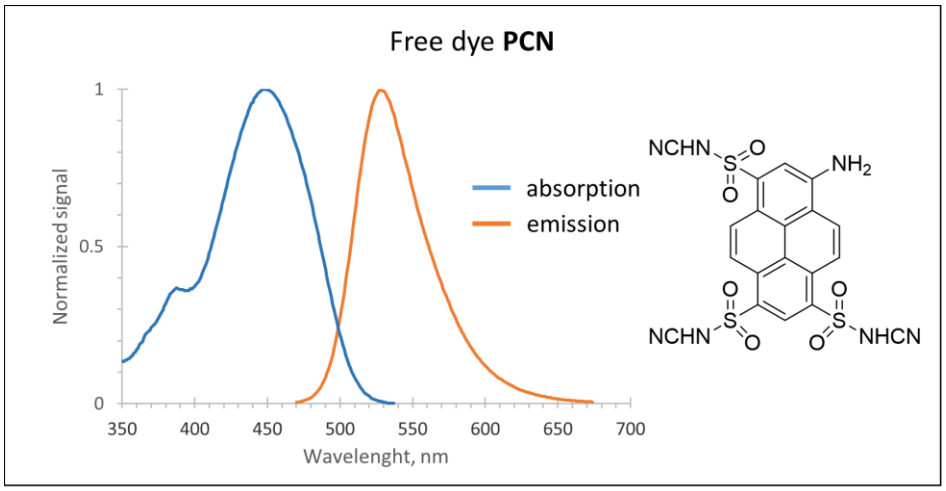

8-Amino-[*N*,*N*′,*N*′′-tris(2-hydroxyethyl)-*N*,*N*′,*N*′′-trimethylpyrene-1,3,6-trisulfonamide]-*O*,*O*′,*O*′′-triphosphate triethylammonium salt (PSN) [2a]

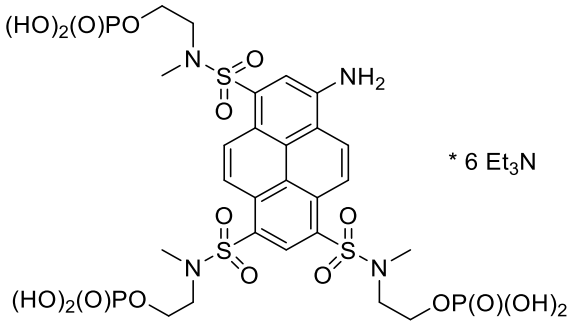

* 6 Et_3N

PSN

Chemical Formula: $C_{25}H_{35}N_4O_{18}P_3S_3$
Exact Mass: 868.03

Direct phosphorylation of 3a (Scheme 4):

Dye **3a** (19 mg, 30 µmol) was dissolved in $(MeO)_3PO$ (0.1 mL), and freshly distilled $POCl_3$ (131 µL, 1.4 mmol) in $(MeO)_3PO$ (0.1 mL) was added with stirring at r.t. A weak exothermic reaction was observed, and the solution turned orange-brown. The reaction mixture was stirred for 3 h at r.t. All volatile components were removed in vacuo, and the residue was further dried by in vacuo. The residue was treated and stirred with 1 M aq. TEAB buffer (pH = 8). Fresh portions of the TEAB buffer were added, when the solution became acidic, until the pH stabilized at 8-9. The title compound was isolated by flash chromatography on reversed phase (15C18AQ-F0025 cartridge) Interchim puriFlash™ (MeCN gradient 0–12% v/v over 12 CV in 25 mM TEAB/MeCN

mix). Freeze-drying of the eluate gave 5 mg of tetrakis triethyammonium salt of the title compound as orange crystals. Yield 16%.

*Deprotection of ^{t}Bu ester **7a** (Scheme 5):*

Ester **7a** (96 mg, 80 μmol) was dissolved in dichloromethane (1 mL), the solution cooled to +5°C in an ice bath, and then TFA (1 mL) was added slowly with stirring. The reaction mixture was allowed to warm-up to r.t. and stirred for 1 h. The volatile materials were removed in vacuo, the residue was co-evaporated with dichloromethane (3 times) and kept in vacuo (0.1 mbar) for 2 h. The residue was treated and stirred with 1 M TEAB buffer (pH = 8-9), until the pH stabilized at 8-9. The title compound was isolated by flash chromatography on reversed phase (15C18AQ-F0025 cartridge) Interchim puriFlash™ (MeCN gradient 0–12% v/v over 12 CV in 25 mM TEAB/MeCN mix). Yield – 89 mg (82%) of the title compound (**PSN**) as hexakis triethylammonium salt.

^{1}H NMR (400 MHz, D_2O) δ 8.76 (s, 1H), 8.69 (d, *J* = 9.7 Hz, 1H), 8.36 (d, *J* = 9.6 Hz, 1H), 8.30 (d, *J* = 9.4 Hz, 1H), 8.07 (d, *J* = 9.6 Hz, 1H), 7.85 (s, 1H), 4.05 – 3.95 (m, 6H), 3.62 – 3.48 (m, 6H), 3.15 (q, *J* = 7.3 Hz, 24H, Et_3N), 2.99 (s, 3H), 2.96 (s, 3H), 2.92 (s, 3H), 1.24 (t, *J* = 7.3 Hz, 36H, Et_3N).

^{13}C NMR (101 MHz, D_2O) δ = 146.6, 135.6, 133.0, 132.0, 129.3, 128.7, 126.9, 126.4, 126.3, 126.2, 125.5, 122.1, 119.6, 117.0, 116.5, 115.6, 62.2, 62.0, 50.7, 50.4, 46.6, 35.6, 35.3, 35.1, 8.2.

^{31}P NMR (162 MHz, D_2O) δ = 1.1, 0.96, 0.91.

ESI-HRMS: found 867.0246 $[M-H]^-$; calculated 867.0249.

λ_{max} (absorption) = 471 nm (H_2O), ε = 18 000 M^{-1} cm^{-1}, λ_{max} (emission) = 544 nm (excitation at 460 nm); Stokes shift 73 nm, fluorescence lifetime 5.6 ns (H_2O; excitation at 440 nm); fluorescence quantum yield: 0.91 (H_2O).

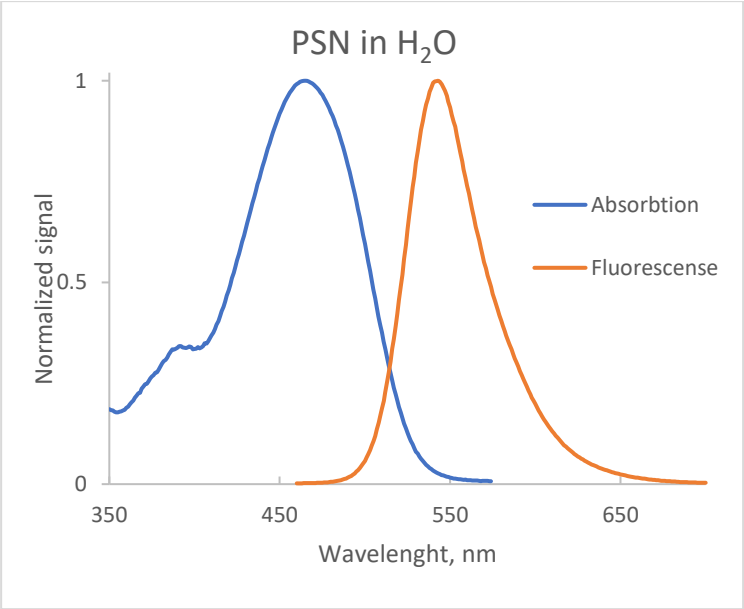

8-Amino-[*N*,*N*',*N*''-*tris*(3-hydroxyazetidine)-1,3,6-trisulfonamide]-*O*,*O*',*O*''-triphosphate triethylammonium salt (PAZ) [2b]

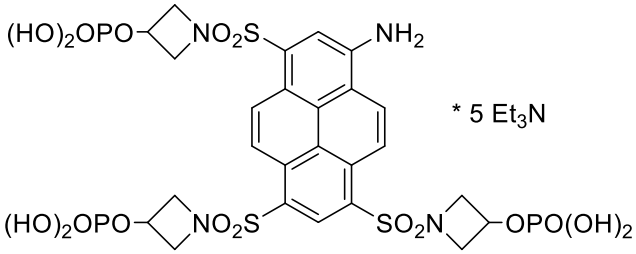

PAZ

Chemical Formula: $C_{25}H_{29}N_4O_{18}P_3S_3$
Exact Mass: 861.99

Direct phosphorylation of 3d (Scheme 4):

Dye **3d** (19 mg, 30 µmol) was dissolved in $(MeO)_3PO$ (0.1 mL), and freshly distilled $POCl_3$ (131 µL, 1.4 mmol) in $(MeO)_3PO$ (0.1 mL) was added with stirring at r.t. A weak exothermic reaction was observed, and the solution turned orange-brown. The reaction mixture was stirred for 3 h at r.t. All volatile components were removed in vacuo, and the residue was further dried by in vacuo. The residue was treated and stirred with 1 M aq. TEAB buffer (pH = 8-9). Fresh portions of the TEAB buffer were added, when the solution became acidic, until the pH stabilized at 8-9. The title compound was isolated by flash chromatography on reversed phase (15C18AQ-F0025 cartridge) Interchim puriFlash™ (MeCN gradient 0–12% v/v over 12 CV in 25 mM TEAB/MeCN mix). Freeze-drying of the eluate gave 5 mg of tetrakis triethyammonium salt of **PAZ** as orange crystals. Yield 13%.

*Deprotection of ^{t}Bu ester **7b** (Scheme 5):*

Ester **7b** (25 mg, 0.02 mmol) was dissolved in dichloromethane (2 mL), the solution cooled to +5°C in an ice bath, and then a solution TFA in DCM (5 %, 5 mL) was added slowly with stirring. The reaction mixture was allowed to warm-up to r.t. and stirred for 2 h. The volatile materials were removed in vacuo. The residue was stirred with 1 M TEAB until the pH stabilized at 8-9. The title compound was isolated as a pentakis triethylammonium salt by flash chromatography on reversed phase (15C18AQ-F0025 cartridge) Interchim puriFlash™ (MeCN gradient 0–12% v/v over 12 CV in 25 mM TEAB/MeCN mix). Yield 88 % (24 mg of a red solid).

ESI-HRMS: found 860.9760 $[M-H]^-$, calculated 860.9779.

^{1}H NMR (400 MHz, D_2O) δ 8.96 (s, 1H), 8.77 (d, *J* = 9.7 Hz, 1H), 8.41 (t, *J* = 9.5 Hz, 2H), 8.15 (d, *J* = 9.6 Hz, 1H), 7.96 (s, 1H), 4.77 – 4.67 (m, 3H), 4.20 – 4.07 (m, 7H), 4.02 (dd, *J* = 8.9, 5.5 Hz, 3H), 3.87 (ddd, *J* = 28.3, 8.9, 5.5 Hz, 4H), 2.90 (q, *J* = 7.3 Hz, 30H, Et_3N), 1.11 (t, *J* = 7.3 Hz, 45H, Et_3N).

^{13}C NMR (101 MHz, D_2O) δ 146.6, 133.5, 132.5, 132.5, 130.5, 128.9, 126.2, 125.4, 125.0, 124.5, 124.2, 122.2, 119.7, 117.1, 116.9, 116.0, 60.9, 60.7, 60.2, 59.7, 59.7, 59.3, 59.3, 46.2, 8.6.

^{31}P NMR (162 MHz, D_2O) δ 2.98, 2.94, 2.91.

λ_{max} (absorption) = 476 nm (H_2O), ε = 19 000 M^{-1} cm^{-1}, λ_{max} (emission) = 543 nm (H_2O; excitation at 450 nm); Stokes shift 67 nm, fluorescence lifetime 5.9 ns (H_2O), fluorescence quantum yield: 0.92 (absolute value in H_2O).

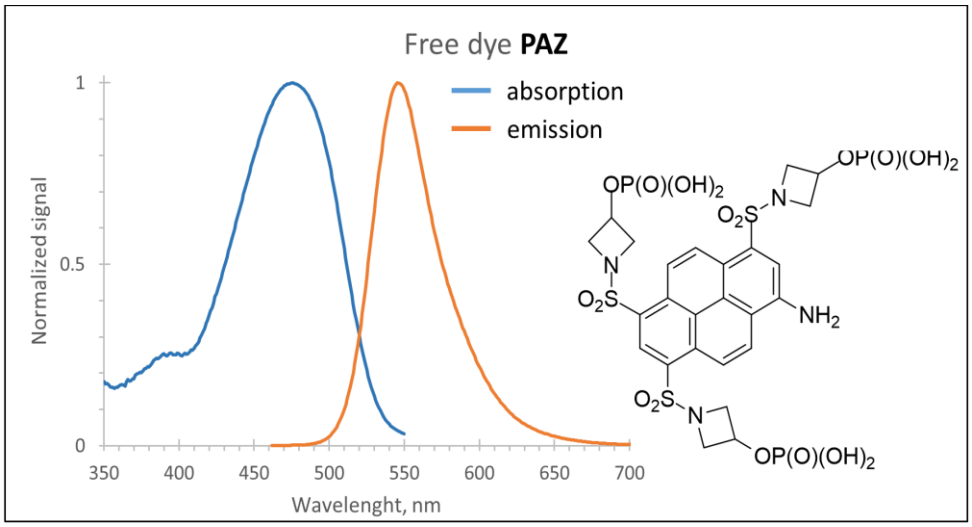

Benzyl *N*-(2-hydroxyethyl)methylcarbamate (4a) [2a; 3]

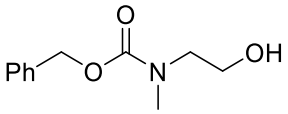

4a

Chemical Formula: $C_{11}H_{15}NO_3$
Exact Mass: 209.11

Benzylchloroformate (1.2 eq, 13.7 g, 81 mmol) and triethylamine (11 mL, 81 mmol) were sequentially and dropwise added at 0 °C to a solution of 2-(methylamino)ethanol (5.0 g, 67 mmol) in dry DCM (150 mL). The cooling bath was removed, and the reaction mixture was stirred overnight at r.t. The reaction mixture was washed with water (2 × 50 mL), brine, and the organic solution was dried over $MgSO_4$ and concentrated in vacuo. TLC (SiO_2): R_f = 0.25 (EtOAc/hexane = 1:1). The title compound was isolated by column chromatography on SiO_2, eluting with 50% EtOAc–hexane to provide 11.2 g of **4a** as a white-yellow solid (yield 80%).

^{1}H NMR (400 MHz, $CDCl_3$): δ 7.39 – 7.28 (m, 5H), 5.12 (s, 2H), 3.74 (br. s, 2H), 3.44 (t, *J* = 5.4 Hz, 2H), 2.99 (s, 3H).

^{13}C NMR (101 MHz, $CDCl_3$): δ 136.7, 128.6, 128.1, 127.9, 67.4, 61.2, 52.0, 35.4.

Benzyl *N*-[[di(*t*-butoxy)phosphoryl]oxy]ethylmethylcarbamate (5a) [2a]

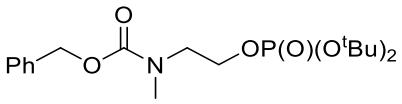

5a

Chemical Formula: $C_{19}H_{32}NO_6P$
Exact Mass: 401.20

Tetrazole (0.45 M solution in CH_3CN, 45 mL, 20 mmol) and di-*t*-butyl *N*,*N*-diisopropylphosphoramidite (5.3 mL, 15 mmol) were added to a solution of **4a** (2.1 g, 10.0 mmol) in THF (50 mL) under Ar, and the mixture was stirred at r.t. for 3 h. HPLC analysis of the reaction mixture indicated that the starting material was consumed. The mixture was cooled to 0 ºC, and H_2O_2 (70% aqueous, 8.0 mL) was added. After 30 min, an aqueous solution of Na_2SO_3 (10%, 50 mL) was added with cooling in an ice bath. Organic solvents were removed under reduced pressure, and the residue was extracted with EtOAc (3 × 50 mL). The combined organic solutions were washed with brine, dried over $MgSO_4$, and evaporated. The residue was subjected to column chromatography on SiO_2 (50 g); elution with 50% EtOAc–petroleum ether provided 2.36 g of **5a** as a colourless oil (yield 59%).

^{1}H NMR (400 MHz, CD_3CN) δ 7.41 – 7.26 (m, 4H), 5.09 (s, 2H), 4.04 – 3.93 (m, 2H), 3.54 – 3.45 (m, 2H), 2.94 (d, *J* = 10.2 Hz, 3H), 1.42 (s, 18H).

^{13}C NMR (101 MHz, CD_3CN) δ 138.3, 129.4, 128.8, 128.7, 83.0, 82.9, 67.6, 67.5, 30.1, 30.0, 29.7, 19.4.

^{31}P NMR (162 MHz, CD_3CN) δ -9.97.

2-(methylamino)ethyl di(*t*-butyl)phosphate (6a) [2a]

6a

Chemical Formula: $C_{11}H_{26}NO_4P$
Exact Mass: 267.16

A Schlenk flask was charged with a stirring bar, Pd/C (10% wt, 0.12 g, oxidized form) was added followed by MeOH (10 mL). The flask was closed with a septum, flushed with argon (outlet through the septum via cannula) and then filled with hydrogen supplied from a balloon attached to the side arm of the flask. After stirring for 30 min, a solution of **5a** (1.2 g, 3.0 mmol) in MeOH (10 mL) was added to a Schlenk flask charged with hydrogen-activated Pd/C. The reaction mixture was stirred at r.t. overnight under hydrogen. The reaction mixture was thoroughly flushed with argon (with stirring) and transferred into centrifugation tubes. The catalyst was removed by centrifugation, washed with MeOH, and the combined organic solutions were evaporated in vacuo to afford 800 mg of **6a** (84% yield) as a colourless oil.

^{1}H NMR (400 MHz, CD_3CN) δ 4.03 – 3.95 (m, 2H), 2.83 – 2.77 (m, 2H), 2.40 (s, 3H), 1.45 (s, 18H).

^{13}C NMR (101 MHz, CD_3CN) δ 83.1, 83.0, 66.3, 66.2, 51.6, 51.5, 35.8, 30.10, 30.06.

^{31}P NMR (162 MHz, CD_3CN) δ -9.74.

8-Amino-[[*N*,*N*′,*N*′′-tris(2-hydroxyethyl)-*N*,*N*′,*N*′′-trimethyl]pyrene-1,3,6-trisulfonamide]-*O*,*O*′,*O*′′-triphosphate hexakis *tert*-butyl ester (7a) [2a]

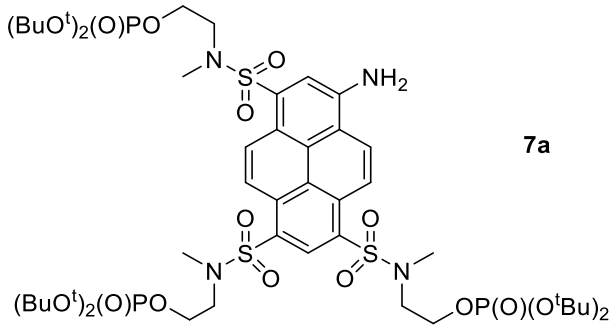

7a

Chemical Formula: $C_{49}H_{83}N_4O_{18}P_3S_3$
Exact Mass: 1204.41

8-aminopyrene-1,3,6-trisulfonyl trichloride **1** (52 mg, 0.10 mmol) was added to a solution of 2-(methylamino)ethyl di(*t*-butyl)phosphate **6a** (0.6 mmol, 160 mg) and triethylamine (0.14 mL,

1.0 mmol) in acetonitrile (2 mL) under Ar. The reaction mixture was stirred at r.t. overnight and concentrated in vacuo. The title compound was isolated by flash chromatography on SiO_2 (SNAP "Ultra" cartridge with 50 g SiO_2, DCM/MeOH with 2-20% MeOH gradient over 13 CV) to afford 96 mg of **7a** (80% yield) as a brown-orange solid.

^{1}H NMR (400 MHz, CD_3OD) δ 9.18 (d, *J* = 9.8 Hz, 1H), 9.06 (s, 1H), 8.95 (d, *J* = 9.7 Hz, 1H), 8.79 (d, *J* = 9.8 Hz, 1H), 8.68 (d, *J* = 9.7 Hz, 1H), 8.13 (s, 1H), 4.13 – 4.08 (m, 6H), 3.63 – 3.55 (m, 6H), 3.05 (s, 3H), 3.01 (s, 3H), 3.00 (s, 3H), 1.51 (d, J = 0.6 Hz, 18H).

^{13}C NMR (101 MHz, CD_3OD) δ 149.1, 138.1, 134.8, 133.8, 131.1, 130.2, 129.3, 128.8, 128.7, 128.0, 127.5, 123.5, 120.6, 118.3, 117.6, 117.0, 85.0, 84.9, 84.8, 84.7, 66.5, 66.4, 66.3, 66.2, 66.1, 51.1, 51.0, 50.9, 50.8, 50.7, 36.5, 36.3, 36.2, 30.7, 30.6, 30.2, 30.1.

^{31}P NMR (162 MHz, CD_3OD) δ -10.22, -10.29, -10.37.

ESI-HRMS: found 1227.3970 $[M+Na]^+$, calculated 1227.3979.

1-Benzyloxycarbonylazetidin-3-ol (4b) [2b]

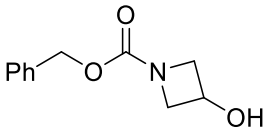

4b

Chemical Formula: $C_{11}H_{13}NO_3$
Exact Mass: 207.09

Benzyl chloroformate (1.68 g, 1.40 mL, 9.65 mmol) was added dropwise at 0 °C to a solution of 3-hydroxyazetidine hydrochloride (1.0 g, 9.0 mmol), K_2CO_3 (2.50 g, 18.1 mmol) in THF-water mixture (70 mL). The cooling bath was removed, and the reaction mixture stirred overnight at r.t. THF was evaporated in vacuo, the residue diluted with EtOAc (50 mL), washed with water (50 mL × 2), and the organic solution dried over $MgSO_4$ and concentrated in vacuo. TLC (SiO_2): R_f = 0.2 (hexane/EtOAc 1:1). The residue was submitted to flash chromatography (SNAP Ultra cartridge with 50 g SiO_2, hexane/EtOAc with 10-70% v/v EtOAc gradient over 15 CV) to provide the title compound **4b** (1.80 g, 96% yield) as a white solid.

^{1}H NMR (400 MHz, $(CD_3)_2CO$) δ 7.47 – 7.24 (m, 5H), 5.06 (d, *J* = 0.7 Hz, 2H), 4.62 – 4.53 (m, 1H), 4.15 (s, 2H), 3.84 – 3.68 (m, 2H).

1-Benzyloxycarbonylazetidin-3-di(*t*-butyl)phosphate (5b) [2b]

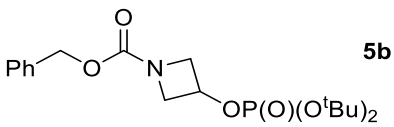

5b

Chemical Formula: $C_{19}H_{30}NO_6P$
Exact Mass: 399.18

1-H tetrazole (840 mg, 12 mmol) and di-*t*-butyl *N*,*N*-diisopropylphosphoramidite (2.8 g, 3.2 mL, 9.6 mmol) were added to a solution of 1-benzyloxycarbonylazetidin-3-ol **4b** (1.0 g, 4.8 mmol) in DMF (8 mL) under Ar and the mixture was stirred at r.t. for 1 h. The formation of the intermediate phosphite was detected by HPLC, t_R = 10.1 min (method A, MeCN gradient 20–100 in 18 min); t_R of starting compound is 7.6 min. Once the reaction was complete, the mixture was cooled to 0 ºC and H_2O_2 (70% aqueous, 1.5 mL) was added. 15 minutes later, the reaction mixture was analysed by HPLC, t_R = 12.07 min (method A, MeCN gradient 20–100 in 18 min); the intermediate phosphite was fully oxidized to phosphate. Then aqueous Na_2SO_3 (10%, 30 mL) was added under ice bath cooling. The organic solvents were removed under reduced pressure and the aqueous residue was extracted with EtOAc (30 mL × 3). The combined organic extracts were washed with brine, dried over $MgSO_4$, and evaporated in vacuo. The residue was submitted to flash chromatography (SNAP Ultra cartridge with 50 g SiO_2, hexane/EtOAc with 20-65% v/v EtOAc gradient over 15 CV) to provide the title compound **5b** (1.18 g, 62% yield) as a white solid.

ESI-HRMS: found 400.1882 $[M+H]^+$, calculated 400.1884; found 422.1703 $[M+Na]^+$, calculated 422.1703.

^{1}H NMR (400 MHz, $(CD_3)_2CO$) δ 7.42 – 7.28 (m, 4H), 5.08 (d, *J* = 0.5 Hz, 2H), 5.02 (tdt, *J* = 6.7, 5.9, 4.2 Hz, 1H), 4.28 (t, *J* = 8.3 Hz, 2H), 4.06 – 3.97 (m, 2H), 1.47 (d, *J* = 0.7 Hz, 18H).

^{13}C NMR (101 MHz, $(CD_3)_2CO$) δ 138.0, 129.2, 128.7, 128.6, 83.2, 83.1, 66.9, 66.0, 65.9, 30.0.

^{31}P NMR (162 MHz, $(CD_3)_2CO$) δ -10.91.

Azetidin-3-di(*t*-butyl)phosphate (6b) [2b]

6b

Chemical Formula: $C_{11}H_{24}NO_4P$
Exact Mass: 265.14

A solution of 1-benzyloxycarbonylazetidin-3-di(*t*-butyl)phosphate **5b** (640 mg, 1.60 mmol) in MeOH (10 mL) was added to a Schlenk flask charged with previously activated Pd/C (25% wt, 160 mg) in THF (3 mL) under H_2. The reaction mixture was stirred in an atmosphere of hydrogen at r.t. overnight. The mixture was centrifuged, and the solution evaporated to give the title compound (390 mg, 92% yield) as a colourless oil.

ESI-HRMS: found 266.1504 $[M+H]^+$, calculated 266.1516; found 288.1346 $[M+Na]^+$, calculated 288.1335.

^{1}H NMR (400 MHz, CD_3CN) δ 5.03 – 4.94 (m, 1H), 4.26 – 4.18 (m, 2H), 4.11 – 4.01 (m, 2H), 1.41 (d, *J* = 0.7 Hz, 18H).

^{13}C NMR (101 MHz, CD_3CN) δ 85.6, 85.5, 67.2, 65.2, 55.3, 54.6, 30.0, 29.9, 1.9, 1.7.

^{31}P NMR (162 MHz, CD_3CN) δ -12.0.

8-Amino-[*N*,*N*',*N*''-*tris*(3-hydroxyazetidine)-1,3,6-trisulfonamide]-*O*,*O*',*O*''-triphosphate hexakis *tert*-butyl ester (7b) [2b]

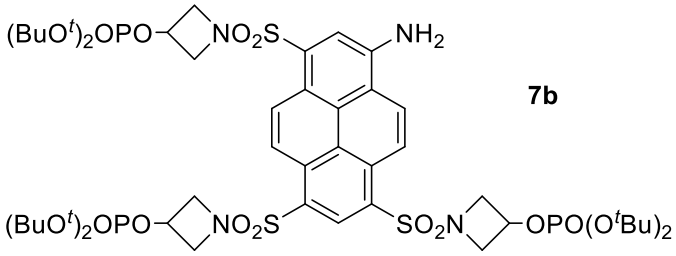

7b

Chemical Formula: $C_{49}H_{77}N_4O_{18}P_3S_3$
Exact Mass: 1198.36

A solid sulfonyl chloride **1** (0.05 mmol, 25 mg) was added in portions to a stirred and cooled (0 °C) solution of azetidin-3-di(*t*-butyl)phosphate **6b** (1.3 mmol, 345 mg) and triethylamine (175 µL, 1.26 mmol) in MeCN (2 mL). 10 minutes later, the reaction mixture was analysed by TLC (DCM/MeOH, 10:1), and a spot with R_f = 0.5 was detected. The reaction mixture was lyophilized, and the residue was submitted to flash chromatography (SNAP Ultra cartridge with 10 g SiO_2, DCM/MeOH with 2-15% v/v MeOH gradient over 15 CV) to provide the title compound **7b** (27 mg, 45 % yield) as an orange solid.

ESI-HRMS: found 1199.3645 $[M+H]^+$, calculated 1199.3681; found 1221.3505 $[M+Na]^+$, calculated 1221.3500

^{1}H NMR (400 MHz, CD_3CN) δ 9.24 (d, *J* = 9.8 Hz, 1H), 9.09 (s, 1H), 9.05 (d, *J* = 9.6 Hz, 1H), 8.89 (d, *J* = 9.8 Hz, 1H), 8.60 (d, *J* = 9.7 Hz, 1H), 8.24 (s, 1H), 4.83 – 4.72 (m, 3H), 4.19 (ddt, *J* = 11.3, 6.5, 2.8 Hz, 6H), 4.01 – 3.85 (m, 6H), 1.29 (s, 18H), 1.29 (s, 18H), 1.24 (s, 18H).

^{31}P NMR (162 MHz, CD_3CN) δ -11.62, -11.65, -11.75.

4.2.1.2 Synthesis of substituted fluorobenzenes

***N*-cyano-4-fluorobenzenesulfonamide (8b)** [2b]

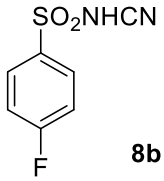

8b

Chemical Formula: $C_7H_5FN_2O_2S$
Exact Mass: 200.01

1. Synthesis of 4-fluorobenzenesulfonyl amide (Scheme 7): Commercially available 4-fluorobenzenesulfonyl chloride (1 mmol, 198 mg) was suspended in 1 mL of THF and cooled to 0 °C in an ice bath. NH_4OH (25 % aq., 5 eq, 0.3 mL) was added dropwise. The reaction mixture was stirred at 0 °C for 30 min, then 1 h at r.t. The formation of sulfonamide was observed by TLC (hexane/EtOAc, 5:1), R_f = 0.2. The reaction mixture was concentrated in vacuo, the crude product was dried and used in the next reaction without further purification.

^{1}H NMR (400 MHz, DMSO-d_6) δ 7.89 – 7.80 (m, 2H), 7.46 – 7.31 (m, 2H).

^{19}F NMR (376 MHz, DMSO-d_6) δ -108.17 (td, J = 8.9, 5.0 Hz).

2. To a stirred and cooled (ice bath) solution of 4-fluorobenzenesulfonyl amide (0.5 mmol, 87 mg) and Et_3N (0.5 mmol, 65 µL) in 1 mL of THF, cyanogen bromide (0.5 mmol, 27 µL) was added. The formation of the *N*-cyanosulfonamide was observed by TLC (DCM/MeOH, 10:1), R_f = 0.45. The reaction mixture was concentrated in vacuo, and the crude residue was submitted to flash chromatography (SNAP Ultra cartridge with 25 g SiO_2, DCM/MeOH with 2-10% v/v MeOH gradient over 10 CV) to provide the title compound **8b** (87 mg, 89 % yield) as a white powder.

^{1}H NMR (400 MHz, DMSO-d_6) δ 7.97 – 7.87 (m, 2H), 7.39 (t, J = 8.9 Hz, 2H).

^{19}F NMR (376 MHz, DMSO-d_6) δ -107.92.

^{13}C NMR (101 MHz, DMSO-d_6) δ 165.1, 162.5, 140.6, 128.7, 128.6, 116.2, 115.9.

ESI-HRMS: found 198.9981 $[M-H]^-$, calculated 198.9983.

***N*-cyano-3-fluorobenzenesulfonamide (8a)** [2b]

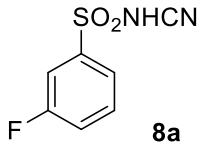

8a

Chemical Formula: $C_7H_5FN_2O_2S$
Exact Mass: 200.01

1. Synthesis of 3-fluorobenzenesulfonyl amide (Scheme 7): Commercially available 3-fluorobenzenesulfonyl chloride (1.00 mmol, 198 mg) was suspended in 1 mL of THF and cooled to 0 °C (ice bath). NH_4OH (25 % aq., 5 eq, 0.30 mL) was added dropwise. The reaction mixture was stirred at 0 °C for 30 min, then 1 h at r.t. The formation of sulfonamide was observed by TLC (hexane/EtOAc, 5:1), R_f = 0.2. The reaction mixture was concentrated in vacuo, the crude product was dried and used in the next reaction without further purification.

^{1}H NMR (400 MHz, DMSO-d_6) δ 7.66 – 7.55 (m, 2H), 7.50 (d, J = 3.1 Hz, 1H), 7.47 – 7.40 (m, 1H).

^{19}F NMR (376 MHz, DMSO-d_6) δ -111.15 (td, J = 8.7, 5.2 Hz).

2. To a stirred and cooled (ice bath) solution of 4-fluorobenzenesulfonyl amide (0.5 mmol, 87 mg) and Et_3N (0.5 mmol, 65 µL) in 1 mL of THF, cyanogen bromide (0.5 mmol, 27 µL) was added. The formation of *N*-cyanosulfonamide was observed by TLC (DCM/MeOH, 10:1), R_f = 0.45. The reaction mixture was concentrated in vacuo and the crude residue was submitted to flash chromatography (SNAP Ultra cartridge with 25 g SiO_2, DCM/MeOH with 2-10% v/v MeOH gradient over 10 CV) to provide the title compound **8a** (78 mg, 78 % yield) as a white powder.

^{1}H NMR (400 MHz, DMSO-d_6) δ 7.70 (ddd, J = 7.8, 1.6, 1.1 Hz, 1H), 7.67 – 7.60 (m, 2H), 7.48 – 7.42 (m, 1H).

^{19}F NMR (376 MHz, DMSO-d_6) δ -111.02 (td, J = 8.8, 5.2 Hz).

^{13}C NMR (101 MHz, DMSO-d_6) δ 162.9, 160.5, 146.3, 131.5, 121.9, 119.0, 112.8.

ESI-HRMS: found 174.0031 $[M\text{-}CN]^-$, calculated 174.0031.

4-Fluoro-*N*-(3-hydroxyazetidinyl)benzenesulfonamide (9b) [2b]

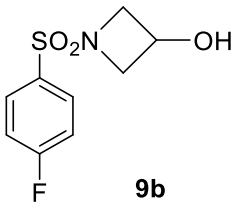

9b

Chemical Formula: $C_9H_{10}FNO_3S$
Exact Mass: 231.04

Commercially available 4-fluorobenzenesulfonyl chloride (0.5 mmol, 100 mg) was suspended in 1 mL of DCM and cooled to 0 °C in an ice bath. 3-Hydroxyazetidine hydrochloride (0.4 mmol, 45 mg) and Et_3N (1 mmol, 130 µL) in 1 mL of DCM were added sequentially. The reaction mixture was stirred at r.t. overnight. The formation of sulfonamide was observed by TLC (hexane/EtOAc, 5:1), R_f = 0.4. The reaction mixture was concentrated in vacuo, and the residue

was submitted to flash chromatography (SNAP Ultra cartridge with 25 g SiO_2, hexane/EtOAc gradient with 10-90% v/v of EtOAc over 15 CV) to provide the title compound **9b** (27 mg, 29%) as a white solid.

^{1}H NMR (400 MHz, DMSO-d_6) δ 7.92 – 7.84 (m, 2H), 7.59 – 7.47 (m, 2H), 5.71 (dd, J = 6.2 Hz, 1H), 4.27 (s, 1H), 3.94 – 3.84 (m, 2H), 3.37 – 3.29 (m, 2H).

^{19}F NMR (376 MHz, DMSO-d_6) δ -105.48 (ddd, J = 14.2, 8.8, 5.2 Hz).

^{13}C NMR (101 MHz, DMSO-d_6) δ 166.1, 163.6, 131.4, 131.3, 116.8, 116.6, 60.4, 58.7.

ESI-HRMS: found 232.0439 $[M+H]^+$, calculated 232.0438.

3-Fluoro-*N*-(3-hydroxyazetidinyl)benzenesulfonamide (9a) [2b]

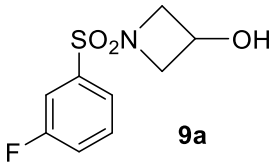

9a

Chemical Formula: $C_9H_{10}FNO_3S$
Exact Mass: 231.04

Commercially available 3-fluorobenzenesulfonyl chloride (0.5 mmol, 100 mg) was suspended in 1 mL of DCM and cooled to 0 °C (ice bath). 3-Hydroxyazetidine hydrochloride (0.4 mmol, 45 mg) and Et_3N (1 mmol, 130 µL) in 1 mL of DCM were added sequentially. The reaction mixture was stirred at r.t. overnight. The formation of the sulfonamide was observed by TLC (hexane/EtOAc, 5:1), R_f = 0.45. The reaction mixture was concentrated in vacuo, and the residue was submitted to flash chromatography (SNAP Ultra cartridge with 25 g SiO_2, hexane/EtOAc gradient with 10-90% EtOAc over 15 CV) to provide the title compound **9a** (25 mg, 27% yield) as a white solid.

^{1}H NMR (400 MHz, DMSO-d_6) δ 7.81 – 7.71 (m, 1H), 7.70 – 7.60 (m, 3H), 5.73 (d, J = 6.2 Hz, 1H), 4.29 (s, 1H), 3.98 – 3.88 (m, 2H), 3.43 – 3.35 (m, 2H).

^{19}F NMR (376 MHz, DMSO-d_6) δ -110.16 (td, J = 8.6, 5.4 Hz).

^{13}C NMR (101 MHz, DMSO-d_6) δ 163.2, 160.7, 131.8, 124.5, 120.7, 115.2, 60.6, 58.7.

ESI-HRMS: found 232.0440 $[M+H]^+$, calculated 232.0438

4.2.1.3 Synthesis of individual conjugates with glucose

General procedure:

1.5 mL Eppendorf tube was charged with a dye (100 µL of 0.1 M solution in water), glucose monohydrate (5 eq., 10 mg, 0.05 mmol), and malonic acid (10 eq, 100 µL of 1 M solution in DMSO). The samples were shaken at 40 °C for 1 h in an Eppendorf ThermoMixer®, and the solvents were completely removed in a freeze-dryer (residual pressure <0.1 mbar, temp. of the cooling coil –80°C). A solution of 2-picoline-borane complex (10 eq, 100 µL of 1 M solution in DMSO) and malonic acid (10 eq, 100 µL of 1 M solution in DMSO) were added, and the samples were stirred at 40°C for 16 h in an Eppendorf ThermoMixer®. The products were isolated by flash chromatography on Interchim puriFlash™ (RP C18, 15C18AQ-F0025 cartridge, MeCN gradient 0–12% v/v over 15 CV in 25 mM TEAB/MeCN mixture).

Conjugate **APTS-G**

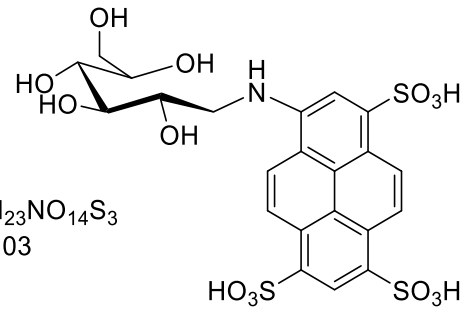

Chemical Formula: $C_{22}H_{23}NO_{14}S_3$
Exact Mass: 621.03

HPLC: t_R = 7.8 min (method C, MeCN gradient 2–10% in 20 min); t_R of the free **APTS** dye = 7.2 min.

Yield 100 %.

ESI-HRMS: found 620.0206 $[M-H]^-$, calculated 620.0208; found 309.5063 $[M-2H]^{2-}$, calculated 309.5068.

λ_{max} (absorption) = 455 nm (H_2O), ε = 17 160 M^{-1} cm^{-1}, λ_{max} (emission) = 511 nm (excitation at 440 nm); Stocks shift 56 nm, fluorescence lifetime 5.1 ns (H_2O; excitation at 440 nm); fluorescence quantum yield: 0.92 (H_2O).

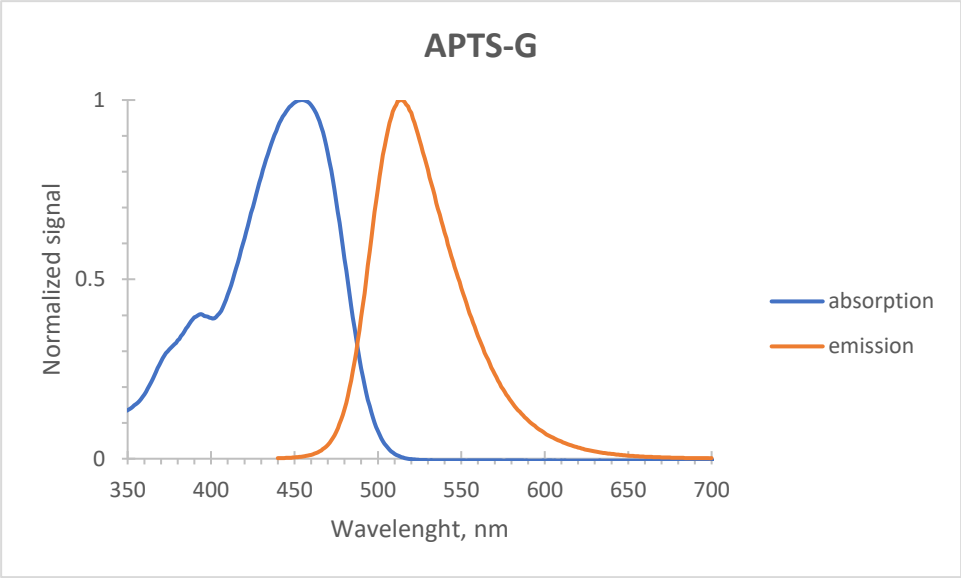

Conjugate **PCN-G** [2b]

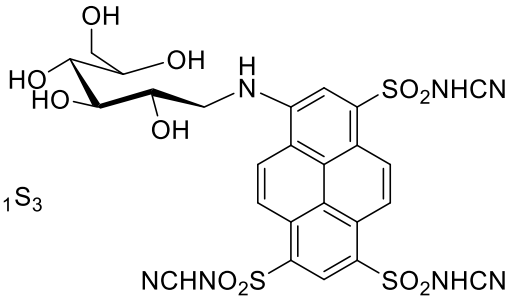

Chemical Formula: $C_{25}H_{23}N_7O_{11}S_3$
Exact Mass: 693.06

93% yield. Analytical HPLC: t_R = 12.9 min (method B, MeCN gradient 1–25% in 20 min) detected at 469 nm; t_R of the free **PCN** dye = 14.2 min.

ESI-HRMS: found 692.0530 $[M-H]^-$, calculated 692.0545; found 345.5235 $[M-2H]^{2-}$, calculated 345.5236.

λ_{max} (absorption) = 484 nm (H_2O), ε = 29 000 M^{-1} cm^{-1}, λ_{max} (emission) = 544 nm (excitation at 470 nm); Stocks shift 60 nm, fluorescence lifetime 5.5 ns (H_2O; excitation at 440 nm); fluorescence quantum yield: 0.92 (H_2O).

^{1}H NMR (400 MHz, D_2O) δ 9.10 (s, 1H), 8.78 (d, *J* = 9.7 Hz, 1H), 8.57 (d, *J* = 9.7 Hz, 1H), 8.45 (d, *J* = 9.8 Hz, 1H), 8.07 (d, *J* = 9.7 Hz, 1H), 7.79 (s, 1H), 4.21 (dt, *J* = 8.6, 4.4 Hz, 1H), 3.99 (dd, *J* = 4.9, 2.0 Hz, 1H), 3.92 – 3.82 (m, 4H), 3.74 (ddd, *J* = 17.2, 11.2, 3.8 Hz, 3H), 3.54 (dd, *J* = 13.8, 8.3 Hz, 1H), 2.61 (q, *J* = 7.3 Hz, 36H, Et_3N), 0.96 (t, *J* = 7.3 Hz, 54H, Et_3N).

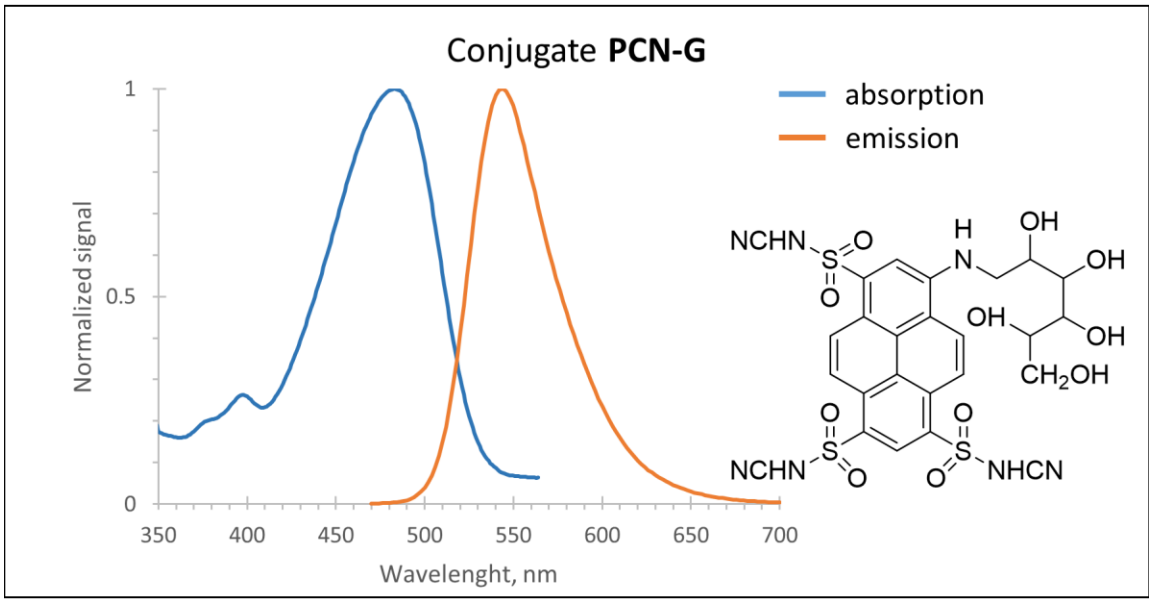

Conjugate **PAZ-G** [2b]

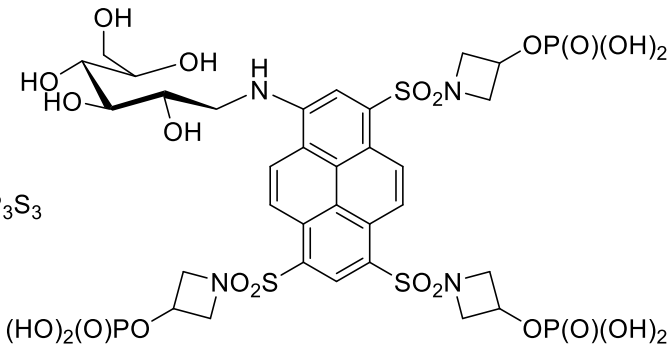

Chemical Formula: $C_{31}H_{41}N_4O_{23}P_3S_3$
Exact Mass: 1026.05

95 % yield. Analytical HPLC: t_R = 12.17 min (method B, MeCN gradient 1–25% in 20 min) detected at 492 nm; t_R of the free **PAZ** dye = 12.5 min.

ESI-HRMS: found 512.0201 $[M-2H]^{2-}$, calculated 512.0196.

λ_{max} (absorption) = 505 nm (H_2O), λ_{max} (emission) = 564 nm (excitation at 490 nm); Stocks shift 59 nm, fluorescence lifetime 5.8 ns (H_2O; excitation at 440 nm); fluorescence quantum yield: 0.90 (H_2O).

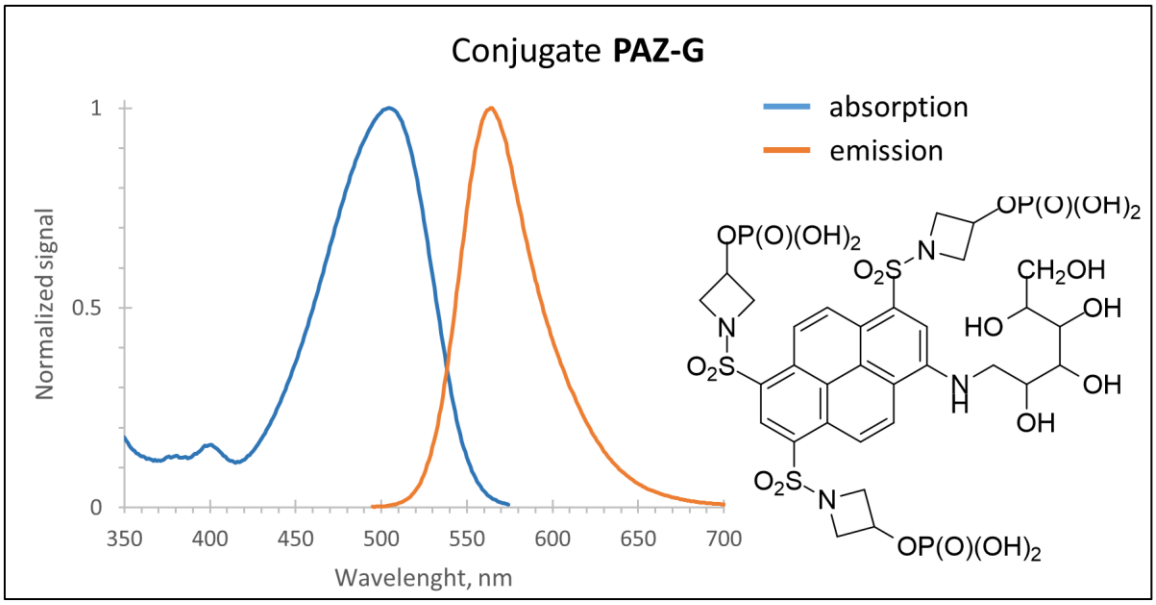

Conjugate **PSN-G** [2b]

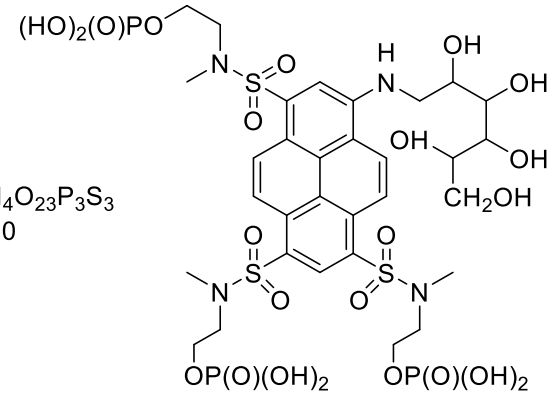

Chemical Formula: $C_{31}H_{47}N_4O_{23}P_3S_3$
Exact Mass: 1032.10

98% yield. Analytical HPLC: t_R = 7.7 min (method C, MeCN gradient 5–60% in 20 min) detected at 500 nm; t_R of the free **PSN** dye = 6.4 min.

ESI-HRMS: found 515.0452 $[M-2H]^{2-}$, calculated 515.0430.

λ_{max} (absorption) = 496 nm (H_2O), ε = 30 000 M^{-1} cm^{-1}, λ_{max} (emission) = 558 nm (excitation at 470 nm); Stocks shift 62 nm, fluorescence lifetime 5.7 ns (H_2O; excitation at 440 nm); fluorescence quantum yield: 0.91 (H_2O).

^{1}H NMR (400 MHz, D_2O) δ 8.76 (d, *J* = 2.5 Hz, 1H), 8.67 (d, *J* = 8.6 Hz, 1H), 8.41 – 8.24 (m, 2H), 8.11 (s, 1H), 7.70 (s, 1H), 4.27 (dt, *J* = 8.8, 4.6 Hz, 1H), 4.09 – 3.82 (m, 13H), 3.73 (d, *J* = 7.5 Hz, 2H), 3.59 (t, *J* = 5.4 Hz, 2H), 3.53 (t, *J* = 5.5 Hz, 2H), 3.41 (s, 2H), 3.16 (q, *J* = 7.3 Hz, 24H, Et_3N), 2.97 (s, 3H), 2.92 (s, 3H), 2.88 (s, 3H), 1.24 (t, *J* = 7.3 Hz, 36H, Et_3N).

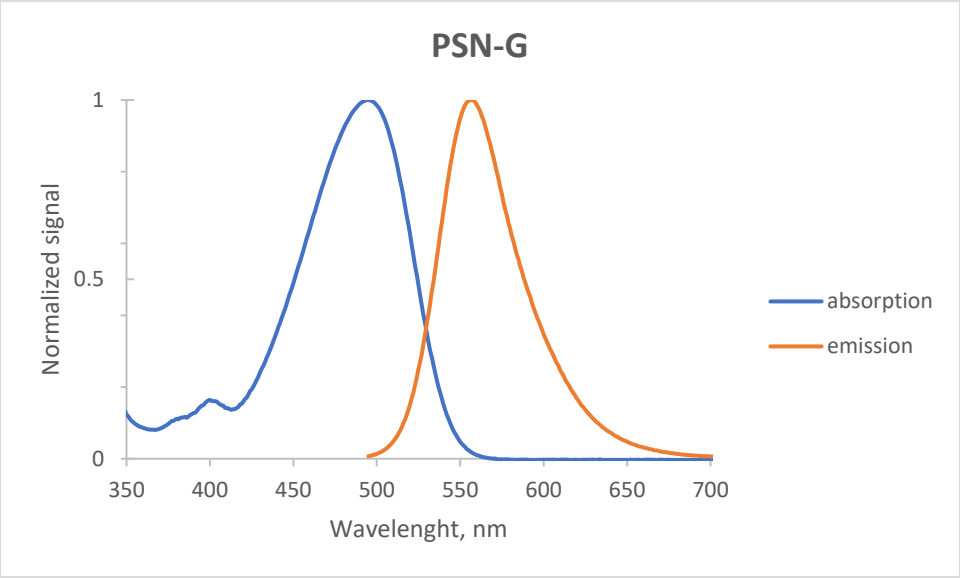

Conjugate **PSU-G** [2b]

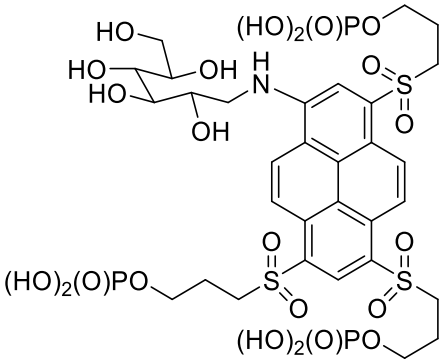

Chemical Formula: $C_{31}H_{44}NO_{23}P_3S_3$
Exact Mass: 987.07

98% yield. Analytical HPLC: t_R = 9.3 min (method C, MeCN gradient 5–60% in 20 min) detected at 500 nm; t_R of the free **PSU** dye = 8.7 min.

Yield 93 %.

ESI-HRMS: found 986.0612 $[M-H]^-$, calculated 986.0606; found 492.5271 $[M-2H]^{2-}$, calculated 492.5267.

λ_{max} (absorption) = 506 nm (H_2O), λ_{max} (emission) = 558 nm (excitation at 490 nm); Stocks shift 52 nm, fluorescence lifetime 5.8 ns (H_2O; excitation at 440 nm); fluorescence quantum yield: 0.95 (H_2O).

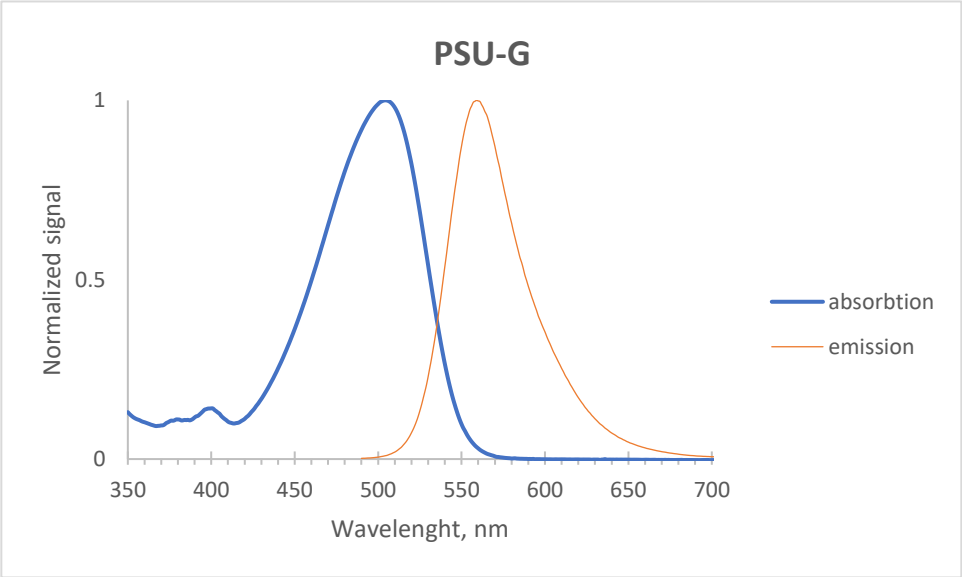

4.2.1.4 Reductive amination of sugars

General method for reductive amination of sugars (water-free protocol):

Method I: 1.5 mL Eppendor tube was charged with a dye (10 µL of 0.1 M solution in water), sugar (5 µL of 0.1 M solution in water), and malonic acid (10 eq, 10 µL of 1 M solution in DMSO). The samples were shaked at 40 °C for 1 h in an Eppendorf ThermoMixer®, and solvents were completely removed in a freeze-dryer (Martin Christ, residual pressute <0.1 mbar, temp. of the cooling coil –80°C: step 1). A solution of 2-picoline-borane complex (10 eq, 10 µL of 1 M solution in DMSO) was added, and the samples were stirred at 40 °C for 16 h in an Eppendorf ThermoMixer® (step 2). The products were isolated by flash chromatography on Interchim puriFlash™ (RP C18, 15C18AQ-F0025 cartridge, MeCN gradient 0–12% v/v over 15 CV in 25 mM TEAB/MeCN mixture).

Method II: 1.5 mL Eppendorf tube was charged with a dye (10 µL of 0.1 M solution in water), sugar (5 µL of 0.1 M solution in water), and citric acid (10 eq, 10 µL of 1 M solution in water). The samples were shaken at 40 °C for 1 h in an Eppendorf ThermoMixer®, and the solvents were completely removed in a freeze-dryer (residual pressure <0.1 mbar, temp. of the cooling coil

–80°C). A solution of $NaBH_3CN$ (10 eq, 10 µL of 1 M solution in THF), and citric acid (10 eq, 10 µL of 1 M solution in water) were added, and the samples were stirred at 40°C for 16 h in an Eppendorf ThermoMixer® (step 2). The products were isolated by flash chromatography on Interchim puriFlash™ (RP C18, 15C18AQ-F0025 cartridge, MeCN gradient 0–12% v/v over 15 CV in 25 mM TEAB/MeCN mixture).

Labelling of the dextran ladder

1.5 mL Eppendorf tube was charged with a dye (25 µL of 0.1 M solution in water), maltodextrin oligosaccharides DP2 to DP15, Carbosynth (1 mg), and malonic acid (10 eq, 25 µL of 1 M solution in DMSO). The samples were shaken at 40 °C for 1 h in an Eppendorf ThermoMixer®, and solvents were completely removed in a freeze-dryer (residual pressure <0.1 mbar, temp. of the cooling coil –80°C). A solution of 2-picoline-borane complex (10 eq, 25 µL of 1 M solution in DMSO) and malonic acid (10 eq, 25 µL of 1 M solution in DMSO) were added, and the samples were stirred at 40°C for 16 h in an Eppendorf ThermoMixer®. The products were isolated by flash chromatography on Interchim puriFlash™ (RP C18, 15C18AQ-F0025 cartridge, MeCN gradient 0–12% v/v over 15 CV in 25 mM TEAB/MeCN mixture).

4.2.1.5 Characterization of conjugates

The constitutions of the products (see structures below) were confirmed by ESI-HRMS.

APTS-derived sugars

APTS + G_3

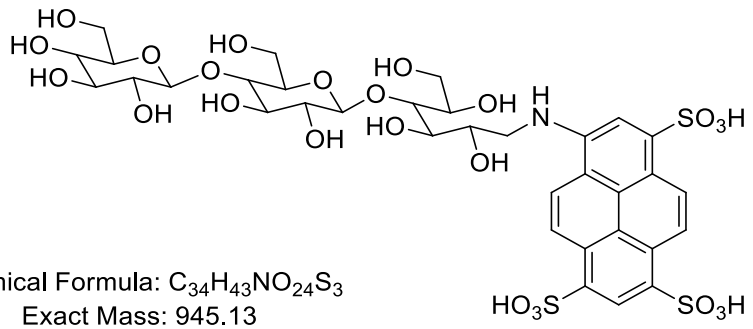

Chemical Formula: $C_{34}H_{43}NO_{24}S_3$
Exact Mass: 945.13

HPLC: t_R = 9.0 min (method C; MeCN (A)/TEAB 0.05 M in water (B)), 2:98 → 10:90 in 20 min detected at 450 nm; λ_{max} (absorption) = 454 nm.

ESI-HRMS: found 944.1261 $[M-H]^-$, calculated 944.1297; found 471.5594 $[M-2H]^{2-}$, calculated 471.5596.

APTS + G_7

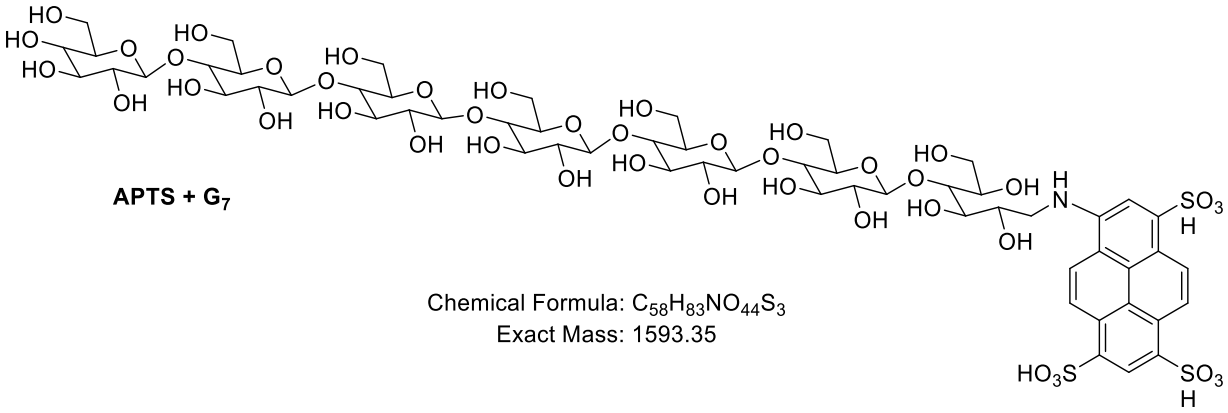

Chemical Formula: $C_{58}H_{83}NO_{44}S_3$
Exact Mass: 1593.35

HPLC: t_R = 8.7 min (method C; MeCN (A)/TEAB 0.05 M in water (B)), 2:98 → 10:90 in 20 min detected at 400 nm; λ_{max} (absorption) = 454 nm.

ESI-HRMS: found 795.6624 $[M-2H]^{2-}$, calculated 795.6652.

APTS + M

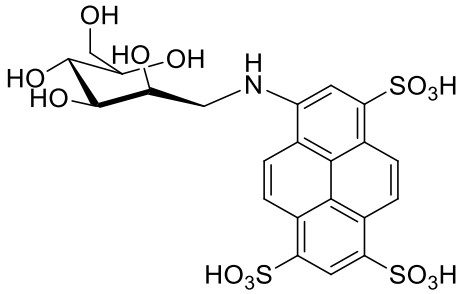

Chemical Formula: $C_{22}H_{23}NO_{14}S_3$
Exact Mass: 621.03

HPLC: t_R = 7.2 min (method B; MeCN (A)/TEAB 0.05 M in water (B)), 1:99 → 30:70 in 20 min detected at 450 nm; λ_{max} (absorption) = 456 nm.

ESI-HRMS: found 309.5065 $[M-2H]^{2-}$, calculated 309.5068; found 206.0022 $[M-3H]^{3-}$, calculated 206.0021.

APTS + M_2 (2-O)

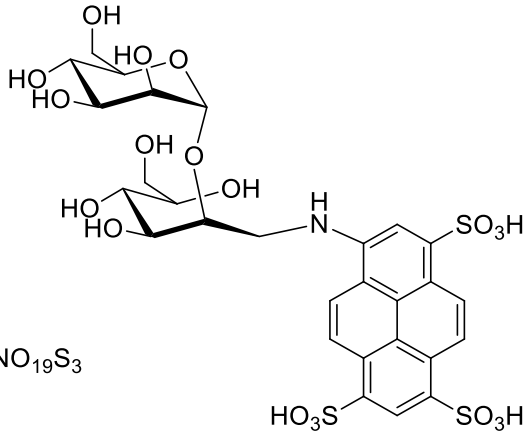

Chemical Formula: $C_{28}H_{33}NO_{19}S_3$
Exact Mass: 783.08

HPLC: t_R = 8.4 min (method B; MeCN (A)/TEAB 0.05 M in water (B)), 1:99 → 25:75 in 20 min detected at 450 nm; λ_{max} (absorption) = 456 nm.

ESI-HRMS: found 782.0741 $[M-H]^-$, calculated 782.0736; found 390.5335 $[M-2H]^{2-}$, calculated 390.5332.

APTS + M_2 (3-O)

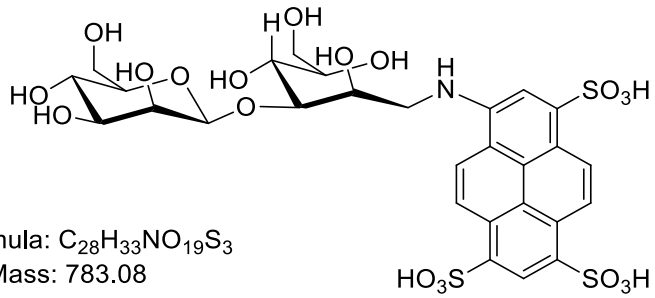

Chemical Formula: $C_{28}H_{33}NO_{19}S_3$
Exact Mass: 783.08

HPLC: t_R = 8.1 min (method B; MeCN (A)/TEAB 0.05 M in water (B)), 1:99 → 25:75 in 20 min detected at 450 nm; λ_{max} (absorption) = 456 nm.

ESI-HRMS: found 782.0734 $[M-H]^-$, calculated 782.0736; found 390.5332 $[M-2H]^{2-}$, calculated 390.5332.

APTS + M_2 (4-O)

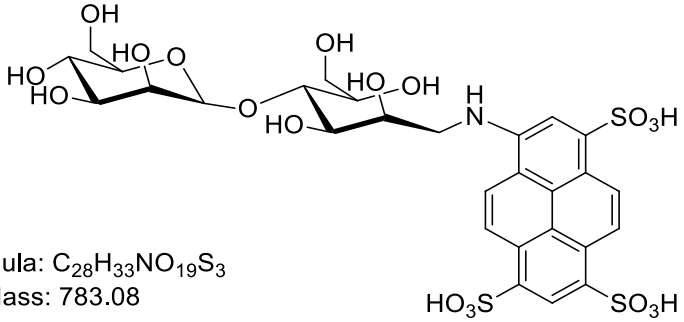

Chemical Formula: $C_{28}H_{33}NO_{19}S_3$
Exact Mass: 783.08

HPLC: t_R = 8.6 min (method B; MeCN (A)/TEAB 0.05 M in water (B)), 1:99 → 25:75 in 20 min detected at 450 nm; λ_{max} (absorption) = 455 nm.

ESI-HRMS: found 782.0720 $[M-H]^-$, calculated 782.0736; found 390.5332 $[M-2H]^{2-}$, calculated 390.5332.

APTS + M_3

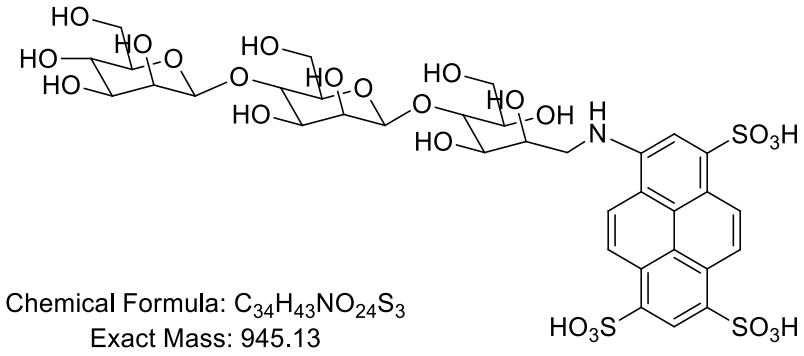

HPLC: t_R = 8.3 min (method B; MeCN (A)/TEAB 0.05 M in water (B)), 1:99 → 25:75 in 20 min detected at 450 nm; λ_{max} (absorption) = 454 nm.

ESI-HRMS: found 944.1251 $[M-H]^-$, calculated 944.1264; found 471.5595 $[M-2H]^{2-}$, calculated 471.5596.

APTS + M_4

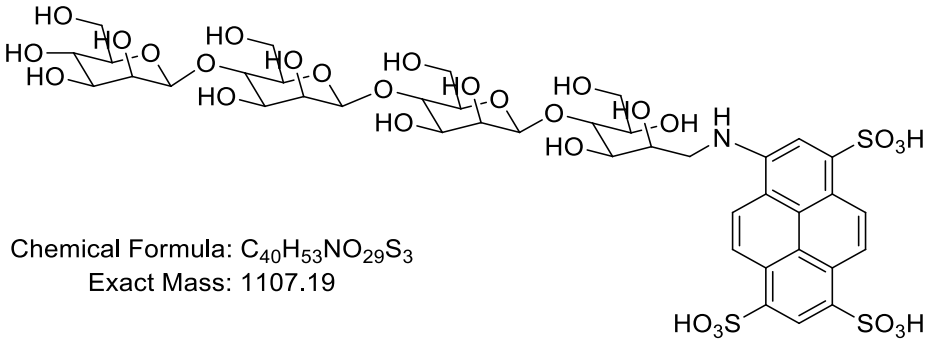

HPLC: t_R = 8.5 min (method B; MeCN (A)/TEAB 0.05 M in water (B)), 1:99 → 25:75 in 20 min detected at 450 nm; λ_{max} (absorption) = 454 nm.

ESI-HRMS: found 1106.1776 $[M-H]^-$, calculated 1106.1793; found 552.5864 $[M-2H]^2$, calculated 552.5860.

APTS + 6'SL

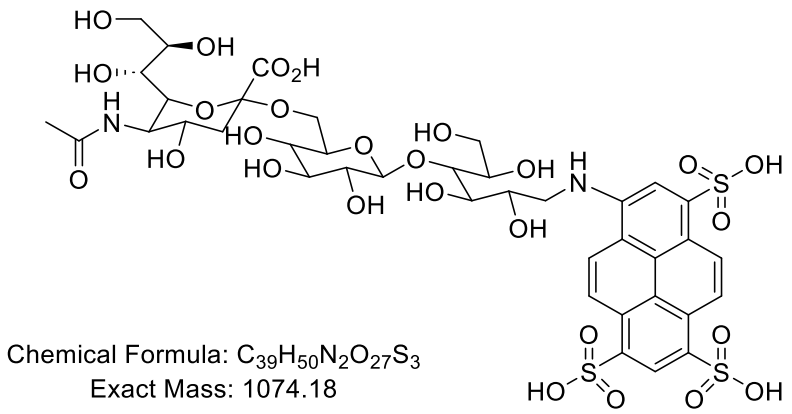

Chemical Formula: $C_{39}H_{50}N_2O_{27}S_3$
Exact Mass: 1074.18

HPLC: t_R = 8.3 min (method B; MeCN (A)/TEAB 0.05 M in water (B)), 1:99 → 25:75 in 20 min detected at 450 nm; λ_{max} (absorption) = 460 nm.

ESI-HRMS: found 536.0817 $[M-2H]^{2-}$, calculated 536.0809; found 357.0512 $[M-3H]^{3-}$, calculated 357.0515.

APTS + 3'SL

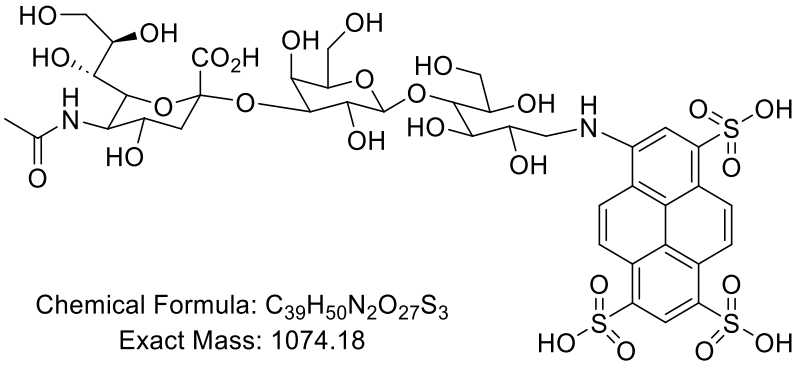

Chemical Formula: $C_{39}H_{50}N_2O_{27}S_3$
Exact Mass: 1074.18

HPLC: t_R = 8.7 min (method B; MeCN (A)/TEAB 0.05 M in water (B)), 1:99 → 25:75 in 20 min detected at 450 nm; λ_{max} (absorption) = 459 nm.

ESI-HRMS: found 536.0813 $[M-2H]^{2-}$, calculated 536.0809; found 357.0507 $[M-3H]^{3-}$, calculated 357.0515.

APTS + L

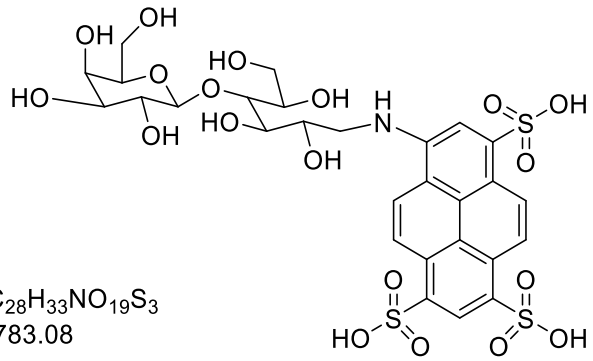

Chemical Formula: $C_{28}H_{33}NO_{19}S_3$
Exact Mass: 783.08

HPLC: t_R = 8.6 min (method B; MeCN (A)/TEAB 0.05 M in water (B)), 1:99 → 25:75 in 20 min detected at 450 nm; λ_{max} (absorption) = 455 nm.

ESI-HRMS: found 782.0730 $[M-H]^-$, calculated 782.0736; found 390.5330 $[M-2H]^{2-}$, calculated 390.5332.

Conjugates of PSU

PSU + G_3

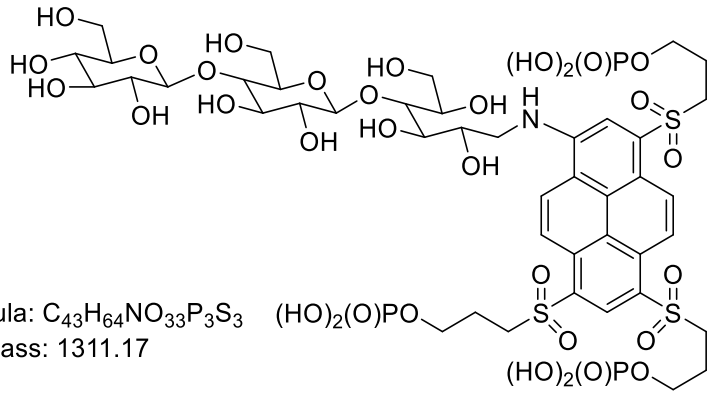

Chemical Formula: $C_{43}H_{64}NO_{33}P_3S_3$
Exact Mass: 1311.17

HPLC: t_R = 10.1 min (method C; MeCN (A)/TEAB 0.05 M in water (B)), 5:95 → 30:70 in 20 min detected at 500 nm; λ_{max} (absorption) = 504 nm.

ESI-HRMS: found 1334.1639 $[M+Na]^+$, calculated 1334.1628; found 654.5797 $[M-2H]^{2-}$, calculated 654.5795.

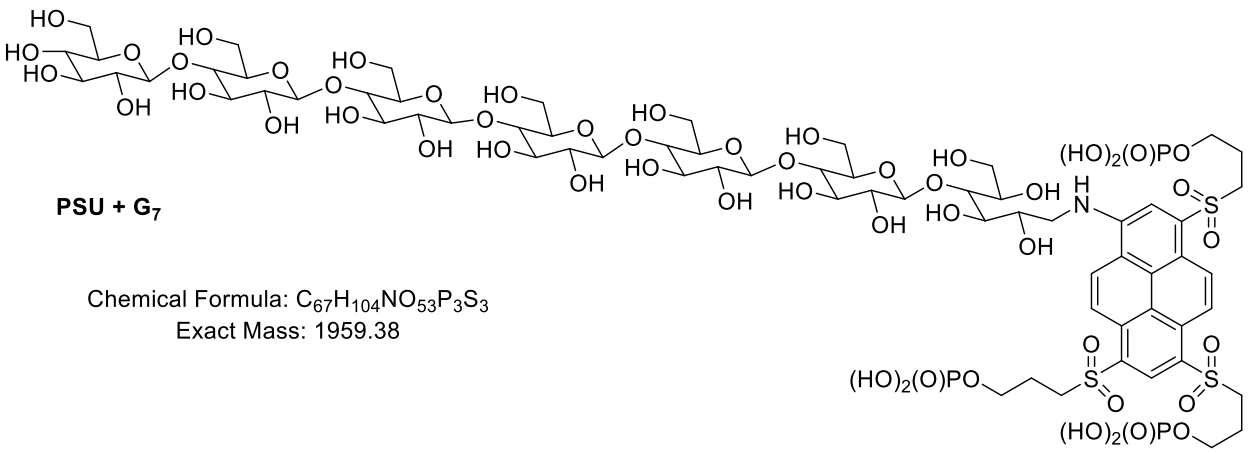

PSU + G_7

Chemical Formula: $C_{67}H_{104}NO_{53}P_3S_3$
Exact Mass: 1959.38

HPLC: t_R = 9.8 min (method C; MeCN (A)/TEAB 0.05 M in water (B)), 5:95 → 30:70 in 20 min detected at 500 nm; λ_{max} (absorption) = 504 nm.

ESI-HRMS: found 2004.6557 $[M-2Na+H]^+$, calculated 2004.3560; found 1958.3786 $[M-H]^-$, calculated 1958.3776; found 978.6857 $[M-2H]^{2-}$, calculated 978.6851.

PSU + M

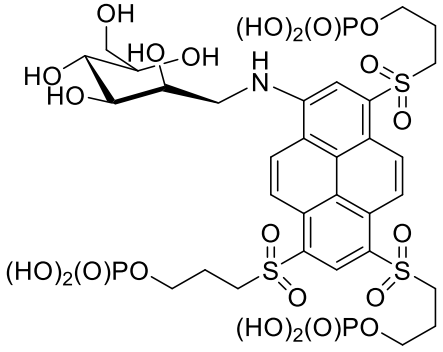

Chemical Formula: $C_{31}H_{44}NO_{23}P_3S_3$
Exact Mass: 987.07

HPLC: t_R = 12.4 min (method B; MeCN (A)/TEAB 0.05 M in water (B)), 1:99 → 25:75 in 20 min detected at 500 nm; λ_{max} (absorption) = 508 nm.

ESI-HRMS: found 492.5263 $[M-2H]^{2-}$, calculated 492.5267; found 328.0154 $[M-3H]^{3-}$, calculated 328.0154.

PSU + M_2 (2-O)

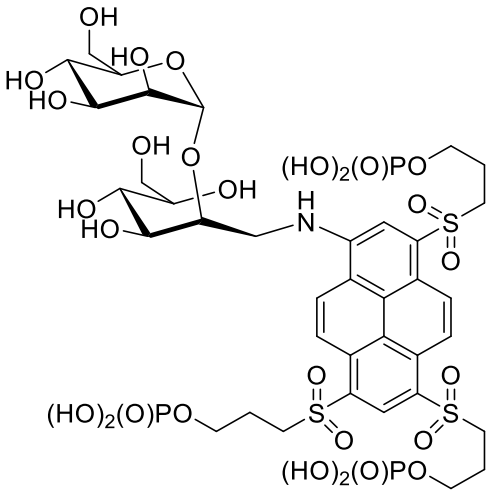

Chemical Formula: $C_{37}H_{54}NO_{28}P_3S_3$
Exact Mass: 1149.12

HPLC: t_R = 12.8 min (method B; MeCN (A)/TEAB 0.05 M in water (B)), 1:99 → 25:75 in 20 min detected at 500 nm; λ_{max} (absorption) = 509 nm.

ESI-HRMS: found 1148.1135 $[M\text{-}H]^-$, calculated 1148.1135; found 573.5535 $[M\text{-}2H]^2$, calculated 573.5531.

PSU + M_2 (3-O)

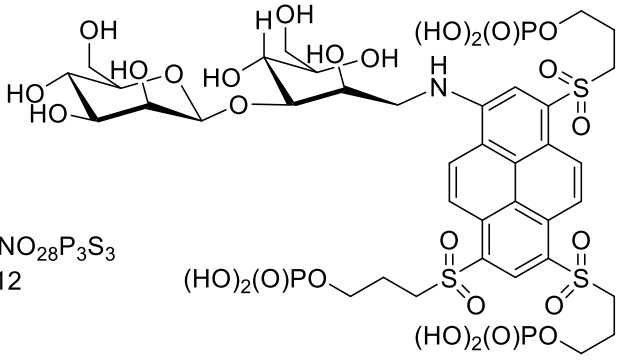

Chemical Formula: $C_{37}H_{54}NO_{28}P_3S_3$
Exact Mass: 1149.12

HPLC: t_R = 12.3 min (method B; MeCN (A)/TEAB 0.05 M in water (B)), 1:99 → 25:75 in 20 min detected at 500 nm; λ_{max} (absorption) = 507 nm.

ESI-HRMS: found 1148.1135 $[M\text{-}H]^-$, calculated 1148.1135; found 573.5537 $[M\text{-}2H]^2$, calculated 573.5531.

PSU + M_2 (4-O)

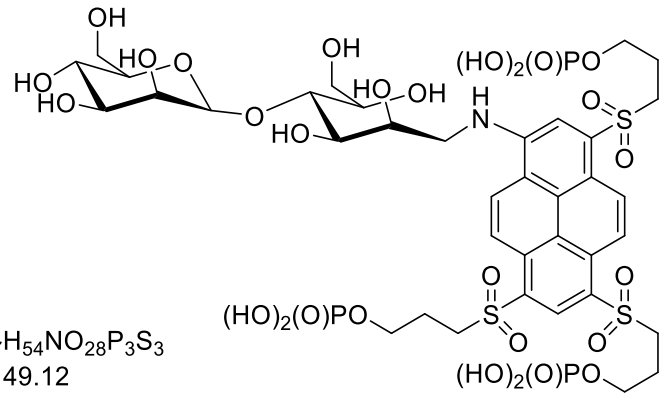

Chemical Formula: $C_{37}H_{54}NO_{28}P_3S_3$
Exact Mass: 1149.12

HPLC: t_R = 12.7 min (method B; MeCN (A)/TEAB 0.05 M in water (B)), 1:99 → 25:75 in 20 min detected at 500 nm; λ_{max} (absorption) = 509 nm.

ESI-HRMS: found 1148.1133 $[M-H]^-$, calculated 1148.1135; found 573.5539 $[M-2H]^{2}$, calculated 573.5531.

PSU + M_3

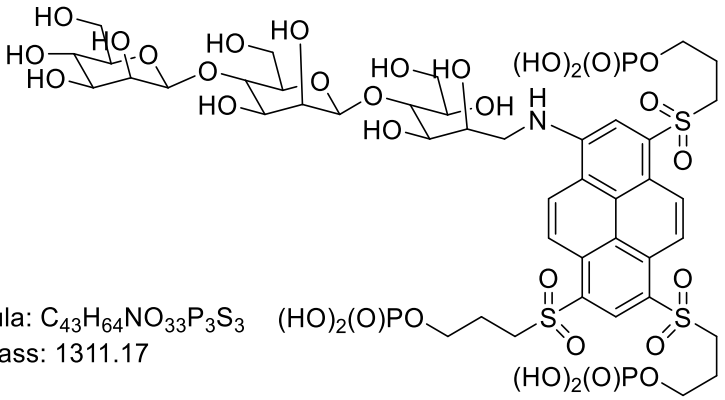

Chemical Formula: $C_{43}H_{64}NO_{33}P_3S_3$
Exact Mass: 1311.17

HPLC: t_R = 11.6 min (method B; MeCN (A)/TEAB 0.05 M in water (B)), 1:99 → 25:75 in 20 min detected at 500 nm; λ_{max} (absorption) = 509 nm.

ESI-HRMS: found 654.5794 $[M-2H]^{2-}$, calculated 654.5795; found 436.0511 $[M-3H]^{3-}$, calculated 436.0506.

PSU + M_4

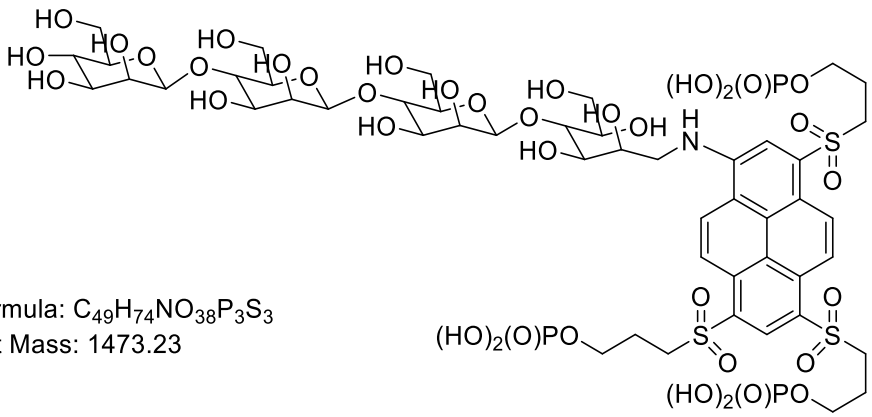

Chemical Formula: $C_{49}H_{74}NO_{38}P_3S_3$
Exact Mass: 1473.23

HPLC: t_R = 12.0 min (method B; MeCN (A)/TEAB 0.05 M in water (B)), 1:99 → 25:75 in 20 min detected at 500 nm; λ_{max} (absorption) = 505 nm.

ESI-HRMS: found 735.6080 $[M-2H]^{2-}$, calculated 735.6059; found 490.0685 $[M-3H]^{3-}$, calculated 490.0682.

PSU + 6'SL

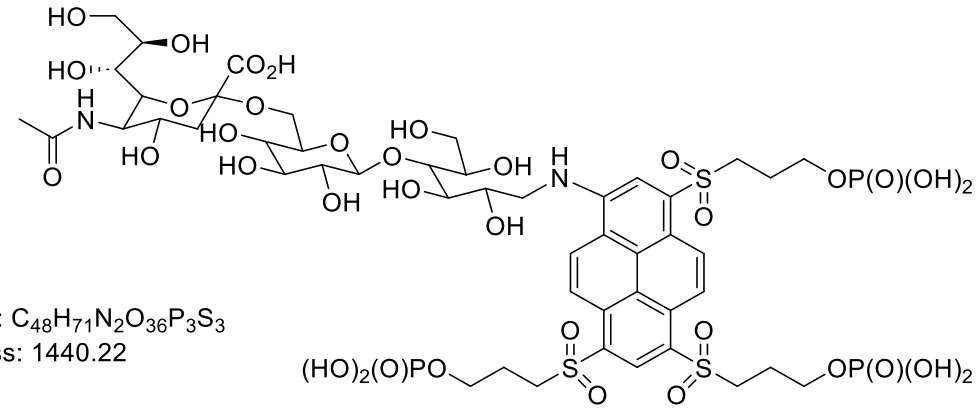

Chemical Formula: $C_{48}H_{71}N_2O_{36}P_3S_3$
Exact Mass: 1440.22

HPLC: t_R = 11.6 min (method B; MeCN (A)/TEAB 0.05 M in water (B)), 1:99 → 25:75 in 20 min detected at 500 nm; λ_{max} (absorption) = 509 nm.

ESI-HRMS: found 719.1016 $[M-2H]^{2-}$, calculated 719.1008; found 479.0647 $[M-3H]^{3-}$, calculated 479.0648.

PSU + 3'SL

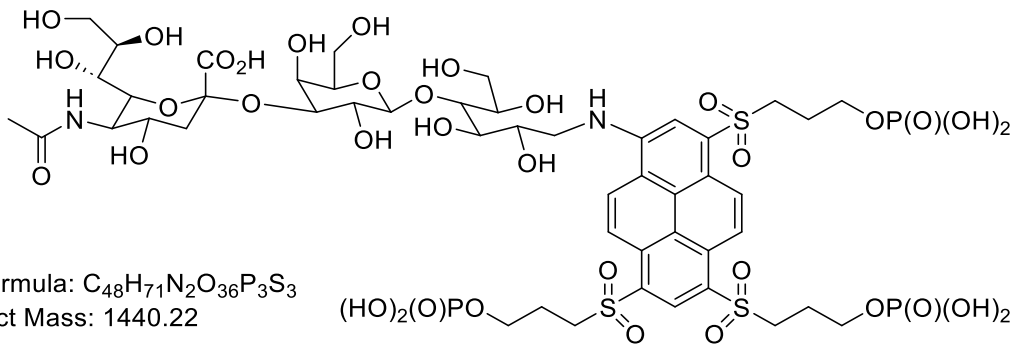

Chemical Formula: $C_{48}H_{71}N_2O_{36}P_3S_3$
Exact Mass: 1440.22

HPLC: t_R = 11.9 min (method; MeCN (A)/TEAB 0.05 M in water (B)), 1:99 → 25:75 in 20 min detected at 500 nm; λ_{max} (absorption) = 508 nm.

ESI-HRMS: found 359.0464 $[M-4H]^{4-}$, calculated 359.0468.

PSN-derived sugars

PSN + G_3

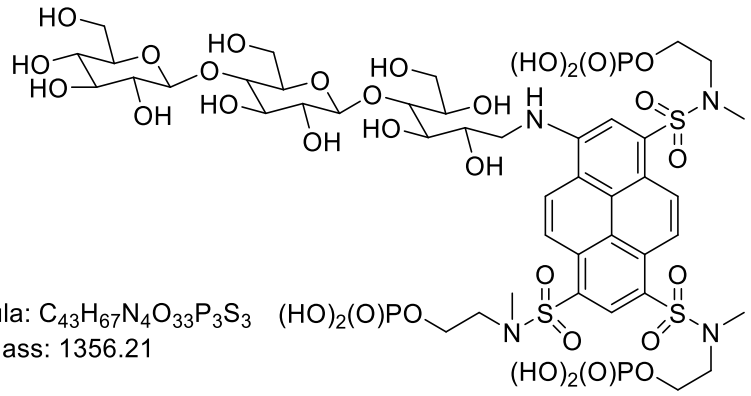

Chemical Formula: $C_{43}H_{67}N_4O_{33}P_3S_3$
Exact Mass: 1356.21

HPLC: t_R = 12.4 min (method B; MeCN (A)/TEAB 0.05 M in water (B)), 1:99 → 25:75 in 20 min detected at 500 nm; λ_{max} (absorption) = 496 nm.

ESI-HRMS: found 677.0971 $[M-2H]^{2-}$, calculated 677.0958.

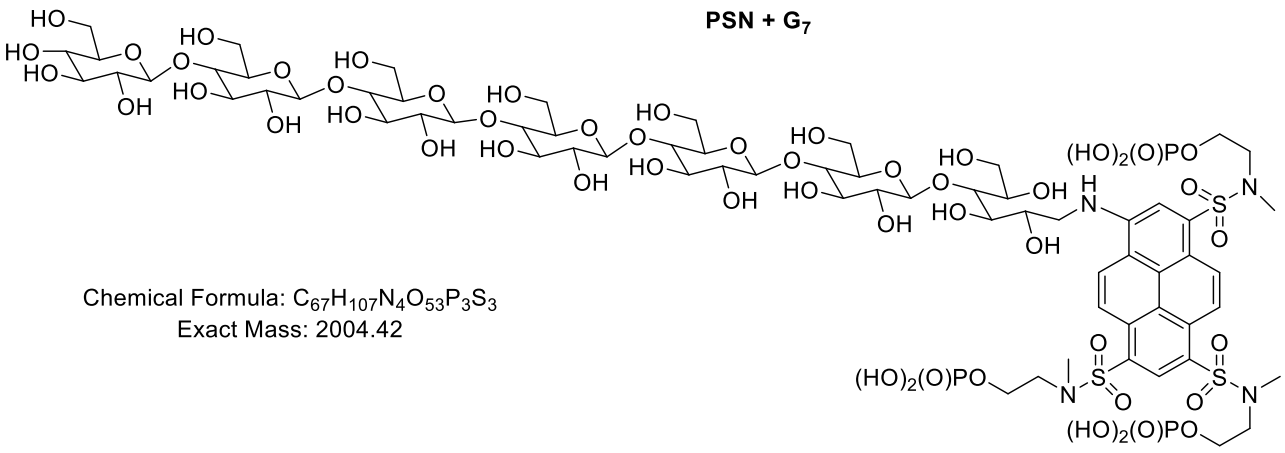

HPLC: t_R = 12.3 min (method B; MeCN (A)/TEAB 0.05 M in water (B)), 1:99 → 25:75 in 20 min detected at 500 nm; λ_{max} (absorption) = 496 nm.

ESI-HRMS: found 1001.2026 $[M-2H]^{2-}$, calculated 1001.2015.

PCN-derived sugars

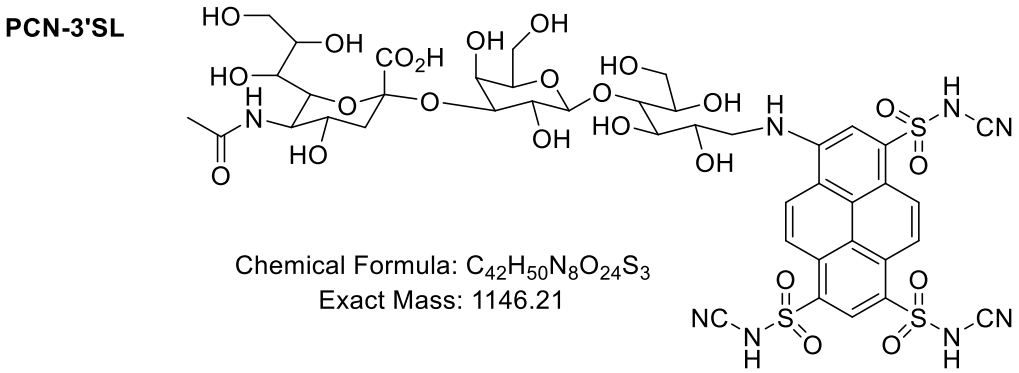

HPLC: t_R = 12.2 min (method B, MeCN gradient 1–25% v/v in 20 min) detected at 485 nm; λ_{max} (absorption) = 486 nm.

ESI-HRMS: Found 1145.2032 $[M-H]^-$, calc. 1145.2027; found 572.0985, $[M-2H]^{2-}$, calc. 572.0977

PCN-6'SL

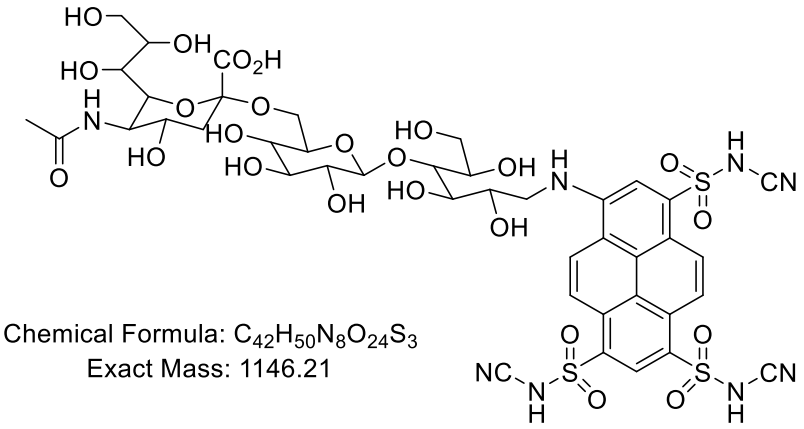

Chemical Formula: $C_{42}H_{50}N_8O_{24}S_3$
Exact Mass: 1146.21

HPLC: t_R = 11.8 min (method B, MeCN gradient 1-25% v/v in 20 min) detected at 485 nm; λ_{max} (absorption) = 486 nm.

ESI-HRMS: Found 1145.2025 $[M-H]^-$, calc. 1145.2027; found 572.0991, $[M-2H]^{2-}$, calc. 572.0977

PCN-L

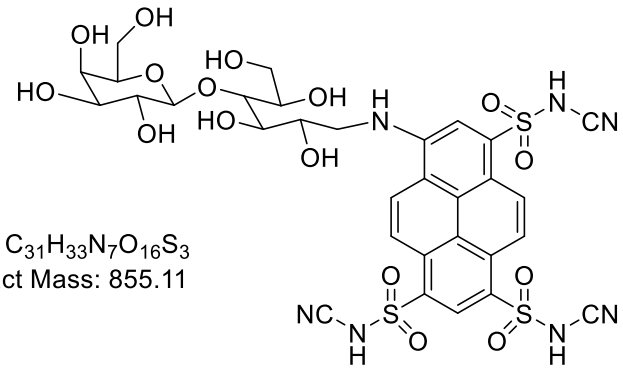

Chemical Formula: $C_{31}H_{33}N_7O_{16}S_3$
Exact Mass: 855.11

HPLC: t_R = 12.5 min (method B, MeCN gradient 1–25% v/v in 20 min) detected at 485 nm; λ_{max} (absorption) = 485 nm.

ESI-HRMS: Found 854.1074 $[M-H]^-$, calc. 854.1073; found 426.5492, $[M-2H]^{2-}$, calc. 426.5500

4.2.1.6 Desialylation studies

3'- and 6' SL as well as lactose were labelled by **PCN** dye (see section reductive amination of sugars). The conversion degrees were determined by measuring peak areas of the residual dye and product(s) at isosbestic point (469 nm). Peak areas are included in HPLC traces.

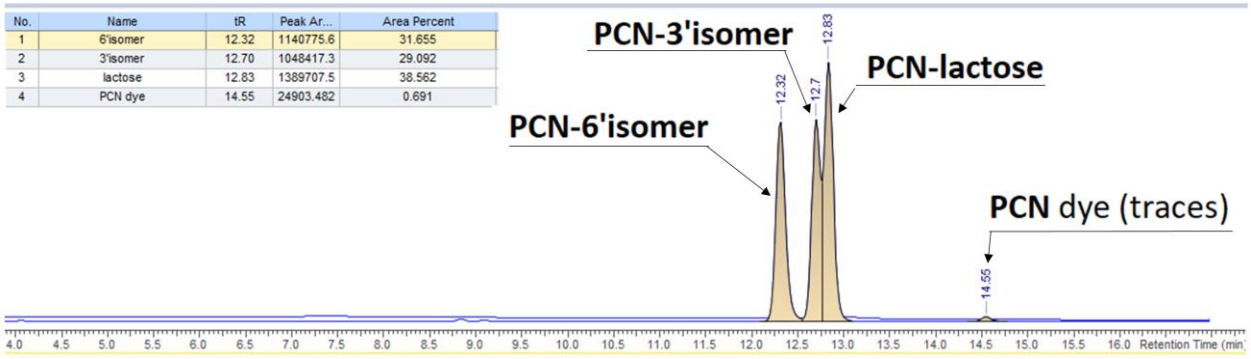

Figure 31. HPLC analysis of the mixture of 3'- and 6'- sialyllactoses and lactose labelled with a **PCN** dye (the traces were recorded at λ 484 nm).

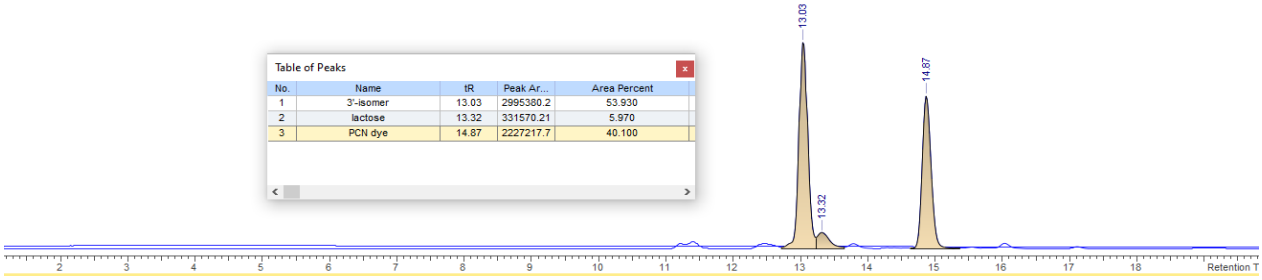

Figure 32. HPLC analysis of the reaction mixture of 3'SL labelled with **PCN** (method I); 6% desialysation is observed.

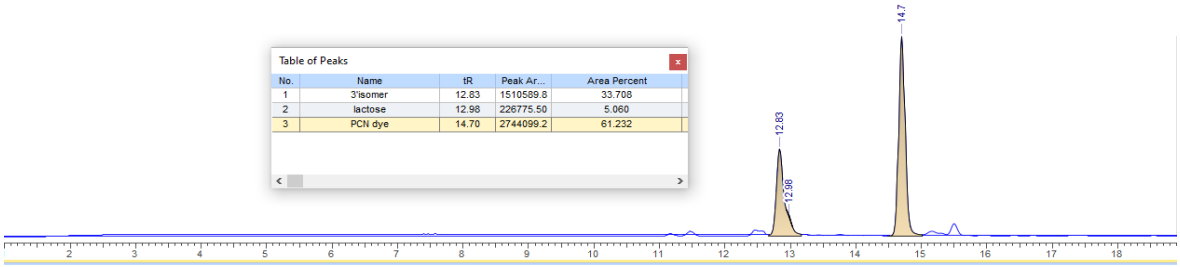

Figure 33. HPLC analysis of the reaction mixture of 3'SL labelled with **PCN** (method II); 5% desialysation is observed.

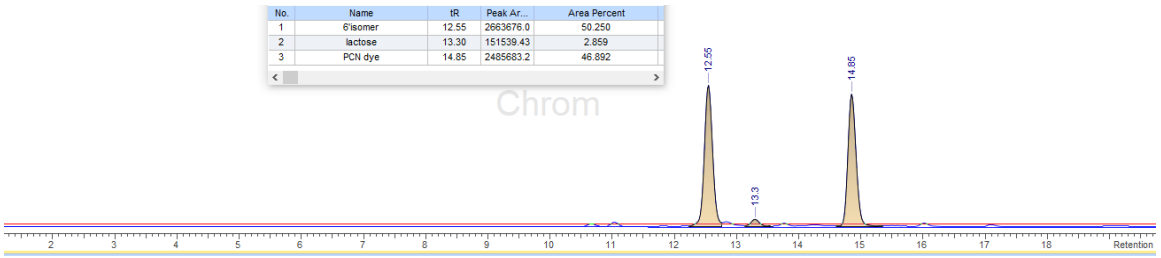

Figure 34. HPLC analysis of the reaction mixture of 6'SL labelled with **PCN** (method I); 3% desialysation is observed.

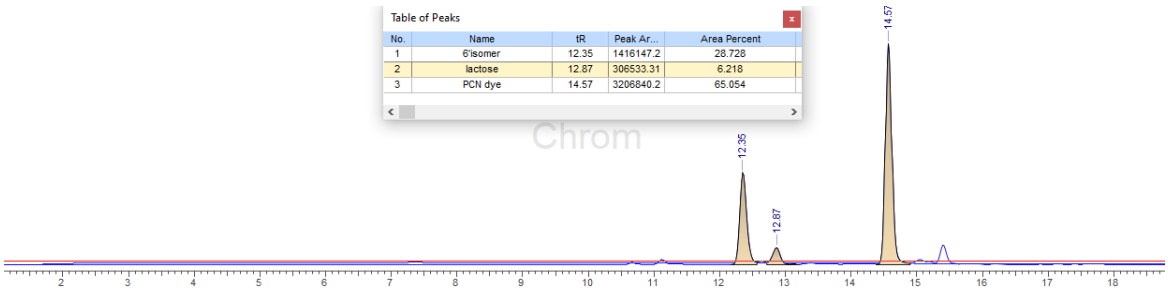

Figure 35. HPLC analysis of the reaction mixture of 6'SL labelled with **PCN** (method II); 6% desialysation is observed.

4.2.2 To chapter 2

4.2.2.1. Preparation of DAK reagent [4]

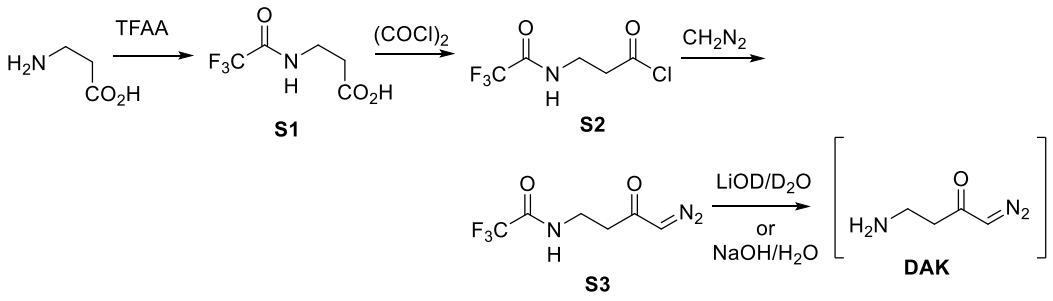

Scheme 60. Preparation of 4-amino-1-diazobutan-2-one (**DAK** reagent)

3-(2,2,2-Trifluoroacetamido)propanoic acid (S1)

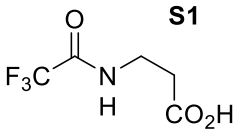

Chemical Formula: $C_5H_6F_3NO_3$
Exact Mass: 185.03

β-alanine (900 mg, 10 mmol) and triethylamine (10 mmol, 1.4 ml) were dissolved in 10 ml of MeOH. The reaction mixtire was colled to 0 ˚C (ice bath) and ethyl trifluoroacetate (1.25 eq, 12.5 mmol, 1.5 ml) was added dropwise. The reaction mixture was stirred overnight at r.t. The volatiles were removed under reduced pressure, the residue acidified with 1.0 M aq. HCl, and stirred for 15 min. The reaction mixture was extracted with EtOAc (3 x 50 ml), the combined organic solutions washed with brine, dried over $MgSO_4$ and concentrated under reduced pressure to give 1.0 g of white crystaline **S1** (54% yield).

^{1}H NMR (400 MHz, CD_3CN) δ 3.51 (td, *J* = 6.6, 6.0 Hz, 2H), 2.58 (t, *J* = 6.7 Hz, 2H).

^{19}F NMR (376 MHz, CD_3CN) δ -76.79.

3-(2,2,2-Trifluoroacetylamino)propanoyl chloride (S2)

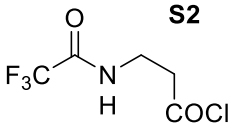

Chemical Formula: $C_5H_5ClF_3NO_2$
Exact Mass: 203.00

To a solution of **S1** (750 mg, 4.00 mmol) in dry DCM (5 ml), oxalyl chloride (2.0 ml) was added followed by a drop of DMF. After stirring at reflux for 1 h, the solution was cooled to r.t. The mixture was concentrated in vacuo and used in the next step without purification.

^{1}H NMR (400 MHz, $CDCl_3$) δ 7.55 (br.s, 1H, NH), 3.63 (q, *J* = 6.1 Hz, 2H), 3.22 (t , *J* = 6.0, 2H).

***N*-(4-Diazo-3-oxobutyl)-2,2,2-trifluoroacetamide (S3)**

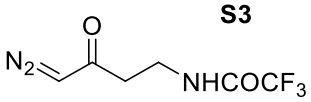

Chemical Formula: $C_6H_6F_3N_3O_2$
Exact Mass: 209.04

The solution of CH_2N_2 in ether was prepared as described.[5] The diazomethane solution was briefly dried over KOH pellets just before use.

S2 (820 mg, 4 mmol) was dissolved in anhydrous DCM (5 ml). To this solution stirred at 0°C, 5.0 mL of the freshly prepared CH_2N_2 in ether were added slowly, and the reaction mixture was kept at +5 °C overnight. At the endpoint of the diazomethane addition, the evolution of nitrogen ceased, and the reaction mixture got pale yellow colour (proof of CH_2N_2 excess). The reaction mixture was diluted with ether (50 ml), washed with 5% aq. $NaHCO_3$ and brine (20 ml each). The combined aqueous solutions ($NaHCO_3$ + brine) were extracted with ether (2x25 ml), and the combined organic solutions were dried with Na_2SO_4 and evaporated in vacuo. The residue (570 mg of the pale yellow oil) was subjected to flash chromatography on *Isolera™ One* system (SNAP Ultra cartridge, 10 g SiO_2, 10 – 90% EtOAc in DCM gradient over 7 CV) to provide compound **S3** (205 mg, 25% yield) as a pale yellow oil.

^{1}H NMR (400 MHz, CD_3CN) δ 7.65 (s, 1H), 5.59 (s, 1H), 3.52 (q, *J* = 6.4 Hz, 2H), 2.60 (q, *J* = 6.4 Hz, 2H).

^{13}C NMR (101 MHz, CD_3CN) δ 192. 8, 156.7, 117.3, 54.7, 38.4, 35.3.

4-amino-1-diazobutan-2-one (DAK)

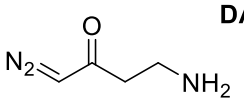

Chemical Formula: $C_4H_7N_3O$
Exact Mass: 113.06

S3 (60 mg, 0.28 mmol) was dissolved in 300 µl of MeCN-*d*$_3$ and 140 µl of 3.0 M solution of LiOD in D_2O were added; the 2nd portion of LiOD was added in 1 h (140 µl of 3.0 M solution).

The deuterated base was allowed to control the reaction progress by NMR. The reaction mixture was stirred at r.t., and the course of the reaction monitored by HPLC (starting compound **S3** t_R 2.9 min, product **DAK** t_R 2.6 min). In 1.5 h the conversion reached 40%, and a precipitate appeared. As desired 4-amino-1-diazobutan-2-one (DAK) was found to be unstable, we worked with this reaction mixture which contained approx. 0.1 mmol of N_2=CHCOCH$_2$CH$_2$NH$_2$.

4.2.2.1 Synthesis and properties of trimethinecyanines (Cy3 dyes)

1-Ethyl-2,3,3-trimethyl-*3H*-indolium iodide (**10**) [6]

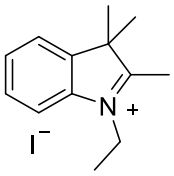

Chemical Formula: $C_{13}H_{18}N^+$
Exact Mass: 188.14

10

2,3,3-Trimethylindolenine (160 mg, 1.00 mmol) and ethyl iodide (3 eq, 3.00 mmol, 470 mg, 244 µl) were dissolved in MeCN (3 ml), placed into a sealed tube and refluxed overnight. The reaction mixture was concentrated under reduced pressure; the resulting solid washed with Et_2O and dried in vacuo. Yield 300 mg, 95%.

^{1}H NMR (400 MHz, CD_3CN) δ 7.74-7.72 (m, 1H), 7.58-7.57 (m, 3H), 4.73 (q, *J* = 7.5 Hz, 2H), 3.12 (s, 3H), 1.64 (s, 6H), 1.62 (t, *J* = 7.5 Hz, 3H).

***N,N′*-Diphenylchloroformamidinium hydrochloride** (**11b**) [7]

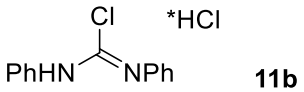

Chemical Formula: $C_{13}H_{11}ClN_2$
Exact Mass: 230.06

11b

N,N′-diphenylthiourea (230 mg, 1.00 mmol) was added in portions over 0.5 h to a stirred 2.2 M solution of $COCl_2$ in toluene (0.5 ml). Brisk evolution of COS occurred, and a yellow precipitate formed. After stirring for 4 h at r.t., the product was filtered off and used directly in the Cy3 synthesis.

ESI-MS, *m/z*: found 231.1 $[M+H]^+$, calculated 231.06 for $C_{13}H_{12}ClN_2$.

General procedure for Cy3 synthesis: (Scheme 17)

Indolium iodide **10** (47 mg, 0.15 mmol) and formamidinium hydrochloride **11b** (20 mg, 0.086 mmol) were placed into a sealed tube, dissolved in the mixture of AcOH-Ac_2O (1:1; 1 ml) and stirred at 130 ˚C for 1 h. The reaction progress was monitored by LCMS. All products were isolated by flash chromatography on a reversed phase cartridge Interchim puriFlash™.

Isolated products:

1-Ethyl-2-(3-(1-ethyl-3,3-dimethylindolin-2-ylidene)prop-1-en-1-yl)-3,3-dimethyl-*3H*-indol-1-ium iodide (12a) [8]

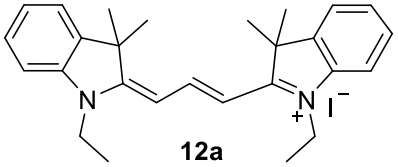

12a

Chemical Formula: $C_{27}H_{33}N_2^+$
Exact Mass: 385.26

Violet solid, 10 mg (23% yield).

^{1}H NMR (400 MHz, CD_3OD) δ 8.56 (t, *J* = 13.5 Hz, 1H), 7.58 – 7.53 (m, 2H), 7.49 – 7.43 (m, 2H), 7.39 – 7.28 (m, 4H), 6.45 (d, *J* = 13.4 Hz, 2H), 4.21 (q, *J* = 7.2 Hz, 4H), 1.77 (s, 12H), 1.43 (t, *J* = 7.2 Hz, 6H).

ESI-MS, *m/z*: found 385.21 $[M]^+$, calculated 385.26 for $C_{27}H_{33}N_2^+$.

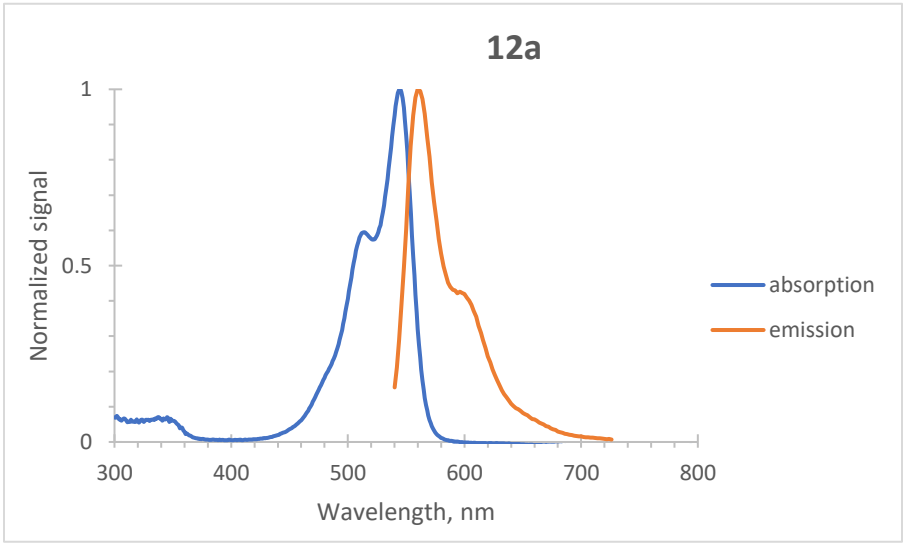

λ_{max} (absorption) 545 nm (ε = 90 000 M^{-1} cm^{-1}, MeCN), λ_{max} (emission) 560 nm (MeCN, excitation at 540 nm); Stokes shift 15 nm; fluorescence quantum yield 0.1 (absolute value in MeCN).

1-Ethyl-2-(3-(1-ethyl-3,3-dimethylindolin-2-ylidene)-2-(phenylamino)prop-1-en-1-yl)-3,3-dimethyl-*3H*-indol-1-ium iodide (12c)

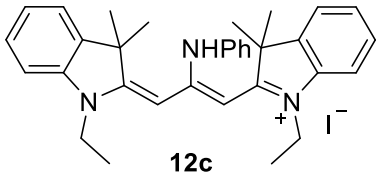

12c

Chemical Formula: $C_{33}H_{38}N_3^+$
Exact Mass: 476.31

Orange solid, 5 mg (10% yield).

^{1}H NMR (600 MHz, CD_3CN) δ 7.44 – 7.39 (m, 4H), 7.37 – 7.33 (m, 4H), 7.24 (ddt, *J* = 8.6, 7.3, 1.1 Hz, 1H), 7.17 (td, *J* = 7.5, 0.9 Hz, 2H), 7.14 (d, *J* = 7.9 Hz, 2H), 5.33 (s, 2H), 4.11 – 3.99 (m, 4H), 1.46 (s, 12H), 1.21 (t, *J* = 7.2 Hz, 6H).

ESI-HRMS: found 476.3056 $[M]^+$, calculated 476.3060 for $C_{33}H_{38}N_3^+$.

λ_{max} (absorption) 498 nm (ε = 72 000 M^{-1} cm^{-1}, MeCN), λ_{max} (emission) 595 nm (MeCN, excitation at 500 nm); Stokes shift 97 nm; fluorescence quantum yield 0.01 (absolute value in MeCN).

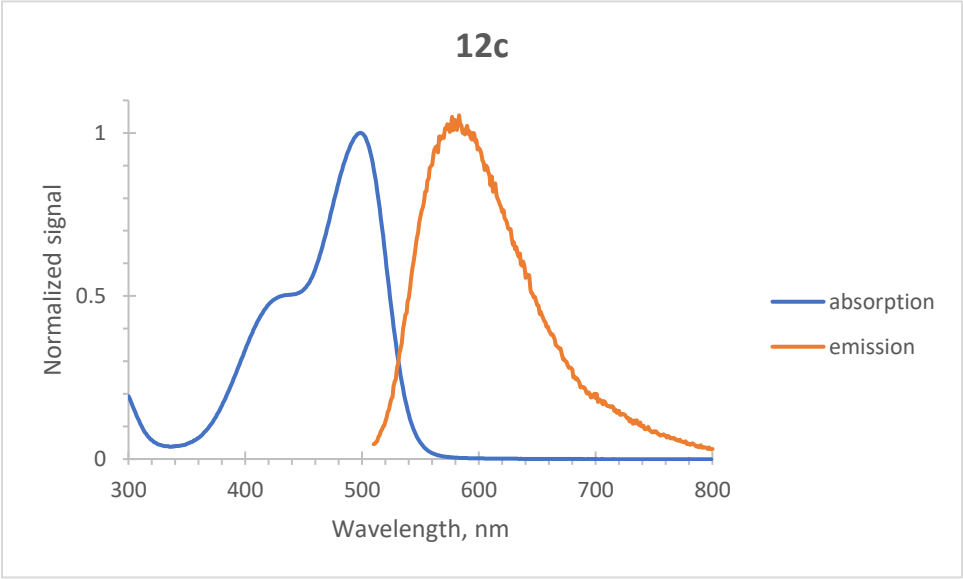

1-Ethyl-3,3-dimethyl-2-(2-(phenylamino)vinyl)-*3H*-indol-1-ium iodide (13) [9]

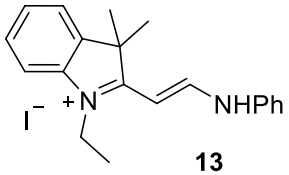

Chemical Formula: $C_{20}H_{23}N_2^+$
Exact Mass: 291.19

13

Dark yellow solid, 8 mg (22% yield).

^{1}H NMR (400 MHz, CD_3OD) δ 8.66 (d, *J* = 12.5 Hz, 1H), 7.60 – 7.26 (m, 8H), 6.16 (d, *J* = 12.5 Hz, 1H), 4.21 (q, *J* = 7.3 Hz, 2H), 1.74 (s, 6H), 1.43 (t, *J* = 7.3 Hz, 3H).

ESI-MS, *m/z*: found 291.16 $[M]^+$, calculated 291.19 for $C_{20}H_{23}N_2^+$.

1-Ethyl-2-(3-(1-ethyl-3,3-dimethylindolin-2-ylidene)-2-((1-ethyl-3,3-dimethylindolin-2-ylidene)methyl)prop-1-en-1-yl)-3,3-dimethyl-*3H*-indol-1-ium iodide (14)

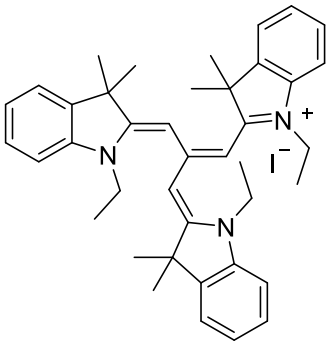

Chemical Formula: $C_{40}H_{48}N_3^+$
Exact Mass: 570.38

14

Violet solid, 12 mg (20% yield).

^{1}H NMR (400 MHz, $CDCl_3$) δ 7.37 (t, *J* = 7.7 Hz, 3H), 7.31 (d, *J* = 7.3 Hz, 3H), 7.19 (t, *J* = 7.5 Hz, 3H), 7.08 (d, *J* = 7.9 Hz, 3H), 5.09 (s, 3H), 4.14 – 4.04 (m, 6H), 1.49 (s, 18H), 1.29 (t, *J* = 7.2 Hz, 9H).

ESI-HRMS: found 570.3842 $[M]^+$, calculated 570.3848 for $C_{40}H_{48}N_3^+$.

λ_{max} (absorption) 553 nm (ε = 65 400 M^{-1} cm^{-1}, MeCN), λ_{max} (emission) 612 nm (MeCN, excitation at 550 nm); Stokes shift 59 nm; fluorescence quantum yield 0 (absolute value in MeCN).

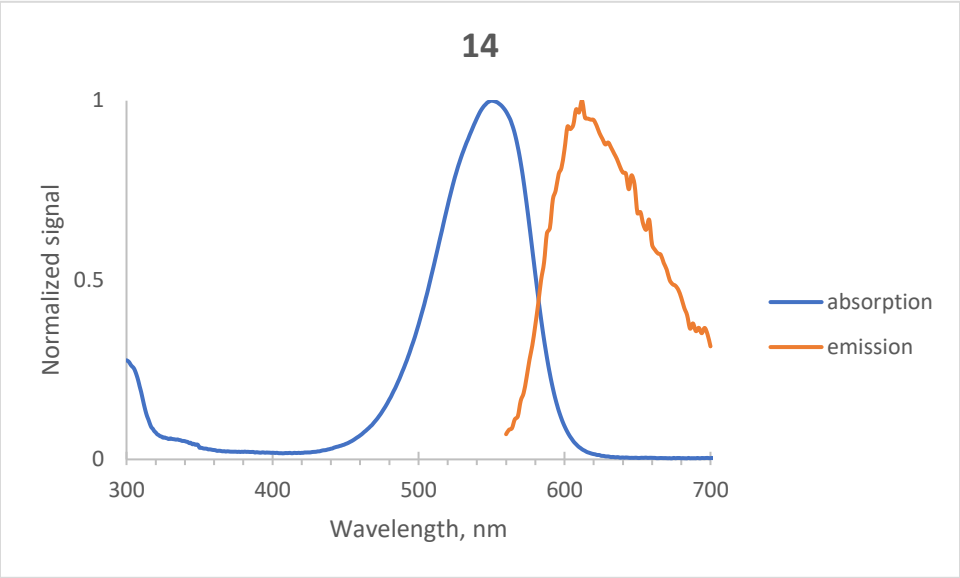

2-(1-(3,3-Dimethyl-*3H*-indol-2-yl)-3-(1-ethyl-3,3-dimethylindolin-2-ylidene)prop-1-en-2-yl)-1-ethyl-3,3-dimethyl-*3H*-indol-1-ium iodide (15)

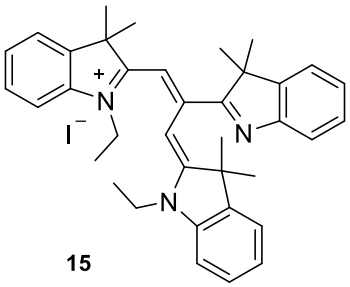

15

Chemical Formula: $C_{37}H_{42}N_3^+$
Exact Mass: 528.34

Violet solid, 11 mg (17% yield).

NMR ^{1}H (600 MHz, CD_3CN) δ 7.52 (ddd, *J* = 7.4, 1.2, 0.6 Hz, 1H), 7.46 – 7.41 (m, 2H), 7.39 (td, *J* = 7.8, 1.3 Hz, 1H), 7.36 – 7.31 (m, 2H), 7.21 (ddd, *J* = 7.3, 1.3, 0.6 Hz, 1H), 7.10 (td, *J* = 7.5, 0.9 Hz, 1H), 7.00 (td, *J* = 7.5, 0.9 Hz, 1H), 6.96 (ddd, *J* = 8.1, 7.6, 1.3 Hz, 1H), 6.93 (dt, *J* = 7.9, 0.7 Hz, 1H), 6.66 (d, *J* = 0.6 Hz, 1H), 5.99 (d, *J* = 0.6 Hz, 1H), 5.40 (dt, *J* = 8.1, 0.8 Hz, 1H), 4.14 – 4.04 (m, 2H), 3.12 (ddt, *J* = 16.8, 14.8, 7.4 Hz, 2H), 1.76 (d, *J* = 14.3 Hz, 6H), 1.59 (d, *J* = 1.7 Hz, 6H), 1.35 (s, 3H), 1.30 (t, *J* = 7.3 Hz, 3H), 1.14 (t, *J* = 7.2 Hz, 3H), 1.10 (s, 3H).

ESI-HRMS: found 528.3373 $[M]^+$, calculated 528.3373 for $C_{37}H_{42}N_3^+$.

λ_{max} (absorption) 577 nm (ε = 92 000 M^{-1} cm^{-1}, MeCN), λ_{max} (emission) 632 nm (MeCN, excitation at 570 nm); Stokes shift 55 nm; fluorescence quantum yield 0 (absolute value in MeCN).

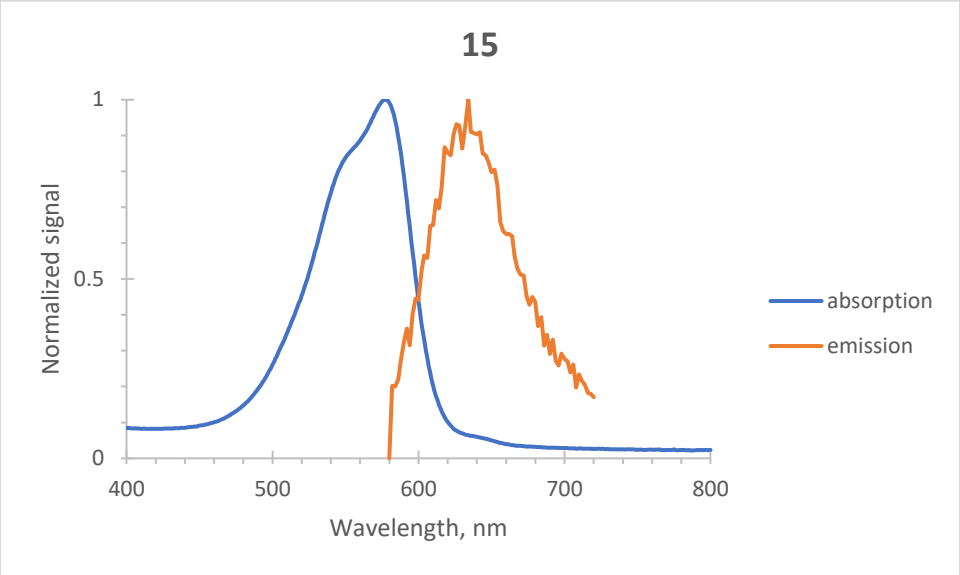

General procedure for the reaction of Fischer base with triphosgene (Scheme 18):

1,3,3-trimethyl-2-metheneindoline **16** (107 µl, 0.60 mmol) and triethylamine (1.2 eq, 102 µl, 0.72 mmol) were dissolved in THF (2 ml) and stirred at 0 ˚C (ice bath) for 30 min. A solution of triphosgene* (90 mg, 0.3 mmol) in THF (0.5 ml) was added dropwise. The reaction mixture was stirred for 5 h at r.t. The reaction mixture was concentrated in vacuo, and the residue submitted to flash chromatography on a reversed phase cartridge Interchim puriFlash™. Squarylium dye **18,** trinuclear dye **20,** 1,3,5-cyclohexanetrione dye **21**, and unsubstituted Cy3 dye **19** were isolated (see below).

*) Similar results were obtained for various amounts of triphosgene. Even with larger excess of **16**, the main isolated product was squarylium dye **18**.

1,3-Bis-(1,3,3-trimethylindolin-2-ylidene)propan-2-one (17) [10]

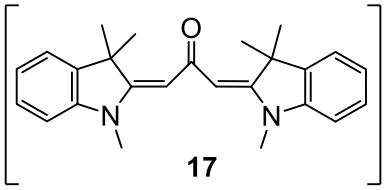

17

Chemical Formula: $C_{25}H_{28}N_2O$
Exact Mass: 372.22

This compound was only observed in the reaction mixture, when the reaction was carried out in THF-d_8 and 1/6 eq. of triphosgene was used. This mixture was subjected to standard workup, but the detected compound **17** disappeared, and squarilium dye **18** was isolated with the yield of 83%. LCMS: t_R 6.0 min; ESI-MS, *m/z*: found 373.34 $[M+H]^+$, calculated 373.22 for $C_{25}H_{29}N_2O^+$.

^{1}H NMR (400 MHz, C_4D_8O) δ 7.06 (dd, *J* = 15.6, 7.4 Hz, 4H), 6.80 (t, *J* = 7.4 Hz, 2H), 6.66 (d, *J* = 7.8 Hz, 2H), 5.42 (s, 2H), 3.10 (s, 6H), 1.76 (s, 12H).

Isolated products:

2,4-Bis(1,3,3-trimethylindolin-2-ylidene)cyclobutane-1,3-dione (18)

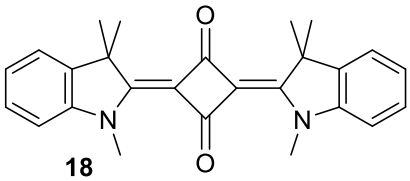

18

Chemical Formula: $C_{26}H_{26}N_2O_2$
Exact Mass: 398.20

Orange solid, 100 mg (83% yield).

^{1}H NMR (400 MHz, $CDCl_3$) δ 7.31 – 7.18 (m, 4H), 7.08 (td, *J* = 7.4, 0.9 Hz, 2H), 6.87 (dt, *J* = 7.9, 0.8 Hz, 2H), 4.00 (s, 3H), 3.97 (s, 3H), 1.76 (s, 6H), 1.76 (s, 6H).

^{13}C NMR (101 MHz, $CDCl_3$) δ 186.4, 185.7, 184.8, 162.3, 162.3, 144.3, 140.6, 140.6, 127.9, 123.3, 121.8, 119.4, 108.9, 49.1, 49.0, 34.5, 34.4, 25.0, 24.9.

ESI-HRMS: found 399.2060 $[M+H]^+$, calculated 399.2067 for $C_{26}H_{27}N_2O_2^+$; found 421.1873 $[M+Na]^+$, calculated 421.1886 for $C_{26}H_{26}N_2O_2Na^+$.

λ_{max} (absorption) = 473 nm (ε = 66 000 M^{-1} cm^{-1}, MeCN; 14 000 M^{-1} cm^{-1} in MeOH), λ_{max} (emission) = 485 nm (MeCN, excitation at 450 nm); Stokes shift 12 nm; fluorescence quantum yield 0.01 (absolute value in MeOH); 0.04 (absolute value in dioxane).

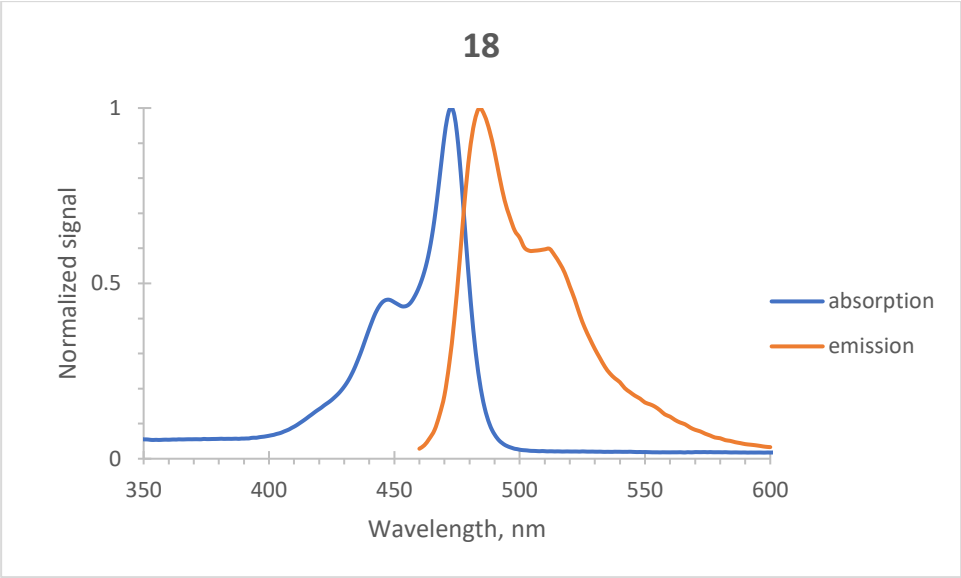

1,3,3-Trimethyl-2-(3-(1,3,3-trimethylindolin-2-ylidene)-2-((1,3,3-trimethylindolin-2-ylidene)methyl)prop-1-en-1-yl)-*3H*-indol-1-ium chloride (20) [11]

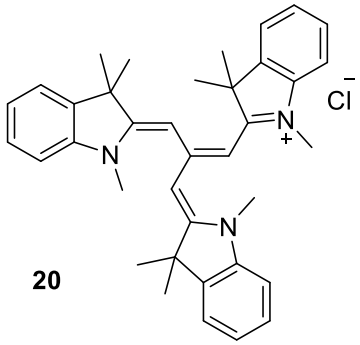

Chemical Formula: $C_{37}H_{42}N_3^+$
Exact Mass: 528.34

Violet solid, 10 mg (9% yield).

^{1}H NMR (400 MHz, $CDCl_3$) δ 7.37 (t, *J* = 7.7 Hz, 3H), 7.31 (d, *J* = 7.4 Hz, 3H), 7.19 (t, *J* = 7.4 Hz, 3H), 7.08 (d, *J* = 7.9 Hz, 3H), 5.09 (s, 3H), 3.43 (s, 9H), 1.49 (s, 18H).

^{13}C NMR (101 MHz, $CDCl_3$) δ 172.3, 159.0, 145.2, 138.6, 128.7, 124.3, 122.2, 110.3, 99.7, 49.2, 37.3, 28.0.

ESI-HRMS: found 528.3366 $[M]^+$, calculated 528.3373 for $C_{37}H_{42}N_3^+$.

λ_{max} (absorption) 554 nm (ε = 65 400 M^{-1} cm^{-1}, MeCN), λ_{max} (emission) 612 nm (MeCN, excitation at 540 nm); Stokes shift 58 nm; fluorescence quantum yield 0 (absolute value in MeCN).

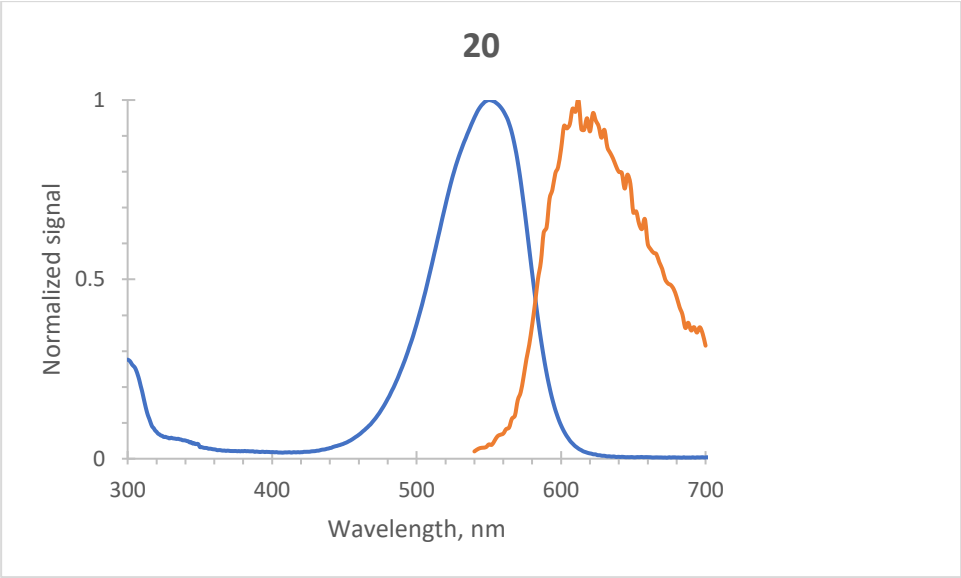

3,5-Dioxo-2,6-bis(1,3,3-trimethyl-*3H*-indol-1-ium-2-yl)-4-(1,3,3-trimethylindolin-2-ylidene)cyclohex-1-en-1-olium chloride (21)

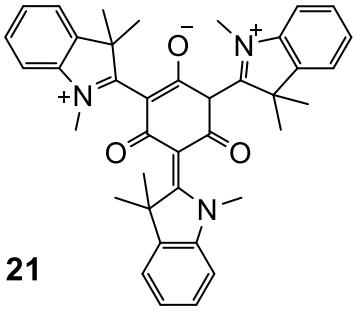

Chemical Formula: $C_{39}H_{40}N_3O_3^+$
Exact Mass: 598.31

21

Orange solid, 25 mg (25% yield).

^{1}H NMR (400 MHz, $CDCl_3$) δ 7.83 (d, *J* = 7.6 Hz, 1H), 7.53 (qd, *J* = 7.8, 7.4, 1.2 Hz, 2H), 7.46 (dd, *J* = 7.2, 1.6 Hz, 1H), 7.42 – 7.35 (m, 3H), 7.30 (d, *J* = 7.4 Hz, 1H), 7.20 (dd, *J* = 9.7, 7.3 Hz, 2H), 7.03 (t, *J* = 7.4 Hz, 1H), 6.78 (d, *J* = 7.9 Hz, 1H), 5.12 (s, 1H), 4.16 (s, 3H), 3.66 (s, 4H), 3.27 (s, 3H), 1.90 (s, 3H), 1.82 (s, 3H), 1.78 (s, 3H), 1.72 (s, 3H), 1.71 (s, 3H), 1.49 (s, 3H).

^{13}C NMR (101 MHz, $CDCl_3$) δ 187.9, 187.3, 174.2, 169.8, 161.6, 160.4, 143.1, 142.9, 142.5, 142.0, 141.9, 140.4, 129.9, 129.3, 128.3, 127.8, 127.5, 122.8, 122.1, 121.7, 116.3, 112.6, 108.6, 98.5, 91.3, 86.2, 57.5, 54.7, 49.0, 38.2, 37.1, 30.7, 27.0, 26.4, 25.4, 25.1, 25.0, 24.1.

ESI-HRMS: found 598.3059 $[M]^+$, calculated 598.3064 for $C_{39}H_{40}N_3O_3^+$.

λ_{max} (absorption) 460 nm (ε = 60 000 M^{-1} cm^{-1}, MeCN), no emission.

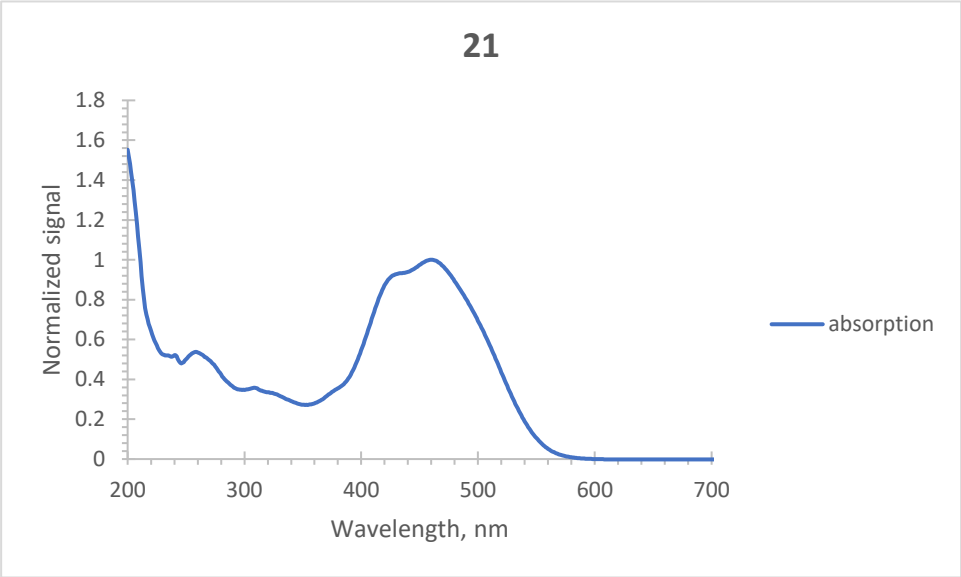

1,3,3-Trimethyl-2-(3-(1,3,3-trimethylindolin-2-ylidene)prop-1-en-1-yl)-*3H*-indol-1-ium chloride (19) [8]

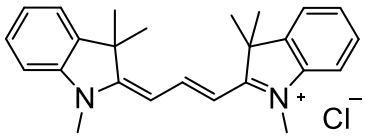

Chemical Formula: $C_{25}H_{29}N_2^+$
Exact Mass: 357.23

19

Violet solid, 4 mg (4% yield).

^{1}H NMR (400 MHz, CD_3OD) δ 8.55 (t, *J* = 13.5 Hz, 1H), 7.54 (ddd, *J* = 7.5, 1.2, 0.6 Hz, 2H), 7.49 – 7.42 (m, 2H), 7.38 – 7.27 (m, 4H), 6.40 (d, *J* = 13.5 Hz, 2H), 3.68 (s, 6H), 1.77 (s, 12H).

λ_{max} (absorption) 545 nm (ε = 90 000 M^{-1} cm^{-1}, MeCN), λ_{max} (emission) 560 nm (MeCN, excitation at 540 nm); Stokes shift 15 nm; fluorescence quantum yield 0.1 (absolute value in MeCN).

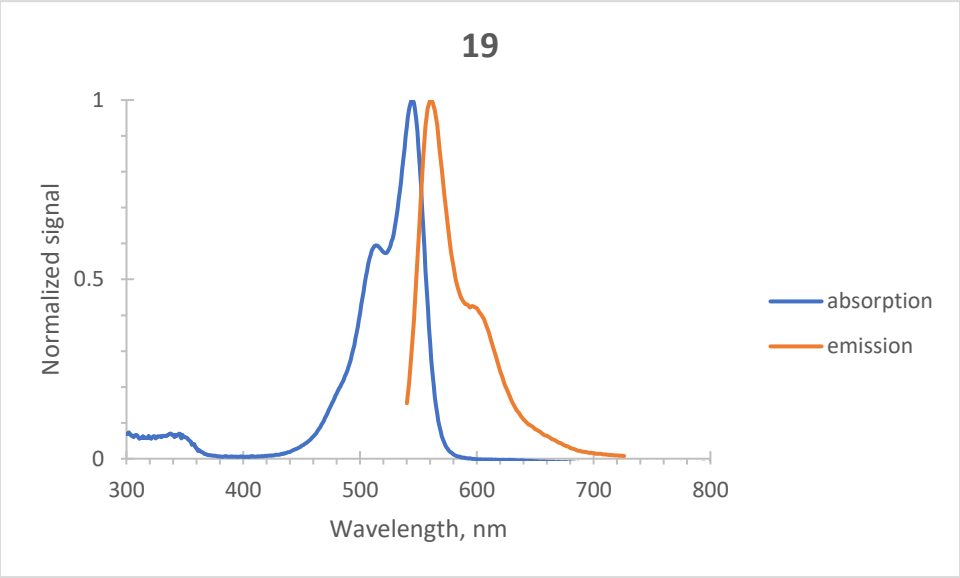

*Synthesis of the meso amino substituted Cy3 derivatives **23** and **24**:*

1,3,3-Trimethyl-2-[1,3,3-trimethylindoline-2-ylidene)prop-1-inyl]-*3H*-indolium chloride (23)

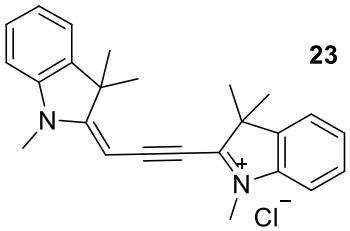

Chemical Formula: $C_{25}H_{27}N_2^+$
Exact Mass: 355.22

A solution of squarilium dye **18** (100 mg, 0.25 mmol), Et_3N (77 µl, 1 mmol) in 1,4-dioxane (5 ml) was heated to 80 ˚C under argon. $POCl_3$ (0.4 ml, 640 mg, 4.2 mmol) was added and the reaction mixture was refluxed for 4 h with the colour change from yellow to red. Analytical LCMS: product **23,** t_R 5.8 min, λ_{abs} 515 nm, ESI M^+ 355.2; starting material **18**, t_R=10.5 min, λ_{abs} 474 nm, ESI M^+ 399.3. The reaction mixture was concentrated in vacuo and separated by flash chromatography on a reversed phase cartridge Interchim puriFlash™; 80 mg of a red powder was obtained after lyophilisation (82% yield of the title compound).

^{1}H NMR (400 MHz, CD_3CN) δ 7.60 – 7.51 (m, 2H), 7.50 – 7.38 (m, 4H), 7.27 – 7.14 (m, 2H), 5.50 (s, 1H), 3.82 (s, 3H), 3.45 (s, 3H), 1.80 (s, 6H), 1.61 (s, 6H).

^{1}H NMR (400 MHz, $CDCl_3$) δ 7.52 (dd, *J* = 7.9, 4.4 Hz, 1H), 7.43 – 7.31 (m, 5H), 7.23 (dd, *J* = 7.5, 0.9 Hz, 1H), 7.05 (d, *J* = 7.9 Hz, 1H), 5.67 (s, 1H), 3.94 (s, 3H), 3.54 (s, 3H), 1.80 (s, 6H), 1.63 (s, 6H).

^{13}C NMR (101 MHz, CD_3CN) δ 179.0, 167.4, 160.7, 160.3, 144.2, 143.2, 140.9, 140.6, 139.8, 130.1, 129.5, 128.6, 125.6, 124.0, 123.1, 113.9, 111.2, 96.1, 71.3, 54.3, 50.3, 35.2, 31.4, 25.8, 25.2.

ESI-HRMS: found 355.2173 $[M]^+$, calculated 355.2169 for $C_{25}H_{27}N_2^+$.

λ_{max} (absorption) 516 nm (ε = 84 000 M^{-1} cm^{-1}, MeCN), λ_{max} (emission) 561 nm (MeCN, excitation at 520 nm); Stokes shift 45 nm; fluorescence quantum yield 0 (absolute value in MeCN).

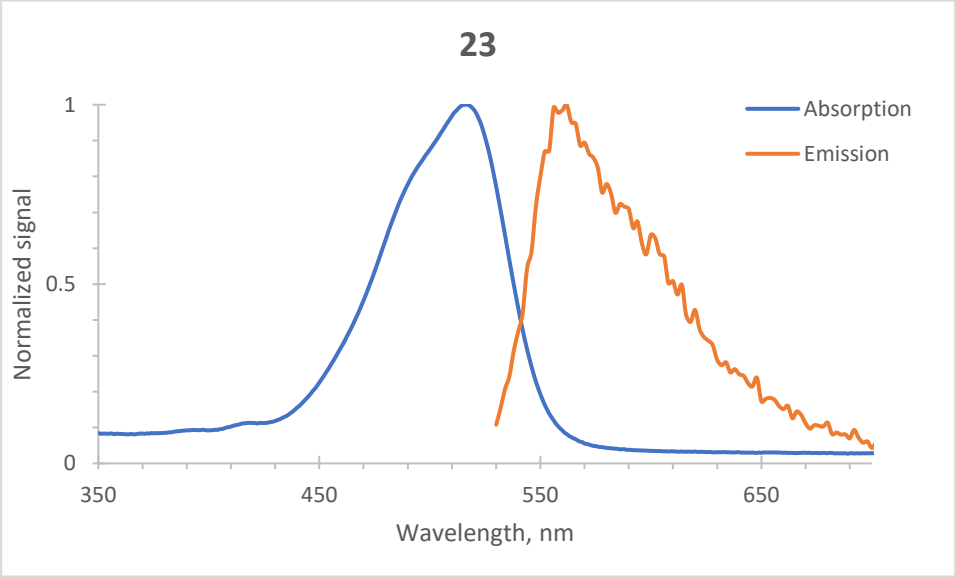

2-(2-((3-(*tert*-Butoxy)-3-oxopropyl)amino)-3-(1,3,3-trimethylindolin-2-ylidene)prop-1-en-1-yl)-1,3,3-trimethyl-*3H*-indol-1-ium chloride (24)

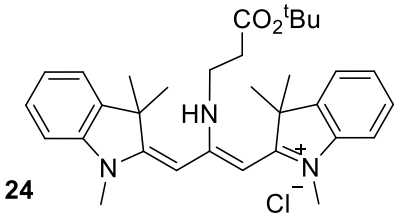

24

Chemical Formula: $C_{32}H_{42}N_3O_2^+$
Exact Mass: 500.33

β-Alanine *t*-butyl ester hydrochloride (2 eq, 19 mg, 0.1 mmol), and K_2CO_3 (2.2 eq, 16 mg, 0.12 mmol) were dissolved in H_2O (0.2 ml) and added dropwise to the solution of **23** (20 mg, 0.05 mmol) in THF (1.0 ml). The resulted mixture was stirred overnight at r.t. The colour changed from red to yellow. The reaction progress was monitored by LCMS (product **24**, t_R 7.2 min, λ_{abs} 458 nm,

ESI M^+ 500.3; starting material **23**, t_R 5.8 min, λ_{abs} 515 nm, ESI M^+ 355.2). The reaction mixture was concentrated in vacuo and applied onto reversed phase cartridge Interchim puriFlash™. 24 mg of a yellow powder was obtained after lyophilisation (90% yield of the title compound).

^{1}H NMR (400 MHz, CD_3CN) δ 7.42 (d, *J* = 7.4 Hz, 1H), 7.35 (q, *J* = 8.3 Hz, 3H), 7.19 (td, *J* = 7.5, 0.9 Hz, 1H), 7.12 (dt, *J* = 7.4, 3.4 Hz, 2H), 7.05 (d, *J* = 7.8 Hz, 1H), 5.26 (s, 1H), 4.85 (s, 1H), 3.74 (q, *J* = 6.4 Hz, 2H), 3.33 (s, 3H), 3.29 (s, 3H), 2.69 (t, *J* = 6.7 Hz, 2H), 1.50 (s, 6H), 1.45 (s, 9H), 1.40 (s, 6H).

^{13}C NMR (101 MHz, CD_3CN) δ 172.0, 171.5, 164.8, 146.3, 140.1, 129.3, 129.2, 125.0, 124.0, 123.2, 123.1, 111.3, 110.2, 86.3, 50.5, 49.6, 41.7, 35.1, 30.9, 28.2, 28.0, 27.7.

ESI-HRMS: found 355.2173 $[M]^+$, calculated 355.2169 for $C_{25}H_{27}N_2^+$.

λ_{max} (absorption) 458 nm (ε = 65 000 M^{-1} cm^{-1}, MeCN), λ_{max} (emission) 534 nm (MeCN, excitation at 450 nm); Stokes shift 76 nm; fluorescence quantum yield 0 (absolute value in MeCN).

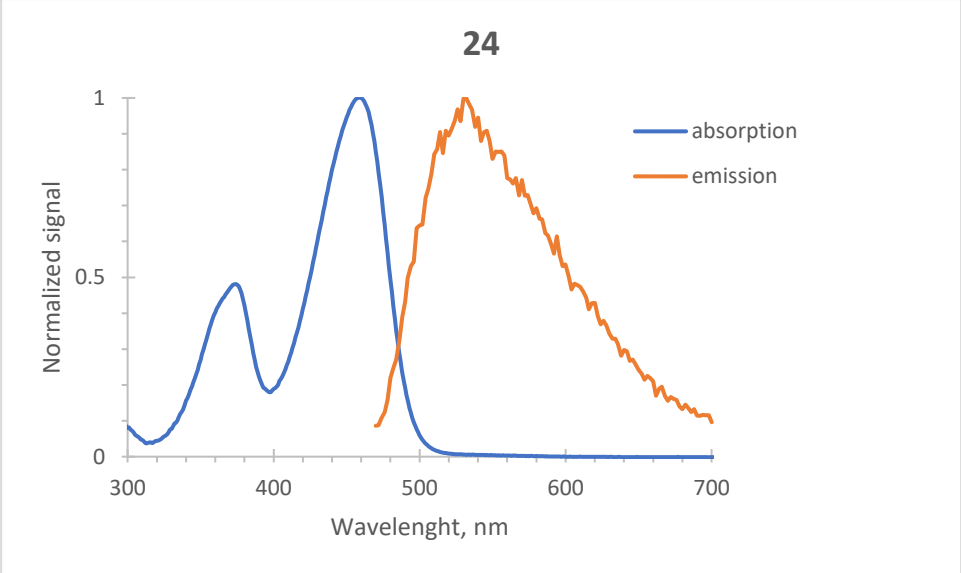

2-(2-((4-Diazo-3-oxobutyl)amino)-3-(1,3,3-trimethylindolin-2-ylidene)prop-1-en-1-yl-3-d)-1,3,3-trimethyl-*3H*-indol-1-ium chloride (25)

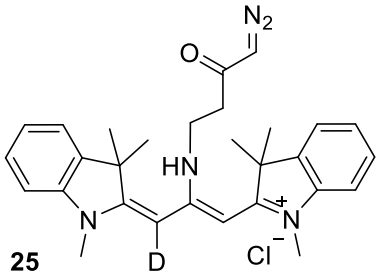

25

Chemical Formula: $C_{29}H_{33}DN_5O^+$
Exact Mass: 469.28

A solution of enyne **23** (15 mg, 0.037 mmol) in 0.5 ml of MeCN was added dropwise to the mixture containing **DAK** (see section 4.2.3 preparation of DAK). The resulted mixture was stirred overnight at r.t. The colour changed from red to yellow. Analytical LCMS: product **25**, t_R 5.6 min, λ_{abs} 458 nm, ESI M^+ 469.4; starting material **23**, t_R 5.8 min, λ_{abs} 515 nm, ESI M^+ 355.2. The reaction mixture was concentrated in vacuo and purified by flash chromatography on a reversed phase cartridge Interchim puriFlash™.Compound **25**: 3 mg of a yellow powder was obtained in this experiment after lyophilisation (16% yield).

^{1}H NMR (400 MHz, CD_3CN) δ 7.42 (d, *J* = 7.3 Hz, 1H), 7.34 (t, *J* = 7.7 Hz, 3H), 7.20 (d, *J* = 7.5 Hz, 1H), 7.12 (t, *J* = 7.2 Hz, 2H), 7.08 – 7.04 (m, 1H), 5.27 (s, 1H), 5.10 (s, 1H), 4.83 (s, 1H), 3.84 – 3.77 (m, 2H), 3.33 (s, 3H), 3.28 (d, *J* = 10.5 Hz, 3H), 2.99 (t, *J* = 6.5 Hz, 1H), 1.50 (s, 6H), 1.40 (s, 6H).

ESI-HRMS: found 469.2819 $[M]^+$, calculated 469.2821 for $C_{29}H_{33}DN_5O^+$; HD exchange found 468.2758 calculated 468.2758 for $C_{29}H_{34}N_5O^+$

λ_{max} (absorption) 458 nm (ε = 65 400 M^{-1} cm^{-1}, MeCN), λ_{max} (emission) 534 nm (MeCN, excitation at 450 nm); Stokes shift 76 nm; fluorescence quantum yield 0 (absolute value in MeCN).

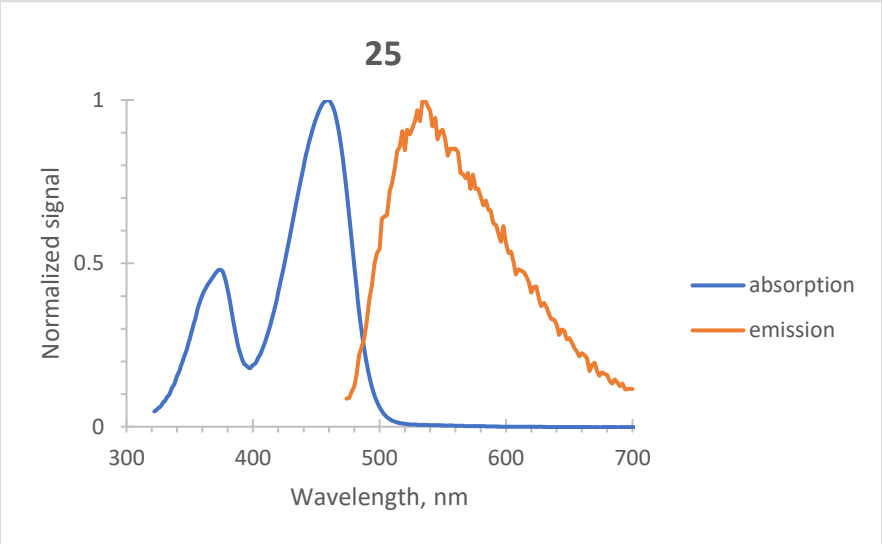

4.2.2.3 Synthesis and properties of pentamethinecyanines (Cy5 dyes)

Synthesis of the meso-halogenated Cy5 derivatives

N-(2-bromo-3-(phenylimino)prop-1-en-1-yl)aniline (28c) [12]

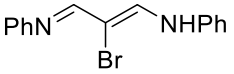

Chemical Formula: $C_{15}H_{13}BrN_2$
Exact Mass: 300.03

1. Commercially available mucobromic acid (2.00 mmol, 530 mg) was dissolved in 1.5 ml of EtOH. A solution of aniline (in EtOH, 4.2 M, 1.0 ml) was added dropwise under stirring, and the reaction mixture heated to 40 °C for 2 h. Then the reaction mixture was cooled down (ice bath), and precooled Et_2O was added to precipitate yellow solid. The solid was filtered off, washed with cold Et_2O and dried on air. The crude product was carried on to the next step without further purification.

ESI-MS, *m/z*: found 301.20 $[M+H]^+$, calculated 301.19 for $C_{15}H_{14}BrN_2$.

2-(3-Chloro-5-(1-ethyl-3,3-dimethylindolin-2-ylidene)penta-1,3-dien-1-yl)-1-ethyl-3,3-dimethyl-*3H*-indol-1-ium iodide (29b) [12]

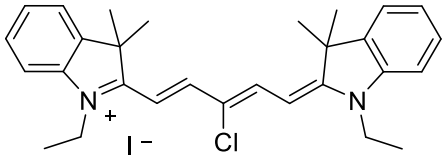

29b

Chemical Formula: $C_{29}H_{34}ClN_2^+$

Exact Mass: 445.24

Commercially available *N*-[2-chloro-3-(phenylamino)-2-propen-1-ylidene]-benzamine hydrochloride (0.1 mmol, 30 mg) and indolium iodide **10** (2 eq, 0.2 mmol, 65 mg) were dissolved in the mixture of Ac_2O-AcOH 1:1 (1 ml). The reaction mixture was stirred for 1 h in a screw-cap tube at 120 °C. The solvents were removed under reduced pressure, and the residue submitted to flash chromatography on *Isolera*™ *One* system (SNAP Ultra cartridge, 50 g SiO_2, DCM/MeOH with 2-25% MeOH gradient over 7 CV) to provide compound **29b** as a dark blue solid (47 mg, 82% yield).

^{1}H NMR (400 MHz, CD_3CN) δ 8.13 (d, *J* = 13.6 Hz, 2H), 7.54 (dd, *J* = 7.4, 1.1 Hz, 2H), 7.49 – 7.40 (m, 2H), 7.40 – 7.24 (m, 4H), 6.39 (d, *J* = 13.5 Hz, 2H), 4.16 (q, *J* = 7.3 Hz, 4H), 1.72 (s, 12H), 1.39 (t, *J* = 7.3 Hz, 6H).

λ_{max} (absorption) 640 nm (ε = 193 700 $M^{-1}cm^{-1}$, MeCN), λ_{max} (emission) 659 nm (MeCN, excitation at 630 nm); Stokes shift 19 nm; fluorescence lifetime 0.22 ns (MeCN), fluorescence quantum yield 0.07 (absolute value in MeCN).

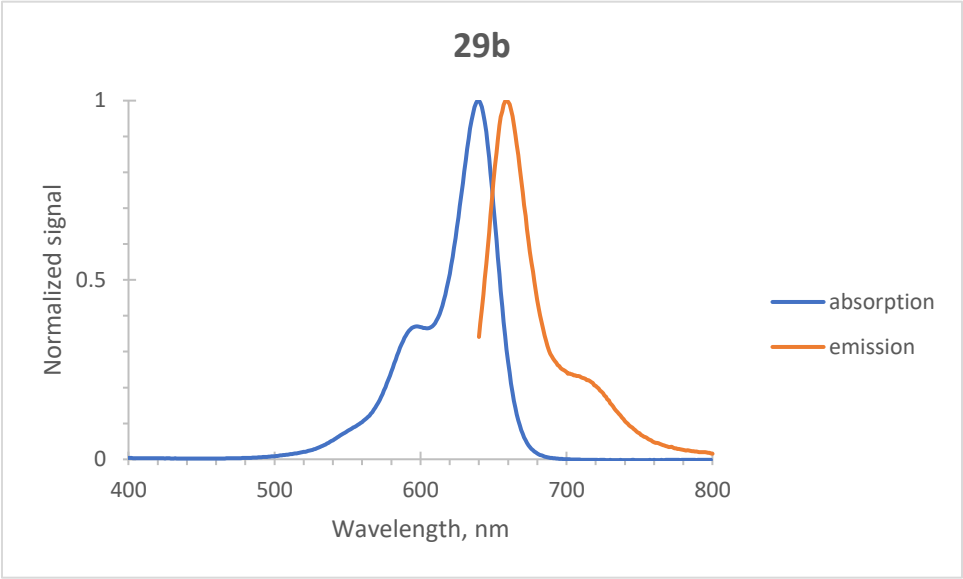

2-(3-Bromo-5-(1-ethyl-3,3-dimethylindolin-2-ylidene)penta-1,3-dien-1-yl)-1-ethyl-3,3-dimethyl-*3H*-indol-1-ium iodide (29c) [12]

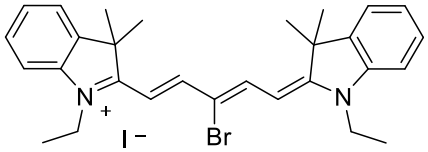

Chemical Formula: $C_{29}H_{34}BrN_2^+$
Exact Mass: 489.19

29c

N-(2-Bromo-3-(phenylimino)prop-1-en-1-yl)aniline **28c** (0.13 mmol, 39 mg) and indolium iodide **10** (0.28 mmol, 82 mg) were dissolved in the mixture of Ac_2O-AcOH 1:1 (1 ml). The reaction mixture was stirred for 1 h in a screw-cap tube at 120 °C. The solvents were removed under reduced pressure, and the residue submitted to flash chromatography on *Isolera™ One* system (SNAP Ultra cartridge, 50 g SiO_2, DCM/MeOH with 2-25% MeOH gradient over 7 CV) to provide compound **29c** as a dark blue solid (40 mg, 50 % yield) and **29a** (10 mg, 14% yield) as a side product.

^{1}H NMR (400 MHz, CD_3CN) δ 8.15 (d, *J* = 13.4 Hz, 2H), 7.53 (dd, *J* = 7.9, 1.1 Hz, 2H), 7.48 – 7.42 (m, 2H), 7.36 – 7.30 (m, 4H), 6.41 (d, *J* = 13.4 Hz, 2H), 4.16 (q, *J* = 7.3 Hz, 4H), 1.72 (s, 12H), 1.40 (t, *J* = 7.3 Hz, 6H).

λ_{max} (absorption) 636 nm (ε = 179 000 $M^{-1}cm^{-1}$, MeCN), λ_{max} (emission) 658 nm (MeCN, excitation at 630 nm); Stokes shift 22 nm; fluorescence lifetime 0.20 ns (MeCN), fluorescence quantum yield 0.05 (absolute value in MeCN).

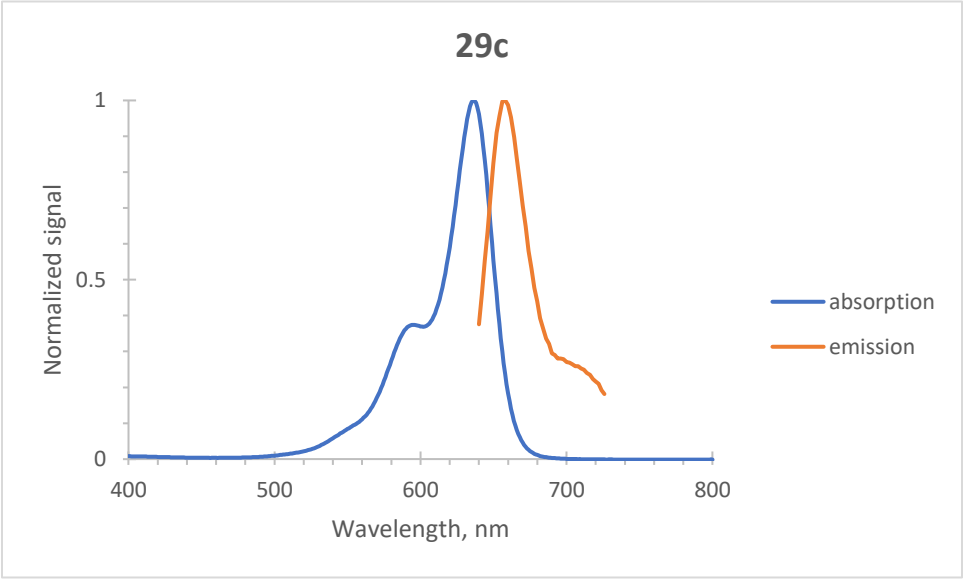

1-Ethyl-2-(5-(1-ethyl-3,3-dimethylindolin-2-ylidene)penta-1,3-dien-1-yl)-3,3-dimethyl-*3H*-indol-1-ium iodide (29a) [12]

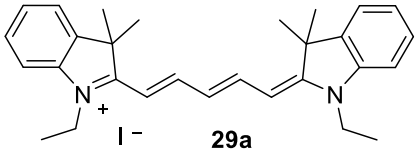

29a

Chemical Formula: $C_{29}H_{35}N_2^+$
Exact Mass: 411.28

Isolated as a side product in the synthesis of **29c**.

^{1}H NMR (400 MHz, CD_3CN) δ 8.09 (dd, *J* = 13.8, 12.5 Hz, 2H), 7.49 (ddd, *J* = 7.4, 1.2, 0.6 Hz, 2H), 7.44 – 7.39 (m, 2H), 7.31 – 7.21 (m, 4H), 6.53 (t, *J* = 12.5 Hz, 1H), 6.22 (d, *J* = 13.8 Hz, 2H), 4.06 (q, *J* = 7.3 Hz, 4H), 1.69 (s, 12H), 1.34 (t, *J* = 7.3 Hz, 6H).

λ_{max} (absorption) 639 nm (ε = 191 000 $M^{-1}cm^{-1}$, MeCN), λ_{max} (emission) 664 nm (MeCN, excitation at 620 nm); Stokes shift 25 nm; fluorescence lifetime 0.78 ns (MeCN), fluorescence quantum yield 0.17 (absolute value in MeCN).

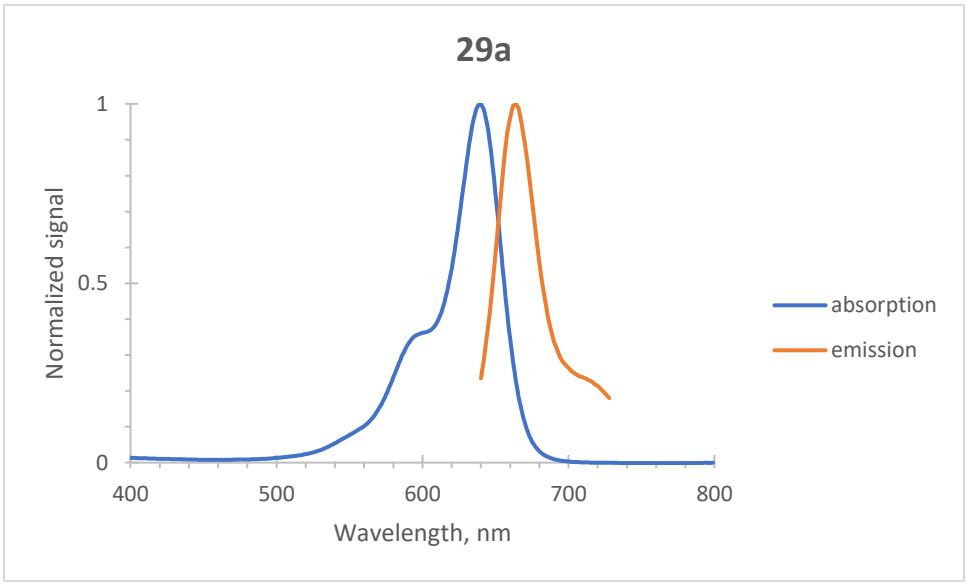

Nucleophilic substitution in the meso-halogenated Cy5 derivatives:

2-(4-((3-(tert-Butoxy)-3-oxopropyl)amino)-3-chlorobuta-1,3-dien-1-yl)-1-ethyl-3,3-dimethyl-*3H*-indol-1-ium iodide (31a)

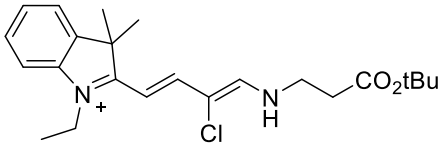

31a

Chemical Formula: $C_{23}H_{32}ClN_2O_2^+$
Exact Mass: 403.21

The starting dye **29b** (46 mg, 0.08 mmol) was placed into a sealed tube and dissolved in dioxane (5 ml). A solution of β-alanine *t*-butyl ester hydrochloride **30a** (2.5 eq, 37 mg, 0.2 mmol), K_2CO_3 (3 eq, 35 mg, 0.25 mmol) in 1 ml of H_2O were added dropwise with stirring. The reaction mixture was stirred at 100 °C for 2 h. The title product **31a** was detected by LCMS: t_R 5.8 min, λ_{abs} 475 nm, ESI M^+ 403 (starting material **29b**, t_R 7.4 min, λ_{abs} 640 nm, ESI M^+ 445). The product was isolated by flash chromatography on a reversed phase cartridge Interchim puriFlash™ together with compound **31c** (LCMS: t_R 7.5 min, detected at 420 nm, ESI M+ 276). Yield 21 mg (49%), brown solid.

^{1}H NMR (400 MHz, CD_3CN) δ 8.06 (d, *J* = 13.7 Hz, 2H), 7.55 – 7.41 (m, 2H), 7.37 – 7.30 (m, 2H), 6.18 (d, *J* = 13.7 Hz, 1H), 4.13 (q, *J* = 7.3 Hz, 2H), 3.72 (t, *J* = 6.3 Hz, 2H), 2.63 (t, *J* = 6.3 Hz, 2H), 1.65 (s, 6H), 1.44 (s, 9H), 1.36 (t, *J* = 7.3 Hz, 3H).

^{13}C NMR (101 MHz, CD_3CN) δ 177.3, 171.2, 158.3, 151.2, 142.5, 142.4, 129.7, 127.0, 123.4, 112.6, 108.7, 97.8, 82.1, 50.9, 46.5, 40.7, 36.0, 28.2, 27.4, 12.4.

ESI-HRMS: found 403.2149 $[M]^+$, calculated 403.2147 for $C_{23}H_{32}ClN_2O_2^+$.

λ_{max} (absorption) 475 nm (MeCN); no emission.

2-(3-Chloro-4-hydroxybuta-1,3-dien-1-yl)-1-ethyl-3,3-dimethyl-*3H*-indol-1-ium iodide (31c)

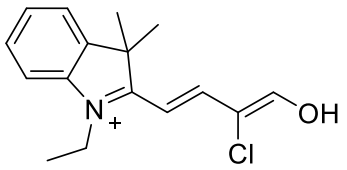

31c

Chemical Formula: $C_{16}H_{19}ClNO^+$
Exact Mass: 276.11

Isolated as a side product in the reaction of **29b** and **30a**.

^{1}H NMR (400 MHz, CD_3CN) δ 9.29 (s, 1H), 7.91 (d, *J* = 12.5 Hz, 1H), 7.34 (s, 1H), 7.29 (td, *J* = 7.7, 1.2 Hz, 1H), 7.06 (td, *J* = 7.4, 0.9 Hz, 1H), 6.98 (d, *J* = 7.9 Hz, 1H), 5.87 (d, *J* = 12.5 Hz, 1H), 3.89 (q, *J* = 7.2 Hz, 2H), 1.62 (s, 6H), 1.27 (t, *J* = 7.2 Hz, 6H).

ESI-HRMS: found 276.1152 $[M]^+$, calculated 276.1150 for $C_{16}H_{19}ClNO^+$.

λ_{max} (absorption) 420 nm (MeCN); no emission.

2-(4-((2-Carboxyethyl)amino)-3-chlorobuta-1,3-dien-1-yl)-1-ethyl-3,3-dimethyl-*3H*-indol-1-ium iodide (31b)

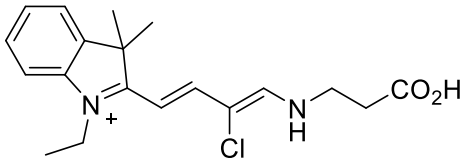

Chemical Formula: $C_{19}H_{24}ClN_2O_2^+$
Exact Mass: 347.15

The starting dye **29b** (46 mg, 0.08 mmol), K_2CO_3 (0.10 mmol, 14 mg), and β-alanine hydrochloride **30b** (1.3 eq, 9 mg, 0.1 mmol) were placed into a sealed tube and dissolved in DMF (2 ml). The reaction mixture was stirred at 110 ℃ overnight. The product **31b** was detected by LCMS: t_R 6.1 min, λ_{abs} 475 nm, ESI M^+ 347 (starting material **29b**, t_R 7.4 min, λ_{abs} 640 nm, ESI M^+ 445). The product was isolated by flash chromatography on a reversed phase cartridge Interchim puriFlash™ together with compound **31c** (LCMS: t_R 7.5 min, detected at 420 nm, ESI M+ 276). Yield 24 mg (62%), brown solid.

^{1}H NMR (400 MHz, CD_3CN) δ 8.09 (d, *J* = 13.6 Hz, 2H), 7.52 (dd, *J* = 7.7, 1.0 Hz, 1H), 7.48 – 7.41 (m, 1H), 7.36 – 7.25 (m, 2H), 6.17 (d, *J* = 13.7 Hz, 1H), 4.13 (q, *J* = 7.3 Hz, 2H), 3.74 (t, *J* = 6.2 Hz, 2H), 2.79 – 2.62 (m, 2H), 1.65 (s, 6H), 1.36 (t, *J* = 7.3 Hz, 3H).

ESI-HRMS: found 347.1517 $[M]^+$, calculated 347.1521 for $C_{19}H_{24}ClN_2O_2^+$.

λ_{max} (absorption) 475 nm (MeCN); no emission.

(2-(3-Chloro-4-(phenylamino)buta-1,3-dien-1-yl)-1-ethyl-3,3-dimethyl-*3H*-indol-1-ium) (31d)

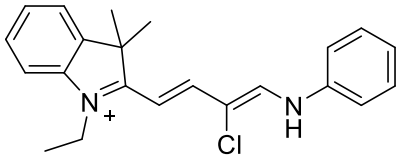

Chemical Formula: $C_{22}H_{24}ClN_2^+$
Exact Mass: 351.16

Dye **29b** (6 mg, 0.01 mmol), K_2CO_3 (0.025 mmol, 4 mg), and aniline **30d** (4 eq, 4 µl, 0.04 mmol) were placed into a sealed tube and dissolved in MeCN (1 ml). The reaction mixture was stirred at 60 ℃ overnight. The product **31d** was detected by LCMS: t_R 5.4 min, λ_{abs} 509 nm, ESI M^+ 351 (starting material **29b**, t_R 7.4 min, λ_{abs} 640 nm, ESI M^+ 445). The product was isolated by flash chromatography on a reversed phase cartridge Interchim puriFlash™. Yield 4 mg (84%), red solid.

^{1}H NMR (400 MHz, CD_3CN) δ 8.48 (s, 1H), 8.25 (d, *J* = 14.0 Hz, 1H), 7.60 (ddd, *J* = 7.4, 1.3, 0.7 Hz, 1H), 7.56 – 7.42 (m, 7H), 7.33 – 7.27 (m, 1H), 6.46 (d, *J* = 14.1 Hz, 1H), 4.27 (q, *J* = 7.3 Hz, 2H), 1.73 (s, 6H), 1.44 (t, *J* = 7.3 Hz, 3H).

ESI-HRMS: found 351.1626 $[M]^+$, calculated 351.1623 for $C_{22}H_{24}ClN_2^+$.

λ_{max} (absorption) 509 nm (MeCN); no emission.

(2-(3-Chloro-4-(3-hydroxyphenoxy)buta-1,3-dien-1-yl)-1-ethyl-3,3-dimethyl-*3H*-indol-1-ium) (31e)

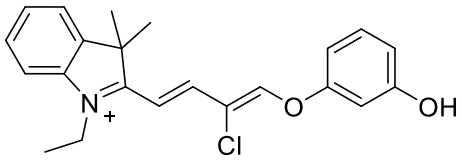

Chemical Formula: $C_{22}H_{23}ClNO_2^+$
Exact Mass: 368.14

The starting dye **29b** (6 mg, 0.01 mmol), K_2CO_3 (4mg, 0.025 mmol), and resorcin **30e** (5 eq, 4 µl, 0.05 mmol) were placed into a sealed tube and dissolved in MeCN (1 ml). The reaction mixture was stirred at 60 °C overnight. The product **31e** was detected by LCMS: t_R10.4 min, λ_{abs} 500 nm, ESI M^+ 368 (starting material **29b**, t_R 7.4 min, λ_{abs} 640 nm, ESI M^+ 445). The product was isolated by flash chromatography on a reversed phase cartridge Interchim puriFlash™. Yield 4 mg (79 %), red solid.

^{1}H NMR (400 MHz, CD_3CN) δ 8.39 (d, *J* = 9.0 Hz, 1H), 8.25 (d, *J* = 14.9 Hz, 1H), 8.22 (s, 1H), 7.70 – 7.63 (m, 2H), 7.62 – 7.55 (m, 2H), 7.01 (d, *J* = 14.9 Hz, 1H), 6.61 (d, *J* = 2.4 Hz, 1H), 6.50 (ddd, *J* = 9.0, 2.4, 0.5 Hz, 1H), 4.44 (q, *J* = 7.4 Hz, 2H), 1.74 (s, 6H), 1.50 (t, *J* = 7.4 Hz, 3H).

ESI-HRMS: found 368.1411 $[M]^+$, calculated 368.1412 for $C_{22}H_{23}ClN_2O_2^+$.

λ_{max} (absorption) 494 nm, λ_{max} (emission) 614 nm (MeCN, excitation at 490 nm); Stokes shift 120 nm; fluorescence quantum yield ~0 (absolute value in MeCN).

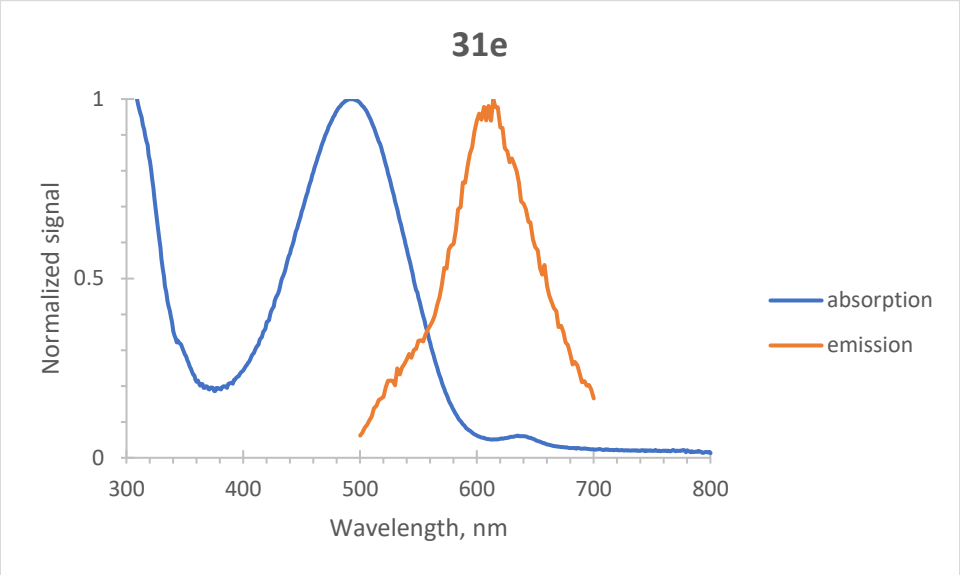

Attempted dehydrohalogenation of the meso-halogenated Cy5 derivatives:

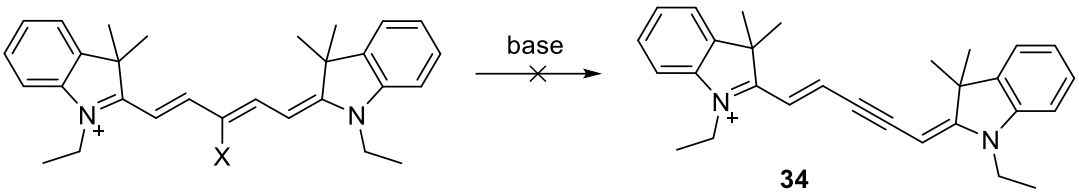

29b (X = Cl), **29c** (X = Br) **34**

Scheme 61. Attempted dehydrohalogenation of Cy5 derivatives.

29b – Et_3N

The starting dye **29b** (0.01 mmol, 5 mg), and triethylamine (0.1 mmol, 14 µl) were dissolved in 0.5 ml of MeCN and refluxed for 1 h. The reaction mixture was analysed by LCMS; only the starting material (t_R 7.4 min, λ_{abs} 640 nm, ESI M^+ 445) and traces of the reduced dye **29a** (t_R 7.1 min, λ_{abs} 638 nm, ESI M^+ 411) were detected.

29b – DBN

The starting dye **29b** (0.02 mmol, 12 mg), and DBN (0.16 mmol, 20 µl) were dissolved in 0.5 ml of DMF and stirred at 100 ˚C for 1 h. The reaction mixture was analysed by LCMS;

numerous compounds (incl. trinuclear cyanine **14**, t_R 7.5 min, λ_{abs} 575 nm, ESI M^+ 528) were detected.

29c – DBN

The starting dye **29c** (0.01 mmol, 5 mg), and DBN (0.08 mmol, 10 µl) were dissolved in 0.5 ml of DMF and stirred at r.t. overnight. The reaction mixture was analysed by LCMS; the starting material (t_R 7.0 min, λ_{abs} 640 nm, ESI M^+ 489), traces of product **34** (t_R 6.5 min, λ_{abs} 623 nm, ESI M^+ 409) and numerous products with short absorption wavelengths (destroyed chromophores) were detected.

29c – DBN

The starting dye **29c** (0.03 mmol, 20 mg), and DBN (0.24 mmol, 30 µl) were dissolved in 1 ml of DMSO and stirred at 100 ˚C for 1 h. The reaction mixture was analysed by LCMS; numerous products were detected.

29c – NaOH

The starting dye **29c** (0.03 mmol, 20 mg), and 1.0 M aq. NaOH (0.06 mmol, 60 µl) were dissolved in 1 ml of DMF and stirred at 100 ˚C for 1 h. The reaction mixture was analysed by LCMS; no reaction occurred.

Synthesis of meso-substituted malonic derivatives:

***N,N*-Dimethyl-*N*-[2-(dimethylaminomethylene)ammonio-3-dimethylamino]prop-2-enylidene-ammonium perchlorate (35)** [13]

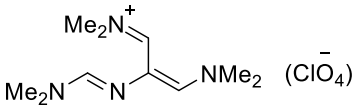

Chemical Formula: $C_{10}H_{21}N_4^+$
Exact Mass: 197.18

DMF (50 ml) was cooled to 0 ˚C (ice bath). $POCl_3$ (0.1 mol, 25 ml) was added dropwise within 25 min. The colour turned orange. The cooling bath was removed, and glycine (2.5 g, 0.03 mol) was added in portions. The reaction mixture was heated to 100…120 ˚C and stirred for 2 h. Then the reaction mixture was cooled down, and poured into crushed ice (100 g). The temperature was maintained at -10 ˚C (external cooling with an ice – acetone bath). Precooled perchloric acid

(60%, 2 × 20 ml) was added under stirring, then the mixture was cooled down to -35 ˚C under continuous stirring and kept at this temperature for 1 h to deposit a precipitate. The dark brown solution was filtered through a Schott filter under reduced pressure, the collected precipitate washed with precooled EtOH; these operations were repeated two more times. The portions of a yellow powder were collected, combined, recrystallized from MeOH, and dried on air. Yield of **35** was 3.9 g. (33%).

^{1}H NMR (400 MHz, CD_3CN) δ 8.50 (d, *J* = 11.7 Hz, 1H), 7.85 – 7.74 (m, 1H), 7.42 (s, 2H), 3.33 (d, *J* = 0.7 Hz, 3H), 3.31 (s, 6H), 3.19 (s, 6H), 3.18 (d, *J* = 0.7 Hz, 3H).

^{13}C NMR (101 MHz, CD_3CN) δ 161.1, 158.1, 49.0, 44.1, 39.7, 37.0.

ESI-HRMS: found 197.1771 $[M]^+$, calculated 197.1761 for $C_{10}H_{21}N_4^+$.

2-(*N*-acetamido)malonaldehyde (36) [13]

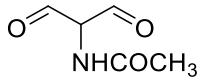

Chemical Formula: $C_5H_4F_3NO_3$
Exact Mass: 183.01

The solid perchlorate **35** (3.9 g, 10 mmol) was dissolved in 60 ml of aq. 1.0 M NaOH (6 eq), and the yellow solution was stirred at 60 ˚C for 3 h. The solution was partially concentrated in vacuo, and then additional amount of 3.0 M aq. solution of NaOH (5.0 ml) was added. The reaction mixture was cooled down to 0 ˚C (ice bath), and 40 ml of DCM were added. A solution of Ac_2O (53 mmol, 5 ml) in 40 ml of DCM was added dropwise with stirring at 0 ˚C. The ice bath was removed, and the reaction mixture stirred for 15 min at r.t. The two layers were separated, the organic layer washed with brine, dried over $MgSO_4$ and concentrated in vacuo to afford 200 mg of yellow crystals. This compound was used in the synthesis of cyanine **40** without further purification.

2-(*N*-trifluoroacetamido)malonaldehyde (37) [13]

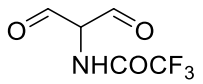

Chemical Formula: $C_5H_4F_3NO_3$
Exact Mass: 183.01

The solid perchlorate **35** (3.9 g, 10 mmol) was dissolved in 60 ml of aq. 1.0 M NaOH (6 eq), and the yellow solution was stirred at 60 ˚C for 3 h. The solution was partially concentrated in vacuo, and then additional amount of 3.0 M aq. solution of NaOH (5.0 ml) was added. The reaction

mixture was cooled down to 0 ˚C (ice bath), and 40 ml of DCM were added. A solution of TFAA (40 mmol, 5 ml) in 40 ml of DCM was added dropwise with stirring at 0 ˚C. The ice bath was removed, and the reaction mixture stirred for 15 min at r.t. The two layers were separated, the organic layer washed with brine, dried over $MgSO_4$ and concentrated in vacuo to afford 90 mg of light brown crystals. This compound was used in the synthesis of cyanine **41** without further purification.

2-Nitromalonaldehyde, sodium salt (38) [14]

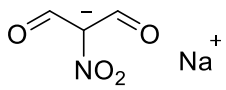

Chemical Formula: $C_3H_2NO_4^-$
Exact Mass: 116.00

A three-necked round-bottom flask equipped with a dropping funnel, thermometer, and gas vent (leading to the hood outlet) was charged with a solution of sodium nitrite (0.2 mol, 14 g) in 15 ml of H_2O. The mixture was stirred at 55 ˚C, until the solid completely dissolved. A solution of mucobromic acid (0.053 mol, 14 g) in 15 ml of warm EtOH was added dropwise within 1 h. The temperature was maintained at 55˚C, the speed of addition was regulated to avoid the violent gas evolution. The solution in the flask became deep red. Once the addition was complete, the reaction mixture was stirred 10 min and then cooled down (0 ˚C, ice bath) to precipitate a yellow solid. This solid was filtered off on a Schott filter, washed with cold aq. EtOH, recrystallized from 20% aq. EtOH, and dried on air to afford 3.0 g of pink powder of **38** (43% yield).

^{1}H NMR (400 MHz, D_2O) δ 9.64 (s, 2H).

ESI-MS, *m/z*: found 116.0 $[M]^-$, calculated 116.0 for $C_3H_2NO_4^-$.

Synthesis of meso-substituted Cy5 dyes from the derivatives of malonic aldehydes (Scheme 24):

2-(3-Acetamido-5-(1-ethyl-3,3-dimethylindolin-2-ylidene)penta-1,3-dien-1-yl)-1-ethyl-3,3-dimethyl-*3H*-indol-1-ium iodide (40)

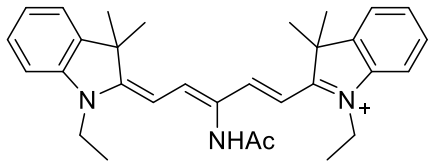

Chemical Formula: $C_{31}H_{38}N_3O^+$
Exact Mass: 468.30

A mixture of indolium iodide **10** (0.3 mmol, 95 mg), perchlorate **35** (0.14 mmol, 56 mg), and sodium acetate (0.2 mmol, 17 mg) in acetic anhydride (1 ml) was heated and stirred at 100 °C

for 1 h. The product was precipitated by addition of diethyl ether and purified by flash chromatography on a reversed phase cartridge Interchim puriFlash™. 71 mg (86% yield) of dye **40** was isolated as a blue solid.

^{1}H NMR (400 MHz, CD_3CN) δ 7.91 (d, *J* = 14.0 Hz, 2H), 7.80 (s, 1H), 7.55 – 7.47 (m, 2H), 7.42 (td, *J* = 7.7, 1.2 Hz, 2H), 7.28 (td, *J* = 8.2, 0.9 Hz, 4H), 6.04 (d, *J* = 14.0 Hz, 2H), 4.09 (q, *J* = 7.3 Hz, 4H), 2.21 (s, 3H), 1.70 (s, 12H), 1.35 (t, *J* = 7.2 Hz, 6H).

^{13}C NMR (101 MHz, CD_3CN) δ 201.1, 174.3, 169.9, 149.9, 142.8, 142.7, 129.6, 126.3, 123.3, 112.0, 100.0, 50.4, 40.2, 27.5, 23.3, 12.4.

ESI-HRMS: found 468.3011 $[M]^+$, calculated 468.3009 for $C_{31}H_{38}N_3O^+$.

λ_{max} (absorption) 637 nm (ε = 180 000 $M^{-1}cm^{-1}$, MeCN), λ_{max} (emission) 660 nm (MeCN, excitation at 620 nm); Stokes shift 23 nm; fluorescence lifetime 0.17 ns (MeCN), fluorescence quantum yield 0.15 (absolute value in MeCN).

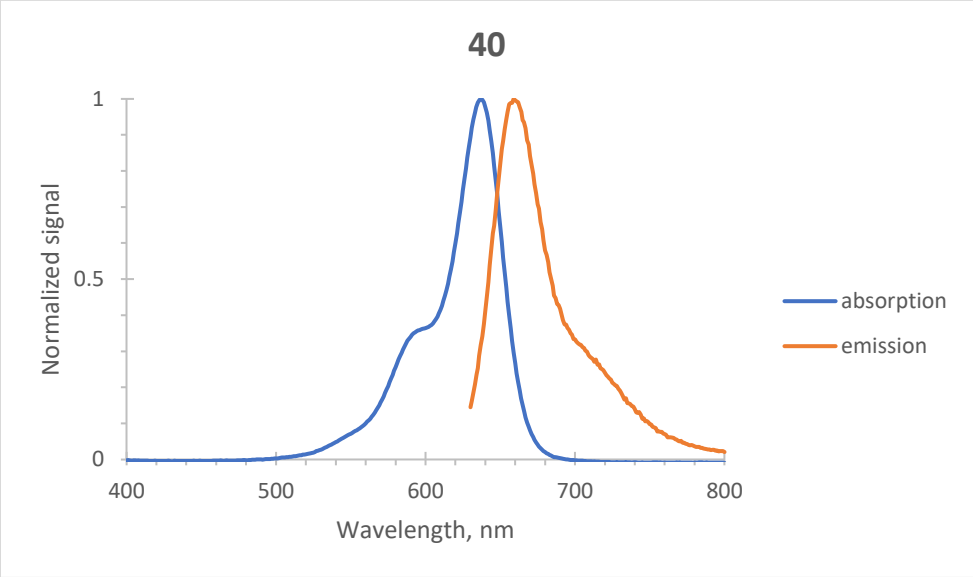

1-Ethyl-2-(5-(1-ethyl-3,3-dimethylindolin-2-ylidene)-3-(2,2,2-trifluoroacetamido)-penta-1,3-dien-1-yl)-3,3-dimethyl-*3H*-indol-1-ium iodide (41)

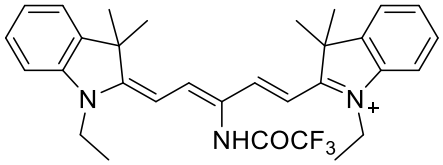

Chemical Formula: $C_{31}H_{35}F_3N_3O^+$
Exact Mass: 522.27

A mixture of indolium iodide **10** (0.3 mmol, 95 mg), 2-(*N*-trifluoro-acetamido)malonaldehyde **37** (0.14 mmol, 26 mg), and sodium acetate (0.2 mmol, 17 mg) in acetic

anhydride (1.0 ml) was heated and stirred at 100 °C for 1 h. The dye was precipitated by addition of diethyl ether and purified by flash chromatography on a reversed phase cartridge Interchim puriFlash™. 65 mg (71% yield) of dye **41** was isolated as a blue solid.

^{19}F NMR (376 MHz, CD_3CN) δ -75.6.

^{1}H NMR (400 MHz, CD_3CN) δ 9.07 (s, 1H), 7.99 (d, *J* = 14.2 Hz, 2H), 7.52 (d, *J* = 7.0 Hz, 2H), 7.44 (td, *J* = 7.7, 1.2 Hz, 2H), 7.31 (t, *J* = 7.6 Hz, 4H), 5.94 (d, *J* = 14.2 Hz, 2H), 4.08 (q, *J* = 7.3 Hz, 4H), 1.72 (s, 12H), 1.34 (t, *J* = 7.3 Hz, 6H).

^{13}C NMR (101 MHz, CD_3CN) δ 175.0, 148.8, 142.7, 142.7, 129.6, 126.6, 123.3, 112.2, 99.3, 50.6, 41.3, 40.4, 27.4, 12.3.

ESI-HRMS: found 522.2727 $[M]^+$, calculated 522.2727 for $C_{31}H_{35}N_3OF_3^+$.

λ_{max} (absorption) 631 nm (ε = 175 000 $M^{-1}cm^{-1}$, MeCN), λ_{max} (emission) 651 nm (MeCN, excitation at 620 nm); Stokes shift 20 nm; fluorescence lifetime 0.16 ns (MeCN), fluorescence quantum yield 0.15 (absolute value in MeCN).

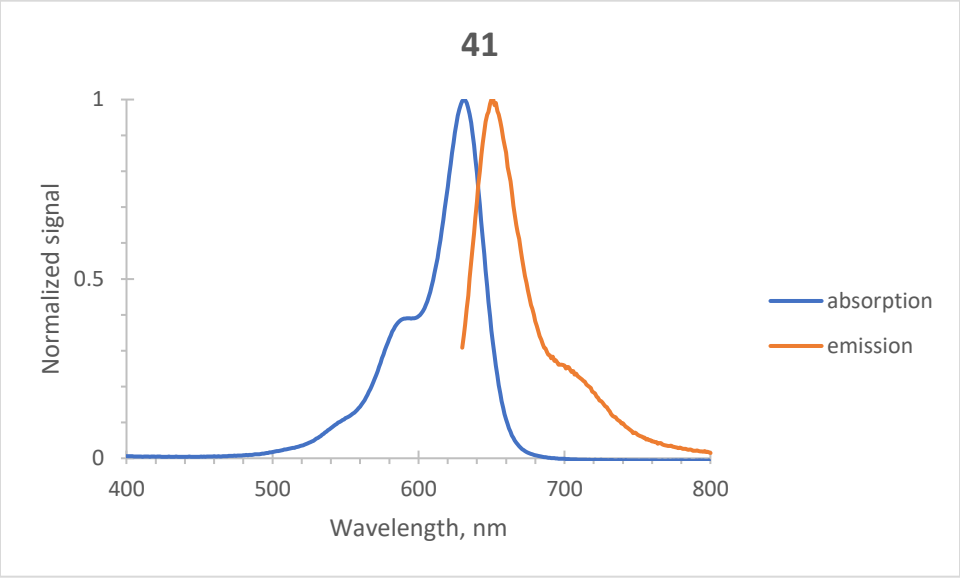

1-Ethyl-2-(5-(1-ethyl-3,3-dimethylindolin-2-ylidene)-3-nitropenta-1,3-dien-1-yl)-3,3-dimethyl-*3H*-indol-1-ium iodide (42)

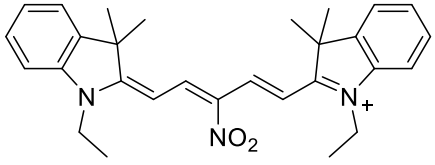

Chemical Formula: $C_{29}H_{34}N_3O_2^+$
Exact Mass: 456.26

A mixture of indolium iodide **10** (0.30 mmol, 95 mg), 2-nitromalonaldehyde (0.14 mmol, 20 mg), and sodium acetate (0.2 mmol, 17 mg) in acetic anhydride (1 ml) was heated and stirred at

100 °C for 1 h. The dye was precipitated by addition of diethyl ether and purified by flash chromatography on a reversed phase cartridge Interchim puriFlash™. 72 mg (88% yield) of dye **42** was isolated as a violet solid.

^{1}H NMR (400 MHz, CD_3CN) δ 8.42 (d, *J* = 15.2 Hz, 2H), 7.64 (ddt, *J* = 7.4, 1.4, 0.7 Hz, 2H), 7.60 – 7.43 (m, 6H), 7.00 (d, *J* = 15.2 Hz, 2H), 4.30 (q, *J* = 7.3 Hz, 4H), 1.79 (d, *J* = 0.6 Hz, 12H), 1.49 (t, *J* = 7.3 Hz, 6H).

^{13}C NMR (101 MHz, CD_3CN) δ 179.8, 143.4, 142.1, 129.9, 128.2, 123.6, 113.6, 102.2, 41.7, 27.7, 12.9, 1.8, 1.6.

ESI-HRMS: found 456.2644 $[M]^+$, calculated 456.2646 for $C_{29}H_{34}N_3O_2^+$.

λ_{max} (absorption) 594 nm (ε = 160 000 $M^{-1}cm^{-1}$, MeCN), λ_{max} (emission) 641 nm (MeCN, excitation at 590 nm); Stokes shift 47 nm; fluorescence lifetime 0.06 ns (MeCN), fluorescence quantum yield 0.02 (absolute value in MeCN).

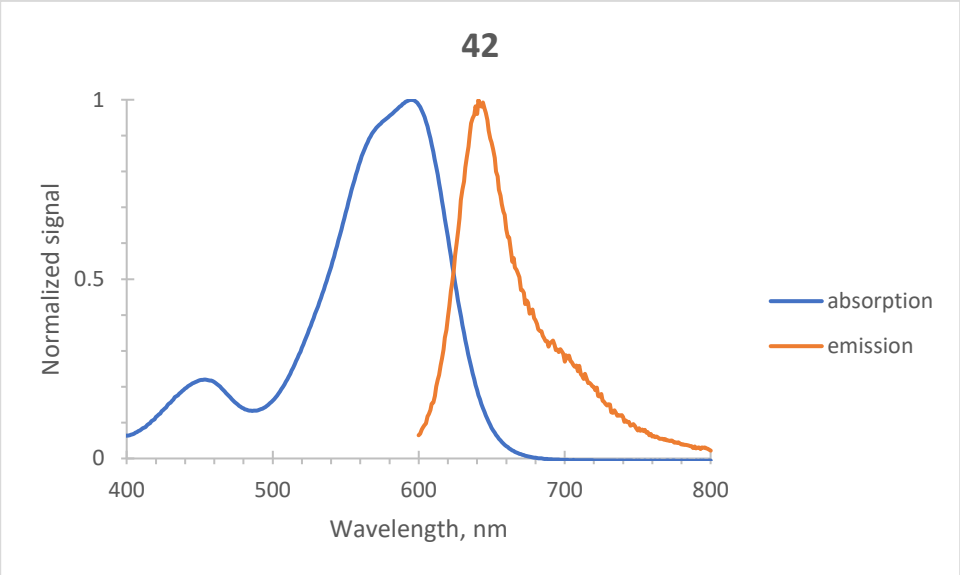

1-Ethyl-2-(5-(1-ethyl-3,3-dimethylindolin-2-ylidene)-3-(*N*-methylacetamido)penta-1,3-dien-1-yl)-3,3-dimethyl-*3H*-indol-1-ium iodide (43)

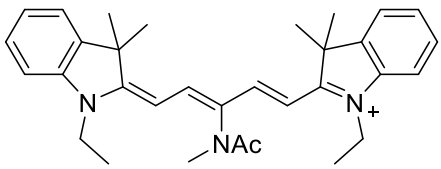

Chemical Formula: $C_{32}H_{40}N_3O^+$
Exact Mass: 482.32

Dye **40** (0.05 mmol, 30 mg), and NaH (60% dispersion in mineral oil, 0.12 mmol, 5 mg) were suspended in dry DMF (1 ml) at 0 °C (ice bath) and stirred for 15 min. MeI (50 µl) was added, and the reaction mixture stirred for 1 h at r.t. The reaction mixture was concentrated in vacuo and

separated by flash chromatography on a reversed phase cartridge Interchim puriFlash™. 22 mg (73% yield) of dye **43** was isolated as a blue solid.

^{1}H NMR (400 MHz, CD_3CN) δ 7.96 (d, *J* = 14.1 Hz, 2H), 7.55 – 7.50 (m, 2H), 7.48 – 7.41 (m, 2H), 7.35 – 7.29 (m, 4H), 5.84 (d, *J* = 14.2 Hz, 2H), 4.08 (qd, *J* = 7.3, 1.9 Hz, 4H), 3.11 (s, 3H), 1.72 (d, *J* = 1.2 Hz, 12H), 1.33 (t, *J* = 7.2 Hz, 6H).

ESI-HRMS: found 482.3169 $[M]^+$, calculated 482.3166 for $C_{32}H_{40}N_3O^+$.

λ_{max} (absorption) 631 nm (ε = 175 000 $M^{-1}cm^{-1}$, MeCN), λ_{max} (emission) 651 nm (MeCN, excitation at 620 nm); Stokes shift 20 nm; fluorescence lifetime 0.51 ns (MeCN), fluorescence quantum yield 0.22 (absolute value in MeCN).

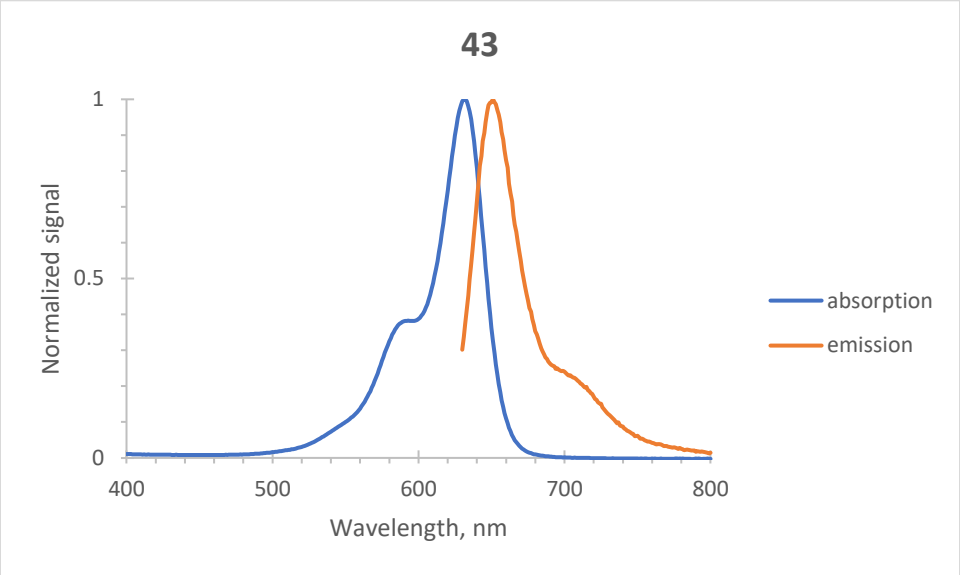

1-Ethyl-2-(5-(1-ethyl-3,3-dimethylindolin-2-ylidene)-3-(2,2,2-trifluoro-*N*-ethyl-acetamido) penta-1,3-dien-1-yl)-3,3-dimethyl-*3H*-indol-1-ium iodide (44)

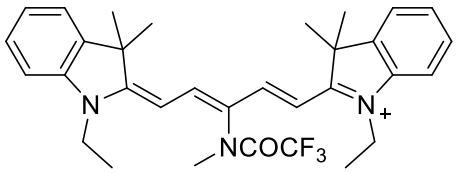

Chemical Formula: $C_{32}H_{37}F_3N_3O^+$
Exact Mass: 536.29

Dye **41** (0.05 mmol, 33 mg), and Cs_2CO_3 (0.1 mmol, 33 mg) were placed into a sealed tube, and dissolved in dry DMF (1 ml). MeI (200 µl) was added, and the reaction mixture stirred at 100 °C for 40 min. The reaction mixture was concentrated in vacuo and separated by flash chromatography on a reversed phase cartridge Interchim puriFlash™. 17 mg (50% yield) of dye **44** was isolated as a blue solid.

^{19}F NMR (376 MHz, CD_3CN) δ -71.1.

^{1}H NMR (400 MHz, CD_3CN) δ 7.98 (d, *J* = 14.3 Hz, 2H), 7.55 – 7.50 (m, 2H), 7.47 – 7.41 (m, 2H), 7.35 – 7.29 (m, 4H), 5.82 (d, *J* = 14.3 Hz, 2H), 4.14 – 4.06 (m, 4H), 3.28 (s, 3H), 1.70 (d, *J* = 6.3 Hz, 12H), 1.30 (t, *J* = 7.3 Hz, 6H).

ESI-HRMS: found 536.2878 $[M]^+$, calculated 536.2883 for $C_{32}H_{37}N_3OF_3^+$.

λ_{max} (absorption) 625 nm (ε = 175 000 $M^{-1}cm^{-1}$, MeCN), λ_{max} (emission) 646 nm (MeCN, excitation at 620 nm); Stokes shift 21 nm; fluorescence lifetime 0.67 ns (MeCN), fluorescence quantum yield 0.22 (absolute value in MeCN).

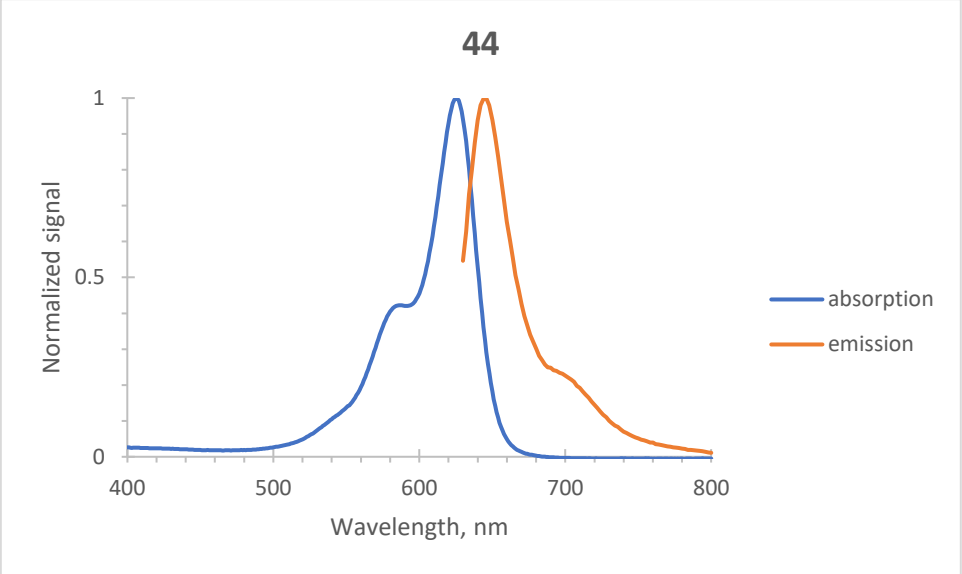

1-Ethyl-2-(5-(1-ethyl-3,3-dimethylindolin-2-ylidene)-3-hydroxypenta-1,3-dien-1-yl)-3,3-dimethyl-*3H*-indol-1-ium iodide (46)

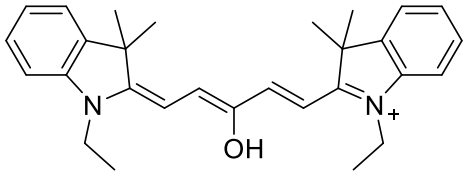

Chemical Formula: $C_{29}H_{35}N_2O^+$
Exact Mass: 427.27

A mixture of indolium iodide **10** (0.3 mmol, 95 mg), 2-hydroxymalonaldehyde **39** (0.14 mmol, 10 mg), and pyridine (0.05 mmol, 4 µl) in a mixture of *n*-BuOH-toluene 1:1 (1 ml) was heated and stirred at 100 °C for 2 h. The reaction mixture was concentrated in vacuo and separated by flash chromatography on a reversed phase cartridge Interchim puriFlash™. 73 mg (94% yield) of dye **46** was isolated as a greenish-blue solid.

^{1}H NMR (400 MHz, CD_3CN) δ 7.51 – 7.44 (m, 2H), 7.40 (td, *J* = 7.8, 1.4 Hz, 4H), 7.22 (d, *J* = 8.6 Hz, 4H), 6.40 (d, *J* = 14.0 Hz, 2H), 4.15 – 4.02 (m, 4H), 1.69 (s, 12H), 1.35 (t, *J* = 7.2 Hz, 6H).

ESI-HRMS: found 427.2749 $[M]^+$, calculated 427.2744 for $C_{29}H_{35}N_2O^+$.

λ_{max} (absorption) 667 nm (ε = 190 000 $M^{-1}cm^{-1}$, MeCN), λ_{max} (emission) 692 nm (MeCN, excitation at 650 nm); Stokes shift 25 nm; fluorescence lifetime 0.26 ns (MeCN), fluorescence quantum yield 0.14 (absolute value in MeCN).

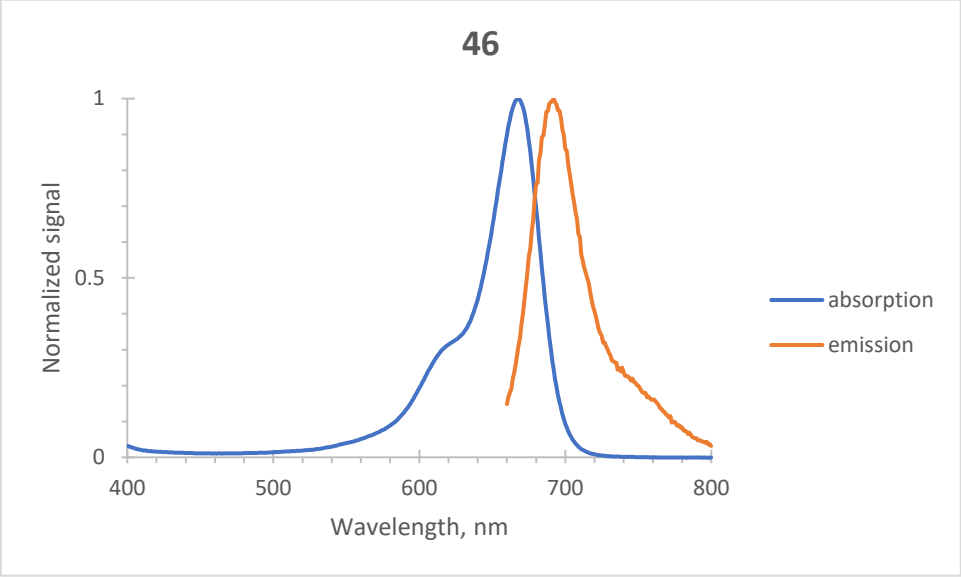

2-(3-Acetoxy-5-(1-ethyl-3,3-dimethylindolin-2-ylidene)penta-1,3-dien-1-yl)-1-ethyl-3,3-dimethyl-*3H*-indol-1-ium iodide (47)

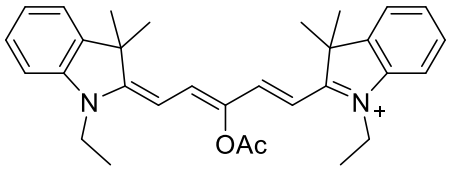

Chemical Formula: $C_{31}H_{37}N_2O_2^+$
Exact Mass: 469.28

A mixture of indolium iodide **10** (0.3 mmol, 95 mg), 2-hydroxymalonaldehyde **39** (0.14 mmol, 10 mg), and sodium acetate (0.2 mmol, 17 mg) in acetic anhydride (1 ml) was heated and stirred at 100 °C for 1 h. The dye was precipitated by addition of diethyl ether and purified by flash chromatography on a reversed phase cartridge Interchim puriFlash™. 72 mg (86% yield) of dye **47** was isolated as a blue solid.

^{1}H NMR (400 MHz, CD_3CN) δ 7.81 (d, *J* = 14.1 Hz, 2H), 7.52 – 7.46 (m, 2H), 7.41 (td, *J* = 7.6, 7.0, 0.9 Hz, 2H), 7.31 – 7.25 (m, 4H), 5.85 (d, *J* = 14.1 Hz, 2H), 4.08 (q, *J* = 7.3 Hz, 4H), 2.43 (s, 3H), 1.66 (s, 12H), 1.30 (t, *J* = 7.2 Hz, 6H).

^{13}C NMR (101 MHz, CD_3CN) δ 173.9, 169.5, 142.8, 142.1, 139.5, 129.1, 126.0, 122.8, 111.6, 97.2, 50.0, 39.7, 26.8, 20.4, 11.9.

ESI-HRMS: found 456.2644 $[M]^+$, calculated 456.2646 for $C_{29}H_{34}N_3O_2^+$.

λ_{max} (absorption) 642 nm (ε = 176 000 $M^{-1}cm^{-1}$, MeCN), λ_{max} (emission) 663 nm (MeCN, excitation at 630 nm); Stokes shift 21 nm; fluorescence lifetime 0.31 ns (MeCN), fluorescence quantum yield 0.11 (absolute value in MeCN).

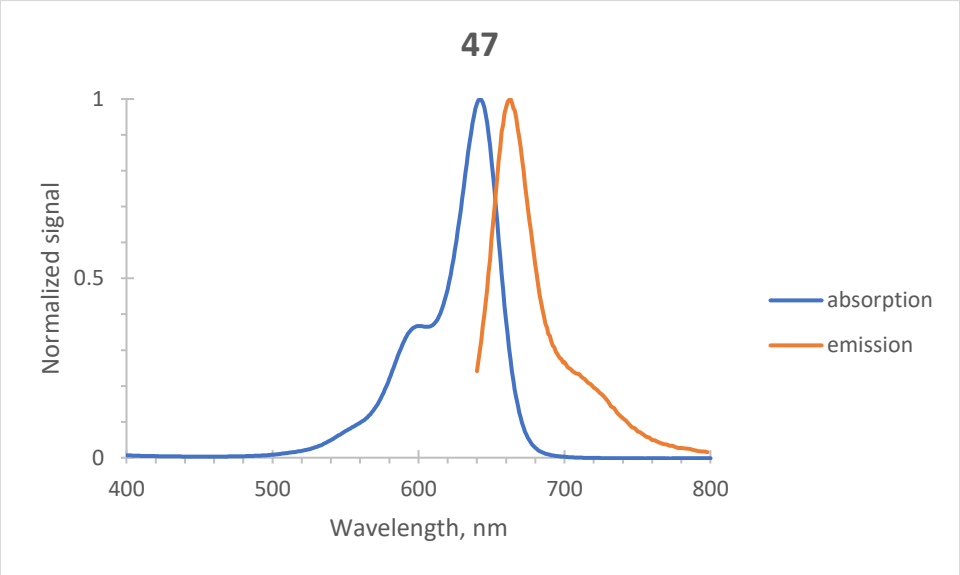

Attempted reduction of the meso nitro-substituted Cy5 derivatives (f, Scheme 24):

a) Dye **43** (0.05 mmol, 30 mg), activated charcoal (100 mg), $FeCl_3$*$6H_2O$ (0.037 mmol, 10 mg) were suspended in MeOH (8 ml) under argon and stirred at 50 ˚C for 10 min. Then, hydrazine hydrate (1 ml) was added dropwise. The colour of the reaction mixture changed to bright red. The reaction mixture was refluxed for 2 h. Then the mixture was cooled down, filtered through Celite, and analysed by LCMS. Unidentified compounds were detected; none of them corresponded to the desired aminosubstituted Cy5.

b) An oven-dried Schlenk flask was evacuated and backfilled with argon. Dye **43** (0.025 mmol, 15 mg), and Pd/C (15 mg) were dissolved in MeOH (5 ml) and placed into the Schlenck flask under Ar. The Schlenck flask was filled with H_2 and the reaction mixture stirred at r.t.

overnight. The bright violet-blue colour of **43** disappeared. On the next day the colourless solution was filtered through Celite, and analysed by LCMS. A number of products was detected; none of them corresponded to the desired aminosubstituted Cy5.

Attempted cleavage of the trifluoroacetyl group (Scheme 25):

To a solution of **44** (7 mg, 0.01 mmol) in 500 µl of MeCN, 50 µl of 3.0 M solution of aq. NaOH were added. The reaction mixture was stirred at r.t. for 1 h. No visible changes were observed, except for the formation of a precipitate. The reaction mixture was stirred overnight at r.t., and the greenish solition analysed by LCMS (Figure 16). The decomposition products with fragments of the Cy5 chromophore were detected; no desired product obtained. No reaction was observed with aq. Na_2CO_3 and NH_3.

4.2.2.4 Introduction of the diazoketone moiety to the *Intermezzo* dye

2-(3-(2-Carboxyphenyl)-5-(1-ethyl-3,3-dimethylindolin-2-ylidene)penta-1,3-dien-1-yl)-1-ethyl-3,3-dimethyl-3H-indol-1-ium iodide (49)

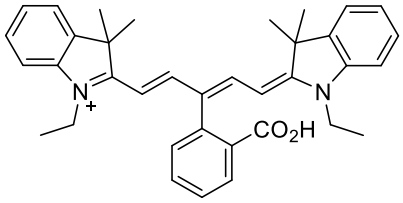

Chemical Formula:
$C_{36}H_{39}N_2O_2^+$
Exact Mass: 531.30

An oven-dried Schlenk tube was charged with $Pd(dppf)Cl_2$ (2 mg, 2.7 µmol, 10 mol %), PPh_3 (10 mg, 0.04 mmol), **29c** (20 mg, 0.03 mmol), Cs_2CO_3 (37 mg, 0.11 mmol), arylboronic acid (0.9 mmol, 15 mg). The Schlenk tube was evacuated, backfilled with argon (this sequence was repeated three times), and 2 ml of 5% aq. 1,4-dioxane were added. The reaction mixture was stirred overnight at 60 ˚C. The reaction progress was monitored by LCMS (product **49**, t_R 5.4 min, λ_{abs} 639 nm, ESI M^+ 531; starting material **29c**, t_R 7.0 min, λ_{abs} 639 nm, ESI M^+ 489;), and the product isolated on a reversed phase cartridge Interchim puriFlash™. Yield 7 mg (35%), blue solid.

^{1}H NMR (400 MHz, CD_3CN) δ 8.16 (d, *J* = 14.1 Hz, 2H), 8.09 (dd, *J* = 7.8, 1.4 Hz, 1H), 7.71 (td, *J* = 7.5, 1.4 Hz, 1H), 7.59 (td, *J* = 7.6, 1.3 Hz, 1H), 7.48 (dd, *J* = 7.5, 1.2 Hz, 2H), 7.37 (td, *J* = 7.7, 1.2 Hz, 2H), 7.28 – 7.22 (m, 3H), 7.16 (dd, *J* = 8.0, 0.8 Hz, 2H), 5.51 (d, *J* = 14.1 Hz, 2H), 3.72 (qd, *J* = 7.2, 1.9 Hz, 4H), 1.72 (s, 12H), 1.08 (t, *J* = 7.2 Hz, 6H).

^{13}C NMR (101 MHz, CD_3CN) δ 173.7, 168.4, 142.8, 142.4, 133.5, 133.3, 132.8, 131.6, 129.4, 129.3, 126.0, 123.2, 111.6, 101.7, 50.2, 39.8, 27.6, 27.5, 12.1.

ESI-HRMS: found 531.3006 $[M]^+$, calculated 531.3006 for $C_{36}H_{39}N_2O_2^+$.

λ_{max} (absorption) 640 nm (ε = 168 000 $M^{-1}cm^{-1}$, MeCN), λ_{max} (emission) 664 nm (MeCN, excitation at 640 nm); Stokes shift 24 nm; fluorescence lifetime 0.26 ns (MeCN), fluorescence quantum yield 0.11 (absolute value in MeCN).

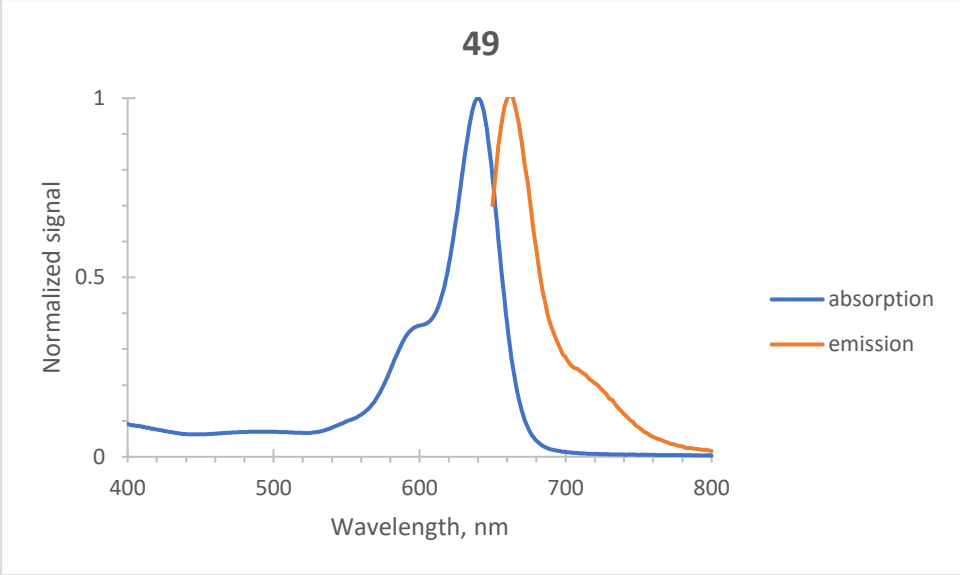

Activation of the carboxylic acid followed by reaction with diazomethane (Scheme 26):

Dye **49** (13 mg, 0.02 mmol), and *N*-methylmorpholine (5µl, 0.044 mmol) were dissolved in 1 ml of dry THF at 0 ˚C (ice bath). Precooled ethyl chloroformate (4 µl, 0.042 mmol) was added and the reaction mixture was stirred at 0 ˚C for 1 h. A solution of diazomethane in Et_2O (0.47 M, 3×50 µl) was added within 1 h. The reaction mixture turned green after 1st addition, and then brown. The reaction progress was monitored by LCMS (Figure 36). The reaction mixture was concentrated in vacuo and separated by flash chromatography on a reversed phase cartridge Interchim puriFlash™. 1 mg of the product was isolated and analysed by LCMS (Figure 37) and ESI-HRMS.

ESI-HRMS: found 527.3047 $[M]^+$, calculated 527.3057 for $C_{37}H_{39}N_2O^+$.

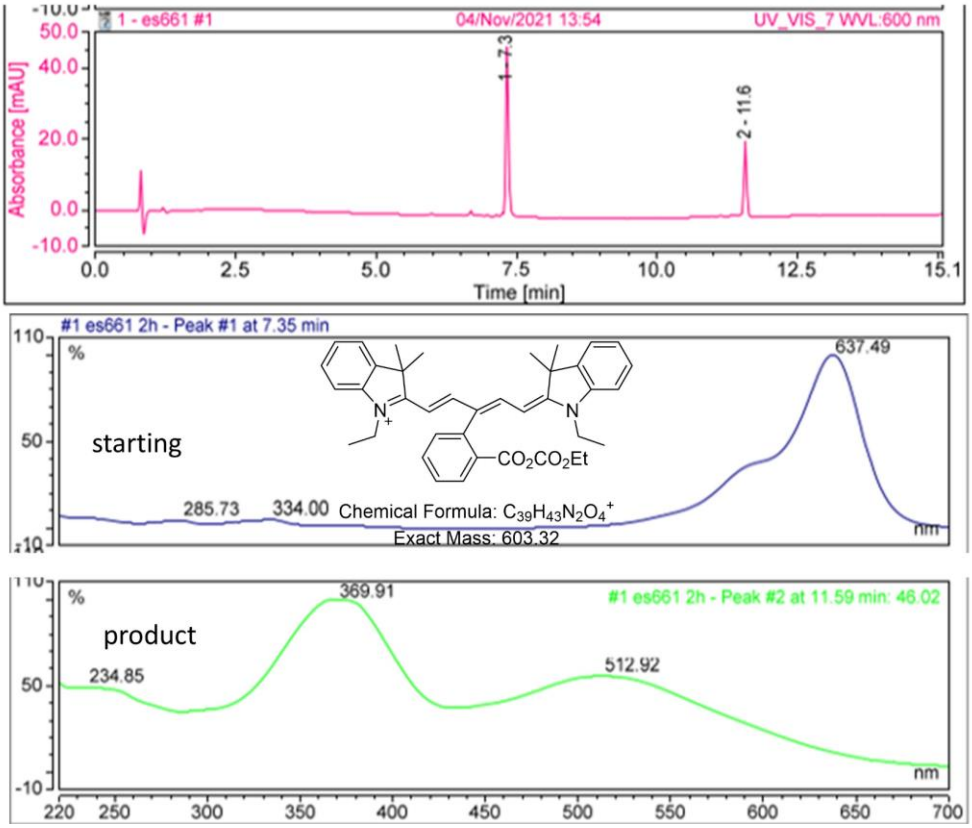

Figure 36. LCMS traces after diazomethane addition

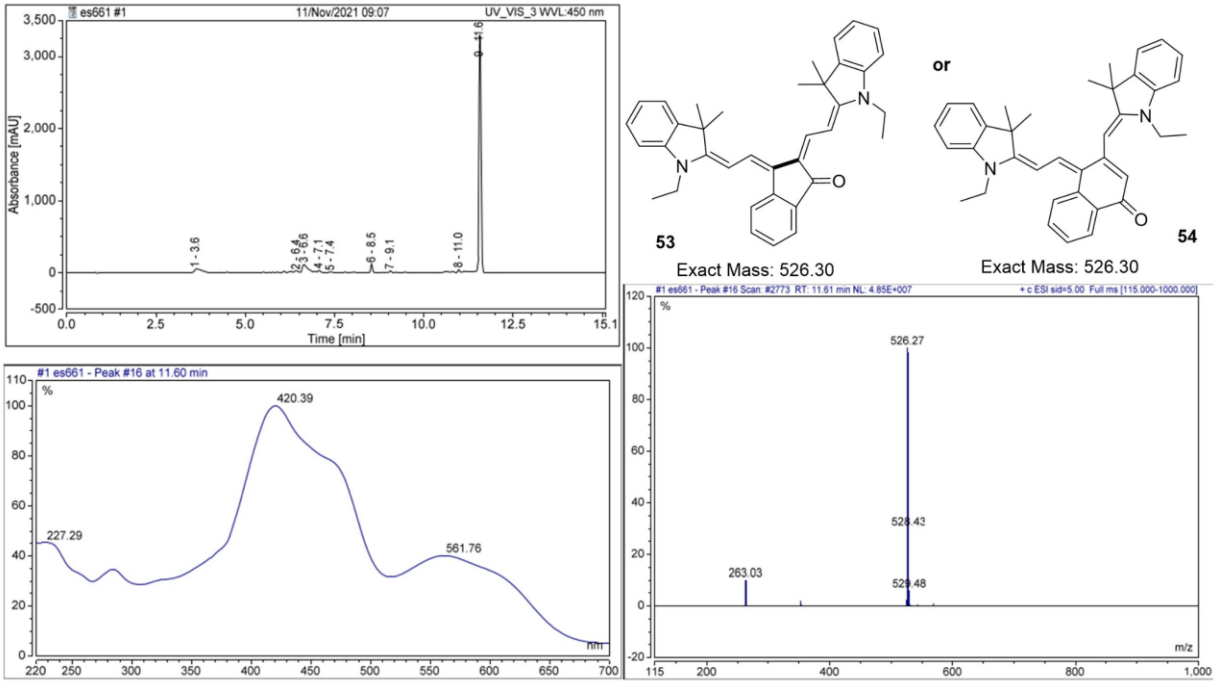

Figure 37. LCMS traces of isolated compound.

2.3.4 Synthesis and properties of squarylium dyes

1-Ethyl-2-((3-((1-ethyl-3,3-dimethylindolin-2-ylidene)methyl)-2-hydroxy-4-oxocyclobut-2-en-1-ylidene)methyl)-3,3-dimethyl-*3H*-indol-1-ium iodide (55)

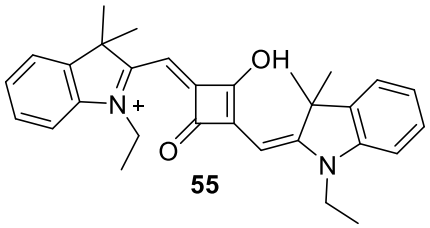

55

Chemical Formula: $C_{30}H_{33}N_2O_2^+$
Exact Mass: 453.25

Indolium iodide **10** (65 mg, 0.2 mmol) and squaric acid (11 mg, 0.1 mmol) were dissolved in 2 ml of an *n*-butanol – toluene 1:1 mixture. The reaction mixture was stirred for 1 h at 120 ˚C. The solvents were removed under reduced pressure, and the residue submitted to flash chromatography on *Isolera™ One* system (SNAP Ultra cartridge, 25 g SiO_2, DCM/MeOH with 1-10 % MeOH gradient over 5 CV) to provide compound **55** as a dark blue solid (47 mg, 81% yield).

^{1}H NMR (400 MHz, $CDCl_3$) δ 7.37 (dd, *J* = 7.4, 1.2 Hz, 2H), 7.33 (td, *J* = 7.7, 1.2 Hz, 2H), 7.18 (td, *J* = 7.4, 0.9 Hz, 2H), 7.03 (d, *J* = 7.9 Hz, 2H), 6.01 (s, 2H), 4.10 (q, *J* = 7.2 Hz, 4H), 1.78 (s, 12H), 1.40 (t, *J* = 7.2 Hz, 6H).

ESI-HRMS: found 453.2533 $[M]^+$, calculated 453.2537 for $C_{30}H_{33}N_2O_2^+$.

λ_{max} (absorption) 631 nm (ε = 210 000 $M^{-1}cm^{-1}$, MeCN), λ_{max} (emission) 644 nm (MeCN, excitation at 640 nm); Stokes shift 13 nm; fluorescence lifetime 0.21 ns (MeCN), fluorescence quantum yield 0.08 (absolute value in MeCN).

2-((2-Chloro-3-((1-ethyl-3,3-dimethylindolin-2-ylidene)methyl)-4-oxocyclobut-2-en-1-ylidene)methyl)-1-ethyl-3,3-dimethyl-*3H*-indol-1-ium iodide (56)

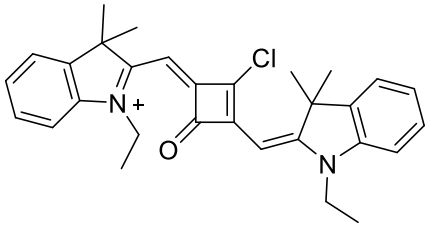

Chemical Formula: $C_{30}H_{32}ClN_2O^+$
Exact Mass: 471.22

Squarylium dye **55** (0.05 mmol, 30 mg), a drop of Et_3N and $POCl_3$ (200 µl) were dissolved in 1,4-dioxane (2 ml) under argon, and the reaction mixture was refluxed for 4 h. No colour change was observed. The reaction mixture was concentrated in vacuo, and the residue analysed by LCMS and ESI-HRMS. Analytical LCMS: full conversion to compound **55** was detected: compound **56**

t_R 6.8 min, λ_{abs} 607 nm, ESI M^+ 471.40 (starting compound **55** t_R 8.0. min, λ_{abs} 625 nm, ESI M^+ 453.33). Compound is unstable and undergoes hydrolysis to the educt **55**. It was used in the next step without further purification.

ESI-HRMS: found 471.2199 $[M]^+$, calculated 471.2198 for $C_{30}H_{32}N_2OCl^+$.

2-((2-((3-(tert-Butoxy)-3-oxopropyl)amino)-3-((1-ethyl-3,3-dimethylindolin-2-ylidene)methyl)-4-oxocyclobut-2-en-1-ylidene)methyl)-1-ethyl-3,3-dimethyl-*3H*-indol-1-ium iodide (57)

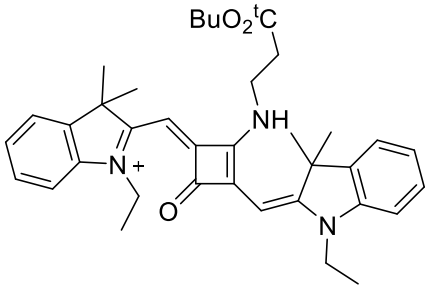

Chemical Formula: $C_{37}H_{46}N_3O_3^+$
Exact Mass: 580.35

Chloride **56** (35 mg, 0.05 mmol) and Et_3N (100 µl, 0.7 mmol) were dissolved in MeCN (3 ml). Then, β-alanine *t*-butyl ester hydrochloride (2 eq, 19 mg, 0.1 mmol) and K_2CO_3 (2.2 eq, 16 mg, 0.12 mmol), were added and the reaction mixture stirred at r.t.. The reaction progress was monitored by LCMS; full conversion to compound **57** was detected after 15 min (product **57** t_R 7.7 min, λ_{abs} 642 nm, ESI M^+ 580; starting material **56** t_R 6.8 min, λ_{abs} 607 nm, ESI M^+ 471). The solvents were removed under reduced pressure, and the residue was purified by flash chromatography on a reversed phase cartridge Interchim puriFlash™. 16 mg (45% yield) of dye **57** was isolated as a blue solid.

^{1}H NMR (400 MHz, $CDCl_3$) δ 7.42 – 7.30 (m, 4H), 7.28 – 7.22 (m, 1H), 7.21 – 7.12 (m, 2H), 7.00 (d, *J* = 7.9 Hz, 1H), 6.80 (s, 1H), 5.94 (s, 1H), 4.57 (q, *J* = 7.3 Hz, 2H), 4.05 (dq, *J* = 21.6, 7.1 Hz, 4H), 2.96 – 2.86 (m, 2H), 1.76 (d, *J* = 5.3 Hz, 12H), 1.48 (t, *J* = 7.1 Hz, 3H), 1.45 (s, 10H), 1.36 (t, *J* = 7.2 Hz, 4H).

^{13}C NMR (101 MHz, $CDCl_3$) δ 174.3, 173.5, 170.7, 169.9, 168.6, 163.3, 157.5, 143.2, 142.0, 141.7, 141.3, 128.2, 128.0, 125.6, 123.9, 122.2, 111.1, 109.3, 90.8, 87.6, 81.1, 54.1, 50.1, 49.2, 40.4, 40.2, 38.7, 36.9, 28.1, 26.9, 26.0, 13.0, 12.0, 1.9.

ESI-HRMS: found 580.3538 $[M]^+$, calculated 580.3534 for $C_{37}H_{46}N_3O_3^+$.

λ_{max} (absorption) 643 nm (ε = 150 000 $M^{-1}cm^{-1}$, MeCN), λ_{max} (emission) 659 nm (MeCN, excitation at 640 nm); Stokes shift 16 nm; fluorescence quantum yield 0 (absolute value in MeCN).

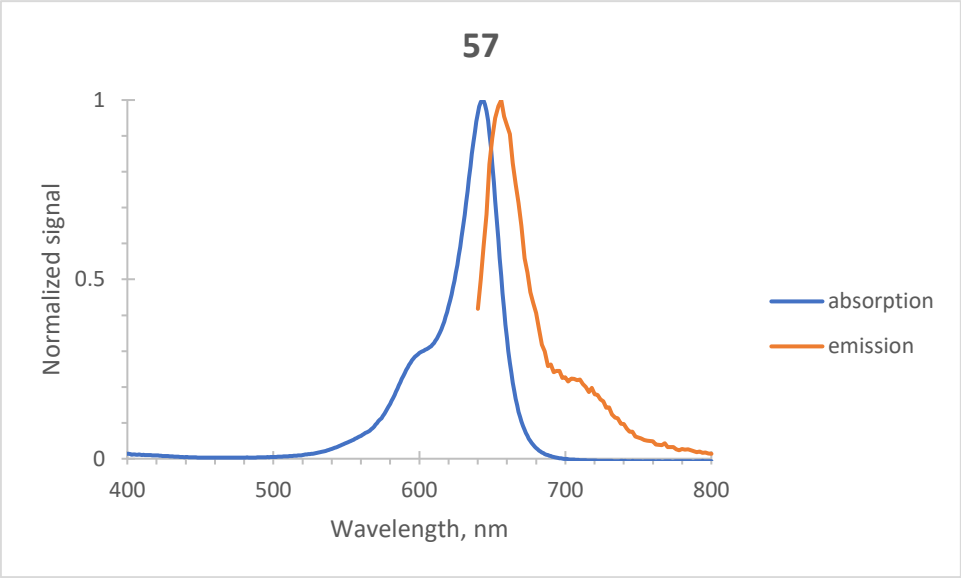

2-((2-((4-Diazo-3-oxobutyl)amino)-3-((1-ethyl-3,3-dimethylindolin-2-ylidene)methyl)-4-oxocyclobut-2-en-1-ylidene)methyl)-1-ethyl-3,3-dimethyl-*3H*-indol-1-ium iodide (58)

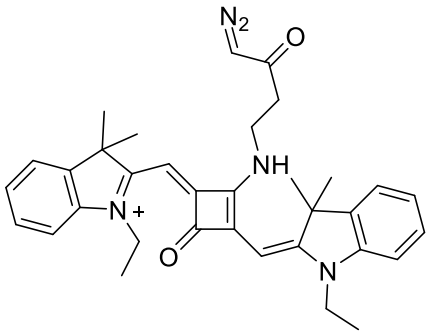

Chemical Formula: $C_{34}H_{38}N_5O_2^+$
Exact Mass: 548.30

Et_3N (0.15 mmol, 21 µl), chloride **56** (30 mg, 0.05 mmol) were dissolved in MeCN (2 ml) and were added dropwise to the solution of **DAK**. The reaction mixture was stirred at r.t., and the progress was monitored by HPLC; full conversion to compound **58** was achieved in 30 min (product **58** t_R 6.7 min, λ_{abs} 643 nm, ESI M^+ 548; starting material **56** t_R 6.8 min, λ_{abs} 607 nm, ESI M^+ 471). The solvents were removed under reduced pressure, and the residue purified by flash chromatography on a reversed phase cartridge Interchim puriFlash™. 5 mg (15% yield) of dye **58** was isolated as a blue solid.

^{1}H NMR (400 MHz, CD_3CN) δ 7.54 – 7.17 (m, 8H), 6.49 (s, 1H), 5.98 (s, 1H), 5.83 (s, 1H) 4.34 (d, *J* = 7.5 Hz, 2H), 4.12 (d, *J* = 7.9 Hz, 2H), 4.03 (t, *J* = 7.0 Hz, 2H), 2.93 (d, *J* = 8.0 Hz, 2H), 1.72 (s, 12H), 1.38 – 1.28 (m, 6H)

ESI-HRMS: found 548.3022 $[M]^+$, calculated 548.3020 for $C_{34}H_{38}N_5O_2^+$.

λ_{max} (absorption) 643 nm (ε = 150 000 $M^{-1}cm^{-1}$, MeCN), λ_{max} (emission) 659 nm (MeCN, excitation at 640 nm); Stokes shift 16 nm; fluorescence quantum yield 0 (absolute value in MeCN).

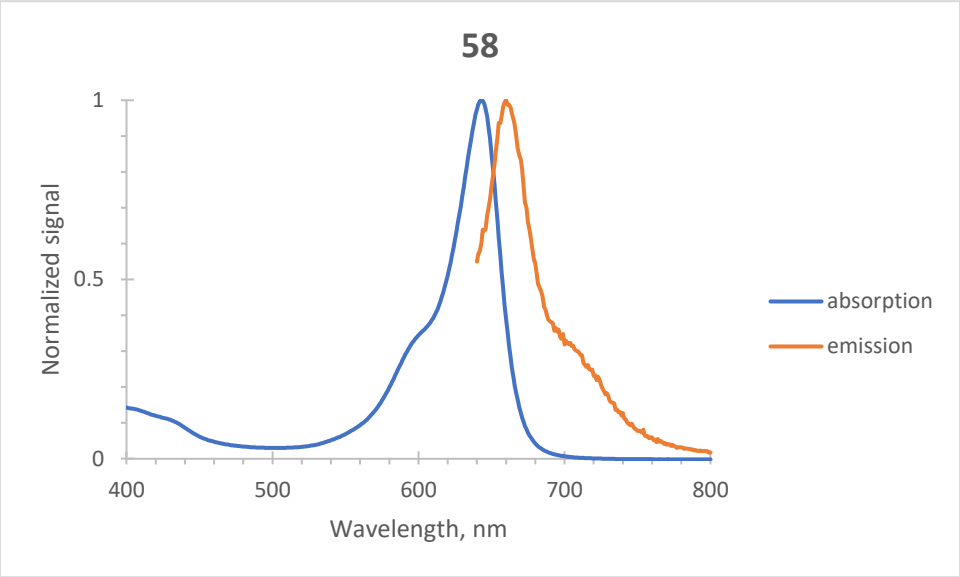

4.2.3 To Chapter 3

4.2.3.1 Oxidative olefination of rhodamines

Synthesis of substrates for C–H activation:

***N,N'*-(3-oxo-3H-spiro[isobenzofuran-1,9'-xanthene]-3',6'-diyl)diacetamide (62)** [15]

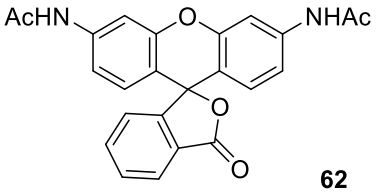

62

Chemical Formula:
$C_{24}H_{18}N_2O_5$
Exact Mass: 414.12

To a solution of rhodamine 110 (250 mg, 0.68 mmol) in 8 mL of dichloromethane, acetic anhydride (150 µl, 2.2 eq., 1.58 mmol) and pyridine (250 µl, 3 mmol) were added. The mixture was stirred at r.t. until the reaction was completed (approx. 2 h), the reaction progress was monitored by TLC (R_f 0.15 in hexane/EtOAc 1:1). Upon completion, the reaction mixture was quenched by the addition of 5 mL of saturated aqueous sodium bicarbonate. The organics were extracted with EtOAc (3 x 20 mL), and dried over $MgSO_4$. The solvents were removed under reduced pressure, and the residue was purified by flash chromatography on *Isolera™ One* system (SNAP Ultra cartridge, 50 g SiO_2, hexane/EtOAc with 20-100 % EtOAc gradient over 5 CV) to to obtain *N,N'*-bis-acetyl rhodamine **62** (240 mg, 85% yield).

^{1}H NMR (400 MHz, DMSO-d_6) δ 7.97 (dt, *J* = 7.5, 1.0 Hz, 1H), 7.80 (d, *J* = 2.0 Hz, 2H), 7.74 (td, *J* = 7.5, 1.3 Hz, 1H), 7.67 (td, *J* = 7.5, 1.1 Hz, 1H), 7.20 (dt, *J* = 7.6, 1.0 Hz, 1H), 7.13 (ddd, *J* = 8.7, 2.1, 0.9 Hz, 2H), 6.67 (d, *J* = 8.7 Hz, 2H), 2.05 (s, 6H).

***N,N'*-(3-oxo-3H-spiro[isobenzofuran-1,9'-xanthene]-3',6'-diyl)di(trifluoro)acetamide (66)** [15]

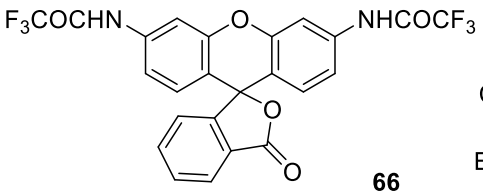

66

Chemical Formula:
$C_{24}H_{18}N_2O_5$
Exact Mass: 414.12

To a solution of rhodamine 110 (250 mg, 0.68 mmol) in 12 mL of DMF, NaH (60% suspension in oil, 125 mg, 3.2 mmol) was added in portions. The mixture was stirred at r.t. for 30 min. Then, trifluoroacetic anhydride (4 eq., 390 µl, 2.8 mmol) was added dropwise and the reaction mixture was stirred at r.t. overnight. The reaction progress was analysed by TLC (R_f 0.4 in hexane/EtOAc 1:1). The reaction mixture was diluted with EtOAc (50 mL), washed with water, followed by brine. The separated organic layer was dried over $MgSO_4$. The solvents were removed under reduced pressure, and the residue was purified by flash chromatography on *Isolera™ One* system (SNAP Ultra cartridge, 50 g SiO_2, hexane/EtOAc with 20-100 % EtOAc gradient over 5 CV) to to obtain *N,N'*-bis-trifluoroacetyl rhodamine **66** (242 mg, 68% yield).

^{1}H NMR (400 MHz, Methanol-d_4) δ 9.29 (dt, *J* = 7.5, 1.0 Hz, 1H), 9.21 (d, *J* = 2.1 Hz, 2H), 9.09 (td, *J* = 7.4, 1.3 Hz, 1H), 9.02 (td, *J* = 7.5, 1.0 Hz, 1H), 8.70 (dd, *J* = 8.7, 2.2 Hz, 2H), 8.62 (dt, *J* = 7.6, 1.0 Hz, 1H), 8.20 (d, *J* = 8.7 Hz, 2H).

*General procedure for optimisation study for Ru-catalysed oxidative olefination of **62** (Scheme 34, Table 8):*

A mixture of *N,N'*-bis-acetyl rhodamine **62** (84 mg, 0.2 mmol), $[RuCl_2(p\text{-cymene})]_2$ (12 mg, 10 mol %), additive (0.04 mmol, 20 mol %), oxidant (1 eq., 0.2 mmol), and ethyl acrylate (1.5 eq., 33 µl, 0.3 mmol), in solvent (2 mL) was stirred at mentioned temperature under Ar (on air) for 20 h. The reaction progress was monitored by LCMS (starting material **62**, t_R 4.7 min, λ_{abs} 283 nm, ESI M^+ 415; products **63a (trans)** t_R 5.3 min, λ_{abs} 289 nm, ESI M^+ 513; **63b (cis)** t_R 4.9 min, λ_{abs} 285 nm, ESI M^+ 513; **63b (trans)** t_R 5.2 min, λ_{abs} 285 nm, ESI M^+ 513; **64a** t_R 6.0 min, λ_{abs} 315 nm, ESI M^+ 609; **64b** t_R 5.84 min, λ_{abs} 300 nm, ESI M^+ 611; **64c** t_R 5.77 min, λ_{abs} 284 nm, ESI M^+ 611; **65a** t_R 6.1 min, λ_{abs} 311 nm, ESI M^+ 709; **65b** t_R 6.3 min, λ_{abs} 316 nm, ESI M^+ 709). The conversion was estimated by integrating peak areas of all peaks associated with rhodamine (sum of peak areas taken as 100%).

Isolation and characterization of individual compounds:

After cooling down to r.t., the reaction mixture was diluted with H_2O (50 mL) and extracted with EtOAc (3 x 50 mL). The combined organic phase was washed with brine and dried over

anhydrous $MgSO_4$. After filtration and evaporation of the solvents under reduced pressure, the individual regioisomers **63-65** were isolated on Interchim puriFlash™ with a 250 × 21.2 mm column (Knauer Eurosphere II 100-5 C18A) from Knauer GmbH. Solvent A: H_2O + 0.05% v/v TFA; solvent B: MeCN + 0.05% v/v TFA. Gradient A/B: 80/20–0/100 (0–20 min), flow rate 18 mL/min, 22°C; detection at 254 nm.

Ethyl-(*E*)-3-(3',6'-diacetamido-3-oxo-3H-spiro[isobenzofuran-1,9'-xanthen]-2'-yl) acrylate (63a)

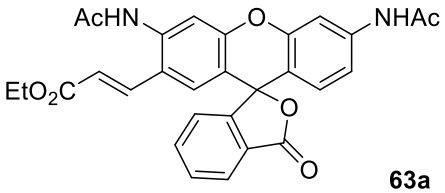

63a

Chemical Formula:
$C_{29}H_{24}N_2O_7$
Exact Mass: 512.16

^{1}H NMR (400 MHz, DMSO-d_6) δ 10.25 (s, 1H), 10.01 (s, 1H) 8.03 (ddd, *J* = 7.2, 1.4, 0.8 Hz, 1H), 7.86 (d, *J* = 2.1 Hz, 1H), 7.78 – 7.72 (m, 2H), 7.68 (d, *J* = 15.8 Hz, 1H), 7.63 (s, 1H), 7.30 (dt, *J* = 7.5, 0.9 Hz, 1H), 7.26 (s, 1H), 7.14 (dd, *J* = 8.7, 2.1 Hz, 1H), 6.69 (d, *J* = 8.7 Hz, 1H), 6.26 (d, *J* = 15.8 Hz, 1H), 4.12 (q, *J* = 7.1 Hz, 2H), 2.13 (s, 3H), 2.07 (s, 3H), 1.20 (t, *J* = 7.1 Hz, 3H).

^{13}C NMR (126 MHz, DMSO-d_6) δ 169.0, 168.7, 166.1, 152.3, 151.6, 150.3, 141.5, 139.1, 138.6, 135.6, 130.2, 128.2, 127.1, 125.8, 125.0, 124.1, 123.8, 118.9, 116.1, 115.4, 113.1, 106.1, 81.1, 60.0, 24.1, 14.2.

ESI-HRMS: found 513.1661 $[M]^+$, calculated 513.1656 for $C_{29}H_{25}N_2O_7$, $[M+H^+]$.

Ethyl-(*E*)-3-(3',6'-diacetamido-3-oxo-3H-spiro[isobenzofuran-1,9'-xanthen]-4'-yl) acrylate (63b)

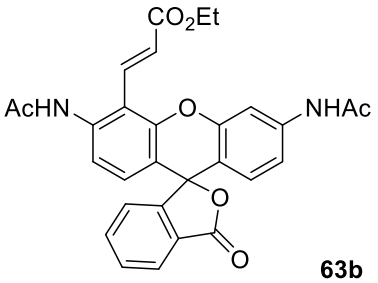

63b

Chemical Formula:
$C_{29}H_{24}N_2O_7$
Exact Mass: 512.16

^{1}H NMR (600 MHz, DMSO-d_6) δ 10.29 (s, 1H), 10.00 (s, 1H), 8.04 (dt, *J* = 7.6, 1.0 Hz, 1H), 7.84 (d, *J* = 2.1 Hz, 1H), 7.81 (td, *J* = 7.5, 1.2 Hz, 1H), 7.79 (d, *J* = 16.3 Hz, 1H), 7.75 (td, *J* = 7.5, 1.0 Hz, 1H), 7.37 (dt, *J* = 7.7, 0.9 Hz, 1H), 7.26 (dd, *J* = 8.7, 2.1 Hz, 1H), 7.20 (d, *J* = 8.6

Hz, 1H), 6.92 (d, *J* = 16.3 Hz, 1H), 6.82 (d, *J* = 8.6 Hz, 1H), 6.77 (d, *J* = 8.7 Hz, 1H), 4.28 (q, *J* = 7.1 Hz, 2H), 2.09 (s, 3H), 2.07 (s, 3H), 1.32 (t, *J* = 7.1 Hz, 3H).

^{13}C NMR (126 MHz, DMSO-d_6) δ 169.0, 168.5, 166.5, 152.3, 150.2, 149.5, 141.6, 139.6, 135.9, 135.7, 130.4, 129.1, 128.3, 125.5, 124.9, 124.1, 123.3, 117.0, 116.1, 115.7, 112.5, 105.9, 81.6, 60.3, 24.1, 14.3.

ESI-HRMS: found 513.1649 $[M]^+$, calculated 513.1656 for $C_{29}H_{25}N_2O_7$, $[M+H^+]$.

Ethyl-(*Z*)-3-(3',6'-diacetamido-3-oxo-3H-spiro[isobenzofuran-1,9'-xanthen]-4'-yl) acrylate (63b-cis)

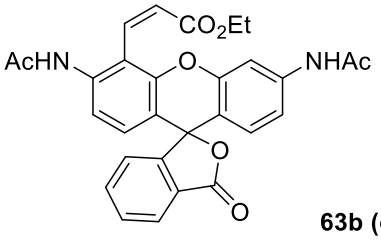

63b (cis)

Chemical Formula:
$C_{29}H_{24}N_2O_7$
Exact Mass: 512.16

^{1}H NMR (400 MHz, DMSO-d_6) δ 10.22 (s, 1H), 9.51 (s, 1H), 8.03 (d, *J* = 7.6 Hz, 1H), 7.84 – 7.70 (m, 2H), 7.76 (d, *J* = 2.1 Hz, 1H), 7.32 (d, *J* = 8.8 Hz, 1H), 7.24 (d, *J* = 7.6 Hz, 1H), 7.11 (dd, *J* = 8.6, 2.1 Hz, 1H), 7.05 (d, *J* = 12.0 Hz, 1H), 6.73 (d, *J* = 8.7 Hz, 1H), 6.71 (d, *J* = 8.6 Hz, 1H), 6.36 (d, *J* = 12.0 Hz, 1H), 3.91 (qd, *J* = 7.1, 2.4 Hz, 2H), 2.06 (s, 3H), 2.02 (s, 3H), 0.98 (t, *J* = 7.1 Hz, 3H).

ESI-HRMS: found 513.1634 $[M]^+$, calculated 513.1656 for $C_{29}H_{25}N_2O_7$, $[M+H^+]$.

Diethyl 3,3'-(3',6'-diacetamido-3-oxo-3H-spiro[isobenzofuran-1,9'-xanthene]-2',7'-diyl) (*2E,2'E*)-diacrylate (64a)

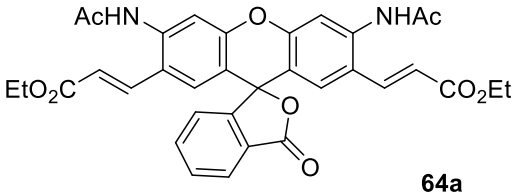

64a

Chemical Formula:
$C_{34}H_{30}N_2O_9$
Exact Mass: 610.20

^{1}H NMR (400 MHz, DMSO-d_6) δ 10.02 (s, 2H), 8.08 – 8.04 (m, 1H), 7.80 – 7.72 (m, 2H), 7.69 (d, *J* = 15.8 Hz, 2H), 7.67 (s, 2H), 7.38 – 7.32 (m, 1H), 7.20 (s, 2H), 6.23 (d, *J* = 15.8 Hz, 2H), 4.13 (q, *J* = 7.1 Hz, 4H), 2.13 (s, 6H), 1.20 (t, *J* = 7.1 Hz, 6H).

ESI-HRMS: found 611.2014 $[M]^+$, calculated 611.2024 for $C_{34}H_{31}N_2O_9$, $[M+H^+]$.

Diethyl 3,3'-(3',6'-diacetamido-3-oxo-3H-spiro[isobenzofuran-1,9'-xanthene]-2',5'-diyl) (*2E,2'E*)-diacrylate (64b)

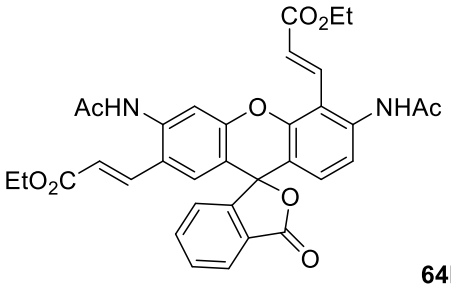

64b

Chemical Formula:
$C_{34}H_{30}N_2O_9$
Exact Mass: 610.20

^{1}H NMR (400 MHz, DMSO-d_6) δ 10.04 (s, 1H), 9.99 (s, 1H), 8.05 (dd, *J* = 7.2, 2.0 Hz, 1H), 7.81-7.73 (m, 2H), 7.77 (d, *J* = 16.3 Hz, 1H), 7.69 (d, *J* = 16.0 Hz, 1H), 7.66 (s, 1H), 7.39 (d, *J* = 7.4 Hz, 1H), 7.33 (s, 1H), 7.22 (d, *J* = 8.7 Hz, 1H), 6.88 (d, *J* = 16.3 Hz, 1H), 6.79 (d, *J* = 8.7 Hz, 1H), 6.34 (d, *J* = 15.8 Hz, 1H), 4.28 (q, *J* = 7.1 Hz, 2H), 4.13 (q, *J* = 7.1 Hz, 2H), 2.14 (s, 3H), 2.07 (s, 3H), 1.32 (t, *J* = 7.1 Hz, 3H), 1.20 (t, *J* = 7.1 Hz, 3H).

ESI-HRMS: found 611.2030 $[M]^+$, calculated 611.2024 for $C_{34}H_{31}N_2O_9$, $[M+H^+]$.

Diethyl 3,3'-(3',6'-diacetamido-3-oxo-3H-spiro[isobenzofuran-1,9'-xanthene]-2',4'-diyl) (*2E,2'E*)-diacrylate (64c)

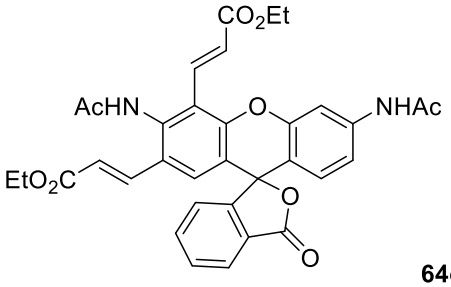

64c

Chemical Formula:
$C_{34}H_{30}N_2O_9$
Exact Mass: 610.20

^{1}H NMR (600 MHz, DMSO-d_6) δ 10.30 (s, 1H), 10.11 (s, 1H), 8.05 (dt, *J* = 7.5, 1.0 Hz, 1H), 7.85 (d, *J* = 2.1 Hz, 1H), 7.80 – 7.73 (m, 2H), 7.76 (d, *J* = 16.3 Hz, 1H), 7.53 (d, *J* = 15.9 Hz, 1H), 7.42 (s, 1H), 7.39 (d, *J* = 7.4 Hz, 1H), 7.26 (dd, *J* = 8.8, 2.0 Hz, 1H), 6.91 (d, *J* = 16.4 Hz, 1H), 6.74 (d, *J* = 8.8 Hz, 1H), 6.39 (d, *J* = 16.0 Hz, 1H), 4.29 (q, *J* = 7.1 Hz, 2H), 4.12 (q, *J* = 7.0 Hz, 2H), 2.12 (s, 3H), 2.07 (s, 3H), 1.32 (t, *J* = 7.1 Hz, 3H), 1.20 (t, *J* = 7.1 Hz, 3H).

^{13}C NMR (126 MHz, DMSO-d_6) δ 169.2, 169.0, 168.6, 166.3, 165.9, 152.1, 150.5, 149.8, 141.6, 138.6, 135.7, 130.4, 128.1, 127.7, 125.7, 125.2, 124.2, 123.9, 121.0, 119.9, 118.7, 115.9, 112.9, 105.9, 80.8, 60.5, 60.1, 24.1, 22.4, 14.2, 14.1, 14.1.

ESI-HRMS: found 611.2039 $[M]^+$, calculated 611.2024 for $C_{34}H_{31}N_2O_9$, $[M+H^+]$.

Triethyl 3,3',3''-(3',6'-diacetamido-3-oxo-3H-spiro[isobenzofuran-1,9'-xanthene]-2',4',7'-triyl) *(2E,2'E,2''E)*-triacrylate (65a)

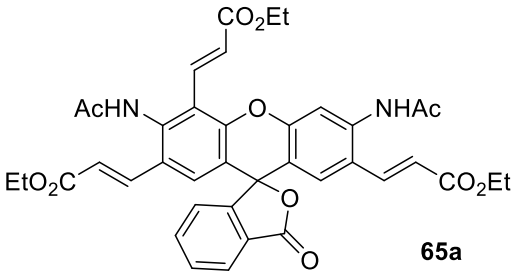

65a

Chemical Formula: $C_{39}H_{36}N_2O_{11}$
Exact Mass: 708.23

^{1}H NMR (600 MHz, DMSO-d_6) δ 10.11 (s, 1H), 10.05 (s, 1H), 8.10 – 8.06 (m, 1H), 7.80 – 7.74 (m, 2H), δ 7.74 (d, *J* = 16.3 Hz, 1H), 7.69 (d, *J* = 15.8 Hz, 2H), 7.69 (s, 1H), 7.53 (d, *J* = 15.9 Hz, 1H), 7.42 (dd, *J* = 6.7, 1.7 Hz, 1H), 7.34 (s, 1H), 7.24 (s, 1H), 6.87 (d, *J* = 16.4 Hz, 1H), 6.34 (d, *J* = 16.0 Hz, 1H), 6.27 (d, *J* = 15.8 Hz, 1H), 4.28 (q, *J* = 7.1 Hz, 2H), 4.13 (qd, *J* = 7.1, 3.9 Hz, 4H), 2.14 (s, 3H), 2.11 (s, 3H), 1.31 (t, *J* = 7.1 Hz, 3H), 1.21 (td, *J* = 7.1, 3.5 Hz, 6H).

^{13}C NMR (126 MHz, DMSO-d_6) δ 169.2, 168.5, 166.2, 165.9, 165.9, 151.9, 150.5, 149.9, 139.2, 138.5, 135.7, 135.5, 130.4, 128.4, 127.2, 126.6, 125.7, 125.5, 124.8, 124.5, 123.7, 121.3, 120.0, 119.3, 119.0, 116.1, 113.0, 80.1, 60.5, 60.2, 60.1, 22.5, 14.2, 14.1.

ESI-HRMS: found 731.2208 $[M]^+$, calculated 731.2211 for $C_{39}H_{36}N_2O_{11}Na$, $[M+Na^+]$.

Triethyl 3,3',3''-(3',6'-diacetamido-3-oxo-3H-spiro[isobenzofuran-1,9'-xanthene]-2',4',5'-triyl) *(2E,2'E,2''E)*-triacrylate (65b)

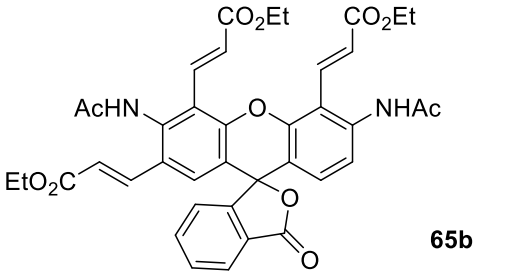

65b

Chemical Formula: $C_{39}H_{36}N_2O_{11}$
Exact Mass: 708.23

^{1}H NMR (600 MHz, DMSO-d_6) δ 10.31 (s, 1H), 10.08 (s, 1H), 8.12 – 8.08 (m, 1H), 7.86 – 7.79 (m, 2H), δ 7.84 (d, *J* = 16.3 Hz, 1H), 7.73 (d, *J* = 15.8 Hz, 2H), 7.69 (s, 1H), 7.63 (d, *J* = 15.9 Hz, 1H), 7.42 (dd, *J* = 6.7, 1.7 Hz, 1H), 7.34 (s, 1H), 7.24 (s, 1H), 7.28 (d, *J* = 16.4 Hz, 1H), 6.94

(d, *J* = 16.2 Hz, 1H), 6.37 (d, *J* = 15.8 Hz, 1H), 4.36 (qd, *J* = 7.1, 3.9 Hz, 4H), 4.26 (q, *J* = 7.1 Hz, 2H), 2.16 (s, 3H), 2.12 (s, 3H), 1.34 (td, *J* = 7.1, 3.5 Hz, 6H) 1.20 (t, *J* = 7.1 Hz, 3H).

ESI-HRMS: found 709.2386 $[M]^+$, calculated 709.2392 for $C_{39}H_{37}N_2O_{11}$, $[M+H^+]$.

*Representative Procedure for Ru-/Rh- catalysed oxidative olefination of N,N'-bis-acetyl rhodamine **62** (Schemes 35, 36):*

A mixture of *N,N'*-bis-acetyl rhodamine **62** (84 mg, 0.2 mmol), $[RuCl_2(p\text{-cymene})]_2$ or $[RhCp^*Cl_2]_2$ (12 mg, 10 mol %), $AgSbF_6$ (14 mg, 0.04 mmol, 20 mol %), $Cu(OAc)_2{}^*H_2O$ (40 mg, 1 eq., 0.2 mmol), and ethyl acrylate (0.5 eq., 11 µl, 0.1 mmol) in acetone (2 mL) was stirred at 70 ºC for 20 h. After cooling down to r.t., the reaction mixture was diluted with H_2O (50 mL) and extracted with EtOAc (3 x 50 mL). The combined organic phase was washed with brine and dried over anhydrous $MgSO_4$. After filtration and evaporation of the solvents under reduced pressure, the products **63** and starting compound **62** were isolated on an Interchim puriFlash™ with a 250 × 21.2 mm column (Knauer Eurosphere II 100-5 C18A) from Knauer GmbH. Solvent A: H_2O + 0.05% v/v TFA; solvent B: MeCN + 0.05% v/v TFA. Gradient A/B: 80/20–0/100 (0–20 min), flow rate 18 mL/min, 22°C; detection at 254 nm.

*General procedure for optimisation study for M-catalysed oxidative olefination of **66** (Scheme 38, Table 10):*

A mixture of *N,N'*-bis-(trifluoro)acetyl rhodamine **66** (110 mg, 0.2 mmol), metal catalyst (0.02 mmol, 10 mol %), additive (0.04 mmol, 20 mol %), oxidant (1 eq., 0.2 mmol), and ethyl acrylate (1.5 eq., 33 µl, 0.3 mmol), in solvent (2 mL) was stirred at mentioned temperature for 18-72 h. The reaction progress was monitored by LCMS (starting material **66**, t_R 7.3 min, λ_{abs} 301 nm, ESI M^+ 523; products **mono** t_R 7.5 min, λ_{abs} 320 nm, ESI M^+ 621; **bis** t_R 7.9 min, λ_{abs} 323 nm, ESI M^+ 719). The conversion was estimated by integrating peak areas of all peaks associated with rhodamine (sum of peak areas taken as 100%).

4.2.3.2 Synthesis and properties of new rhodamine dyes

*Deprotection of the amino groups in compounds **63-64** (Schemes 39-41):*

(*E*)-6-amino-9-(2-carboxyphenyl)-7-(3-ethoxy-3-oxoprop-1-en-1-yl)-3H-xanthen-3-iminium chloride (67)

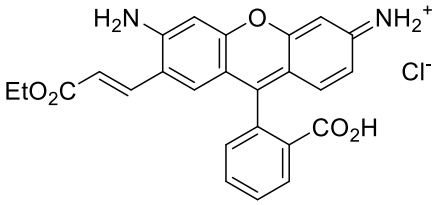

Chemical Formula: $C_{25}H_{21}N_2O_5^+$
Exact Mass: 429.14

67

To a solution of **63a** (15 mg, 0.03 mmol) in 2 ml of EtOH, 2 ml of 25% solution of aq. HCl was added. The reaction mixture was stirred at 90 ºC overnight. The reaction progress was monitored by LCMS (starting material **63a**, t_R 5.3 min, λ_{abs} 289 nm, ESI M^+ 513; products **67** t_R 4.1 min, λ_{abs} 518 nm, ESI M^+ 429). Compound **67** was isolated on an Interchim puriFlash™ with a 250 × 21.2 mm column (Knauer Eurosphere II 100-5 C18A) from Knauer GmbH. Solvent A: H_2O + 0.05% v/v TFA; solvent B: MeCN + 0.05% v/v TFA. Gradient A/B: 70/30–0/100 (0–20 min), flow rate 18 mL/min, 22°C; detection at 500 nm. Yield 29% (4 mg) of a red solid.

^{1}H NMR (400 MHz, Acetonitrile-d_3) δ 8.20 (d, *J* = 7.3 Hz, 1H), 7.84 – 7.73 (m, 2H), 7.64 (d, *J* = 15.8 Hz, 1H), 7.31 (d, *J* = 7.4 Hz, 1H), 7.11 (s, 1H), 6.89 (d, *J* = 8.6 Hz, 1H), 6.82 (s, 1H), 6.73 (s, 1H), 6.69 (d, *J* = 9.2 Hz, 1H), 6.08 (d, *J* = 15.7 Hz, 1H), 4.15 (q, *J* = 7.1 Hz, 2H), 1.23 (t, *J* = 7.1 Hz, 3H).

ESI-HRMS: found 429.1435 $[M]^+$, calculated 429.1445 for $C_{25}H_{21}N_2O_5$, $[M^+]$.

(*E*)-6-amino-9-(2-carboxyphenyl)-7-(2-carboxyvinyl)-3H-xanthen-3-iminium chloride (68)

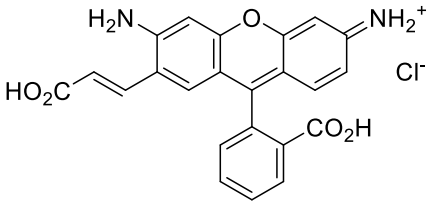

Chemical Formula: $C_{23}H_{17}N_2O_5^+$
Exact Mass: 401.11

68

To a solution of **63a** (15 mg, 0.03 mmol) in 2 ml of EtOH, 2 ml of 20% solution of aq. NaOH was added. The reaction mixture was stirred at 90 ºC overnight. The reaction progress was

monitored by LCMS (starting material **63a**, t_R 5.3 min, λ_{abs} 289 nm, ESI M^+ 513; products **68** t_R 2.8 min, λ_{abs} 518 nm, ESI M^+ 401). Compound **68** was isolated on an Interchim puriFlash™ with a 250 × 21.2 mm column (Knauer Eurosphere II 100-5 C18A) from Knauer GmbH. Solvent A: H_2O + 0.05% v/v TFA; solvent B: MeCN + 0.05% v/v TFA. Gradient A/B: 70/30–0/100 (0–20 min), flow rate 18 mL/min, 22°C; detection at 500 nm. Yield 54% (7 mg) of a red solid.

^{1}H NMR (400 MHz, Acetonitrile-d_3) δ 8.26 (dd, J = 7.4, 1.7 Hz, 1H), 7.84 – 7.73 (m, 2H), 7.64 (d, J = 15.7 Hz, 1H), 7.31 (dd, J = 7.1, 1.7 Hz, 1H), 7.20 (s, 1H), 7.03 (d, J = 9.7 Hz, 1H), 6.88 (s, 1H), 6.82 – 6.74 (m, 2H), 6.08 (d, J = 15.7 Hz, 1H).

ESI-HRMS: found 401.1128 $[M]^+$, calculated 401.1132 for $C_{23}H_{17}N_2O_5$, $[M^+]$.

λ_{max} (absorption) 518 nm (ε = 77 000 $M^{-1}cm^{-1}$, EtOH), λ_{max} (emission) 548 nm (EtOH, excitation at 510 nm); Stokes shift 30 nm; fluorescence lifetime 3.6 ns (EtOH), fluorescence quantum yield 0.88 (absolute value in EtOH).

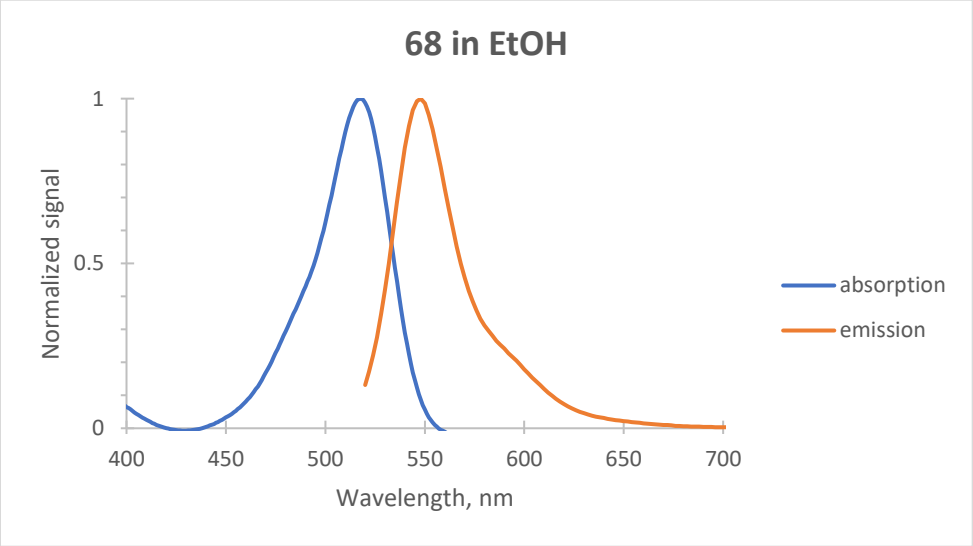

(*E*)-6-amino-9-(2-carboxyphenyl)-5-(2-carboxyvinyl)-3H-xanthen-3-iminium chloride (70)

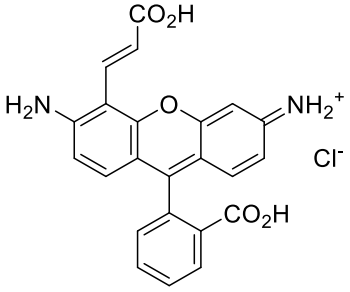

Chemical Formula: $C_{23}H_{17}N_2O_5^+$
Exact Mass: 401.11

70

To a solution of **63b** (15 mg, 0.03 mmol) in 2 ml of EtOH, 2 ml of 20% solution of aq. NaOH was added. The reaction mixture was stirred at 90 ºC overnight. The reaction progress was monitored by LCMS (starting material **63b**, t_R 5.2 min, λ_{abs} 285 nm, ESI M^+ 513; products **70** t_R 3.06 min, λ_{abs} 506 nm, ESI M^+ 401). Compound **70** was isolated on an Interchim puriFlash™ with a 250 × 21.2 mm column (Knauer Eurosphere II 100-5 C18A) from Knauer GmbH. Solvent A: H_2O + 0.05% v/v TFA; solvent B: MeCN + 0.05% v/v TFA. Gradient A/B: 70/30–0/100 (0–20 min), flow rate 18 mL/min, 22°C; detection at 500 nm. Yield 54% (7 mg) of a red solid.

^{1}H NMR (400 MHz, Acetonitrile-d_3) δ 8.25 (dd, J = 7.4, 1.5 Hz, 1H), 7.83 (d, J = 16.3 Hz, 1H), 7.77 (ddd, J = 9.9, 7.3, 1.5 Hz, 2H), 7.29 (dd, J = 7.0, 1.7 Hz, 1H), 7.05 (d, J = 9.1 Hz, 1H), 7.01 (d, J = 9.2 Hz, 1H), 6.94 (d, J = 2.1 Hz, 1H), 6.86 (d, J = 16.3 Hz, 1H), 6.85 – 6.81 (m, 2H).

ESI-HRMS: found 401.1125 $[M]^+$, calculated 401.1132 for $C_{23}H_{17}N_2O_5$, $[M^+]$.

λ_{max} (absorption) 505 nm (ε = 74 000 $M^{-1}cm^{-1}$, EtOH), λ_{max} (emission) 533 nm (EtOH, excitation at 500 nm); Stokes shift 28 nm; fluorescence lifetime 3.2 ns (EtOH), fluorescence quantum yield 0.77 (absolute value in EtOH).

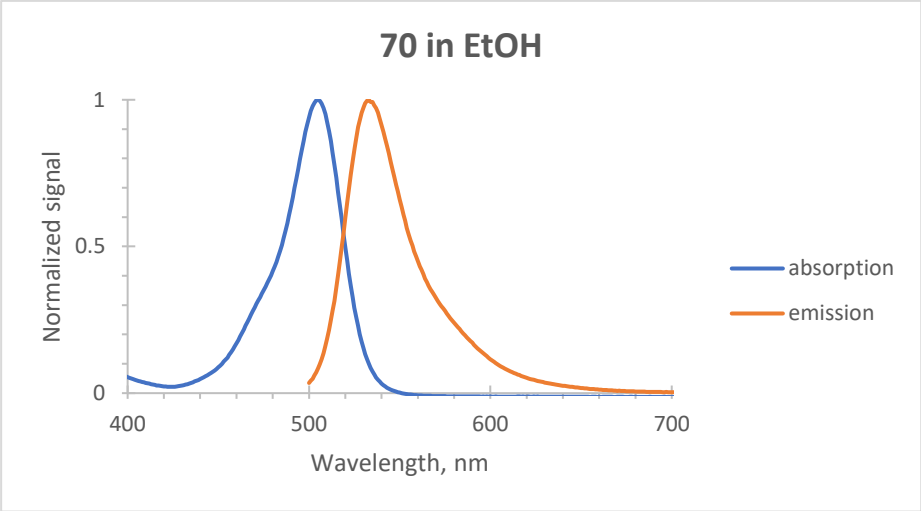

6-amino-9-(2-carboxyphenyl)-2,7-bis((*E*)-2-carboxyvinyl)-3H-xanthen-3-iminium chloride (72)

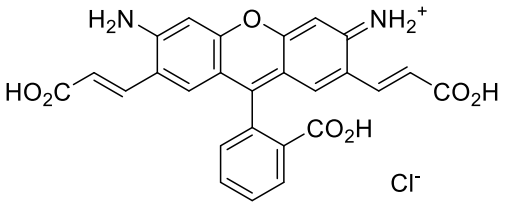

Chemical Formula: $C_{26}H_{19}N_2O_7^+$
Exact Mass: 471.12

72

To a solution of **64a** (18 mg, 0.03 mmol) in 2 ml of EtOH, 2 ml of 20% solution of aq. NaOH was added. The reaction mixture was stirred at 90 ºC overnight. The reaction progress was monitored by LCMS (starting material **64a**, t_R 6.0 min, λ_{abs} 315 nm, ESI M^+ 609; products **72** t_R 2.9 min, λ_{abs} 535 nm, ESI M^+ 471). Compound **72** was isolated on an Interchim puriFlash™ with a 250 × 21.2 mm column (Knauer Eurosphere II 100-5 C18A) from Knauer GmbH. Solvent A: H_2O + 0.05% v/v TFA; solvent B: MeCN + 0.05% v/v TFA. Gradient A/B: 70/30–0/100 (0–20 min), flow rate 18 mL/min, 22°C; detection at 500 nm. Yield 53% (8 mg) of a red solid.

^{1}H NMR (400 MHz, Acetonitrile-d_3) δ 8.21 (d, J = 7.6 Hz, 1H), 7.83 – 7.75 (m, 2H), 7.63 (d, J = 15.6 Hz, 2H), 7.31 (d, J = 7.1 Hz, 1H), 7.10 (s, 2H), 6.83 (s, 2H), 6.05 (d, J = 15.7 Hz, 2H).

ESI-HRMS: found 471.1184 $[M]^+$, calculated 471.1187 for $C_{26}H_{19}N_2O_7$, $[M^+]$.

λ_{max} (absorption) 545 nm (ε = 77 000 $M^{-1}cm^{-1}$, EtOH), λ_{max} (emission) 580 nm (EtOH, excitation at 540 nm); Stokes shift 35 nm; fluorescence lifetime 3.5 ns (EtOH), fluorescence quantum yield 0.88 (absolute value in EtOH).

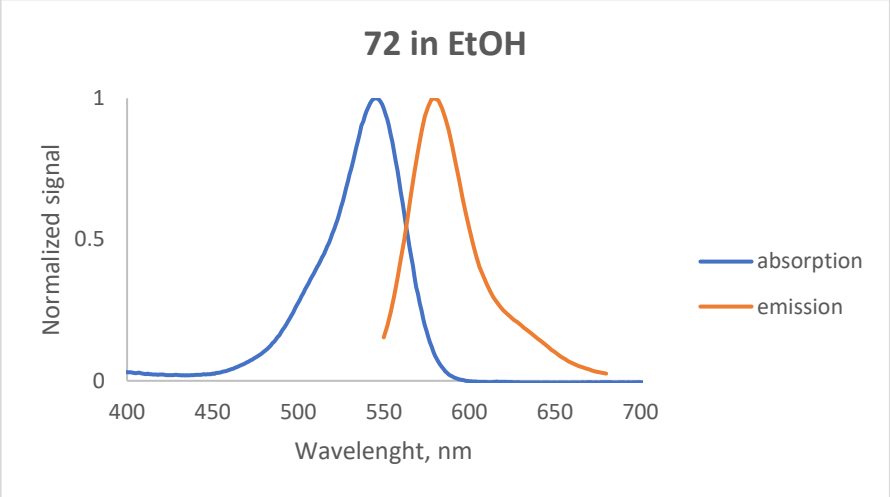

6-(2-carboxyphenyl)-2,10-dioxo-10,11-dihydro-2H-pyrano[3,2-g:5,6-g']diquinolin-1-ium chloride (73)

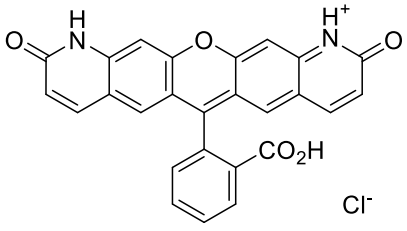

Chemical Formula: $C_{26}H_{15}N_2O_5^+$
Exact Mass: 435.10

73

To a solution of **64a** (18 mg, 0.03 mmol) in 2 ml of EtOH, 2 ml of 20% solution of aq. NaOH was added. The reaction mixture was stirred at 90 ºC overnight. The reaction progress was monitored by LCMS (starting material **64a**, t_R 6.0 min, λ_{abs} 315 nm, ESI M^+ 609; products **73** t_R 4.0 min, λ_{abs} 347 nm, ESI M^+ 435). Compound **73** was isolated on an Interchim puriFlash™ with a 250 × 21.2 mm column (Knauer Eurosphere II 100-5 C18A) from Knauer GmbH. Solvent A: H_2O + 0.05% v/v TFA; solvent B: MeCN + 0.05% v/v TFA. Gradient A/B: 70/30–0/100 (0–20 min), flow rate 18 mL/min, 22°C; detection at 500 nm. Yield 35% (5 mg) of a light-rose solid.

^{1}H NMR (400 MHz, DMSO-d_6) δ 8.11 – 8.07 (m, 1H), 7.85 – 7.74 (m, 2H), 7.81 (d, J = 9.7 Hz, 2H), 7.38 – 7.33 (m, 1H), 7.28 (s, 2H), 7.22 (s, 2H), 6.37 (dd, J = 9.5, 1.6 Hz, 2H).

ESI-HRMS: found 435.0971 $[M]^+$, calculated 435.0975 for $C_{26}H_{14}N_2O_5$, $[M^+]$.

4.2.3.3 Oxidative olefination of phenoxazines

Synthesis of substrates for C–H activation

3,7-dinitro-*10H*-phenoxazine (76) [16]

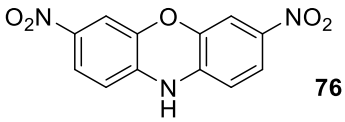

76

Chemical Formula: $C_{12}H_7N_3O_5$
Exact Mass: 273.04

To a solution of phenoxazine (1.0 g, 5.5 mmol) and sodium nitrite (760 mg, 11 mmol) in acetone (100 ml), glacial acetic acid (2 ml, 35 mmol) was added. The mixture was stirred at r.t. for 3 days. The reaction progress was monitored by LCMS (starting material, t_R 4.7 min, λ_{abs} 238 nm, ESI M^- 182; products **76**: t_R 6.8 min, λ_{abs} 475 nm, ESI M^- 272; **79**: t_R 6.7 min, λ_{abs} 457 nm, ESI M^- 227; **80**: t_R 7.1 min, λ_{abs} 468 nm, ESI M^- 317). The reaction mixture was poured in 80 m1 of NaOH (0.1 M). The precipitate was filtered under vacuo, washed with water and dried under vacuum. The residue (1.3 g) was submitted to flash chromatography in portions (approx. 200 mg each; due to poor solubility of target compound **76** in common organic solvents) on Isolera™ One system (SNAP Ultra cartridge, 50 g SiO_2, DCM/MeOH with 0-25% MeOH gradient over 7 CV) to provide compound **76** as a red solid (600 mg in total, 40% yield).

^{1}H NMR (400 MHz, Acetone-d_6) δ 7.75 (dd, J = 8.7, 2.5 Hz, 2H), 7.46 (d, J = 2.5 Hz, 2H), 6.74 (d, J = 8.7 Hz, 2H).

7-amino-*3H*-phenoxazin-3-iminium chloride (81) [16, 17]

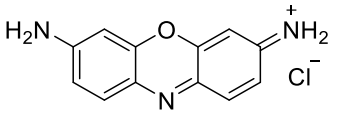

81

Chemical Formula: $C_{12}H_{10}N_3O^+$
Exact Mass: 212.08

To a stirred suspension of **76** (27 mg, 0.1 mmol) and iron powder (30 mg, 0.5 mmol) in ethanol (4 ml), hydrochloric acid (25%, 0.35 ml) was added. The mixture was refluxed for 1 h. The reaction progress was monitored by LCMS (gradient 5/95-50/50, starting material **76**: t_R 9.6 min, λ_{abs} 475 nm, ESI M^- 272; product **81**: t_R 4.3 min, λ_{abs} 580 nm, ESI M^+ 212). The reaction mixture was cooled down to r.t. and filtered off. After filtration, the organic solvent was removed under vacuum and the residue was washed with Et_2O to afford 20 mg of **81** (80% yield) as a blue-violet solid.

^{1}H NMR (400 MHz, Methanol-d_4) δ 7.73 (d, J = 9.2 Hz, 2H), 7.16 (dd, J = 9.2, 2.1 Hz, 2H), 6.79 (d, J = 2.1 Hz, 2H).

3,7-dinitro-(10-acetyl-*10H)*-phenoxazine (82)

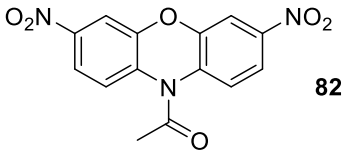

82

Chemical Formula: $C_{14}H_9N_3O_6$
Exact Mass: 315.05

A mixture of mono- (**79**), bis-(**76**), and tris-(**80**) nitrophenoxazines (1.2 g) obtained after nitration of phenoxazine (see the procedure for preparation of **76**) was suspended in acetic anhydride (35 ml) and refluxed for 3 h. The reaction progress was monitored by LCMS (starting material **76**: t_R 6.7 min, λ_{abs} 475 nm, ESI M^- 272; product **82**: t_R 6.5 min, λ_{abs} 337 nm, ESI M^- 272 $[M\text{-}Ac]^-$). The reaction mixture was concentrated in vacuo, and the residue was submitted to flash chromatography on Isolera™ One system (SNAP Ultra cartridge, 50 g SiO_2, hexane/EtOAc with 20-100% EtOAc gradient over 7 CV) to provide compound **82** as a beige solid (875 mg, 73% yield).

^{1}H NMR (400 MHz, Acetone-d_6) δ 8.13 (dd, J = 8.9, 2.5 Hz, 2H), 8.02 (d, J = 2.5 Hz, 2H), 7.94 (d, J = 8.9 Hz, 2H), 2.46 (s, 3H).

^{13}C NMR (101 MHz, Acetone-d_6) δ 169.4, 150.9, 147.0, 135.7, 126.7, 120.4, 113.0, 23.4.

ESI-HRMS: found 316.0641 $[M]^+$, calculated 316.0642 for $C_{14}H_{10}N_3O_6$, $[M+H^+]$.

***N,N'*-(10-acetyl-*10H*-phenoxazine-3,7-diyl)diacetamide (78)**

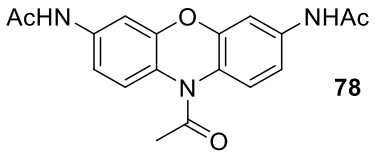

78

Chemical Formula: $C_{18}H_{17}N_3O_4$
Exact Mass: 339.12

An oven-dried Schlenk flask was charged with Pd/C (60 mg) in Ac_2O (10 ml) and kept under hydrogen for 10 min. Then, a solution of **82** (56 mg, 0.2 mmol) in 4 ml of Ac_2O was added via syringe, and the reaction mixture vigorously stirred at r.t. under hydrogen for 8 h. The reaction completion was monitored by LCMS (starting material **82**: t_R 6.5 min, λ_{abs} 337 nm, ESI M^- 272 [M-Ac]$^-$; product **78**: t_R 3.0 min, λ_{abs} 234, 258 nm, ESI M^+ 340); although full conversion was achieved, the LCMS analysis revealed some side products (the puridication was needed). The reaction mixture was either diluted with water, and organics extracted with EtOAc (3 x 30 ml), or just filtered through Celite. The solvents were removed under reduced pressure, and the residue (approx. 70 mg) was purified by column chomatography. This procedure was repeated several times, each time the full conversion was achieved (no traces of starting material by LCMS detection). Different chromatography techniques were used: normal silica SiO_2 40-60 mesh, or basic alumina Al_2O_3, or SNAP Ultra cartridge, 25 g sfär silica HC; eluents: hexane/EtOAc, DCM/MeOH, DCM/Me_2CO. Purification of reversed phase was also used (Interchim puriFlash™ with a 250 × 21.2 mm column (Knauer Eurosphere II 100-5 C18A). Solvent A: H_2O + 0.05% v/v TFA; solvent B: MeCN + 0.05% v/v TFA. Gradient A/B: 80/20–0/100 (0–20 min), flow rate 18 mL/min, 22°C; detection at 250 nm.) The best result (isolation of 3 mg (4% yield) of compound **78** was achieved by using flash chromatography on *Isolera™ One* system (SNAP Ultra cartridge, 25 g sfär silica HC, DCM/acetone with 2-25 % gradient of acetone over 6 CV).

^{1}H NMR (400 MHz, Acetone-d_6) δ 9.34 (br s, 2H), 7.70 (d, J = 2.3 Hz, 2H), 7.48 (d, J = 8.7 Hz, 2H), 7.27 (dd, J = 8.7, 2.3 Hz, 2H), 2.27 (s, 3H), 2.08 (s, 6H).

^{1}H NMR (400 MHz, Methanol-d_4) δ 7.58 (d, J = 2.3 Hz, 2H), 7.47 (d, J = 8.7 Hz, 2H), 7.25 (dd, J = 8.7, 2.3 Hz, 2H), 2.31 (s, 3H), 2.13 (s, 7H).

ESI-HRMS: found 340.1291 $[M]^+$, calculated 340.1297 for $C_{18}H_{18}N_3O_4$, $[M+H^+]$.

3,7-diamino-(10-acetyl-*10H*)-phenoxazine (83)

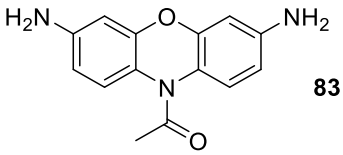

83

Chemical Formula: $C_{14}H_{13}N_3O_2$
Exact Mass: 255.10

An oven-dried Schlenk flask was charged with Pd/C (100 mg) in EtOAc (5 ml) and kept under hydrogen for 10 min. Then, a solution of **82** (170 mg, 0.54 mmol) in 5 ml of EtOAc was added via syringe, and the reaction mixture vigorously stirred at r.t. under hydrogen overnight. The reaction completion was monitored by LCMS (gradient 5/95-50/50, starting material **82**: t_R 8.2 min, λ_{abs} 337 nm, ESI M^- 272 $[M\text{-}Ac]^-$; product **83**: t_R 2.9 min, λ_{abs} 225, 260 nm, ESI M^+ 256); full conversion was achieved and no side products detected. The reaction mixture filtered through Celite, and the solvent was removed under reduced pressure to afford 130 mg of bluish solid (96% yield of compound **83**).

^{1}H NMR (400 MHz, Acetonitrile-d_3) δ 7.16 (d, J = 9.2 Hz, 2H), 6.38 (dd, J = 6.6, 2.3 Hz, 2H), 6.36 (d, J = 2.3 Hz, 1H), 2.15 (s, 3H).

^{13}C NMR (101 MHz, Acetonitrile-d_3) δ 170.4, 152.6, 148.0, 126.6, 120.8, 109.9, 102.8, 23.0.

ESI-HRMS: found 256.1080 $[M]^+$, calculated 256.1081 for $C_{14}H_{14}N_3O_2$, $[M+H^+]$.

*General procedure for M-catalysed oxidative olefination of **82** (Scheme 48):*

A mixture of 3,7-dinitro-(10-acetyl-*10H)*-phenoxazine **82** (63 mg, 0.2 mmol), metal catalyst (0.02 mmol, 10 mol %), additive (0.04 mmol, 20 mol or 30 mol %), oxidant (1 eq., 0.2 mmol), and ethyl acrylate (1.5 eq., 33 µl, 0.3 mmol), in solvent (2 mL) was stirred at mentioned temperature for 18-72 h. The reaction progress was monitored by LCMS (starting material **82**: t_R 6.5 min, λ_{abs} 337 nm, ESI M^- 272 $[M\text{-}Ac]^-$; no conversion was detected).

di-*tert*-Butyl (10-acetyl-*10H*-phenoxazine-3,7-diyl)dicarbamate (88)

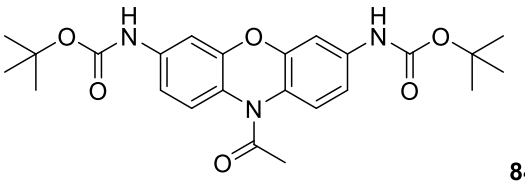

84

Chemical Formula: $C_{24}H_{29}N_3O_6$
Exact Mass: 455.21

To a solution of **83** (130 mg, 0.5 mmol) in ethanol (4 ml) was added Boc_2O (1.2 eq., 1.2 mmol, 270 mg) and the reaction mixture was stirred at r.t. overnight. The formation of *N,N'*-bis-boc-protected compound **84** was observed by TLC (hexane/EtOAc, 1:1), R_f = 0.3; and confirmed by LCMS (product **84**: t_R 7.8 min, λ_{abs} 256 nm, ESI M^+ 456). The reaction mixture was concentrated in vacuo and the crude residue was submitted to flash chromatography (SNAP Ultra cartridge with 25 g SiO_2, hexane/EtOAc with 10-100% EtOAc gradient over 5 CV) to provide compound **84** (200 mg, 88 % yield) as a yellowish powder.

^{1}H NMR (400 MHz, Acetone-d_6) δ 8.58 (s, 2H), 7.54 (d, *J* = 2.4 Hz, 2H), 7.48 (d, *J* = 8.8 Hz, 2H), 7.26 (dd, *J* = 8.8, 2.4 Hz, 2H), 2.27 (s, 3H), 1.49 (s, 18H).

^{13}C NMR (101 MHz, Acetone-d_6) δ 169.5, 153.6, 151.8, 139.4, 126.1, 124.9, 113.6, 107.0, 80.4, 30.6, 28.5, 23.0.

ESI-HRMS: found 456.2121 $[M]^+$, calculated 456.2129 for $C_{24}H_{30}N_3O_6$, $[M+H^+]$.

*Representative Procedure for Rh- or Ru-catalysed oxidative olefination of N,N'-bis-boc phenoxazine **84** (Scheme 50):*

A mixture of *N,N'-bis-boc phenoxazine **84*** (92 mg, 0.2 mmol), $[RuCl_2(p\text{-cymene})]_2$ or $[RhCp^*Cl_2]_2$ (12 mg, 10 mol %), $AgSbF_6$ (14 mg, 0.04 mmol, 20 mol %), $Cu(OAc)_2{*}H_2O$ (40 mg, 1 eq., 0.2 mmol), and *tert*-butyl acrylate (1.5 eq., 44 µl, 0.3 mmol) in acetone (2 mL) was stirred at 70 ºC for 20 h. The reaction completion was monitored by LCMS (starting material **84**: t_R 7.8 min, λ_{abs} 256 nm, ESI M^+ 456; product **85a**: t_R 9.2 min, λ_{abs} 261, 331 nm, ESI M^+ 582; product **85b**: t_R 9.5 min, λ_{abs} 286, 340 nm, ESI M^+ 582). After cooling down to r.t., the reaction mixture was diluted with H_2O (50 mL) and extracted with EtOAc (3 x 50 mL). The combined organic phase was washed with brine and dried over anhydrous $MgSO_4$. After filtration and evaporation of the solvents under reduced pressure, the crude residue was submitted to flash chromatography (SNAP Ultra cartridge with 50 g SiO_2, hexane/EtOAc with 10-100% EtOAc gradient over 6 CV) to provide product **85**.*

*in case of Rh-catalysed reaction, a mixture containing compounds **85a** and **85b** was obtained after purification by column chromatography. The individual regioisomers **85a,b** were isolated on Interchim puriFlash™ with a 250 × 21.2 mm column (Knauer Eurosphere II 100-5 C18A). Solvent A: H_2O + 0.05% v/v TFA; solvent B: MeCN + 0.05% v/v TFA. Gradient A/B: 80/20–0/100 (0–20 min), flow rate 18 mL/min, 22°C; detection at 254 nm.

***tert*-Butyl *(E)*-3-(10-acetyl-3,7-bis((tert-butoxycarbonyl)amino)-*10H*-phenoxazin-2-yl) acrylate (85a)**

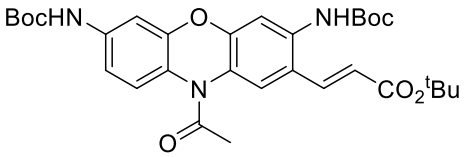

Chemical Formula: $C_{31}H_{39}N_3O_8$
Exact Mass: 581.27

85a

^{1}H NMR (400 MHz, Acetone-d_6) δ 8.62 (s, 1H), 8.44 (s, 1H), 7.95 (s, 1H), 7.78 (d, *J* = 15.7, 1H), 7.57 – 7.51 (m, 2H), 7.50 (d, *J* = 8.8 Hz, 1H), 7.30 (dd, *J* = 8.8, 2.4 Hz, 1H), 6.35 (d, *J* = 15.7 Hz, 1H), 2.34 (s, 3H), 1.51 (s, 9H), 1.50 (s, 9H), 1.49 (s, 9H).

ESI-HRMS: found 582.2803 $[M]^+$, calculated 582.2810 for $C_{31}H_{40}N_3O_8$, $[M+H^+]$.

tert-Butyl *(E)*-3-(10-acetyl-3,7-bis((tert-butoxycarbonyl)amino)-*10H*-phenoxazin-4-yl) acrylate (85b)

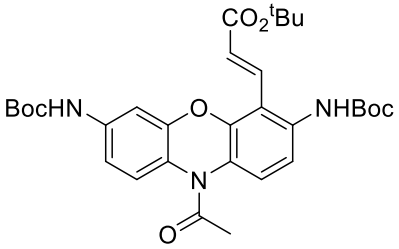

Chemical Formula: $C_{31}H_{39}N_3O_8$
Exact Mass: 581.27

85b

^{1}H NMR (400 MHz, Acetone-d_6) δ 8.66 (s, 1H), 8.61 (s, 1H), 7.77 (d, J = 2.3 Hz, 1H), 7.64 (d, J = 15.9 Hz, 1H), 7.62-7.57 (m, 2 H), 7.58 (d, J = 8.7 Hz, 1H), 7.34 (dd, J = 8.7, 2.4 Hz, 1H), 6.38 (d, J = 16.0 Hz, 1H), 2.17 (s, 3H), 1.52 (s, 9H), 1.50 (s, 9H), 1.50 (s, 9H).

ESI-HRMS: found 582.2798 $[M]^+$, calculated 582.2810 for $C_{31}H_{40}N_3O_8$, $[M+H^+]$.

***tert*-Butyl 3-(10-acetyl-3,7-bis((tert-butoxycarbonyl)amino)-*10H*-phenoxazin-4-yl) propanoate (86)**

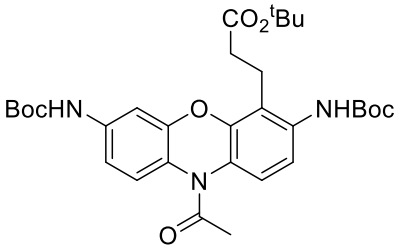

Chemical Formula: $C_{31}H_{41}N_3O_8$
Exact Mass: 583.29

86

An oven-dried Schlenk flask was charged with Pd/C (20 mg) in EtOAc (2 ml) and kept under hydrogen for 10 min. Then, a solution of **85b** (35 mg, 0.06 mmol) in 2 ml of EtOAc was

added via syringe, and the reaction mixture vigorously stirred at r.t. under hydrogen overnight. The reaction completion was monitored by LCMS (starting material **85b**: t_R 9.5 min, λ_{abs} 286, 340 nm, ESI M^+ 582; product **86**: t_R 8.8 min, λ_{abs} 284 nm, ESI M^+ 584); full conversion was achieved and no side products detected. The reaction mixture filtered through Celite, and the solvent was removed under reduced pressure to afford 34 mg of white solid (97% yield of compound **86**).

^{1}H NMR (400 MHz, Acetone-d_6) δ 7.68 (dd, *J* = 8.6, 0.4 Hz, 1H), 7.07 (dd, *J* = 2.5, 0.4 Hz, 1H), 7.03 (dd, *J* = 8.6, 2.5 Hz, 1H), 6.93 – 6.90 (m, 2H), 3.01 (dt, *J* = 15.3, 7.9 Hz, 1H), 2.87 (ddd, *J* = 15.3, 8.8, 6.9 Hz, 1H), 2.64 (ddd, *J* = 14.9, 8.4, 6.5 Hz, 1H), 2.55 (ddd, *J* = 15.9, 8.5, 7.0 Hz, 1H), 1.30 (s, 9H).

^{13}C NMR (101 MHz, Acetone-d_6) δ 172.5, 170.8, 169.5, 169.5, 153.5, 150.8, 150.5, 140.4, 129.7, 127.3, 127.0, 118.7, 118.4, 111.9, 109.5, 80.5, 35.5, 28.3, 27.9, 22.5, 21.0.

ESI-HRMS: found 584.2969 $[M]^+$, calculated 584.2966 for $C_{31}H_{42}N_3O_8$, $[M+H^+]$.

4.2.3.4 Synthesis and properties of new oxazines

*Acidic hydrolysis of compound **85a**:*

Ester **85a** (9 mg, 15 μmol) was dissolved in dichloromethane (2 mL), the solution cooled to +5°C in an ice bath, and then TFA (200 μl) was added dropwise with stirring. The reaction mixture was allowed to warm-up to r.t. and stirred for 1 h. The volatile materials were removed in vacuo, the residue was co-evaporated with dichloromethane (3 times) and kept in vacuo (0.1 mbar) for 2 h. The title compound was isolated by flash chromatography on Interchim puriFlash™ with a 250 × 21.2 mm column (Knauer Eurosphere II 100-5 C18A). Solvent A: H_2O + 0.05% v/v TFA; solvent B: MeCN + 0.05% v/v TFA. Gradient A/B: 80/20–0/100 (0–20 min), flow rate 18 mL/min, 22°C; detection at 580 nm. 1 mg of pink powder of compound **87** was isolated (20 % yield) together with compounds **88** (1 mg, 16% yield), **89** (2 mg, 42% yield), and **90** (traces).

***(E)*-3-(10-acetyl-3,7-diamino-*10H*-phenoxazin-2-yl) acrylic acid (87)**

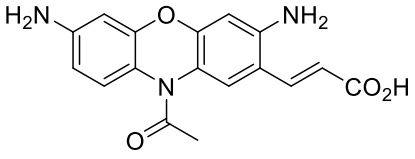

Chemical Formula: $C_{17}H_{15}N_3O_4$
Exact Mass: 325.11

87

^{1}H NMR (400 MHz, DMSO-d_6) δ 7.75 (d, J = 15.7 Hz, 1H), 7.60 (s, 1H), 7.17 (d, J = 9.2 Hz, 1H), 6.44 (s, 1H), 6.41 – 6.30 (m, 2H), 6.22 (d, J = 15.7 Hz, 1H), 2.18 (s, 3H).

ESI-HRMS: found 326.1141 $[M]^+$, calculated 326.1135 for $C_{17}H_{16}N_3O_4$, $[M+H^+]$.

(E)-7-amino-2-(2-carboxyvinyl)-*3H*-phenoxazin-3-iminium trifluoroacetate (88)

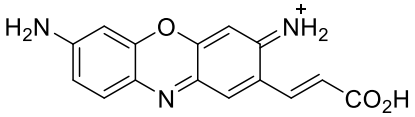

88

Chemical Formula: $C_{15}H_{12}N_3O_3^+$
Exact Mass: 282.09

^{1}H NMR (600 MHz, Methanol-d_4) δ 7.93 (d, J = 0.7 Hz, 1H), 7.78 (d, J = 9.2 Hz, 1H), 7.44 (d, J = 15.5 Hz, 1H), 7.16 (dd, J = 9.2, 2.2 Hz, 1H), 6.82 (s, 1H), 6.77 (d, J = 2.3 Hz, 1H), 6.57 (d, J = 15.6 Hz, 1H).

ESI-HRMS: found 282.0874 $[M]^+$, calculated 282.0873 for $C_{15}H_{12}N_3O_3$, $[M^+]$.

λ_{max} (absorption) 604 nm (ε = 100 000 $M^{-1}cm^{-1}$, EtOH), λ_{max} (emission) 630 nm (EtOH, excitation at 590 nm); Stokes shift 30 nm; fluorescence lifetime 2.4 ns (EtOH), fluorescence quantum yield 0.41 (absolute value in EtOH).

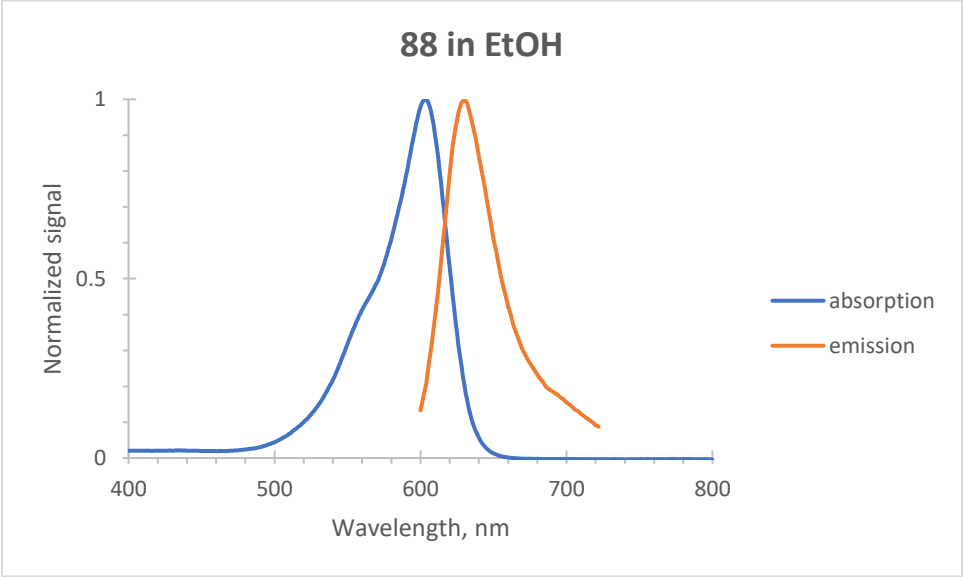

6-acetyl-9-amino-1,6-dihydro-*2H*-pyrido[3,2-b]phenoxazin-2-one (89)

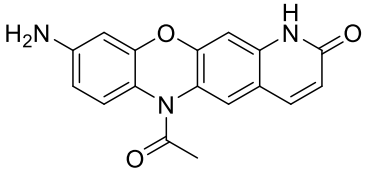

89

Chemical Formula: $C_{17}H_{13}N_3O_3$
Exact Mass: 307.10

^{1}H NMR (400 MHz, DMSO-d_6) δ 7.88 (d, J = 9.6 Hz, 1H), 7.86 (s, 1H), 7.21 (d, J = 8.5 Hz, 2H), 6.99 (s, 1H), 6.45 – 6.31 (m, 3H), 2.22 (s, 3H).

ESI-HRMS: found 308.1039 $[M]^+$, calculated 308.1035 for $C_{17}H_{14}N_3O_3$, $[M+H^+]$.

*Acidic hydrolysis of compound **85b**:*

Ester **85b** (9 mg, 15 μmol) was placed into amber glass flask, 2 ml of dichloromethane was added under Ar, and the solution cooled to +5°C in an ice bath. TFA (200 μl) was added dropwise with stirring. The reaction mixture was allowed to warm-up to r.t. and stirred for 1 h. The volatile materials were removed in vacuo, the residue was co-evaporated with dichloromethane (3 times) and kept in vacuo (0.1 mbar) for 2 h. The title compound was isolated by flash chromatography on Interchim puriFlash™ with a 250 × 21.2 mm column (Knauer Eurosphere II 100-5 C18A). Solvent A: H_2O + 0.05% v/v TFA; solvent B: MeCN + 0.05% v/v TFA. Gradient A/B: 80/20–0/100 (0–20 min), flow rate 18 mL/min, 22°C; detection at 580 nm. 3 mg of pink powder of compound **91** was isolated (61 % yield) together with dye **92** (1 mg, 16% yield).

***(E)*-3-(10-acetyl-3,7-diamino-*10H*-phenoxazin-4-yl) acrylic acid (91)**

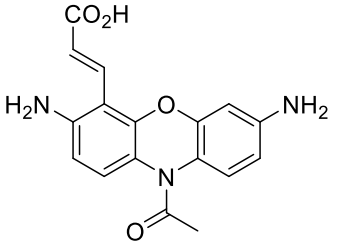

91

Chemical Formula: $C_{17}H_{15}N_3O_4$
Exact Mass: 325.11

^{1}H NMR (400 MHz, Methanol-d_4) δ 7.63 (d, J = 16.1 Hz, 1H), 7.32 (d, J = 9.1 Hz, 1H), 6.90 (d, J = 2.3 Hz, 1H), 6.66 – 6.63 (m, 2H), 6.62 (d, J = 2.4 Hz, 1H), 6.44 (d, J = 16.0 Hz, 1H), 2.14 (s, 3H).

ESI-HRMS: found 326.1143 $[M]^+$, calculated 326.1135 for $C_{17}H_{16}N_3O_4$, $[M+H^+]$.

***(E)*-7-amino-6-(2-carboxyvinyl)-*3H*-phenoxazin-3-iminium trifluoroacetate (92)**

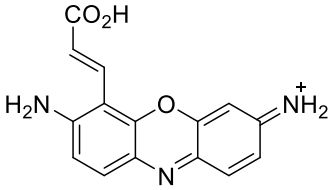

92

Chemical Formula: $C_{15}H_{12}N_3O_3^+$
Exact Mass: 282.09

^{1}H NMR (400 MHz, Methanol-d_4) δ 8.20 (d, J = 16.2 Hz, 1H), 7.84 (d, J = 9.3 Hz, 1H), 7.36 (d, J = 2.2 Hz, 1H), 7.14 (dd, J = 9.3, 2.2 Hz, 1H), 6.81 (d, J = 16.3 Hz, 1H), 6.73 (dd, J = 5.9, 2.3 Hz, 2H).

ESI-HRMS: found 282.0876 $[M]^+$, calculated 282.0873 for $C_{15}H_{12}N_3O_3$, $[M^+]$.

λ_{max} (absorption) 597 nm (ε = 105 000 $M^{-1}cm^{-1}$, EtOH), λ_{max} (emission) 607 nm (EtOH, excitation at 590 nm); Stokes shift 10 nm; fluorescence lifetime 3.4 ns (EtOH), fluorescence quantum yield 0.46 (absolute value in EtOH).

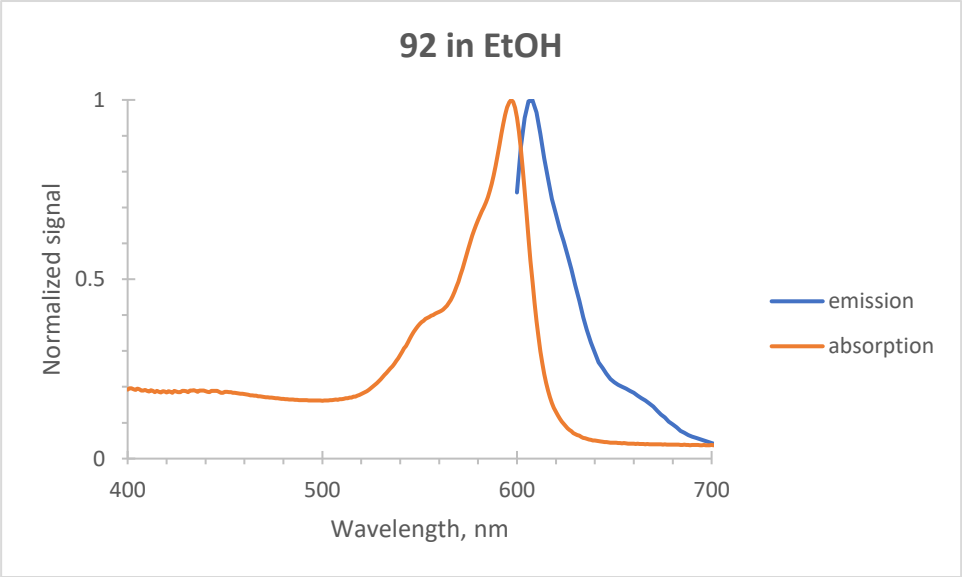

*Acidic hydrolysis of compound **86**:*

Ester **86** (9 mg, 15 µmol) was dissolved in 2 ml of dichloromethane and TFA (200 µl) was added dropwise. The reaction mixture turned fuxia immediately. The reaction mixture was stirred at r.t. for 1 h. The volatile materials were removed in vacuo, the residue was co-evaporated with dichloromethane (3 times) and kept in vacuo (0.1 mbar) for 2 h. The title compound was isolated by flash chromatography on Interchim puriFlash™ with a 250 × 21.2 mm column (Knauer Eurosphere II 100-5 C18A). Solvent A: H_2O + 0.05% v/v TFA; solvent B: MeCN + 0.05% v/v

TFA. Gradient A/B: 80/20–0/100 (0–20 min), flow rate 18 mL/min, 22°C; detection at 580 nm. 4 mg of red powder of compound **94** was isolated (61 % yield).

7-amino-6-(2-carboxyethyl)-*3H*-phenoxazin-3-iminium trifluoroacetate (94)

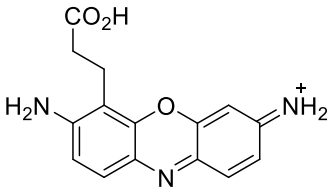

Chemical Formula: $C_{15}H_{14}N_3O_3^+$
Exact Mass: 284.10

94

^{1}H NMR (400 MHz, Methanol-d_4) δ 8.20 (d, J = 16.2 Hz, 1H), 7.84 (d, J = 9.3 Hz, 1H), 7.36 (d, J = 2.2 Hz, 1H), 7.14 (dd, J = 9.3, 2.2 Hz, 1H), 6.81 (d, J = 16.3 Hz, 1H), 6.73 (dd, J = 5.9, 2.3 Hz, 2H).

ESI-HRMS: found 284.1031 $[M]^+$, calculated 284.1035 for $C_{15}H_{14}N_3O_3$, $[M^+]$.

λ_{max} (absorption) 589 nm (ε = 100 000 $M^{-1}cm^{-1}$, EtOH), λ_{max} (emission) 599 nm (EtOH, excitation at 580 nm); Stokes shift 10 nm; fluorescence lifetime 3.6 ns (EtOH), fluorescence quantum yield 0.54 (absolute value in EtOH).

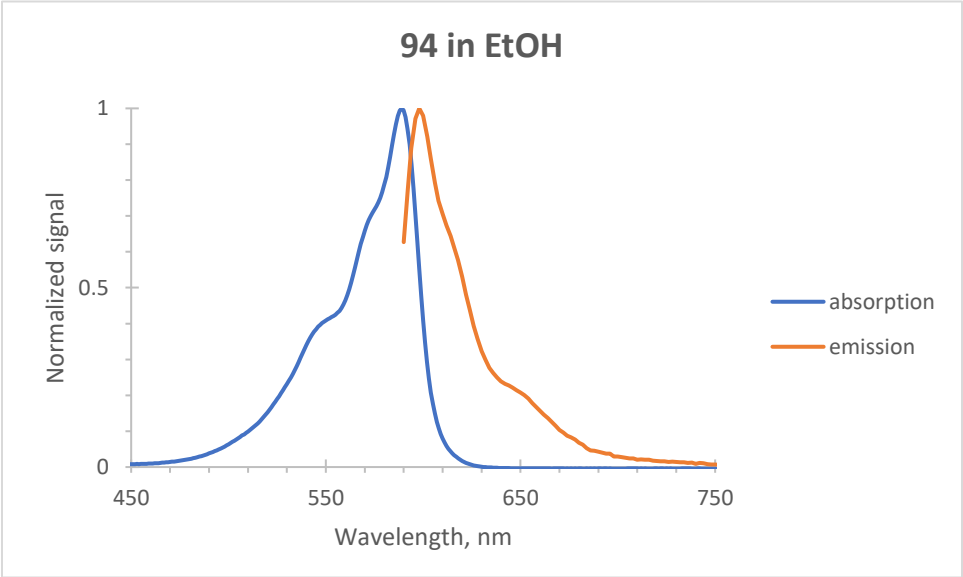

4.2.3.5 Oxidative olefination of compound 95

10-acetyl-*10H*-phenoxazine-3,7-diyl diacetate (95)

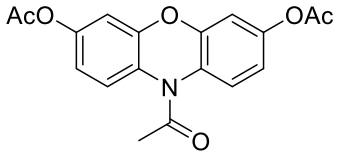

95

Chemical Formula: $C_{18}H_{15}NO_6$
Exact Mass: 341.09

A solution of zinc powder (300 mg, 4.6 mmol), resazurin sodium salt (300 mg, 1.2 mmol), glacial acetic acid (8 ml) and acetyc anhydride (6 ml) were stirred under Ar at r.t. overnight, then 1 h at reflux. The reaction completion was monitored by TLC (hexane/EtOAc 1:1, R_f 0.3) and LCMS (product **95** t_R 5.6 min, λ_{abs} 281 nm, ESI M^+ 342). The reaction mixture was diluted with water (50 ml) and extracted with EtOAc (3×150 ml). The combined organic extract was washed with brine, dried over anhydrous $MgSO_4$, and evaporated to get a brown crude product which was purified by column chromatography (SNAP Ultra cartridge with 50 g SiO_2, hexane/EtOAc with 20-100% EtOAc gradient over 5 CV) to provide product **95** as a yellow solid (380 mg, yield 93%).

^{1}H NMR (400 MHz, Acetone-d_6) δ 7.63 (dd, J = 8.7, 0.4 Hz, 2H), 7.00 (d, J = 2.3 Hz, 2H), 6.97 (dd, J = 8.7, 2.6 Hz, 2H), 2.32 (s, 3H), 2.27 (s, 6H).

ESI-HRMS: found 342.0968 $[M]^+$, calculated 342.0972 for $C_{18}H_{16}NO_6^+$, $[M+H]^+$.

(*E*)-10-acetyl-4-(3-(*tert*-butoxy)-3-oxoprop-1-en-1-yl)-*10H*-phenoxazine-3,7-diyl diacetate (96)

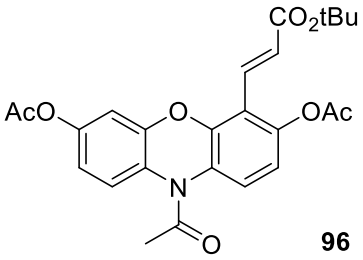

96

Chemical Formula: $C_{25}H_{25}NO_8$
Exact Mass: 467.16

Triacetate (**95**) (340 mg, 1 mmol), *tert*-butyl acrylate (1.5 eq, 220 µl, 196 mg, 1.5 mmol), $[RuCl_2(p\text{-cymene})]_2$ (60 mg, 10 mol %), $AgSbF_6$ (70 mg, 20 mol %) and $Cu(OAc)_2 \cdot H_2O$ (200 mg, 1 mmol) were suspended in 20 ml of acetone and placed in a sealed tube. The reaction mixture was stirred at 80 °C overnight. The reaction completion was monitored by TLC (hexane-EtOAc 1:1, R_f 0.5; starting material R_f 0.3) and LCMS (strarting compound **95** t_R 5.6 min, λ_{abs} 281 nm, ESI M^+ 342; product **96** t_R 7.5 min, λ_{abs} 280 nm, ESI M^+ 468). The mixture was diluted with water (50 ml)

and extracted with EtOAc (3x50 ml). The combined organic extract was washed with brine and dried over anhydrous $MgSO_4$. After filtration and evaporation of the solvents under reduced pressure, the crude product was purified by column chromatography (SNAP Ultra cartridge with 50 g SiO_2, hexane/EtOAc with 20-100% EtOAc gradient over 5 CV). Yield 49% (230 mg of a yellow solid of **96**).

^{1}H NMR (400 MHz, Acetone-d_6) δ 7.74 (dd, *J* = 8.5, 0.4 Hz, 1H), 7.62 (d, *J* = 16.0 Hz, 1H), 7.45 (dd, *J* = 2.4, 0.4 Hz, 1H), 7.09 – 7.02 (m, 3H), 6.51 (d, *J* = 16.0 Hz, 1H), 2.28 (d, *J* = 2.2 Hz, 6H), 2.20 (s, 3H), 1.97 (s, 1H), 1.51 (s, 9H).

^{13}C NMR (101 MHz, Acetone-d_6) δ 170.9, 169.4, 166.2, 153.5, 152.6, 150.7, 150.5, 139.0, 133.0, 128.8, 127.4, 118.4, 115.8, 112.8, 111.7, 80.9, 28.3, 22.4, 20.9.

ESI-HRMS: found 490.1473 $[M+Na]^+$, calculated 490.1472 for $C_{25}H_{25}NO_8Na^+$, $[M+Na^+]$.

10-acetyl-4-(3-(*tert*-butoxy)-3-oxopropyl)-*10H*-phenoxazine-3,7-diyl diacetate (97)

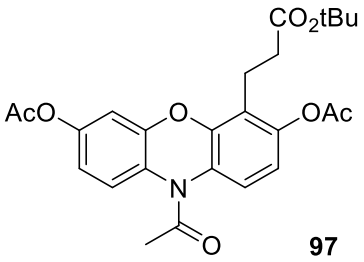

97

Chemical Formula: $C_{25}H_{27}NO_8$
Exact Mass: 469.17

An oven-dried Schlenk flask was charged with Pd/C (50 mg) in EtOAc (2 ml) and kept under hydrogen for 10 min. Then, a solution of **96** (102 mg, 0.22 mmol) in 4 ml of EtOAc was added via syringe, and the reaction mixture vigorously stirred at r.t. overnight. The reaction completion was monitored by LCMS (strarting compound **96** t_R 7.5 min, λ_{abs} 280 nm, ESI M^+ 468; products **97** t_R 7.1 min, λ_{abs} 277 nm, ESI M^+ 470). The reaction solution was filtered through Celite, and concentrated in vacuo. Yield 98% (100 mg of a yellow solid of **97**). No purification needed.

^{1}H NMR (400 MHz, Acetone-d_6) δ 7.68 (dd, *J* = 8.6, 0.4 Hz, 1H), 7.07 (dd, *J* = 2.5, 0.4 Hz, 1H), 7.03 (dd, *J* = 8.6, 2.5 Hz, 1H), 6.92 (q, *J* = 2.5 Hz, 2H), 3.07 – 2.96 (m, 1H), 2.87 (ddd, *J* = 14.9, 8.6, 6.7 Hz, 2H), 2.70 – 2.50 (m, 2H), 2.26 (d, *J* = 7.7 Hz, 6H), 2.21 (s, 3H), 1.31 (s, 9H).

^{13}C NMR (101 MHz, Acetone-d_6) δ 172.3, 170.6, 169.4, 169.3, 153.3, 150.6, 150.4, 140.2, 129.6, 127.2, 126.9, 118.6, 118.3, 111.7, 109.4, 80.3, 35.4, 28.1, 27.7, 22.3, 20.9.

ESI-HRMS: found 414.1180 $[M-^tBu+2H]^+$, calculated 414.1183 for $C_{21}H_{20}NO_8^+$, $[M-C_4H_9+2H]^+$.

tert-Butyl 3-(10-acetyl-3,7-dihydroxy-_10H_-phenoxazin-4-yl) propanoate (100)

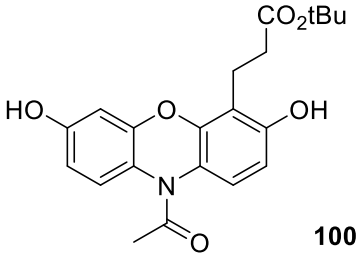

100

Chemical Formula: $C_{21}H_{23}NO_6$
Exact Mass: 385.15

To a solution of diacetate **97** (100 mg, 0.21 mmol) in EtOH (6 ml) was added 5 M NaOH dropwise (200 µl, 1 mmol, 5 eq). The colour immediately turned fuxia. The reaction was stirred at r.t. for 4 h. The reaction completion was monitored by TLC (EtOAc, R_f 0.5, starting material R_f 0.75) and LCMS (strarting compound **97** t_R 7.1 min, λ_{abs} 277 nm, ESI M^+ 470, product **100** t_R 5.0 min, λ_{abs} 282 nm, ESI M^+ 330 $[M\text{-}^tBu+2H]^+$). The resulting red solution was acidified with 1 M HCl (5 ml), the colour turned yellow, the mixture diluted with water, and organics extracted with EtOAc (2×50 ml). The combined organic extract was washed with brine and dried over anhydrous $MgSO_4$. The solvents were evaporated under reduced pressure to provide a red solid (100 mg of a crude product) which was used in the next step without further purification.

ESI-HRMS: found 408.1418 $[M+Na]^+$, calculated 408.1418 for $C_{21}H_{23}NO_6Na^+$.

10-Acetyl-4-(3-(_tert_-butoxy)-3-oxopropyl)-_10H_-phenoxazine-3,7-diyl ditriflate

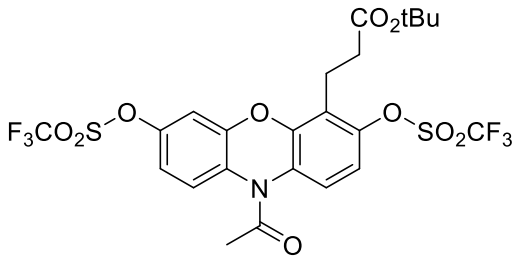

98

Chemical Formula: $C_{23}H_{21}NO_{10}F_6S_2$
Exact Mass: 649.05

The crude solid of **100** was suspended in DCM (5 mL) and cooled to 0 °C. Pyridine (135 µl, 1.7 mmol, 8 eq) and trifluoromethanesulfonic anhydride (140 µl, 0.84 mmol, 4 eq) were added, and the ice bath was removed. The reaction was stirred at r.t. for 1 h. The reaction completion was monitored by TLC (hexane/EtOAc 9:1, R_f 0.4; starting compound Rf 0) and LCMS (strarting compound **100** t_R 5.0 min, λ_{abs} 282 nm, ESI M^+ 330 $[M\text{-}^tBu+2H]^+$; product **98** t_R 9.8 min, λ_{abs} 281 nm, ESI M^+ 594 $[M\text{-}^tBu+2H]^+$). It was subsequently diluted with water and extracted with DCM (2×50 ml). The combined organic extract was dried over anhydrous $MgSO_4$, filtered, and evaporated. The crude product was purified by column chromatography (Isolera SNAP Ultra

cartridge with 50 g SiO_2, hexane/EtOAc with 2-50-100% EtOAc gradient over 5 CV). Yield 66% of **98** (90 mg of a white-yellow solid).

^{1}H NMR (400 MHz, Chloroform-*d*) δ 7.54 – 7.48 (m, 1H), 7.19 – 7.14 (m, 2H), 7.05 – 7.00 (m, 2H), 2.96 (dh, *J* = 15.1, 7.1 Hz, 2H), 2.71 – 2.46 (m, 2H), 1.33 (s, 9H).

^{19}F NMR (376 MHz, Chloroform-*d*) δ -72.63, -72.73.

^{13}C NMR (101 MHz, Chloroform-*d*) δ 171.6, 169.9, 152.5, 147.7, 140.7, 130.6, 127.8, 127.0, 120.4, 117.8, 117.4, 117.2, 111.3, 108.8, 81.0, 34.9, 28.0, 26.9, 22.3.

ESI-HRMS: found 672.0403 $[M+Na]^+$, calculated 672.0403 for $C_{23}H_{21}NO_{10}F_6S_2Na^+$.

tert-Butyl 3-(10-acetyl-3,7-di(azetidin-1-yl)-*10H*-phenoxazin-4-yl) propanoate (99)

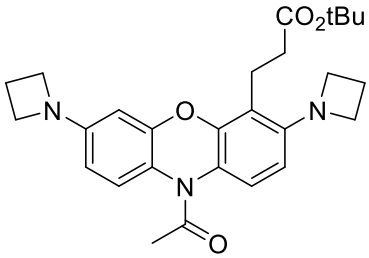

Chemical Formula: $C_{27}H_{33}N_3O_4$
Exact Mass: 463.25

99

A vial was charged with ditriflate **98** (90 mg, 0.14 mmol), $Pd(dba)_2$ (16 mg, 0.028 mmol, 0.2 eq), XPhos (26 mg, 0.054 mmol, 0.4 eq), and Cs_2CO_3 (130 mg, 0.4 mmol, 2.8 eq). The vial was sealed and evacuated/backfilled with Ar 3 times. Dioxane (2 ml) was added, then azetidine (23 µl, 2.4 eq, 0.34 mmol), and the reaction mixture was stirred at 100 °C (oil bath temperature) for 18 h.

The reaction completion was monitored by TLC (hexane/EtOAc 4:1, R_f 0.25; starting compound Rf 0) and LCMS (strarting compound **98** t_R 9.8 min, λ_{abs} 281 nm, ESI M^+ 594 $[M-{}^tBu+2H]^+$; product **99** t_R 9.0 min, λ_{abs} 264 nm, ESI M^+ 464 $[M+H]^+$). The reaction mixture was diluted with water and extracted with DCM (2×50 ml). The combined organic extract was washed with brine, and evaporated. The crude product was purified by column chromatography (Isolera SNAP Ultra cartridge with 50 g SiO_2, hexane/EtOAc with 20-100% EtOAc gradient over 5 CV). Yield 80 % (52 mg of a white-rose solid).

^{1}H NMR (400 MHz, Acetone-d_6) δ 7.30 (dd, *J* = 8.1, 0.6 Hz, 1H), 6.23 – 6.16 (m, 2H), 6.11 (d, *J* = 2.4 Hz, 1H), 6.05 (d, *J* = 2.5 Hz, 1H), 3.84 (q, *J* = 7.5 Hz, 8H), 3.00 – 2.71 (m, 2H), 2.62 – 2.44 (m, 2H), 2.32 (h, *J* = 7.4 Hz, 4H), 2.09 (s, 3H), 1.36 (s, 9H).

^{13}C NMR (101 MHz, Acetone-d_6) δ 172.7, 171.3, 154.3, 154.2, 152.6, 152.3, 127.1, 126.7, 120.6, 107.5, 106.7, 99.8, 97.9, 80.1, 53.0, 35.8, 31.6, 28.2, 28.0, 26.0, 24.5, 23.4, 22.4, 17.2.

ESI-HRMS: found 464.2542 $[M+H]^+$, calculated 464.2549 for $C_{27}H_{34}N_3O_4^+$, $[M+H]^+$.

3-(10-Acetyl-3,7-di(azetidin-1-yl)-*10H*-phenoxazin-4-yl) propanoic acid (102)

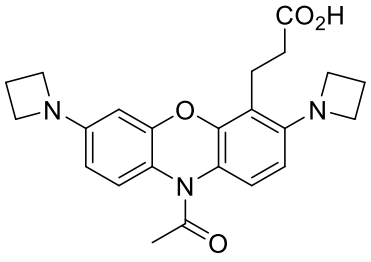

Chemical Formula: $C_{23}H_{25}N_3O_4$
Exact Mass: 407.18

102

Ester **99** (9 mg, 20 μmol) was placed into amber glass flask, 2 ml of deoxigenated dichloromethane was added under Ar, and the solution cooled to +5°C in an ice bath. TFA (170 μl in 0.5 ml of DCM) was added dropwise with stirring. The reaction mixture was allowed to warm-up to r.t. and stirred for 1 h. The volatile materials were removed in vacuo, the residue was co-evaporated with dichloromethane (3 times) and kept in vacuo (0.1 mbar) for 2 h. The title compound was isolated by flash chromatography on Interchim puriFlash™ with a 250 × 21.2 mm column (Knauer Eurosphere II 100-5 C18A). Solvent A: H_2O + 0.05% v/v TFA; solvent B: MeCN + 0.05% v/v TFA. Gradient A/B: 80/20–0/100 (0–20 min), flow rate 18 mL/min, 22°C; detection at 580 nm. 5 mg of bluish powder of compound **102** was isolated (61 % yield).

4.3 References to Chapter 4

1. a) R. W. Taft, E. Price, I. R. Fox, I. C. Lewis, K. K. Andersen, G. T. Davis, *J. Am. Chem. Soc.* **1963**, *85*, 709-724; b) R. W. Taft, E. Price, I. R. Fox, I. C. Lewis, K. K. Andersen, G. T. Davis, *J. Am. Chem. Soc.* **1963**, *85*, 3146-3456.

2. a) E. A. Savicheva, G. Y. Mitronova, L. Thomas, M. J. Boehm, J. Seikowski, V. N. Belov, S. W. Hell, *Angew. Chem. Int. Ed*. **2020**, *59*, 5505-5509; b) E. A. Savicheva, J. Seikowski, J. I. Kast, C. R. Grünig, V. N. Belov, S. W. Hell, *Angew. Chem. Int. Ed.* **2021**, *60*, 3720-3726.

3. D. L. Mohler, G. Shen, *Org. Biomol. Chem*. **2006**, *4*, 2082-2087.

4. E. A. Savicheva, M. L. Bossi, V. N. Belov, S. W. Hell, *ChemPhotoChem* **2022**, e202200222.

5. Diazald® and Diazomethane Generators, Sigma Aldrich Technical Information Bulletin AL-180.

6. D.-Y. Zhou, Y. Li, W.-L. Jiang, Y. Tian, J. Fei, C.-Y. Li, *Chem. Comm.* **2018,** *54*, 11590-11593.

7. H. Eilingsfeld, G. Neubauer, M. Seefelder, H. Weidinger, *Chem. Ber.* **1964**, *97*, 1232-1245.

8. Z.-H. Peng, L. Qun, X.-F. Zhou, S. Carroll, H. J. Geise, B. Peng, R. Dommisse, R. Carleer, *J. Mater. Chem*. **1996**, *6*(4), 559-565.

9. X. Jia, Q. Chen, Y. Yang, Y. Tang, R. Wang, Y. Xu, W. Zhu, X. Qian, *J. Am. Chem. Soc.* **2016**, *138*, 34, 10778-10781.

10. M. Coenen, *Chem. Ber.* **1949**, *82*, 66-72.

11. C. Reichardt, W. Mormann, *Chem. Ber*. **1972**, *105*, 1815-1839.

12. E. A. Owens, H. Hyun, T. L. Dost, J. H. Lee, G. L. Park, D. H. Pham, M. H. Park, H. S. Choi, M. Henary, *J. Med. Chem*. **2016**, *59*, 5311-5323.

13. Z. Arnold, J. Sauliova, V. Krchnak *Coll. Czech. Chem. Commun*. **1973**, *38*, 2633-2640

14. P.E. Fanta, *Org. Synth*. **1952**, 32, 95.

15. K. K. Abney, S. J. Ramos-Hunter, I. M. Romaine, J. S. Goodwin, G. A. Sulikowski, C. D. Weaver, *Chem. Eur. J.* **2018**, *24*(36), 8985-8988.

16. H. Maas, A. Khatyr, G. Calzaferri, *Microporous Mesoporous Mater*. **2003**, *65*, 233-242.

17. D. Creed, N. C. Fawcett, R. L. Thompson, *J. C. S. Chem. Commun*. **1981**, 497-499.

Acknowledgements

I would like to express my deepest gratitude to Prof. Stefan W. Hell, who provided me with an excellent opportunity to pursue my doctoral studies in the competitive and interdisciplinary environment of the Department of Nanobiophotonics of the MPI NAT. I am very grateful to Prof. Lutz Ackermann for the productive thesis committee meetings, his feedback, and careful reading of the manuscript. Special thanks go to Dr. Vladimir Nikolaevich Belov for proposing interesting topics for my PhD thesis, providing exceptional guidance, and for always supporting me during my time in Göttingen. I could not have imagined a better advisor and mentor. I also would like to thank other members of my thesis committee – Prof. Marina Bennati, Dr. Daniel Janßen-Müller, and Dr. Grazvydas Lukinavicius – for their attention and evaluation of my work and assistance in my graduation.

I would like to thank all members of the organic synthesis group in the Nanobiophotonics Department at MPI NAT (Göttingen). In particular, I would like to thank Dr. Dušan Kolarski and Dr. Marie Auvray for interesting discussions and knowledge sharing. I am immensely grateful to Dr. Mariano Bossi for help with photolysis experiments and to Dr. Alexey Butkevich for sharing his knowledge and experience in the synthesis of organic fluorophores. I would like to thank the staff of the chemical facility (MPI NAT) where I was kindly allowed to work, especially Jan Seikowski for help with electrophoresis experiments, Jürgen Bienert for recording numerous NMR spectra, and performing LCMS and HPLC analysis.

At the Department of Chemistry, University of Göttingen, I would like to thank Dr. Holm Frauendorf and his team for promptly providing HR-MS spectra and Dr. Michael John for recording NMR spectra. I had the opportunity to collaborate with a private company during the thesis and I would like to thank Jeannette Kast and Dr. Christoph Grünig (Microsynth AG, Switzerland) for the CGE-LIF analysis of my probes and fruitful discussions on this topic.

I thank my family and friends for their support during my PhD thesis.